



# University of HUDDERSFIELD

## University of Huddersfield Repository

Xu, Qihua

Development of Advanced Creep Damage Constitutive Equations for Low CR Alloy Under Long-Term Service

### Original Citation

Xu, Qihua (2016) Development of Advanced Creep Damage Constitutive Equations for Low CR Alloy Under Long-Term Service. Doctoral thesis, University of Huddersfield.

This version is available at <http://eprints.hud.ac.uk/id/eprint/27858/>

The University Repository is a digital collection of the research output of the University, available on Open Access. Copyright and Moral Rights for the items on this site are retained by the individual author and/or other copyright owners. Users may access full items free of charge; copies of full text items generally can be reproduced, displayed or performed and given to third parties in any format or medium for personal research or study, educational or not-for-profit purposes without prior permission or charge, provided:

- The authors, title and full bibliographic details is credited in any copy;
- A hyperlink and/or URL is included for the original metadata page; and
- The content is not changed in any way.

For more information, including our policy and submission procedure, please contact the Repository Team at: [E.mailbox@hud.ac.uk](mailto:E.mailbox@hud.ac.uk).

<http://eprints.hud.ac.uk/>

**DEVELOPMENT OF ADVANCED CREEP  
DAMAGE CONSTITUTIVE EQUATIONS FOR  
LOW CR ALLOY UNDER LONG-TERM SERVICE**

**QIHUA XU**

A thesis submitted to the University of Huddersfield in partial fulfilment of the requirements for the degree of Doctor of Philosophy

School of Computing and Engineering  
The University of Huddersfield

January 2016

## Copyright statement

- i. The author of this thesis (including any appendices and/or schedules to this thesis) owns any copyright in it (the “Copyright”) and s/he has given The University of Huddersfield the right to use such copyright for any administrative, promotional, educational and/or teaching purposes.
- ii. Copies of this thesis, either in full or in extracts, may be made only in accordance with the regulations of the University Library. Details of these regulations may be obtained from the Librarian. This page must form part of any such copies made.
- iii. The ownership of any patents, designs, trademarks and any and all other intellectual property rights except for the Copyright (the “Intellectual Property Rights”) and any reproductions of copyright works, for example graphs and tables (“Reproductions”), which may be described in this thesis, may not be owned by the author and may be owned by third parties. Such Intellectual Property Rights and Reproductions cannot and must not be made available for use without the prior written permission of the owner(s) of the relevant Intellectual Property Rights and/or Reproductions.

## Abstract

Low Cr alloys are mostly utilized in structural components such as steam pipes, turbine generators and reactor pumps operating at high temperatures from 400°C to 700°C in nuclear power plants. For safe operation, it is necessary at the design stage to predict and understand the creep damage behaviour of low Cr alloys under long-term service conditions but under low stress levels. Laboratory creep tests can be utilized in the investigation of creep damage behaviour, however, these are usually expensive and time-consuming. Thus, constitutive modelling is considered here for both time and economic efficiency.

Existing constitutive equations for describing creep are mostly proposed based on experimental data for materials under high stresses. For low stress levels, the computational determination of a current state is extrapolated from those constitutive equations by simply using a power-law or sinh law. However, experimental observation has shown that this method is not satisfactory. The aim of the current research is to utilize continuum damage mechanics (CDM) to improve the constitutive equations for low Cr alloys under long-term service.

This project provides three main contributions. The first is a more accurate depiction of the relationship between minimum creep rate and stress levels. The predicted creep rates show good agreement with creep data observed experimentally for both 2.25Cr-1Mo steel and 0.5Cr-0.5Mo-0.25V steel creep specimens. Secondly, it gives a more comprehensive description of the relationship between creep damage and creep cavitation. The CDM approach has been used and a reasonable agreement has also been achieved between predicted creep strain and experimental data for 0.5Cr-0.5Mo-0.25V base material under the critical stress of 40MPa at 640°C. Thirdly, it proposes a more accurate creep rupture criterion in the creep damage analysis of low Cr alloys under different stress levels. Based on investigation of creep cavitation for

2.25Cr-1Mo steel, the area fraction of cavitation at rupture time obviously differs under different stress levels.

This thesis contributes to computational creep damage mechanics in general and in particular to the design of a constitutive model for creep damage analysis of low Cr alloys. The proposed constitutive equations are only valid at low and intermediate stress levels. Further work needs to be undertaken when more experimental data are available.

## Acknowledgements

I am very grateful to my supervisors Dr Qiang Xu, Professor Zhongyu Lu and Dr Yongxin Pang for their guidance and continuous encouragement over the course of this research. I would also like to thank them for providing opportunities to attend international conferences and meetings during this study.

My sincere gratitude is reserved for my first supervisor, Dr Qiang Xu, the ideas in the development of minimum creep rate constitutive equations and the design of the rupture criterion for low Cr alloys are firstly proposed by my first supervisor.

I would also like to take this opportunity to thank Dr Donglai Xu and Dr Fengshou Gu - my first and second year progression viva examiners - for their very helpful comments and suggestions.

I would like to express my sincere acknowledgement to Dr Dezheng Liu and Maggie Mundy, for their careful proof reading of my thesis.

Words cannot express the feelings I have for my parents for their constant, unconditional support - both emotionally and financially; without my mother and father's financial support and encouragement, this thesis would not have been finished.

Partial financial support from the School Scholarship scheme is also appreciated.

Finally, I would like to thank Dr Qiang Xu and Dr Dezheng Liu again. There were times during the past four years when everything seemed hopeless I can honestly say that it was only their determination and constant encouragement that ultimately made it possible for me to see this project through to the end.

## **Declaration**

This dissertation is submitted for the degree of Doctor of Philosophy at the University of Huddersfield. I declare that the work in this dissertation was carried out in accordance with the Regulations of the University of Huddersfield.

The first two years of this research were conducted at Teesside University under the supervision of Dr Qiang Xu, Dr Yongxin Pang and Dr Michael Short, while Dr Qiang Xu was working at Teesside University.

This work is original except where acknowledgment and references are made to previous work. Neither this nor any substantially similar dissertation has been or is being submitted for a degree, diploma or other qualification at any other university.

## Publications list

1. **Xu, Q. H.**, Xu, Q., Pang, Y. X., and Short, M. (2012). 'Current state of developing creep damage constitutive equation for 0.5Cr0.5Mo0.25V ferritic steel'. Advanced Materials Research, vol.: 510, pp.812-816, ISSN 1662-8985
2. **Xu, Q. H.**, Xu, Q., Pang, Y. X., and Short, M. (2013). 'Review of creep cavitation and rupture of low Cr alloy and its weldment. Advanced Materials Research, vol: 744, pp. 407-411, ISSN 1662-8985
3. **Xu Q. H.** Xu, Q., Pang, Y. X., and Short, M. (2013). 'A review of creep deformation and rupture mechanisms of low Cr-Mo alloy for the development of creep damage constitutive equations under lower stress'. In: Proceedings of the 2013 World Congress in Computer Science and Computer Engineering and Application, Nevada, USA, 22-25 July 2013, CSREA Press. ISSN 1-60132-238-0
4. Liu, D., Xu, Q., Lu, Z., Xu, D. and **Xu, Q. H.** (2013). 'The techniques in developing finite element software for creep damage analysis'. Advanced Materials Research, 744, pp. 199-204. ISSN 1662-8985
5. **Xu Q. H.**, Xu Q., Lu Z. and Barrans S. (2013). 'A review of creep deformation and rupture mechanisms of Cr-Mo alloy for the development of creep damage constitutive equations under lower stress'. Journal of Computer and Communication, vol: 10, pp.72-81, ISSN 1548-7709
6. **Xu Q. H.**, Xu Q., and Lu Z. (2013). 'The development of creep damage constitutive equation for low Cr-Mo alloy steel and its weldment at low stress'. In: 6th International 'HIDA' Conference: Life/Defect Assessment & Failures in High Temperature Plant, Nagasaki, Japan, 2-4 December 2013

# Contents

<b><u>ABSTRACT .....</u></b>	<b><u>3</u></b>
<b><u>ACKNOWLEDGEMENTS .....</u></b>	<b><u>5</u></b>
<b><u>DECLARATION .....</u></b>	<b><u>6</u></b>
<b><u>PUBLICATIONS LIST.....</u></b>	<b><u>7</u></b>
<b><u>CONTENTS .....</u></b>	<b><u>8</u></b>
<b><u>LIST OF TABLES .....</u></b>	<b><u>13</u></b>
<b><u>LIST OF FIGURES .....</u></b>	<b><u>13</u></b>
<b><u>LIST OF ABBREVIATIONS.....</u></b>	<b><u>17</u></b>
<b><u>CHAPTER 1 INTRODUCTION.....</u></b>	<b><u>18</u></b>
1.1 RESEARCH BACKGROUND .....	18
1.2 AIM AND OBJECTIVES .....	20
1.3 PROJECT APPROACH.....	21
1.4 STRUCTURE OF THE THESIS .....	23
<b><u>CHAPTER 2 BACKGROUND.....</u></b>	<b><u>25</u></b>
2.1 INTRODUCTION .....	25
2.2 CREEP BEHAVIOUR IN LOW CR ALLOYS .....	26
2.2.1 LOW CR ALLOY STEELS.....	26
2.2.2 CREEP CHARACTERISTICS IN LOW CR ALLOY STEELS .....	27
2.3 STRESS LEVEL DEFINITION.....	29
2.4 STRESS BREAKDOWN PHENOMENON .....	32
2.4.1 PREMATURE FAILURE .....	32
2.4.2 STRESS BREAKDOWN IN LOW CR ALLOYS.....	33
2.5 SUMMARY .....	36
<b><u>CHAPTER 3 LITERATURE SURVEY OF CREEP DAMAGE CONSTITUTIVE EQUATIONS.....</u></b>	<b><u>37</u></b>
3.1 INTRODUCTION .....	37
3.2 CURRENT APPROACHES TO PREDICTING CREEP FAILURE TIME.....	38

3.2.1 REVIEW OF EXISTING APPROACHES TO PREDICTING CREEP FAILURE TIME.....	38
3.2.2 PREFERENCE FOR CDM-BASED APPROACH .....	40
3.3 CLASSICAL CREEP DAMAGE CONSTITUTIVE EQUATIONS BASED ON CDM .....	41
3.3.1 REVIEW OF KACHANOV-RABOTNOV EQUATION.....	41
3.3.2 REVIEW OF DYSON’S EQUATION .....	45
3.3.3 REVIEW OF HAYHURST’S EQUATION .....	48
3.3.4 REVIEW OF XU QIANG’S EQUATION.....	50
3.3.5 REVIEW OF YIN’S EQUATION .....	51
3.4 MOTIVATIONS FOR DEVELOPING A NOVEL SET OF CREEP DAMAGE CONSTITUTIVE EQUATIONS FOR LOW CR ALLOYS.....	53
3.5 SUMMARY .....	55

**CHAPTER 4 DEVELOPMENT STRATEGY..... 56**

4.1 INTRODUCTION .....	56
4.2 GENERAL DEVELOPMENT STRATEGY .....	57
4.3 DEVELOPMENT APPROACH FOR MINIMUM CREEP RATE EQUATION.....	59
4.3.1 EXPERIMENT DATA FOR DESCRIPTION OF MINIMUM CREEP RATE .....	59
4.3.2 DEVELOPMENT OF MINIMUM CREEP RATE EQUATION.....	60
4.4 DEVELOPMENT APPROACH FOR DAMAGE EVOLUTION EQUATION AND RUPTURE CRITERION.....	60
4.4.1 EXPERIMENT DATA FOR DESCRIPTION OF THE EVOLUTION OF CREEP CAVITY .....	60
4.4.2 DEVELOPMENT OF DAMAGE EVOLUTION EQUATION AND RUPTURE CRITERION.....	61
4.5 SUMMARY .....	62

**CHAPTER 5 INVESTIGATION OF MECHANISMS FOR LOW CR ALLOYS ..... 63**

5.1 INTRODUCTION .....	63
5.2 CREEP DEFORMATION MECHANISMS .....	63
5.2.1 DEFORMATION MECHANISMS BASED ON DISLOCATION CREEP .....	65
5.2.1.1 Dislocation glide creep mechanism.....	65
5.2.1.2 Dislocation climb creep mechanism.....	67
5.2.2 DEFORMATION MECHANISMS BASED ON DIFFUSION CREEP .....	69
5.2.2.1 Nabarro-Herring creep (volume diffusion) mechanism.....	69
5.2.2.2 Coble creep (GB diffusion) mechanism .....	71
5.3 CREEP DAMAGE MECHANISMS .....	73
5.3.1 CAVITY SITE .....	73
5.3.2 CAVITY NUCLEATION MECHANISM .....	74
5.3.2.1 Cavity nucleation mechanism based on dislocation creep .....	75
5.3.2.2 Cavity nucleation mechanism based on diffusion creep .....	77
5.3.3 CGM.....	79
5.3.3.1 CGM-based on dislocation creep.....	80
5.3.3.2 CGM-based on diffusion creep.....	81
5.4 CREEP RUPTURE MECHANISMS.....	84

5.4.1 CREEP RUPTURE MECHANISMS UNDER HIGH STRESS LEVELS.....	87
5.4.2 CREEP RUPTURE MECHANISMS UNDER LOW STRESS LEVELS .....	88
5.5 SUMMARY .....	89

**CHAPTER 6 ANALYSIS OF THE EFFECTS OF STRESS LEVEL ON CREEP DAMAGE BEHAVIOUR FOR LOW CR ALLOYS..... 91**

6.1 INTRODUCTION .....	91
6.2 ANALYSIS OF THE EFFECTS OF STRESS LEVEL ON CREEP CURVE .....	92
6.2.1 TYPICAL CREEP CURVE.....	92
6.2.2 ANALYSIS OF THE EFFECTS OF STRESS LEVEL ON CREEP CURVE FOR LOW CR ALLOYS .....	93
6.3 ANALYSIS OF THE EFFECTS OF STRESS LEVEL ON CREEP PARAMETER.....	95
6.3.1 ANALYSIS OF THE EFFECTS OF STRESS LEVEL ON MINIMUM CREEP RATE .....	95
6.3.2 ANALYSIS OF THE EFFECTS OF STRESS LEVEL ON RUPTURE TIME .....	98
6.3.3 ANALYSIS OF THE EFFECTS OF STRESS LEVEL ON CREEP STRAIN AT FAILURE.....	100
6.3.4 STRESS LEVEL DEFINITION IN CREEP DAMAGE ANALYSIS OF LOW CR ALLOYS.....	101
6.4 ANALYSIS OF THE EFFECTS OF STRESS LEVEL ON CREEP CAVITY.....	102
6.4.1 EFFECT OF STRESS LEVEL ON CAVITY SHAPE.....	103
6.4.2 EFFECT OF STRESS LEVEL ON CREEP CAVITY SITE .....	104
6.4.3 CREEP CAVITY BEHAVIOUR UNDER LOW STRESS LEVELS .....	106
6.4.3.1 Cavity nucleation rate induced stress dependence under low stress level .....	108
6.4.3.2 Cavity density induced strain dependence under low stress level .....	110
6.4.4 CREEP CAVITY BEHAVIOUR UNDER HIGH STRESS LEVEL.....	110
6.4.4.1 Cavity growth rate induced stress dependence under high stress level .....	111
6.4.4.2 Cavity nucleation rate induced stress dependence under high stress level .....	112
6.5 SUMMARY .....	113

**CHAPTER 7 MINIMUM CREEP RATE AND STRESS EQUATION FOR LOW CR ALLOYS UNDER LONG-TERM SERVICE..... 114**

7.1 INTRODUCTION .....	114
7.2 INVESTIGATION OF CLASSICAL CONSTITUTIVE LAWS FOR MINIMUM CREEP RATE.....	115
7.2.1 INVESTIGATION OF THE DIFFUSION LAW .....	116
7.2.2 INVESTIGATION OF THE POWER-LAW .....	118
7.2.3 INVESTIGATION OF THE LINEAR + POWER-LAW.....	122
7.2.4 INVESTIGATION OF THE HYPERBOLIC SINE LAW .....	127
7.3 DEVELOPMENT OF A NOVEL MINIMUM CREEP RATE EQUATION.....	132
7.3.1 DATA FITTING METHOD FOR DETERMINATION OF THE CONSTANTS IN THE CONSTITUTIVE EQUATIONS.....	132
7.3.2 INVESTIGATION OF THE EFFECTS OF PARAMETER A ON MINIMUM CREEP RATE .....	137
7.3.3 INVESTIGATION OF THE EFFECTS OF PARAMETER B ON MINIMUM CREEP RATE .....	138

7.3.4 INVESTIGATION OF THE EFFECTS OF STRESS EXPONENT ON MINIMUM CREEP RATE .....	140
7.4 VALIDATION OF THE NEWLY DEVELOPED MINIMUM CREEP RATE EQUATION.....	141
7.4.1 VALIDATION OF THE NEWLY DEVELOPED MINIMUM CREEP RATE EQUATION BASED ON 2.25Cr-1Mo STEEL EXPERIMENT TEST.....	141
7.4.2 VALIDATION OF THE NEWLY DEVELOPED MINIMUM CREEP RATE EQUATION BASED ON 1Cr-1Mo-1V STEEL EXPERIMENT TEST .....	145
7.5 SUMMARY .....	148

**CHAPTER 8 DAMAGE EVOLUTION EQUATION AND RUPTURE CRITERION FOR LOW CR ALLOYS UNDER LONG-TERM SERVICE .....** 150

8.1 INTRODUCTION .....	150
8.2 INVESTIGATION OF THE EVOLUTION OF CREEP CAVITY DURING RUPTURE PROCESS .	151
8.2.1 CREEP CAVITY AT INITIAL DAMAGE TIME .....	151
8.2.2 CREEP CAVITY AT RUPTURE TIME .....	153
8.2.3 DISCUSSION .....	156
8.3 DESIGN OF THE RUPTURE CRITERION FOR CONSTITUTIVE EQUATION .....	158
8.3.1 INVESTIGATION OF THE TYPICAL CREEP RUPTURE CRITERION .....	158
8.3.2 NEW PHYSICALLY-BASED CREEP RUPTURE CRITERION .....	159
8.4 DEVELOPMENT AND VALIDATION OF NEW DAMAGE EVOLUTION EQUATION.....	162
8.4.1 DEVELOPMENT OF NEW DAMAGE EVOLUTION EQUATION .....	162
8.4.2 VALIDATION OF NEW DAMAGE EVOLUTION EQUATION.....	164
8.5 SUMMARY .....	167

**CHAPTER 9 IMPLEMENTATION AND VERIFICATION OF CREEP DAMAGE CONSTITUTIVE EQUATIONS FOR CREEP DAMAGE ANALYSIS.....** 169

9.1 INTRODUCTION .....	169
9.2 IMPLEMENTATION OF THE NEWLY DEVELOPED MINIMUM CREEP RATE EQUATION AND DAMAGE EVOLUTION EQUATION INTO CONSTITUTIVE EQUATIONS .....	169
9.3 VERIFICATION OF THE NEW CONSTITUTIVE EQUATIONS BY COMPARING WITH RESULTS FROM THE RESPECTED KACHANOV-RABOTNOV CONSTITUTIVE EQUATIONS AND EXPERIMENT DATA .....	171
9.4 VERIFICATION OF THE NEW CONSTITUTIVE EQUATIONS VIA EXTENSION OF THE LOW STRESS LEVEL TO INTERMEDIATE STRESS LEVEL .....	175
9.5 SUMMARY .....	177

**CHAPTER 10 CONCLUSION AND FUTURE WORK.....** 178

10.1 CONTRIBUTIONS AND CONCLUSIONS .....	178
10.1.1 BACKGROUND OF LOW CR ALLOYS IN HIGH TEMPERATURE INDUSTRIES .....	178
10.1.2 LITERATURE SURVEY OF CLASSICAL CREEP DAMAGE CONSTITUTIVE EQUATIONS .....	179

<b>10.1.3 DEVELOPMENT STRATEGY IN DEVELOPING CREEP DAMAGE CONSTITUTIVE EQUATIONS .....</b>	<b>179</b>
<b>10.1.4 INVESTIGATION OF CREEP MECHANISMS FOR LOW Cr ALLOYS.....</b>	<b>180</b>
<b>10.1.5 ANALYSIS OF THE EFFECTS OF STRESS LEVEL ON CREEP BEHAVIOUR FOR LOW Cr ALLOYS .....</b>	<b>181</b>
<b>10.1.6 NEW CONSTITUTIVE EQUATION TO DEPICT RELATIONSHIP BETWEEN MINIMUM CREEP RATE AND STRESS.....</b>	<b>182</b>
<b>10.1.7 NEW CONSTITUTIVE EQUATION TO DEPICT RELATIONSHIP BETWEEN DAMAGE EVOLUTION AND RUPTURE CRITERION.....</b>	<b>182</b>
<b>10.1.8 IMPLEMENTATION AND VERIFICATION OF CREEP CONSTITUTIVE EQUATIONS FOR LOW Cr ALLOYS .....</b>	<b>183</b>
<b>10.2 FUTURE WORK.....</b>	<b>183</b>
<b><u>REFERENCES.....</u></b>	<b><u>185</u></b>

# List of Tables

Table 2.1: Review of existing stress level definition methods.....	30
Table 3.1: Existing approaches to predicting creep failure time.....	38
Table 4.1: Physically-based experiment data for developing minimum creep rate equation....	59
Table 4.2: Experiment data for developing damage evolution equation and rupture criterion .....	61
Table 6.1: Stress level definitions involved in developing constitutive equations for low Cr alloys .....	101
Table 6.2: Creep cavity site under different stress levels for low Cr alloys .....	105
Table 6.3: Initiation time for development of cavitation process.....	108
Table 6.4: Summary of stress index for power-law behaviour under low stress.....	109
Table 6.5: Cavity growth rate versus stress in low Cr-Mo alloy under high stress (Rediel, 1987) .....	111
Table 6.6: Summary of stress index for power law behaviour under high stress .....	112
Table 7.1: Typical well-known constitutive laws for minimum creep rate.....	116
Table 7.2: Material parameters under the diffusion law.....	117
Table 7.3: Material parameters under the power-law .....	119
Table 7.4: Stress exponents under the power-law .....	120
Table 7.5: Material parameters under the diffusion + power-law .....	123
Table 7.6: Stress exponents under the linear + power-law.....	125
Table 7.7: Parameter B under the diffusion + power-law .....	126
Table 7.8: Parameter A under the hyperbolic sine law .....	128
Table 7.9: Parameter B under the hyperbolic sine law .....	130
Table 7.10: Parameter A in newly designed constitutive equation .....	137
Table 7.11: Parameter B in newly designed constitutive equation .....	139
Table 7.12: Stress exponent parameters in newly designed constitutive equation.....	140
Table 7.13: Material parameters in newly developed constitutive equation for 2.25Cr-1Mo steel .....	142
Table 7.14: Material parameters in conventional sine law for 2.25Cr-1Mo steel.....	143
Table 7.15: Material parameters in newly developed constitutive equation for 0.5Cr-0.5Mo-0.25V steel .....	145
Table 7.16: Material parameters in conventional sinh law for 0.5Cr-0.5Mo-0.25V steel .....	146
Table 8.1: Evolution of creep cavities in 1Cr-0.5Mo steel .....	157
Table 8.2: Summary of typical rupture criteria for low Cr alloy creep damage constitutive equations .....	158
Table 8.3: Material parameters in validating newly developed damage evolution equation for 0.5Cr-0.5Mo-0.25V base material (Dyson and Osgerby, 1993) .....	164
Table 9.1: Material parameters in Kachanov-Rabotnov constitutive equations for 0.5Cr-0.5Mo-0.25V base material.....	171
Table 9.2: Material parameters in newly developed constitutive equations for 0.5Cr-0.5Mo-0.25V base material.....	173
Table 9.3: Material parameters in newly developed constitutive equations for 0.5Cr-0.5Mo-0.25V base material at the stress 54MPa.....	176

# List of Figures

Figure 2.1: General schematic diagram of creep curve for low Cr alloys .....	28
Figure 2.2: Stress versus time to rupture at 450, 500, 600 and 650 °C for quenched and tempered 2.25Cr-1Mo steel plates (M/CDS/No. 36B/2003, 2003) .....	34
Figure 2.3: Fracture mechanism map under different stress levels (Lee et al., 2006) .....	35
Figure 5.1: Schematic diagram of creep deformation mechanism map (Riedel, 1987) .....	64
Figure 5.2: Schematic diagram of dislocation glide creep mechanism .....	66
Figure 5.3: Schematic diagram of dislocation climb creep .....	68
Figure 5.4: Schematic diagram of volume diffusion creep.....	70
Figure 5.5: Schematic diagram of GB diffusion .....	72
Figure 5.6 Schematic diagram of the formation and condensation of vacancy on GB under the dislocation process .....	76
Figure 5.7: Schematic diagram of how dislocation creep influences the cavity nucleation associated with carbides or particles .....	77
Figure 5.8: Schematic diagram of the formation and condensation of vacancy on GB under the diffusion process.....	78
Figure 5.9: Schematic diagram of the generation of cavity nucleation associated with particles caused by GB sliding.....	79
Figure 5.10: Schematic diagram of the effect of dislocation creep on cavity growth associated with the triple point.....	80
Figure 5.11: Schematic diagram of the effect of diffusion creep on cavity growth .....	82
Figure 5.12: Schematic diagram of the effect of GB sliding on cavity growth at GB.....	83
Figure 5.13: Schematic diagram of the effect of GB sliding on cavity growth at triple junction.....	83
Figure 5.14: Schematic diagram of the effect of cavity nucleation on creep fracture .....	85
Figure 5.15: Schematic diagram of the effect of cavity growth on creep fracture .....	85
Figure 5.16: Schematic diagram of creep fracture mechanism map (Riedel, 1987) .....	86
Figure 6.1: The typical creep curve (Viswanathan, 1989) .....	93
Figure 6.2: Creep curves under the stresses 40MPa ( $0.31\sigma_Y$ ), 54MPa ( $0.42\sigma_Y$ ) and 70MPa ( $0.54\sigma_Y$ ) at 640 °C for 0.5Cr-0.5Mo-0.25V steel .....	94
Figure 6.3: Schematic diagram of stress dependence of steady-state creep rate (Yavari and Langdon, 1982).....	96
Figure 6.4: Log-log plot of stress versus minimum creep rate for low Cr alloys.....	97
Figure 6.5: Log-log plot of stress versus creep rupture time for low Cr alloys .....	99
Figure 6.6: Relationship between creep strain at failure and stress levels for low Cr alloys..	100
Figure 6.7: Wedge shape creep cavities in 0.5Cr-0.5Mo-0.25V steel under constant stress 110MPa ( $0.55\sigma_Y$ ) at 600 °C (Singh and Kamaraj, 2009).....	103

Figure 6.8: Round shape creep cavities in 1Cr-0.5Mo steel under constant stress 35MPa (0.22 $\sigma_Y$ ) at 520°C (Dobrzański et al., 2006) .....	104
Figure 6.9: Typical damage microstructures associated with the typical curve reflecting dominant creep damage processes (cavitation) with typical creep curve for low Cr-Mo alloy steel at low stresses (0.2~0.4 $\sigma_Y$ ).....	107
Figure 7.1: Log-log plot of stress versus minimum creep rate based on experiment data.....	115
Figure 7.2: Log-log plot of material parameter versus minimum creep rate under the diffusion law .....	118
Figure 7.3: Log-log plot of material parameter versus minimum creep rate under the power-law.....	120
Figure 7.4: Log-log plot of stress exponent versus minimum creep rate under the power-law.....	121
Figure 7.5: Log-log plot of material parameter versus minimum creep rate under the linear + power-law.....	124
Figure 7.6: Log-log plot of stress exponent versus minimum creep rate under the linear + power-law.....	125
Figure 7.7: Log-log plot of parameter B versus minimum creep rate under the linear + power-law.....	126
Figure 7.8: Log-log plot of parameter A versus minimum creep rate under the hyperbolic sine law .....	129
Figure 7.9: Log-log plot of parameter B versus minimum creep rate under the hyperbolic sine law .....	130
Figure 7.10: Comparison of hyperbolic sine law and experiment data.....	131
Figure 7.11 General flow chart of the optimization process for determination of material constants (Iguar and Xu, 2015).....	136
Figure 7.12: Log-log plot of parameter A versus minimum creep rate using newly designed constitutive equation .....	138
Figure 7.13: Log-log plot of parameter B versus minimum creep rate using newly designed constitutive equation .....	139
Figure 7.14: Log-log plot of stress exponent versus minimum creep rate in newly designed constitutive equation .....	140
Figure 7.15: Comparison of newly developed constitutive equation with experiment data for 2.25Cr-1Mo steel .....	142
Figure 7.16: Comparison of conventional sinh law with experiment data for 2.25Cr-1Mo steel.....	143
Figure 7.17: Comparison of the conventional sinh law with newly designed constitutive equation for 2.25Cr-1Mo steel .....	144
Figure 7.18: Comparison of newly developed constitutive equation with experiment data for 0.5Cr-0.5Mo-0.25V steel .....	146

Figure 7.19: Comparison of conventional sinh law with experiment data for 0.5Cr-0.5Mo-0.25V steel .....	147
Figure 7.20: Comparison of conventional sinh law with newly designed constitutive equation for 0.5Cr-0.5Mo-0.25V steel.....	148
Figure 8.1: Cavity at initial damage stage of 1Cr-0.5Mo steel under stress range from 35MPa at temperature of 520°C (Dobrzański et al., 2006) .....	151
Figure 8.2: Cavity semi-axis schematic diagram .....	152
Figure 8.3: Radii of initial cavities of 1Cr-0.5Mo steel in semi-minor axis .....	152
Figure 8.4: Radii of initial cavities of 1Cr-0.5Mo steel in semi-major axis .....	153
Figure 8.5: Cavities at coalescence stage of 1Cr-0.5Mo steel under stress range from 35MPa at temperature of 520°C (Dobrzański et al., 2006) .....	154
Figure 8.6: Schematic diagram of cavity linkup behaviour at rupture stage (Westwood et al., 2004) .....	154
Figure 8.7: Radii of cavities of 1Cr-0.5Mo steel in semi-minor axis at rupture time .....	155
Figure 8.8: Radii of cavities of 1Cr-0.5Mo steel in semi-major axis at rupture time .....	156
Figure 8.9: Area fraction of cavitation versus time for 2.25Cr-1Mo under the stresses 55.6MPa, 60.6MPa and 70.6MPa at temperature of 565°C .....	160
Figure 8.10: Area fraction of cavitation at rupture time versus stress for 2.25Cr-1Mo under the stresses 55.6MPa, 60.6MPa and 70.6MPa at temperature of 565°C, and assumption of the area fraction of cavitation at 600°C and 640°C .....	161
Figure 8.11: Comparison of Dyson's damage evolution equation with experiment data for 0.5Cr-0.5Mo-0.25V base material.....	165
Figure 8.12: Comparison of newly developed damage evolution equation with the experiment data for 0.5Cr-0.5Mo-0.25V base material .....	166
Figure 8.13: Comparison of newly developed damage evolution equation with Dyson's damage evolution equation for 0.5Cr-0.5Mo-0.25V base material.....	167
Figure 9.1: Comparison of creep strain predicted by Kachanov-Rabotnov constitutive equations and experiment data for 0.5Cr-0.5Mo-0.25V base material.....	172
Figure 9.2: Comparison of initial creep strain predicted by Kachanov-Rabotnov constitutive equations and experiment data for 0.5Cr-0.5Mo-0.25V base material.....	173
Figure 9.3: Comparison of creep strain predicted by new constitutive equations and experiment data for 0.5Cr-0.5Mo-0.25V base material .....	174
Figure 9.4: Comparison of initial creep strain predicted by new constitutive equations and experiment data for 0.5Cr-0.5Mo-0.25V base material .....	175
Figure 9.5: Comparison of creep strain predicted by new constitutive equations and experiment data for 0.5Cr-0.5Mo-0.25V base material under intermediate stress level and low stress level.....	176

## List of Abbreviations

CDM	Continuum Damage Mechanics
CEGB	Central Electricity Generating Board
CGM	Cavity Growth Mechanism
CPT	Classical Plastic Theory
ECCC	European Creep Collaborative Committee
EPRI	Electric Power Research Institute
ETD	European Technology Development Ltd
GB	Grain Boundary
GCC	German Creep Committee
TEM	Transmission Electron Microscopy
TTP	Time-Temperature-Parameter
NIMS	National Research Institute for Metals
NPL	National Physical Laboratory
UMIST	University of Manchester Institute of Science and Technology

# Chapter 1 Introduction

## 1.1 Research background

Creep damage is a time dependent behaviour which occurs with components operating under high temperatures (over  $1/3T_m$ , where  $T_m$  is the melting temperature) (Finnie and Heller, 1959). Creep damage behaviour plays a dominant role in fields involving structural components at high temperature, and it leads to the final rupture of such components. The fields where creep damage has been of importance in the interpretation of structural response are the design and construction of nuclear power plants, gas turbine engines, refining and chemical plants (Gooch, 2003; Shibli et al., 2005; Abe et al., 2008). In the nuclear industry, low Cr alloy steels have been widely utilized in the construction of steam pipes, turbine generators and reactor pumps, etc. These low Cr alloy steels are often operated in conditions under stress ranges from 25MPa to 60MPa and high temperature ranges from 400°C to 700°C, and the dominant failure mechanism of this type of steel is creep damage (Shibli and Holdsworth, 2009; Wilshire and Bache, 2009; Whittaker and Wilshire, 2013).

In recent decades, creep damage behaviour has caused significant safety and economic problems. For instance, in 1996 the creep failure of a steam pipe (SH link piping) utilized by the Mt. Storm company caused a serious explosion (Rodgers and Tilley, 1999). In order to meet both design safety and economic requirements, it is essential to understand and predict the rupture lifetime and damage evolution of structural components that are operated under long-term service. It is notable that numerous research institutes (such as the Electric Power Research Institute (EPRI), European Creep Collaborative Committee (ECCC), National Institute for Material Science (NIMS), European Technology Development Ltd (ETD), National Physical Laboratory (NPL), University of Manchester Institute of Science and Technology (UMIST), and Central Electricity Generating Board (CEGB)) have utilized either creep damage constitutive equations or experimental methods to describe creep damage behaviour in structural

components (Martin and Leckie, 1972; Lonsdale and Flewitt, 1979; Dyson and Osgerby, 1993; Perrin and Hayhurst, 1996; Dyson and McLean, 2001; Yin and Faulkner, 2006; Abe et al., 2008; Shibli and Holdsworth, 2009). However, some deficiencies still exist and such deficiencies can be outlined as follows:

- 1) Only a few creep damage constitutive equations are designed to predict the lifetime and creep rupture behaviour for structural materials at high temperature. Furthermore, those constitutive equations are mostly proposed based on experimental data for materials under high stress levels. For a low stress level, the computational capability to determine a current state is extrapolated from those constitutive equations by simply using a power-law or sinh law. However, experimental observation has shown that this method is not satisfactory because the damage mechanisms under a high stress level are different from those of a low stress level (Evans, 1984; Viswanathan, 1989; Abe et al., 2008). To date, no constitutive equations have been specifically designed for low Cr alloys under low stress levels.
- 2) The relationship between minimum creep rate and stress is unclear in describing creep behaviour for low Cr alloy steels under a low stress level. The minimum creep rate represents a vital role in the development of creep damage constitutive equations because this parameter influences almost 70% of the creep deformation process at low stress levels (Viswanathan, 1989; Shibli et al., 2005; Abe et al., 2008). Thus, the creep deformation process, particularly at the tertiary creep stage, cannot be accurately modelled.
- 3) The relationship between cavitation and creep damage is still bewildering in the investigation of creep damage behaviour for low Cr alloy steels under low stress levels, yet the evolution of cavity is a dominant factor in accurately describing the accumulation of creep damage and final rupture. As a result, the lack of an accurate rupture criterion has a significant influence on the prediction of

creep rupture time for low Cr alloy steels under low stress conditions.

Therefore, the development of a novel set of creep damage constitutive equations should be considered in order to predict long-term rupture lifetime and describe the creep deformation and damage behaviour of low Cr alloys. Due to open international cooperation, there is a large amount of up-to-date experimental creep data from multiple sources at various time points that can be employed in the development of constitutive equations to describe creep deformation and creep damage. With authoritative permission to use these experimental data, the possible development of a new set of creep damage constitutive equations, specifically designed for low Cr alloys under long-term service, could be achieved. The experimental creep data used in this project are predominantly from studies carried out by research institutes such as EPRI, ECCC, NIMS, ETD, NPL and CEGB.

## **1.2 Aim and objectives**

The aim of this project was to develop a new set of creep damage constitutive equations for low Cr alloy steels under low stress levels. These constitutive equations should be able to describe how the microstructure develops during creep processes and how stress level influences creep damage. In order to achieve this aim, there were several objectives:

- To provide a critical investigation of current issues relating to the application of low Cr alloys at high temperatures under long-term industrial service.
- To provide a critical literature review of the performance of existing creep damage constitutive equations in modelling the creep behaviour of low Cr alloys.
- To provide an integrated development strategy to develop creep damage constitutive equations for creep damage analysis of low Cr alloy steels under long-term service.

- To provide a unified knowledge acquisition and knowledge representation mechanism to retrieve and organize knowledge from various creep damage documents.
- To provide a critical analysis of the effects of stress level on the creep damage behaviour of low Cr alloys under long-term service.
- To develop a new physically-based constitutive equation to describe the relationship between minimum creep rate and stress.
- To provide a new, physically-based damage evolution equation and rupture criterion to evaluate creep rupture behaviour.
- To implement the newly developed constitutive equations in combination with existing constitutive equations for creep damage analysis.
- To validate the newly developed constitutive equations for low Cr alloys under a low stress level.

### **1.3 Project approach**

This project started with an extensive review of state-of-the-art literature on current issues regarding the application of low Cr alloys, knowledge-based stress breakdown phenomena and the current state of classical creep damage constitutive equations for low alloy steels. Based upon the domain research outlined in the literature review, the development of creep damage constitutive equations for low alloy steels used the following development processes:

#### **1) Development strategy design**

The overall project development strategy was produced taking into account all aspects of problem domains and the requirements involved in developing constitutive equations for creep damage analysis of low alloy steels. To address the aim and the objectives highlighted in Section 1.2, this research was conducted to develop creep damage constitutive equations based on CDM. The development approaches for the minimum creep rate equation, damage evolution equation and

rupture criterion were designed within the CDM framework. The main advantage of using CDM is that the physical mechanisms of material deformation and deterioration can be represented by explicit state variables (Dyson, 2000).

## **2) Proving validity**

Proposed approaches or schemes must be proven to be appropriate to address the proposed aim and objectives. The correctness of the development of creep damage constitutive equations is demonstrated by the investigation of creep mechanisms and analysis of the effects of stress level on creep behaviour. The validity of the proposed scheme for developing creep damage constitutive equations is thus proven by the use of a strict mathematical method.

## **3) Creep data analysis**

The creep data of low alloy steels under long-term service were analysed. A new constitutive equation to describe the relationship between minimum creep rate and stress was proposed, based on the analysis of creep data for low Cr alloys under low stress levels. Furthermore, the creep data for cavity nucleation and growth were analysed, and then a damage evaluation constitutive equation designed to depict the relationship between cavity and creep damage was proposed. Finally, a new rupture criterion was proposed based on the analysis of experimental data on the evolution of creep cavity during the rupture process for low alloy steels.

## **4) Testing and evaluation**

The proposed constitutive equations have been strictly tested and verified to evaluate their performance and accuracy through comparison with existing experimental creep data. The tests mainly focused on proving the correctness and functionality of the proposed constitutive equations. In this research, testing and evaluations were mainly undertaken at a low stress level to determine performance under long-term service conditions. It was understood that further

revisions of the proposed constitutive equations might be required based on the outcome of these tests and evaluations.

## **5) Prototype implementation**

A prototype for a set of creep damage constitutive equations was developed by the integration of a creep rate equation, hardening rate equation, particle rate equation and damage evolution equation. This facilitated the refinement and completion of the approaches and schemes, and led to an improved understanding of some implementation issues. The implementation also served as a demonstration of the capabilities of the final constitutive equations through feedback from various tests.

## **1.4 Structure of the thesis**

Chapter 1 has introduced the need for computational capability in creep damage analysis and provided the justification for the development of a set of creep damage constitutive equations to describe the creep damage behaviour of low Cr alloys under long-term service. The aim and objectives of this project have been described, followed by a summary of the project approach. An explanation of the thesis structure is also presented.

Chapter 2 reports the background knowledge relative to the application of low Cr alloys in high temperature industry. The contents of this chapter mainly focus on the creep characteristics of low Cr alloys, the method of stress definition and the stress breakdown phenomenon.

Chapter 3 provides a literature review regarding the performance of existing creep damage constitutive equations in modelling the creep behaviour of low Cr alloys. Current approaches and the effectiveness of existing creep damage constitutive equations in predicting creep failure time are presented. The specific areas which need to be enhanced in developing constitutive equations for low Cr alloys are reported.

Chapter 4 presents the development strategy for the proposed constitutive equations. An integrated development strategy, involving seven

development stages to provide creep damage constitutive equations for low Cr alloys, is proposed. The development approach for the constitutive equation to depict the minimum creep rate under different stress regions, and that for the constitutive equation to depict creep damage and rupture time under the different creep stages, are detailed.

Chapter 5 presents the investigation of mechanisms in creep damage analysis of low Cr alloys. A critical consideration of which mechanism is dominative in the process of creep is presented, covering the mechanisms of creep deformation, damage, rupture behaviour and creep failure.

Chapter 6 presents a critical analysis of the effects of stress level on creep behaviour for low Cr alloys. A critical discussion of the effects of stress level on creep damage constitutive equations is presented, which covers the effects of stress level on creep curve, creep parameter and creep cavitation.

Chapter 7 presents the development of a constitutive equation to depict the relationship between minimum creep rate and stress level. The classical constitutive laws for depicting the relationship between minimum creep rate and stress are firstly investigated; then, the development and validation of a new minimum creep rate constitutive equation are demonstrated.

Chapter 8 presents the development of the damage evolution equation and the rupture criterion for creep analysis of low Cr alloys. The evolution of creep cavity during rupture process is firstly investigated; then, the development and validation of a new damage evolution equation and rupture criterion are presented.

Chapter 9 provides the implementation and verification of creep constitutive equations for low Cr alloys. The new minimum creep rate equation and damage evolution equation are implemented firstly, followed by verification of the integrated constitutive equations.

Chapter 10 focuses on a summary of this research and its contribution to knowledge; this is followed by suggestions for future work.

# Chapter 2 Background

## 2.1 Introduction

High temperature creep of structural components has been of interest to scientists and engineers for over 100 years. Demands for thermal efficiency have led to an increase in the operating temperature of structural components, so that such components suffer more severe creep deformation and damage resulting in final rupture. In the past few decades, some research institutes such as those of EPRI (Viswanathan, 1989), NPL (Dyson and Osgerby, 1993) and ECCC (Shibli and Holdsworth, 2009) have reported the development of creep damage constitutive equations to depict creep deformation and creep rupture. However, the definition of stress levels is still vague and the stress breakdown phenomenon has not been considered in the development of constitutive equations for creep damage analysis of low Cr alloys. This chapter focuses on introducing and explaining this domain of knowledge and thus provides the background for this research.

The specific knowledge explored in detail within this chapter includes the following areas of enquiry:

- 1) To understand the creep behaviours in low Cr alloys. Three creep deformation stages (primary, secondary and tertiary stages) involved with the mechanical properties of low Cr alloys are studied in order to understand the creep-resistant performance of low Cr alloys at elevated temperatures.
- 2) To investigate stress level definition. Existing stress level definition methods are investigated in order to understand the current state of stress level definition in the development of creep damage constitutive equations.
- 3) To investigate the stress breakdown phenomenon. The premature failure phenomenon is first introduced and then the issue of stress breakdown in low Cr alloys is investigated.

## **2.2 Creep behaviour in low Cr alloys**

Considerable attention has recently been paid to the creep failure of low alloy steels under long-term service at elevated temperatures, and a number of researchers have evaluated creep behaviour through investigation of three creep deformation stages (primary, secondary and tertiary stage) related to the mechanical properties of low Cr alloys (Parker, 1995; Perrin and Hayhurst, 1999; Tu et al., 2004; Vakili et al., 2005; Maharaj et al., 2009; Kassner, 2015). To address this research, it is necessary to interpret creep properties at the different creep stages in order to develop physically-based constitutive equations for depicting the evolution of creep damage behaviour in low Cr alloys.

### **2.2.1 Low Cr alloy steels**

Creep is a time-dependent inelastic deformation; in creep tests, it occurs when a material is subjected to a constant stress at constant temperature (Hult, 1966). Especially at elevated temperatures, this behaviour plays an important role in the fracture mechanism of metallic materials in engineering applications. Creep resistance is significantly influenced by the mechanical properties of the structural components.

Low Cr alloy steels exhibit a good performance in creep resistance. Various microstructures can be developed by the utilization of low Cr alloy; for example, T/P22 steel can enable different combinations of properties for various extreme environments in advanced nuclear systems (Boyle and Spence, 2013).

The properties which make low Cr alloy steels appropriate for high temperature applications in industry can be summarised as:

- The low alloy content makes them relatively inexpensive and most low alloy steels are readily weldable.
- Low alloy steels are usually tough and corrosion resistant at high temperatures.

- Low alloy steels exhibit excellent creep resistance in the temperature range 400°C to 700°C.

Low Cr alloys are widely utilized in structural components such as steam pipes, turbine generators and reactor pumps in nuclear power plants. Nuclear power generates almost one sixth of the United Kingdom's electricity by using 16 operational nuclear reactors at nine plants (Adamantiades and Kessides, 2009). On the present nuclear closure trajectory, there are four nuclear reactors which will reach the end of their nominal 30-year-design lifetimes by 2023. However, the operating lives of nuclear reactors can usually be extended with additional investment in reactor maintenance upgrades. For example, in 2012, EDF announced that it expected seven-year life extensions on average across all advanced gas-cooled reactors and twenty-year life extensions on a pressurized water reactor (Zinkle and Was, 2013). To meet both safety and economic requirements, lifetime assessments are required for low Cr alloy structural components operating at high temperatures.

The dominant mechanism of material deformation and fracture in nuclear power plants can be observed from creep-tested specimens. Having identified the dominant creep mechanisms, the correct physically-based creep damage constitutive equation can be used in structural calculations.

### **2.2.2 Creep characteristics in low Cr alloy steels**

The characteristics of creep deformation behaviour at different creep stages can generally be described by typical creep curves. Based on the studies of Frost and Ashby (1982), Nabarro and Villiers (1995) and Hyde et al. (2013), a general schematic diagram of the creep curve for low Cr alloys can be plotted.

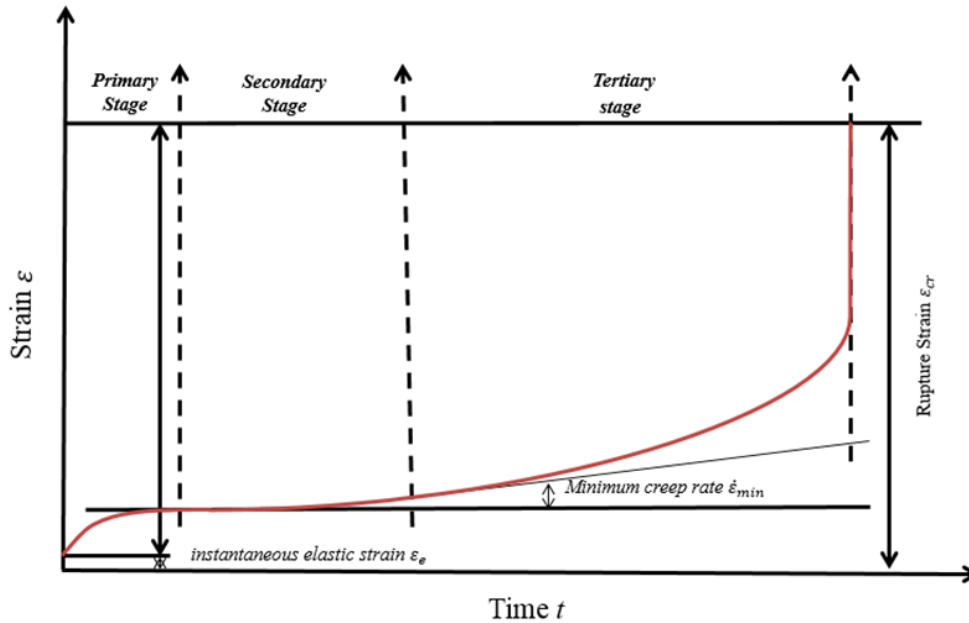


Figure 2.1: General schematic diagram of creep curve for low Cr alloys

Figure 2.1 shows the general creep curve for low Cr alloys. The process of creep behaviour can be divided into three particular stages: non-stationary or primary creep stage; steady-state or secondary creep stage; and accelerated or tertiary creep stage. They correspond to the decrease, constancy and increase in creep rate, respectively (Hyde et al., 2013). The primary and secondary creep stages are usually analysed within the framework of the creep deformation process, and the tertiary stage is strongly associated with the creep damage and final rupture process. The characteristics of creep behaviour at the different creep stages can be summarised as follows:

- a) Primary creep: primary creep takes place at the very beginning of the creep test and is characterized first by a high strain rate, which then decelerates to a constant value denoting the beginning of secondary creep (Souni, 2000). In the primary creep stage, there is competition between time-dependent strain hardening and creep recovery. Unloading in the primary creep process leads to substantial creep recovery, and higher primary creep strains lead to higher recoverable strains (Frost and Ashby, 1982). Two experiential laws, which are logarithmic creep (Mott, 1951) and Andrade creep (Berry, 1976), are usually adopted in the analysis of primary creep. Primary creep is

usually logarithmic at a low stress level and Andrade at high stress level (Cottrell, 1997).

- b) Secondary creep: secondary creep takes place after primary creep and is typified by an approximate constant strain rate (Frost and Ashby, 1982). The creep behaviour of metals and alloys is most commonly analysed in terms of steady state creep, where the dependence of the steady state creep rate on stress and temperature is described using different analytical or empirical approaches such those of Nabarro (1967), Frost and Ashby (1982), Viswanathan (1989), Shibli et al. (2005) and Abe et al. (2008). In the secondary creep stage, the strain hardening rate is balanced by the rate of creep recovery, which is by gliding softening at low temperatures with cross-slip as the main cause, or by climb softening at higher temperatures (Frost and Ashby, 1982). Dislocation flow creep and diffusional flow creep can contribute to creep deformation in secondary creep stage.
- c) Tertiary creep: tertiary creep occurs after secondary creep, and this is where failure takes place (Kouichi et al., 2001). In the tertiary creep stage, the strain rate exponentially increases with stress because of the necking phenomenon (Parker, 1995). Furthermore, the increase of creep rate is also caused by metallurgical changes such as recrystallization and the increase of stress as the area is reduced, either by the thinning of a specimen under constant load, or by internal fracture or the nucleation of a creep cavity (Goldhoff and Woodford, 1972).

### **2.3 Stress level definition**

The need for stress level definition was initially brought about by the development of creep damage constitutive equations in the latter half of the 20<sup>th</sup> century. Notably, Sherby and Burke (1968) proposed that a steady state creep rate can exhibit a variety of stress-dependent behaviour, and that stress sensitivity varies widely between high and low stress levels. Furthermore, extensive studies (Frost and Ashby, 1982; Riedel, 1987; Nabarro and Villiers, 1995; Hyde et al., 2013; Kassner, 2015) have shown

that applied stress provides a driving force for the movement of atoms. As the stress is increased, the rate of deformation also increases. In general, it can be illustrated by the power-law creep:

$$\dot{\varepsilon}_{min} = A\sigma^n \quad (2.1)$$

where  $A$  is a temperature-dependent material parameter,  $\sigma$  is the applied stress and  $n$  is the stress exponent. Prediction of the value of  $n$  is dependent on which mechanism of creep is in operation. As the stress is varied, the changing value of  $n$  can conveniently represent the changing stress dependence.

Approaches to stress level definition have typically been to divide stresses into a high stress level and low stress level (Hayhurst, 1972; Petry and Lindet, 2009; Bueno and Sobrinho, 2012). However, Chen et al. (2012) suggest that an intermediate stress level, between the high stress and low stress levels, should be considered; they also propose the concept of the intermediate stress level for creep damage analysis of high Cr alloys.

In order to define the stress levels for the development of new creep damage constitutive equations for low Cr alloys under long-term service, the existing stress level definition methods have been reviewed and presented in Table 2.1.

Table 2.1: Review of existing stress level definition methods

Method & authors	Stress level definition	Characteristics and comments
The constant stress dependence method: the constant stress $\sigma = A(MPa)$ (Chen et al., 2012)	<p>High stress level: <math>&gt;110(MPa)</math></p> <p>Intermediate stress level: <math>70-110(MPa)</math></p> <p>Low stress level: <math>\leq 70(MPa)</math></p>	<p>This method is simple and easy to operate; however, it can only be utilized in relation to specific high Cr alloys, temperatures and particular heat treatment materials.</p> <p>At extremely low stresses, the value of <math>n = 1</math>. At intermediate stresses, values of <math>n</math> range from 4.2 to 6.9 in annealed metals and unique alloys. At high stress levels, the exponential creep laws are utilized to define the value of <math>n</math>.</p>

<p>The yield stress dependence method: the applied stress divided by yield stress <math>\frac{\sigma}{\sigma_y}</math> (Hayhurst, 1972)</p>	<p>High stress level: <math>\geq 0.4</math></p> <p>Low stress level: 0.2-0.4</p>	<p>This method can be utilized with a wide range of temperatures and materials. The yield stress varies with temperature and should be defined at different temperatures.</p> <p>The range of ratio is defined from 0 to 1.</p> <p>The intermediate stress level has not been considered in this modified stress dependence method.</p>
<p>The parameter dependence method: the applied stress divided by Young's modulus <math>\frac{\sigma}{E}</math> (Bueno and Sobrinho, 2012)</p>	<p>High stress level: <math>&gt; 6 \times 10^{-5}</math></p> <p>Low stress level: <math>&lt; 6 \times 10^{-5}</math></p>	<p>Young's modulus of a material should have an effect on secondary creep rate, since the stress field around any obstacle to dislocation motion increases with Young's modulus (Robin, 1978). The creep rate is independent of grain size.</p> <p>The intermediate and high stress levels have not been considered and this method can only be utilized with specific temperatures.</p>
<p>The strain dependence method: the constant strain at failure <math>\epsilon_f = A</math> (Petry and Lindet, 2009)</p>	<p>High stress level: <math>&gt; 10\%</math></p> <p>Low stress level: <math>\leq 5\%</math></p>	<p>The intermediate and high stress levels have not been considered. The time to reach 10% strain is considered an accurate prediction of the time-to-rupture. As the applied stress decreases, the model progressively tends to overestimate times to rupture, this effect being more pronounced as temperature increases.</p> <p>This method can only be utilized with specific temperatures.</p>

Table 2.1 has summarised the current state of stress level definition methods. The characteristics of each method have been commented on. From the comparison of stress level definition methods in Table 2.1, it is clear that the yield stress dependence method exhibits an obvious advantage in creep damage analysis at a wide temperature range. However, the limitation of the current yield stress dependence method is that the intermediate stress level has not been defined (Hayhurst, 1972). According to Garofalo (1963), at extremely low stresses, diffusion creep is

a dominant mechanism involving stress-directed atomic migration, while at a high stress level, creep rate is much greater than that predicted by extrapolation of intermediate stress data, and the exponent  $n$  is increased rapidly with stress. The constant stress dependence method proposed by Chen et al. (2012) defines the intermediate stress level, but the main disadvantage of the use of this method is the limited temperature and material property range.

The creep deformation and creep damage process can be illustrated as one in which the controlling creep mechanism changes as a function of stress. For creep damage analysis of low Cr alloys, there is no standard method to define the stress level. In this project, in order to depict the creep deformation and damage more accurately and clearly, it was decided to consider the yield stress dependence method in combination with the concept of an intermediate stress level.

## **2.4 Stress breakdown phenomenon**

### **2.4.1 Premature failure**

The long-term creep properties of structural materials to be used at high temperature in power plants can be evaluated from short-term rupture data with the aid of time-temperature-parameter (TTP) methods (Lee et al., 2006). However, the activation energy for rupture life of materials at high temperature often decreases in long-term creep, and the conventional TTP methods overestimate the long-term rupture life of structural materials (Armaki et al., 2008; Maruyama et al., 2015). The above phenomenon is usually called premature failure.

Premature failure may bring some unexpected accidents in high temperature industries; for instance, the premature failure of an advanced high Cr ferritic steel resulted in the unexpected shutdown of a power plant in 2004 (Lee et al., 2006). This urgent engineering issue raised engineers' awareness of the need to detect and prevent such premature failure. Many experimental studies, such as those of Riedel (1987), Jovanovic (2003) and Boyle and Spence (2013), have attempted to explain the

premature failure phenomenon and the possible causes of this phenomenon can be summarised as follows:

- If the design is poor, so that unforeseen high local stresses occur, then the local creep deformation may exceed the creep ductility and lead to premature failure.
- If the structures are not stress relieved, residual stresses may be superimposed on the applied stress and again lead to premature failure.

#### **2.4.2 Stress breakdown in low Cr alloys**

Creep is a behaviour of microstructural deformation which is due to the supply of activation energy (at over 1/3 of melting temperature, high temperature supplies the activation energy for diffusion and dislocation; the diffusion mechanism requires less energy and the dislocation mechanism requires higher energy). Based on the investigations of Pharr (1981), Yavari and Langdon (1982) and (Raj, 2002), Lee et al. (2006) first proposed the concept of stress breakdown. According to Lee et al. (2006), the postponement of the decrease of activation energy in the long-term creep of a component can substantially extend the service life of the high temperature component, because the decrease in activation energy is always accompanied by a decrease in the stress exponent for rupture life. Thus, the stress breakdown phenomenon can be regarded as the result of changes in both activation energy and the stress exponent. For low Cr alloys, experimental data concerning the dependence of time to failure upon stress are given in Figure 2.2.

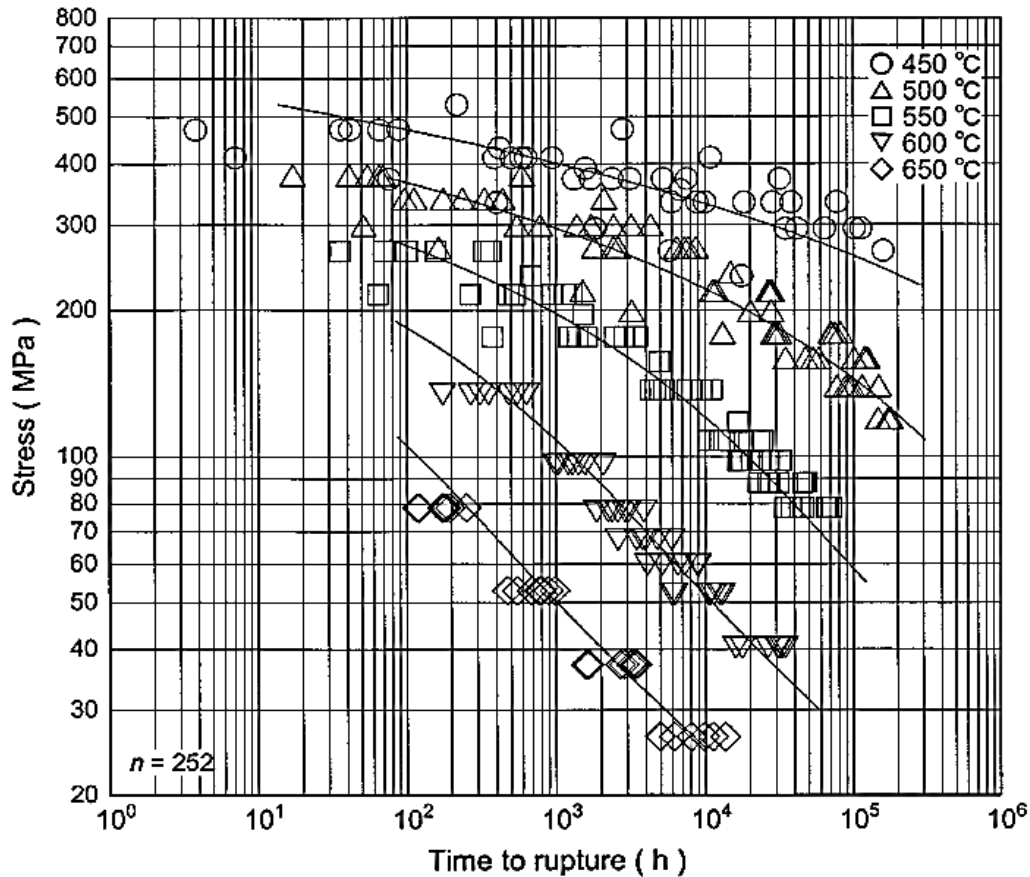


Figure 2.2: Stress versus time to rupture at 450, 500, 600 and 650°C for quenched and tempered 2.25Cr-1Mo steel plates (M/CDS/No. 36B/2003, 2003)

Figure 2.2 shows the distinctive changes of rupture lifetime at different stress and temperature ranges. According to Figure 2.2, the slope of stress against rupture life has obviously decreased from short-term creep to long-term creep, and this phenomenon confirms the existence of stress breakdown phenomenon in the creep evolution of low Cr alloys. Especially at the tertiary creep stage, there is an increase in stress as the cross-section area is reduced, either by the specimen's thinning under constant load, or by internal fracture or the nucleation of creep cavity. Furthermore, the reduction of the cross-section area can lead to the stress concentration phenomenon and in turn, the stress concentration leads to the change in the fracture-driving mechanism.

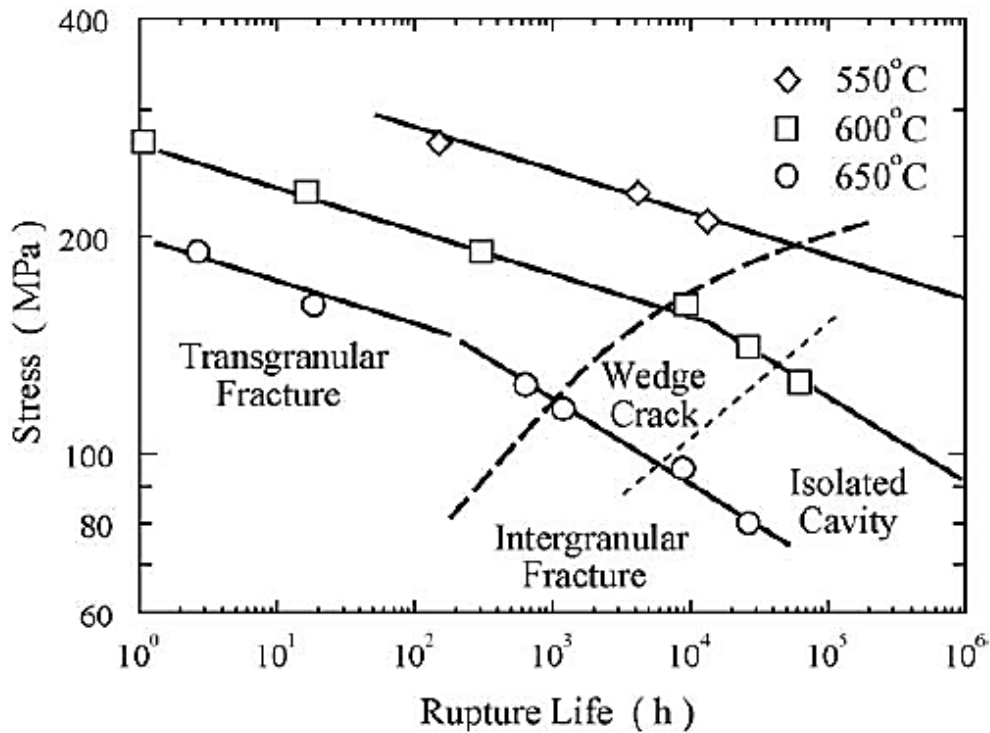


Figure 2.3: Fracture mechanism map under different stress levels (Lee et al., 2006)

Figure 2.3 shows the fracture mechanism map under different stress levels. The dashed line is the boundary between trans-granular and inter-granular fracture modes. The inter-granular fracture field is further divided into wedge cracking and isolated creep cavities (Lee et al., 2006). The stress breakdown phenomenon is caused by the changing fracture mechanisms which influence microstructural changes at different stress levels. However, the stress breakdown phenomenon has not been included into the current computational approaches for creep.

Stress breakdown of creep strength is a significant problem which needs to be resolved in long-term creep of structural components at high temperature. In order to describe the creep deformation and rupture time for low Cr alloy steels more accurately, it is essential to consider stress breakdown in the development of creep damage constitutive equations within this project.

## **2.5 Summary**

This chapter has given a brief overview and discussion of the problem domains relating to this project. Creep behaviour and characteristics in low Cr alloys have been reviewed in order to understand the nature of the creep damage problem. The importance of the investigation of creep damage behaviour in low Cr alloys has been identified.

The chapter has also illustrated the methods of stress level definition and the stress breakdown phenomenon involved in creep damage analysis. In particular, the importance of the stress breakdown phenomenon and stress level definition in developing constitutive equations has been demonstrated.

# Chapter 3 Literature Survey of Creep Damage Constitutive Equations

## 3.1 Introduction

This chapter is a review of literature covering existing approaches to predicting creep failure time and the classical CDM-based creep damage constitutive equations. The overall aim of this chapter is to provide a general understanding of computational creep damage mechanics and summarise the critical issues that need to be addressed through a comprehensive literature review, specifically concentrating on the characteristics of CDM-based creep damage constitutive equations.

The specific knowledge reviewed in detail within this chapter includes the following areas of enquiry:

- 1) To review existing approaches to predicting creep failure time. Three approaches (the classical plastic theory (CPT) based approach, the cavity growth mechanism (CGM) based approach and the CDM-based approach) are reviewed, concluding with a preference for the CDM-based approach in the development of creep damage constitutive equations for low Cr alloys.
- 2) To review existing CDM-based creep damage constitutive equations. The Kachanov-Rabotnov equation, Dyson's equation, Hayhurst's equation, Xu's equation and Yin's equation are investigated, and the advantages and disadvantages of each constitutive equation are commented on.
- 3) To demonstrate why new creep damage constitutive equations need to be created. The deficiencies of the existing constitutive equations are summarised and the expectations of the new constitutive equations for creep damage analysis of low Cr alloys are outlined.

## 3.2 Current approaches to predicting creep failure time

### 3.2.1 Review of existing approaches to predicting creep failure time

In order to obtain a sound understanding of creep mechanisms, and to develop an accurate engineering design criterion for high temperature components, many theories and creep design approaches have been developed. These theories and creep design approaches can be grouped into three categories: the CPT-based approach, the CGM-based approach and the CDM-based approach (Segle, 2002; Yao et al., 2007). The characteristics of the current approaches in predicting creep failure time are commented on in Table 3.1.

Table 3.1: Existing approaches to predicting creep failure time

Approaches	Characteristics and comments
CPT-based approach	The CPT-based approach was first used in creep damage analysis during the first half of the 20 <sup>th</sup> century. It is popular for its simplicity in application to stress analysis because the process of creep deformation can be regarded as the process of plastic deformation (Hill, 1998). However, the CPT-based approach is limited in practical application because its derivation and use has aimed mainly at conventional creep damage situations in structures exposed to high temperature; it is usually derived from the criteria of yielding failure and does not account for the physical damage process (Webster and Ainsworth, 1994). Furthermore, the mathematical description of tertiary creep, where the significant damage occurs, is not available in the use of the CPT-based approach (Yao et al., 2007).

<p>CGM-based approach</p>	<p>The CGM-based approach was first proposed by Kachanov and Rimmer (1959) and was established based on understanding of the cavity growth process. The CGM-based approach is used in creep damage analysis because the creep failure of components operated at elevated temperature is usually controlled by creep cavity growth, and studies of cavity growth mechanisms such as plasticity-controlled growth, diffusion-controlled growth and constrained cavity growth have recently received more attention (Hales, 1994; Spindler, 2004; Zhang et al., 2015). However, the cavity growth rate in the whole creep failure process is not always controlled by the fastest growth mechanism through the use of CGM-based approach. In addition, applications of such approaches are usually expensive and time-consuming.</p>
<p>CDM-based approach</p>	<p>The CDM-based approach was initially proposed by Kachanov (1958). It was developed based on continuum mechanics and then a damage parameter was introduced by Rabotnov (1969) and Murakami (1983). In applications, a damage parameter is defined through the use of the CDM-based approach that ranges from zero (no damage) to a critical damage value (full damage), and is then measured throughout the creep processes. Creep failure time is defined as the time taken for the continuum damage level to move from no damage to full damage (Lasa, 2013). Physically-based CDM for creep provides a suitable framework for quantifying the shapes of creep curve caused by several microstructural damage mechanisms (Kowalewski et al., 1994).</p>

### 3.2.2 Preference for CDM-based approach

The CDM-based approach has been combined with the finite element method through the work of Vakili et al. (2005), Hayhurst et al. (2008) and Liu et al. (2013) for the investigation of creep damage behaviour. The literature on CDM has now reached a mature level. Initially, the CDM-based approach was developed for assessing the manufacture of components from a single material (Kachanov 1958); later on, it came to be used extensively in the creep damage analysis of multi-material structures such as damage evolution (Hayhurst et al., 2005).

In comparison with the CPT-based approach and the CGM-based approach, the CDM-based approach has obvious advantages. The advantages of the use of CDM for creep damage analysis can be summarised as follows:

- 1) The characteristics of the CDM-based approach are that the way in which the material becomes damaged does not essentially have to be understood in detail, and that the damage parameter can assess the damage level of creep (Segle, 2002).
- 2) The CDM-based approach allows the physical mechanisms of material deformation and deterioration to be represented by explicit state variables (Perrin and Hayhurst, 1996).
- 3) A mathematical description of tertiary creep, where the significant damage occurs, can be achieved through the use of CDM-based approaches (Perrin and Hayhurst, 1996).
- 4) CDM-based constitutive equations can be easily implemented with the finite element program in the analysis of creep damage behaviour, which can significantly improve efficiency in terms of both time and economy (Maharaj et al., 2009).

It is notable that most creep damage constitutive equations are developed based on the CDM approach. The CDM-based approach has also been adopted in this project for the development of creep damage constitutive equations for low Cr alloys. The CDM-based creep damage model can be

used to consider a variety of both thermal-induced and stress-induced creep damage mechanisms, and provides very useful information on the predicted creep behaviour of the material (Vakili et al., 2005). Creep failure time can be defined through the use of CDM as the time taken for the continuum damage level to move from no damage to full damage. With the CDM-based approach, the developer can develop new creep damage constitutive equations that inherit many of the reliable achievements of older, existing theories (Dyson and Osgerby, 1993).

### **3.3 Classical creep damage constitutive equations based on CDM**

The computational capability for creep damage analysis relies on the availability of a set of creep damage constitutive equations. The CDM-based approach has been widely used in the development of creep damage constitutive equations for describing the creep behaviour of ferritic steels, where the dominant mechanisms of material degradation are creep cavitation and the coarsening of the carbide precipitates. Here, the existing CDM-based creep damage constitutive equations such as Kachanov-Rabotnov's equation, Dyson's equation, Hayhurst's equation, Xu Qiang's equation and Yin's equation are reviewed. The advantages and deficiencies of each constitutive equation are commented on.

#### **3.3.1 Review of Kachanov-Rabotnov equation**

The prototype of the Kachanov-Rabotnov equation was first proposed by Kachanov (1958), then was extensively developed to include the mathematical description of tertiary creep by Kachanov (1958) and Rabotnov (1969). The Kachanov-Rabotnov equation is a nonlinear first order differential rate equation which contains one variable. Creep damage manifests itself as an accelerating (tertiary) rate in a standard constant rate test. Although loss of strength can be caused by numerous mechanisms of degradation, the pragmatic engineering solution introduced by Kachanov (1958) and Rabotnov (1969) was able to quantify these changes through the use of a single empirical mathematical parameter. Kachanov (1958) and Rabotnov (1969) used a power-law

creep rate formulation, coupled with a power-law dependence of damage evolution equation, as illustrated in Equation 3.1 and Equation 3.2.

$$\frac{d\varepsilon}{dt} = A' \left( \frac{\sigma}{1-\omega} \right)^n \quad (3.1)$$

$$\frac{d\omega}{dt} = B' \left( \frac{\sigma}{1-\omega} \right)^v \quad (3.2)$$

where  $\varepsilon$  is creep strain,  $\omega$  is the creep damage and the  $\sigma$  is the applied stress;  $A'$  and  $B'$  are material constants;  $n$  and  $v$  are stress exponents.

The relatively simple one state variable model, which can describe the effect of cavitation damage, has been widely used, although the extrapolation of results from this model should be carried out with great caution (Hyde et al., 2006). For implementation of the concept of different stress regimes and materials, the above equations can be expressed as follows:

$$\frac{d\varepsilon}{dt} = A'' \left( \frac{\sigma}{1-\omega} \right)^n \quad (3.3)$$

$$\frac{d\omega}{dt} = B'' \frac{\sigma^x}{(1-\omega)^\emptyset} \quad (3.4)$$

where  $\varepsilon$  is creep strain,  $\omega$  is the creep damage and  $\sigma$  is the applied stress; where  $A''$  and  $B''$  are material constants; and  $n$ ,  $x$  and  $\emptyset$  are stress exponents which depend on different stress regimes and materials.

Constant volume is maintained during creep, so the rate of volume creep strain is zero:

$$\dot{\varepsilon}_1 + \dot{\varepsilon}_2 + \dot{\varepsilon}_3 = 0 \quad (3.5)$$

where  $\dot{\varepsilon}_1$ ,  $\dot{\varepsilon}_2$  and  $\dot{\varepsilon}_3$  are the principal strain rate.

The principal shear strain rates are proportional to the principal shear stresses.

Then,

$$\frac{\dot{A}_1}{\dot{B}_1} = \frac{\dot{A}_2}{\dot{B}_2} = \frac{\dot{A}_3}{\dot{B}_3} = 2\delta \quad (3.6)$$

where,

$$\begin{aligned} A_1 &= (\sigma_1 - \sigma_2), & A_2 &= (\sigma_2 - \sigma_3), & A_3 &= (\sigma_3 - \sigma_1), \\ B_1 &= (\varepsilon_1 - \varepsilon_2), & B_2 &= (\varepsilon_2 - \varepsilon_3), & B_3 &= (\varepsilon_3 - \varepsilon_1), \end{aligned}$$

where  $\sigma_1$ ,  $\sigma_2$  and  $\sigma_3$  are the principal stresses, and

$$\sigma_m = \frac{1}{3}(\sigma_1 + \sigma_2 + \sigma_3) \quad (3.7)$$

Thus,

$$\begin{cases} \dot{\varepsilon}_1 = \delta(\sigma_1 - \sigma_m) \\ \dot{\varepsilon}_2 = \delta(\sigma_2 - \sigma_m) \\ \dot{\varepsilon}_3 = \delta(\sigma_3 - \sigma_m) \end{cases} \quad (3.8)$$

Equivalent creep strain rate,  $\bar{\dot{\varepsilon}}$  is shown as below:

$$\bar{\dot{\varepsilon}} = \frac{2}{3}\delta\bar{\sigma} \quad (3.9)$$

So,

$$\delta = \frac{3\bar{\dot{\varepsilon}}}{2\bar{\sigma}} \quad (3.10)$$

Assuming  $\delta$  is related to the function of  $f(t)$  and  $f(\bar{\sigma})$ :

$$\delta = \frac{3}{2} \frac{f(t)f(\bar{\sigma})}{\bar{\sigma}} \quad (3.11)$$

Therefore, the constitutive equation could be written as:

$$\dot{\varepsilon} = \frac{3}{2}(\sigma_1 - \sigma_m) \frac{f(t)f(\bar{\sigma})}{\bar{\sigma}} \quad (3.12)$$

The multi-axial creep damage constitutive equation is normally described by the von Mises stress; and at the isotropic damage situation the strain evolution equation is derived as:

$$\frac{d\varepsilon_{ij}}{dt} = \frac{3}{2}K[\sigma_v^{n-1}S_{ij}/(1 - \omega)^m] \quad (3.13)$$

Thus, the damage evolution equation can be defined as:

$$\frac{d\omega}{dt} = A[\sigma_{eq}^p / (1 - \omega)^k] \quad (3.14)$$

where  $d\varepsilon_{ij}$  is the creep strain tensor,  $S_{ij}$  is the deviatoric tensor of stress,  $\sigma_v$  is the von Mises stress and  $\sigma_{eq}$  is the equivalent stress which is defined by the multi-axial stress state.  $K$ ,  $n$ ,  $A$ ,  $p$ ,  $k$  and  $m$  are material parameters. These parameters are defined from the creep curve fitting.  $\omega$  ( $0 < \omega < 1$ ) is a variable which describes cavitation creep damage (Hall, 1990).

The Kachanov-Rabotnov equation has been widely used in the description of creep damage behaviour, such as the numerical investigation of the creep damage behaviour of a Cr-Mo-V steam pipe weldment which was undertaken by Hall and Hayhurst (1991). Although there are many advantages to the use of the Kachanov-Rabotnov equation in creep damage analysis, some deficiencies still exist. The advantages and deficiencies of the use of the Kachanov-Rabotnov equation in creep damage analysis are summarised as follows:

- **Advantages:**

- 1) The function of the mathematical description of tertiary creep is included in the Kachanov-Rabotnov equation (Gorash, 2008).
- 2) This equation can be easily utilized at varying temperatures and stresses by simply changing the value of  $n$  ( Hall and Hayhurst, 1991).
- 3) The material parameters are easily to fit and the implementation of this equation into the finite element program is very convenient (Gaffard, 2004).
- 4) The inherent simplification of a single empirical damage parameter formulation has an obvious advantage for computation and it can be used in the analysis of multi-materials such as weldment (Hall, 1990).

- **Deficiencies:**

- 1) The Kachanov-Rabotnov equation does not include related mechanisms such as hardening (deceleration of strain at primary stage) or particle coarsening (accumulation of strain at tertiary stage) (Dyson and McLean, 1983).
- 2) Stress level definition has not been considered in this equation as a result of the inaccurate description of the relationship between minimum creep rate and stress, particularly with regard to the prediction of long-term creep damage behaviour (Gaffard, 2004).
- 3) At the primary creep stage, the relationship between time-dependent strain hardening and creep recovery has not been clearly demonstrated as a result of the inaccurate prediction of creep deformation at this stage (Gorash et al., 2005).
- 4) The stress breakdown phenomenon has not been involved in this equation as a result of lack of consideration of the effect of changing fracture mechanisms due to microstructural changes under different stress levels.

### 3.3.2 Review of Dyson's equation

With the development of various remnant lifetime techniques and predictive models of creep behaviour, Dyson and Osgerby (1993) proposed a new set of physical creep damage equations for creep deformation in particle-hardened alloys. These equations provide the function of predicting creep parameters such as rupture life, minimum creep rate and various measures of remnant lifetime. Dyson's equation was developed based on the mechanism of creep in particle-hardened alloys, whereby the process of climb and glide occurs as a parallel rather than a sequential process (Dyson and Osgerby, 1993). The formulations of Dyson's creep damage constitutive equation (Dyson and Osgerby, 1993) are shown below:

$$\dot{\varepsilon} = \dot{\varepsilon}_0 \sinh \left[ \frac{\sigma(1-H)}{\sigma_0(1-\phi)(1-\omega)} \right] \quad (3.15)$$

$$\dot{H} = \left(\frac{h\dot{\varepsilon}}{3}\right) \left[1 - \left(\frac{H}{H^*}\right)\right] \quad (3.16)$$

$$\dot{\emptyset} = \left(\frac{K_P}{3}\right) (1 - \emptyset)^4 \quad (3.17)$$

$$\dot{\omega} = N \left(\frac{K_N}{\varepsilon_{fu}}\right) \dot{\varepsilon} \quad (3.18)$$

where  $N = 1$  when  $\sigma_1 > 0$  and  $N = 0$  when  $\sigma_1 \leq 0$ . The parameters of  $\dot{\varepsilon}_0$ ,  $\sigma_0$ ,  $h$ ,  $K_P$  are material constant and the details of these parameter calculations can be found in Dyson and Osgerby (1993). The parameter of  $K_N$  has a maximum value of  $1/3$ , where  $\varepsilon_{fu}$  is the uniaxial strain at failure.

Variable  $\varepsilon$  represents the creep strain and variable  $\sigma$  represents the applied stress. Variable  $H$  is the strain hardening which can take on values ranging from zero to a microstructure-dependent maximum of  $H^*$  ( $<1$ ). Variable  $\emptyset$  increases from its initial value of zero towards a theoretical upper limit of unity (never achievable in practice); therefore, decreasing the magnitude of  $\sigma_0$  will increase creep rate. Variable  $\omega$  represents the damage induced by continuous cavity nucleation.

The mathematical equation for creep analysis at primary creep was originally proposed by Ion et al. (1986); Dyson and Osgerby (1993) then modified this equation through the implementation of the particle coarsening theory (Greenwood, 1956; Lifshitz and Slyozov, 1961; Wagner, 1961). In Dyson's equation, three variable equations can be used to represent more complex failure mechanisms (Yao et al., 2007).

Dyson's equation has been widely utilized in the creep damage analysis of high temperature structures, such as by Dyson and Osgerby (1993) for 1Cr-1/2Mo ferritic steel, Perrin and Hayhurst (1996) for 0.5Cr-0.5Mo-0.25V ferritic steel, Kowalewski et al. (1994) for aluminium alloy and Dyson (2009) for Nimonic 90. Although there are many advantages to the use of Dyson's equation in creep damage analysis, some deficiencies still exist.

The advantages and deficiencies of the use of Dyson's equation for creep damage analysis are summarised as follows:

- **Advantages:**

- 1) The softening mechanism operates in low alloy steels due to the thermal coarsening of matrix carbide particles; the contribution of this to material degradation was first incorporated by Dyson and Osgerby (1993).
- 2) Improvement in the accuracy of a discrepancy is achieved through the use of hyperbolic sine law to replace the power-law; this has been demonstrated by comparing it with an experiment test (Jaffee, 2013).
- 3) The capability to describe primary creep strain deceleration behaviour is achieved because the initial strain hardening has been considered in Dyson's equation (Dyson and Osgerby, 1993).
- 4) The accuracy of depiction of tertiary creep strain is improved through identification of the dominant mechanism in microstructural degradation within the CDM framework.
- 5) Stress level definition is considered in Dyson's equation and this equation can be used in extrapolating the short-term creep to long-term creep condition.

- **Deficiencies:**

- 1) At a temperature of 530°C, predictions through the use of Dyson's equation overestimate lifetimes, particularly at low stress level, due to lack of consideration of the cavitation on strain trajectories (Dyson and Osgerby, 1993).
- 2) At low stress level there are major discrepancies, in particular at 550°C, and the values of minimum creep rate are influenced due to the constant values of  $h'$  and  $H^*$  reflecting the material parameter.
- 3) The rupture criterion used in Dyson's equation follows conventional creep damage mechanics, and the material is deemed to fail when the creep damage reaches a constant value. However, the damage

at failure time may not be a constant in physical practice (Dyson and Osgerby, 1993).

- 4) The stress breakdown phenomenon has not been involved in this equation as a result of lack of consideration of the effects of changing fracture mechanisms on microstructural changes under different stress levels.

### 3.3.3 Review of Hayhurst's equation

Hayhurst's equation includes both uniaxial and multi-axial forms (Perrin and Hayhurst, 1996). Hayhurst's equation is developed based on Dyson's equation and the uniaxial form is the same as Dyson's equation. In order to achieve the computational capability for creep damage analysis on multi-materials and complex geometry components, the uniaxial constitutive equation was expanded through the implementation of multi-axial stress states by Perrin and Hayhurst (1996).

Hayhurst's creep damage constitutive equations (Perrin and Hayhurst, 1996) are shown below:

$$\dot{\varepsilon}_{ij} = \frac{3S_{ij}}{2\sigma_e} A \sinh \left[ \frac{B\sigma_e(1-H)}{(1-\phi)(1-\omega)} \right] \quad (3.19)$$

$$\dot{H} = \left( \frac{h\dot{\varepsilon}_e}{\sigma_e} \right) \left( 1 - \left( \frac{H}{H^*} \right) \right) \quad (3.20)$$

$$\dot{\phi} = \left( \frac{K_c}{3} \right) (1 - \phi)^4 \quad (3.21)$$

$$\dot{\omega} = CN\dot{\varepsilon}_e(\sigma_1/\sigma_e)^v \quad (3.22)$$

where  $\sigma_1$  is the maximum principal stress.  $N = 1$  when  $\sigma_1 > 0$  and  $N = 0$  when  $\sigma_1 < 0$ . The multi-axial parameters  $A$ ,  $B$ ,  $C$ ,  $h$ ,  $H^*$  and  $k_c$  are constants to be determined from the uniaxial creep behaviour. The parameter  $v$  is the multi-axial stress sensitivity index, where  $\sigma_{eq} = (3S_{ij}S_{ij}/2)^{1/2}$  is the effective stress,  $S_{ij} = \sigma_{ij} - \delta_{ij}\sigma_{kk}/3$  is the stress deviator and  $\varepsilon_e = (2\varepsilon_{ij}\varepsilon_{ij}/3)^{1/2}$  is the effective creep strain.

The advantages and deficiencies of the use of Hayhurst's equation for creep damage analysis are summarised as follows:

- **Advantages:**

- 1) The function of the mathematical description of the accumulation of inter-granular cavitation and the coarsening of carbide precipitates has been involved in Hayhurst's equation (Kowalewski et al., 1994).
- 2) Implementation of the multi-axial stress state extends the computational capability in complex geometry components such as notched-bar and butt-welded pipework (Hayhurst et al., 1984).
- 3) Hayhurst's equation is easily implemented into the finite element program for creep damage analysis (Hayhurst et al., 2005).
- 4) The multi-axial stress rupture criterion of 0.5Cr-0.5Mo-0.25V ferritic steel has been determined by Perrin and Hayhurst (1996).

- **Deficiencies:**

- 1) When stresses exceed 100MPa, at which the mechanism of rupture is thought to switch from an inter-granular mode to a trans-granular mode, significant deficiency will occur in Hayhurst's equation (Perrin and Hayhurst, 1996).
- 2) Hayhurst's equation cannot predict a combination of the inter-granular and trans-granular modes of failure at low stress level, where the effects of the coarsening of carbide precipitates on creep deformation are significant (Perrin and Hayhurst, 1996).
- 3) This equation is developed based on lifetime consistency, and inaccuracy of predicted creep strain may occur due to a lack of creep deformation consistency (Zhang et al., 2015).
- 4) The stress breakdown phenomenon has not been involved in this equation as a result of lack of consideration of the effects of changing fracture mechanisms due to microstructural changes under different stress levels.

### 3.3.4 Review of Xu Qiang's equation

In order to overcome shortcomings such as the lack of consideration of inconsistencies in creep deformation within Hayhurst's equation, Xu (2001) implemented two functions to describe the effects of stress state on creep damage evolution and strain, respectively. Based on Hayhurst's multi-axial constitutive equation (Perrin and Hayhurst, 1996) and the constrained cavity growth theory (Spindler et al., 1997), Xu (2001) proposed a new set of multi-axial creep damage constitutive equations.

Xu Qiang's constitutive equations (Xu, 2001; Xu, 2004) are shown below:

$$\dot{\varepsilon}_{ij} = \frac{3s_{ij}}{2\sigma_e} A \sinh \left[ \frac{B\sigma_e(1-H)}{(1-\phi)(1-\omega)} \right] \quad (3.23)$$

$$\dot{H} = \left( \frac{h\dot{\varepsilon}_e}{\sigma_e} \right) \left( 1 - \left( \frac{H}{H^*} \right) \right) \quad (3.24)$$

$$\dot{\phi} = \left( \frac{K_c}{3} \right) (1 - \phi)^4 \quad (3.25)$$

$$\dot{\omega} = N\dot{\varepsilon}_e * f_2 \quad (3.26)$$

$$\dot{\omega}_d = \dot{\omega} * f_1 \quad (3.27)$$

$$f_1 = \left( \frac{2\sigma_e}{3S_1} \right)^a \exp \left( b \left( \frac{3\sigma_m}{S_s} - 1 \right) \right) \quad (3.28)$$

$$f_2 = \exp \left( p \left( 1 - \frac{\sigma_1}{\sigma_e} \right) + q \left( \frac{1}{2} - \frac{3\sigma_m}{2\sigma_e} \right) \right) \quad (3.29)$$

where  $f_1$  and  $f_2$  are functions of stress state. The  $f_2$  is introduced to describe the effect of the state of stress on damage evolution. The additional function  $f_1$  is introduced to better represent the phenomenological coupling between damage and tertiary deformation and creep rupture (Xu, 2001), where  $S_s = \sqrt{\sigma_1^2 + \sigma_2^2 + \sigma_3^2}$ ,  $\sigma_m = \frac{1}{3}(\sigma_1 + \sigma_2 + \sigma_3)$  and  $S_1 = \sigma_1 - \sigma_m$ ;  $a$  and  $b$  are two material parameters which reflect stress sensitively.

The advantages and deficiencies of the use of Xu Qiang's equation in creep damage analysis can be summarised as follows:

- **Advantages:**

- 1) With the implementation of the effects of stress state on damage evolution and strain, the creep computational capability can be extended to analyse plane stress, plane strain and multi-axial stress state problems (Xu et al., 2011).
- 2) Xu Qiang's equation offers the capability to produce results consistent with experimental measurement of lifetime and strain at failure under selected stress states with proportional loading conditions.
- 3) Under pure shear conditions, the accuracy of prediction of creep deformation and rupture time has been significantly improved through the use of Xu Qiang's equation (Xu et al., 2011).
- 4) Xu Qiang's equation is easily implemented into the finite element program for creep damage analysis.

- **Deficiencies:**

- 1) The material is deemed to have failed when the damage reaches a critical value, but this may not be physically sound (Xu et al., 2011).
- 2) Inaccuracy in creep damage analysis may occur at extremely high stress conditions.
- 3) The formulation fits strain at failure correctly; however, there is no further validation to ensure that it fits the tertiary stage of creep deformation under multi-axial stress state (Xu et al., 2011).
- 4) The stress breakdown phenomenon has not been involved in this equation as a result of lack of consideration of the effects of changing fracture mechanisms on microstructural changes under different stress levels.

### **3.3.5 Review of Yin's equation**

In order to overcome the shortcomings of Dyson's (1993) equation, Yin and Faulkner (2006) proposed the use of two types of damage for creep

analysis. The two types of damage are: 1) thermally induced damage, including damage due to particle coarsening and solute depletion from the matrix; and 2) strain induced damage, including damage due to cavity nucleation growth and multiplication of mobile dislocations. Based on Dyson's equation, Yin and Faulkner (2006) proposed a new set of creep damage equations.

Yin's constitutive equations (Yin and Faulkner, 2006) are shown below:

$$\dot{\varepsilon} = \dot{\varepsilon}_0 \sinh \left[ \frac{\sigma(1-H)}{\sigma_0(1-\phi)(1-\omega)} \right] \quad (3.30)$$

$$\dot{H} = \left( \frac{h\dot{\varepsilon}}{3} \right) \left[ 1 - \left( \frac{H}{H^*} \right) \right] \quad (3.31)$$

$$\dot{\phi} = \left( \frac{K_P}{3} \right) (1 - \phi)^4 \quad (3.32)$$

$$\dot{\omega} = A' \varepsilon^{B'} \dot{\varepsilon} \quad (3.33)$$

where  $A' = AB$ ,  $B' = B - 1$ ,  $A = 1.5$ ,  $B = 2$ . These represent the damage parameters for cavity nucleation and growth, and  $\omega$  is defined as the fraction of Grain boundary (GB) facets cavitated. When cavities nucleate continuously, the evolution of  $\omega$  can be described by the following equation:

$$\dot{\omega} = \left( \frac{K_N}{\varepsilon_{fu}} \right) \dot{\varepsilon} \quad (3.34)$$

where  $\varepsilon_{fu}$  is the uniaxial strain at failure and the value of  $k_N$  has an upper limit of 1/3. This equation implies that damage due to cavitation is directly proportional to strain rate and  $\omega = A\varepsilon$ .

The advantages and deficiencies of the use of Yin's equation in creep damage analysis can be summarised as follows:

- **Advantages:**

- 1) GB cavitation has been considered according to experimental observations; therefore, creep rupture behaviour may be predicted more accurately (Yin and Faulkner, 2006).

- 2) The influence of different creep damage mechanisms (thermally induced damage and strain induced damage) on overall creep behaviour has been considered in Yin's equation.
- 3) Yin's equation is easily implemented into the finite element program for creep damage analysis.

- **Deficiencies:**

- 1) There is a lack of consideration of vacancy condensation on GB cavitation; this is due to the fact that the effects of temperature on creep damage owing to cavitation are not considered (Abe et al., 2008).
- 2) According to Yin et al. (2008), at high stress levels there are major discrepancies, in particular at a temperature of 600°C.
- 3) This equation can be utilized under stress ranges from 81MPa to 180MPa at a relatively high temperature of 600°C. However, in a low stress situation there is no justification or validation for the use of Yin's equation for creep analysis (Yin and Faulkner, 2006).
- 4) The stress breakdown phenomenon has not been involved in this equation as a result of lack of consideration of the effects of changing fracture mechanisms due to microstructural changes under different stress levels.

### **3.4 Motivations for developing a novel set of creep damage constitutive equations for low Cr alloys**

This project is conducted in order to develop a novel set of creep damage constitutive equations for low Cr alloys under low stress levels. Although some CDM-based creep damage constitutive equations have been proposed, some deficiencies still exist in the mathematical modelling of creep damage behaviour. Especially at low stress levels, the current constitutive equations exhibit many significant shortcomings for low Cr alloys. Thus, the development of a novel set of physically-based constitutive equations for low Cr alloys under long-term service remains

valuable. Based on the literature review of creep damage constitutive equations, the motivations for undertaking this project can be summarised as follows:

- 1) The existing creep damage constitutive equations are not specifically designed to predict the lifetime and creep rupture behaviour for low Cr alloy steels under low stress levels. Furthermore, those constitutive equations are mostly proposed based on experimental data obtained under high stress levels. For low stress levels, the computational capability for a current state is extrapolated from those constitutive equations by simply using a power-law or sinh law. However, this method is not consistent with experimental observation, since the damage mechanisms under a high stress level are different from those at low stress level (Viswanathan, 1989; Abe et al., 2008). To date, no constitutive equations have been specifically designed on the basis of physically-based experiment data for low Cr alloys under a low stress level.
- 2) The relationship between minimum creep rate and damage fields is unclear in describing creep behaviour for low Cr alloy steels under a low stress level. The minimum creep rate represents a vital role in the development of creep damage constitutive equations because this parameter influences almost 70% of the creep deformation process under low stress levels (Viswanathan, 1989; Shibli et al., 2005; Abe et al., 2008). As a result, the creep deformation process, particularly at the tertiary creep stage, cannot be accurately modelled.
- 3) The relationship between cavitation and creep damage is still bewildering in the investigation of rupture behaviour for low Cr alloy steels under low stress levels, yet the evolution of cavity is a dominant factor in accurately describing the accumulation of creep damage and final rupture. As a result, the lack of an accurate rupture criterion has a significant influence on the accuracy of

prediction of creep rupture time for low Cr alloy steels under long-term creep conditions.

- 4) With the CDM-based approach, current creep damage constitutive equations have exhibited a good performance in the description of hardening and particle coarsening, and it is evident from the literature survey that further enhancements to advance knowledge should only be focused on an accurate minimum creep rate equation, damage evolution equation and rupture criterion for creep damage analysis of low Cr alloys. Furthermore, a large amount of experimental creep data for describing creep behaviour in low Cr alloys has recently been compiled from studies undertaken by multiple research institutes such as EPRI, ECCC, NIMS and NPL (Shibli and Holdsworth, 2009; Whittaker and Wilshire, 2011; Roy et al., 2013). With authoritative permission to access these experimental data, the possibility of developing new creep damage constitutive equations could be achieved through the use of experimental creep data specific to low Cr alloys, combined with an advanced CDM approach.

### **3.5 Summary**

This chapter has investigated the current state of development of creep damage constitutive equations for creep damage analysis. Three approaches for predicting creep failure time have been investigated and the advantages of the use of the CDM-based approach have been demonstrated.

Existing classical CDM-based creep damage constitutive equations have also been investigated. The advantages and deficiencies of each constitutive equation for creep analysis have been commented on. The chapter has also illustrated why this project needs to be undertaken and which areas should be enhanced in order to address the development of new creep damage constitutive equations for low Cr alloys.

# Chapter 4 Development Strategy

## 4.1 Introduction

Recent technological advances, which do not just originate in CDM but also come from the field of the physically-based experiment methods, have been applied to investigate the creep damage behaviour of low Cr alloys. However, a set of creep damage constitutive equations which are specifically designed to accurately describe the creep behaviour of low Cr alloys at low stress levels is still demanded by high temperature industries. To understand the physics in a creep damage constitutive equation, and then to correct its undesirable features, it is essential to investigate the creep mechanisms which lead to creep rupture; it is also vital to understand the physically-based experiment data involving the minimum creep rate under different stress levels and damage behaviour at the different creep stages. In order to develop such constitutive equations, the following development strategy was proposed based on analysis of the CDM approach and experiment data:

- 1) For the general development strategy: a step-by-step strategy involving seven development stages in developing creep damage constitutive equations for low Cr alloys was proposed.
- 2) For the development approach for the constitutive equation to describe the minimum creep strain rate under different stress conditions: the relevant experiment data sources; the classical equations for minimum creep rate under different stress levels; the validation of the classical constitutive equations; and the minimization of deficiencies in existing constitutive equations would be investigated.
- 3) For the development approach for the constitutive equations to describe creep damage and the rupture criterion at different creep stages: the relative experiment data sources; investigation of the relationship between cavitation and creep damage accumulation; and the definition of the creep rupture criterion would be analysed.

## 4.2 General development strategy

The development process for creep damage constitutive equations has been reported by Dyson and Osgerby (1993) and Xu (2001). However, there is still no integrated system for describing the development strategy. In order to develop the constitutive equations in a step-by-step fashion, and in a logical and cohesive manner, an integrated development strategy for low Cr alloys was proposed based on the studies of Dyson and Osgerby (1993) and Xu (2001). The development strategy employed to address this project can be illustrated in seven main stages:

- **Stage 1:** Understanding the background of creep fields
  - 1) To precisely describe the stress regimes in creep damage analysis of low Cr alloys.
  - 2) To accurately describe the stress breakdown phenomenon.
  - 3) To understand the importance of creep damage behaviour under low stress conditions.
- **Stage 2:** Investigating the classical, physically-based creep damage constitutive equations within the framework of the CDM approach
  - 1) To critically review the existing classical creep damage constitutive equations.
  - 2) To evaluate the advantages and deficiencies of the current constitutive equations.
  - 3) To find the key factors which can significantly influence the development of creep damage constitutive equations.
  - 4) To identify the further enhancements which should be undertaken (relationships between minimum creep rate and stress level, damage evolution and rupture criterion).

- **Stage 3:** Critically evaluating and investigating the creep mechanisms for low Cr alloys
  - 1) To investigate the creep deformation mechanisms.
  - 2) To investigate the creep damage mechanisms.
  - 3) To investigate the creep rupture mechanisms.
- **Stage 4:** Analysing the long-term creep microstructural experiment data obtained under different stress regimes
  - 1) To analyse the effects of stress level on creep curve.
  - 2) To identify the dominative creep mechanism at the different stress levels.
  - 3) To analyse the effects of stress level on minimum creep rate.
  - 4) To analyse the effects of stress level on rupture time.
  - 5) To analyse the effects of stress level on strain at failure.
  - 6) To analyse the effects of stress level on creep cavity.
- **Stage 5:** Developing a new constitutive equation to depict relationships between minimum creep rate and stress regions
  - 1) To analyse the existing constitutive laws for describing minimum creep rate under different stress levels.
  - 2) To evaluate and test the classical existing constitutive equations.
  - 3) To minimise deficiencies through the development of a new minimum creep rate equation.
- **Stage 6:** Developing a new constitutive equation and rupture criterion to describe creep damage evolution and rupture time
  - 1) To analyse experiment data relating to the evolution of creep cavity.

- 2) To investigate the relationship between cavitation and creep damage accumulation.
  - 3) To define the creep rupture criterion.
- **Stage 7:** Implementing and validating the creep damage constitutive equations for low Cr alloys
    - 1) To implement the new minimum creep rate equation, damage evolution equation and rupture criterion into the constitutive equation system.
    - 2) To validate the newly developed creep damage constitutive equations for low Cr alloys under low stress levels.

### 4.3 Development approach for minimum creep rate equation

#### 4.3.1 Experiment data for description of minimum creep rate

With authoritative permission to access relevant physically-based experiment data, the constitutive equation to describe relationships between minimum creep rate and stress regions could be determined. The experiment data used in developing the minimum creep rate equation are listed in Table 4.1.

Table 4.1: Physically-based experiment data for developing minimum creep rate equation

Experiment data source	Material type	Analysis aspect	Temperature and stress range
Cane (1979; 1980; 1981)	2.25Cr-1Mo steel	Minimum creep rate versus applied stress	565°C; 68-200MPa
NIMS (M/CDS/No. 3B, 1986)	2.25Cr-1Mo steel	Stress versus time to rupture	450-650°C; 30-300MPa
NPL (Dyson and Osgerby, 1993)	1Cr-0.5Mo steel	Minimum creep rate versus applied stress	450-650°C; 30-300MPa

<b>EPRI (Parker, 1995)</b>	2Cr-1Mo steel; 0.5Cr-0.5Mo- 0.25V steel	Minimum creep rate versus applied stress	600°C; 60-180MPa
<b>University of Nottingham (Hyde et al., 1998)</b>	0.5Cr-0.5Mo- 0.25V steel	Creep curve fitting	640°C; 40,54,70MPa
<b>NIMS (M/CDS/No. 35B, 2002)</b>	1Cr-0.5Mo steel	Minimum creep rate versus applied stress	550°C; 40-270MPa
<b>NIMS (M/CDS/No. 36B, 2003)</b>	2.25Cr-1Mo steel	Stress versus time to rupture	450-650°C; 30-300MPa

#### 4.3.2 Development of minimum creep rate equation

Based on the experiment data in Table 4.1, the approach for the development of a constitutive equation to describe relationships between minimum creep rate and stress level was proposed as follows:

- 1) To analyse the experiment data related to minimum creep rate under different stress levels; the stress levels addressed in this project should also be defined.
- 2) To identify the constitutive law involved in developing the minimum creep rate equation.
- 3) To develop the new minimum creep rate equation. The new equation should be able to deal with the stress breakdown phenomenon.
- 4) To validate the newly developed minimum creep rate equation.

#### 4.4 Development approach for damage evolution equation and rupture criterion

##### 4.4.1 Experiment data for description of the evolution of creep cavity

The experiment data used in developing the creep damage evolution equation and rupture criterion are listed in Table 4.2.

Table 4.2: Experiment data for developing damage evolution equation and rupture criterion

Experiment data source	Material type	Analysis aspect	Temperature and stress ranges
<b>Cane (1979; 1980); Cane and Middleton (1981)</b>	2.25Cr-1Mo	Cavity density	60-210MNm <sup>-2</sup> at 565°C, both interrupted and ruptured tests
<b>Lonsdale and Flewitt (1979)</b>	2.25Cr-1Mo	Cavity density	55-76MNm <sup>-2</sup> at 600°C, 66.5MNm <sup>-2</sup> at 565-650°C, interrupted and ruptured tests in argon
<b>Needham (1983)</b>	2.25Cr-1Mo (grain size d was either 18 or 155µm)	Cavity density	550°C with different $\sigma$ , uniaxial and multi-axial tests
<b>Cane (1980); Cane and Middleton (1981)</b>	2.25Cr-1Mo	$N_R$ , cavity density at rupture	62-208MPa at 565°C, uniaxial and multi-axial tests
<b>Needham and Gladman (1986)</b>	1Cr-0.5Mo (three batches)	Cavity density rate	550°C with different stress levels
<b>Bollerup et al. (1986)</b>	1Cr-0.5Mo (new and service-exposed material)	Cavity density	100MPa at 547-627°C, both interrupted and ruptured tests
<b>Tipler and Hopkins (1976)</b>	Commercial and high purity 1Cr-1Mo-0.25V and 0.5Cr-0.5Mo-0.25V	Cavity density	262-355MPa at 550°C both interrupted and ruptured tests
<b>Fedeli and Mori (1993)</b>	Service-exposed 0.5Cr-0.5Mo-0.25V	Cavity density	66 MPa at 640°C and 675°C
<b>Singha and Kamaraj (2009)</b>	Aged 1Cr-1Mo-1/4V	Cavity characteristics	110MPa at 500°C and 600°C

#### 4.4.2 Development of damage evolution equation and rupture criterion

Based on the experiment data in Table 4.2, the approach for the development of the damage evolution equation and rupture criterion was proposed as follows:

- 1) To analyse the effects of stress level on creep cavity behaviour.
- 2) To investigate the current creep rupture criteria.
- 3) To design the new rupture criterion.

- 4) To develop the new damage evolution equation; this equation should be able to deal with a combined inter-granular and trans-granular mode of failure under long-term creep conditions.
- 5) To validate the newly developed creep damage equation and rupture criterion.

## **4.5 Summary**

An integrated development strategy, involving seven development stages to develop the creep damage constitutive equations for low Cr alloys, has been proposed in this chapter.

The chapter has also illustrated the development approach for the constitutive equation to depict the minimum creep strain rate under different stress regions, and the development approach for the constitutive equation to depict creep damage and the rupture criterion at different time stages.

# Chapter 5 Investigation of Mechanisms for Low Cr Alloys

## 5.1 Introduction

This chapter focuses on explaining and investigating the domain mechanisms and contexts that are heavily used in this project. These do not just originate in fundamental creep behaviour but also come from the field of computational creep damage mechanics. The overall aim of this chapter is to present a critical understanding of which mechanism is dominative in the process of creep deformation under different stress levels, specifically concentrating on the characteristics of physically-based creep behaviour through investigation of the mechanisms of creep deformation, damage, rupture behaviour and creep failure in low Cr alloy.

The specific areas of focus for this chapter include the following:

- 1) To investigate creep deformation mechanisms. The creep deformation mechanism map, deformation mechanisms based on dislocation creep and those based on diffusion creep are analysed in order to identify creep behaviour under different temperature and stress ranges.
- 2) To investigate creep damage mechanisms. Cavity sites are firstly investigated, then the cavity nucleation mechanism and CGM are analysed in order to understand the mechanisms with cavitation characteristics involved in creep damage behaviour.
- 3) To investigate creep rupture mechanisms. The rupture mechanisms under high and low stress levels are investigated in order to understand the nature of creep failure behaviour.

## 5.2 Creep deformation mechanisms

Materials are deformed by different creep deformation mechanisms, depending on different stress levels, temperatures and the states of materials (Ashby and Brown, 2014). Physically-based creep mechanism

maps can be used in identifying which is the dominant deformation mechanism as a function of the variables of interest; for instance, stress versus temperature range (Riedel, 1987).

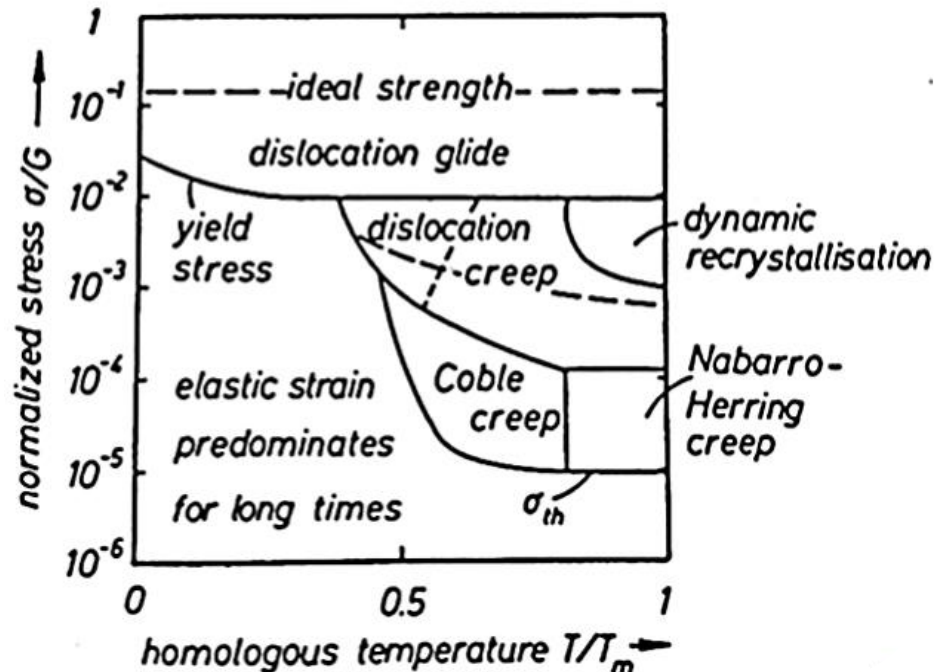


Figure 5.1: Schematic diagram of creep deformation mechanism map (Riedel, 1987)

Figure 5.1 shows the dominant deformation mechanism varying with stress versus temperature range. It should note that yield stress is decreasing with the decreasing of temperature; therefore, the yield stress value in Figure 5.1 should not be fixed value. Different regions are presented for a range of stresses and temperatures over which a specific mechanism is anticipated to be the principle process of creep (Riedel, 1987). There are two main creep processes involved in the mechanism of creep deformation (Ashby and Verrall, 1983). The first process is called dislocation creep, in which the factor controlling the creep rate is the ability of dislocations to glide (Langdon and Mohamed, 1978). The second process is called diffusion creep, in which the factor controlling the creep rate is continuous annealing at high temperatures (Svensson and Dunlop, 1981). These two creep processes are unavoidably interconnected, as they may both take place at the same time (Hall, 1990).

The mechanisms appearing on the creep deformation mechanism map can be described according to the category of creep process as:

- I. Creep deformation mechanisms based on the creep process of dislocation.
- II. Creep deformation mechanisms based on the creep process of diffusion.

### **5.2.1 Deformation mechanisms based on dislocation creep**

Dislocation creep tends to dominate at high stresses and relatively low temperatures, and is normally associated with lattice defects such as impurities or larger interstitial particles (Greenwood et al., 1954; Raj, 1975; Hull and Bacon, 2001). The atoms in the crystal-graphic planes, or so-called crystal-graphic bands, are preferentially forced by the shear stress, and this movement requires less energy to slip or glide from one band to another than the energy required to diffuse over a whole plane at once. Dislocation creep involves the movement of dislocations through the crystal lattice of the material and the permanent deformation of the individual crystals (Mott, 1951). The mechanisms of creep dislocation can be identified as two main types, which are dislocation glide creep and dislocation climb creep (Greenwood, 1956; Ratcliffe and Greenwood, 1965; Mohamed and Langdon, 1974b; Yoo and Trinkaus, 1986).

#### **5.2.1.1 Dislocation glide creep mechanism**

The glide dislocation mechanism is the motion along a crystallographic direction which allows dislocations a further degree of freedom. In certain cases, this may impede dislocation movement through dislocation integration (Nieh and Nix, 1980). Dislocation motion may also be arrested by obstacles such as second phase particles and inclusions (Yamaguchi and Umakoshi, 1990). This mechanism of creep tends to dominate at high stresses and relatively low temperatures.

It is noted that the diffusion of atoms can unlock dislocations from obstacles (Stanley, 1978). Such behaviour can involve movement by gliding in a slip plane, this process requiring little thermal activation to

enable the forces (Stanley, 1978). This deformation mechanism is controlled by a local shear stress in an appropriate direction on the dislocation for the glide (Stanley, 1978). Dislocation glide allows plastic deformation to occur at a much lower stress than would be required to move a whole plane of atoms past one another (Orowan, 1940; Watanabe and Davies, 1978).

A schematic diagram of the mechanism of dislocation glide creep deformation can be plotted through the investigations of Bauer (1965), Rollason (1973), Poirier (1985), Mainprice et al. (1986) and Galiyev et al. (2001).

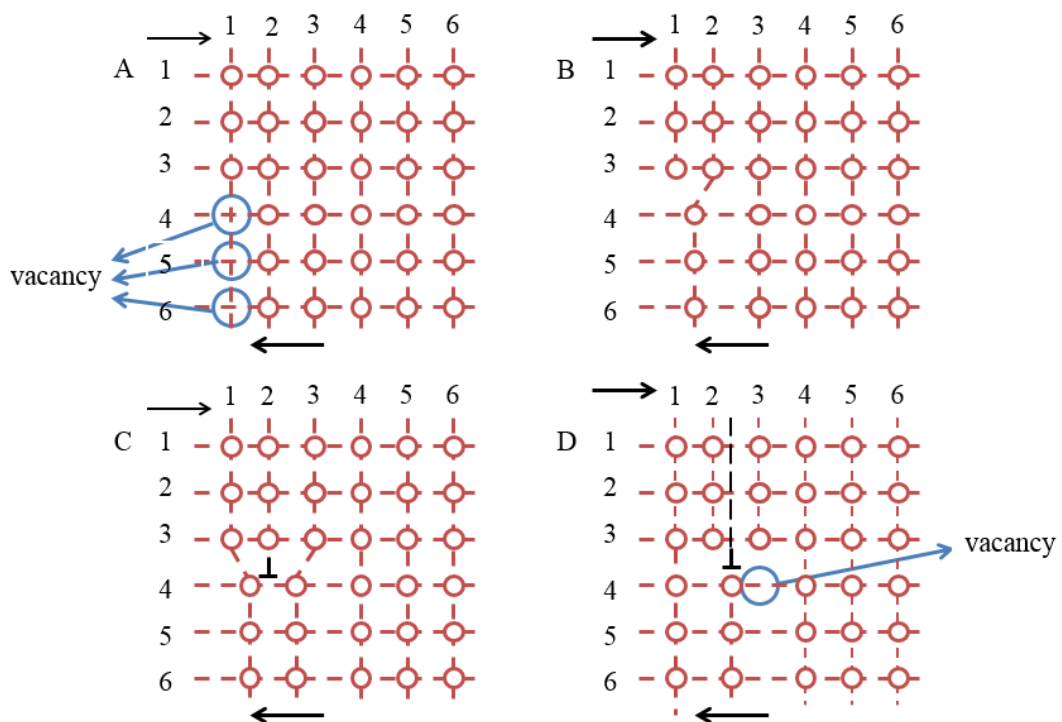


Figure 5.2: Schematic diagram of dislocation glide creep mechanism

Figure 5.2 shows the schematic diagram of how dislocation glide creep deformation occurs in the square lattice, and how the atoms glide from one slip plane (slip band) to another by the mechanism known as cross-slip, which allows dislocations a further degree of freedom (Nicolas and Poirier, 1976). Its preferentiality depends on the shear stress that drives the movement of atoms (Yamaguchi and Umakoshi, 1990). According to Figure 5.2, the process of dislocation glide is always associated with

crystal structure defects in which an atom is 'missing' from the ideal crystal structure, and this behaviour will cause the generation of a vacancy. Furthermore, if the vacancy exists within normally empty regions (interstices) in the host lattice, this will cause distortion of the host lattice to occur around the vacancy (Milne et al., 2003). With the increase in the movement of atoms, more vacancies will occur, and these could contribute to creep deformation.

#### **5.2.1.2 Dislocation climb creep mechanism**

The climb dislocation mechanism is the motion along a crystallographic direction which allows dislocations a further degree of freedom (Rediel, 1987). In certain cases, this may impede dislocation movement through dislocation inter-action, causing dislocation to become entangled or locked (Weertman, 1955). Dislocation motion may also be arrested by obstacles such as second phase particles and inclusions (Burton, 1972). Vacancies diffuse into the dislocation core, allowing the dislocation to climb (Balluffi, 1969).

Diffusion of atoms can unlock dislocations from obstacles, allowing them to climb and enable further slip. This behaviour is linked to both the climb mechanism and the dislocation creep process (Balluffi, 1969). However, the rate-determining step for the motion of atoms is usually associated with the climb mechanism, which requires high temperature (Rediel, 1987). Obstacles such as dislocations, precipitates or grain boundaries in the slip plane can lead to dislocation climb (Speight and Beere, 1975).

Based on the literature of Weertman (1957), Evans and Wilshire (1970), Burton (1972), Stanley (1978), Langdon (1985) and Milne et al. (2003), a schematic diagram of the mechanism of dislocation climb creep deformation can be plotted as shown in Figure 5.3 to illustrate climb dislocation behaviour.

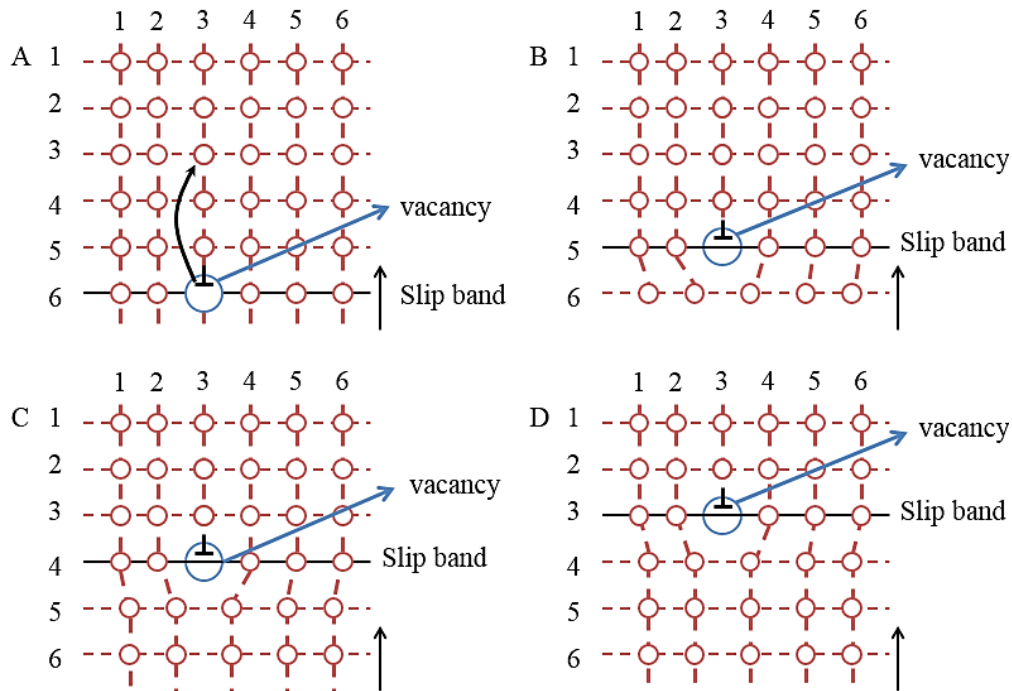


Figure 5.3: Schematic diagram of dislocation climb creep

Figure 5.3 shows a schematic diagram of how dislocation climb creep occurs in the square lattice and illustrates the movement of atoms from one slip plane (slip band) to another. This behaviour is also preferentially dependent on the shear stress that drives the atoms to move from one side to another (Stanley, 1978). With the climb of atoms, the stress concentration in the crystal could be relieved (Stanley, 1978). Dislocation climb creep can therefore result in recovery and softening behaviour which could balance the strain hardening caused by the dislocation glide process (Weertman, 1957).

The deformation process of dislocation climb creep usually happens at the secondary creep stage. Weertman (1957) proposed a model based on the theory of dislocation climb for steady state creep. In this model, the creep deformation behaviour is controlled by the dislocation climb behaviour, which is the dominant interaction movement within the microstructure of the material. The derived empirical expression of this model is shown as follows:

$$\dot{\epsilon}_s \propto D_L \sigma^{4.5} / b^{0.5} N^{0.5} G^{3.5} kT \quad (5.1)$$

where  $N$  is the number of dislocation sources per unit volume,  $G$  is the shear modulus and  $b$  is the Burger vector. The stress exponent has been estimated as 4.5. This model obeys the power-law and it can predict the relationship between steady state creep rate and the empirical stress observed in pure metals.

### **5.2.2 Deformation mechanisms based on diffusion creep**

Diffusion occurs when vacancies exist in the metal crystal lattice (Balluffi and Mehl, 1982). The creep process is controlled by stress-directed atomic diffusion through the structural components (Rediel, 1987). The applied stress changes the chemical potential of atoms at the surfaces of grains, and when an atom has enough thermal energy it can move into a neighbouring vacancy (Seitz, 1952). The process of diffusion creep was first proposed for the diffusion of vacancies through their crystal lattice by Nabarro (1948) and Herring (1950). Later, Coble (1963a) proposed that grain boundaries can also provide an alternative path for stress-directed diffusional mass transport to take place.

The diffusion creep process occurs at relatively low stresses. There are two main mechanisms in the diffusion creep process: 1) Coble creep (Coble, 1963a), which occurs when the diffusion paths are predominantly through the grain boundaries under lower temperatures; and 2) Nabarro-Herring creep (Nabarro, 1948; Herring, 1950), when the diffusion paths are predominantly through the grains themselves under higher temperatures.

#### **5.2.2.1 Nabarro-Herring creep (volume diffusion) mechanism**

Nabarro-Herring diffusion was proposed by Nabarro (1948) and Herring (1950), and this mechanism considers the possibility of creep occurring by stress-assisted diffusional mass transport through the lattice (Viswanathan, 1989). In this creep deformation mechanism, the crystal lattice is diffused through the grain at high temperature ( $>0.7T_m$ ).

The process of this mechanism is controlled by stress-directed atomic diffusion through the bulk of a metallic crystal (Stanley, 1978). Based on

the investigations of Nabarro (1948), Herring (1950) and Ashby (1969), a schematic diagram of volume diffusion creep can be plotted to illustrate volume diffusion behaviour.

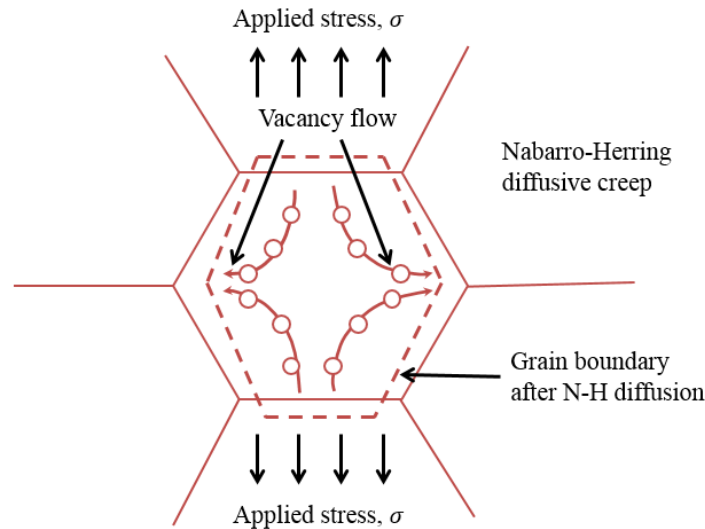


Figure 5.4: Schematic diagram of volume diffusion creep

Figure 5.4 shows a schematic diagram of how volume diffusion creep occurs in a crystal lattice. In the volume diffusion creep deformation mechanism, the vacancy is driven by the applied stress, and this mechanism usually occurs at elevated temperatures and low stresses. According to Figure 5.4, the upside and downside of the GB are forced by the applied stress when the stress is applied on the grain. The energy for the vacancy to form is very low, but the density of the vacancy is very high due to the fact that the left and right hand sides of the GB are forced by the applied stress (Greenwood, 1970). Furthermore, these vacancies through the lattice are concentrated within the grain boundaries due to the differences in density of the vacancies (Beere and Speight, 1978). Simultaneously atoms flow in the opposite direction and diffuse from the sides to the tops and bottoms in the direction of the stress applied (Nabarro, 2002).

Herring (1950) expresses diffusional flux as a function of the gradient of chemical potential of atoms and vacancies. The derived formulation for volume diffusion creep is presented as follows:

$$\dot{\epsilon} = \frac{BD\sigma\Omega}{d^2kT} \quad (5.2)$$

where  $B$  is a constant associated with the shape of grains and the types of loads.  $\sigma$  is the applied stress,  $d$  is the crystal size,  $\Omega$  is the atomic volume and  $D$  is the self-diffusion coefficient of atoms, which is expressed as follows:

$$D = D_v C_0 \Omega \quad (5.3)$$

where  $D_v$  is the diffusion vacancy and  $C_0$  is the vacancy concentration.

### 5.2.2.2 Coble creep (GB diffusion) mechanism

The Coble creep mechanism normally occurs through the diffusion of atoms along the grain boundaries in a material, and it is considered that grain boundaries can also provide an alternative path for stress-directed diffusional mass transport to take place based on the Nabarro-Herring creep mechanism (Hondros and Henderson, 1983; Penny and Marriott, 1995). In the Coble creep deformation mechanism, the crystal lattice is diffused along the boundary at low temperature ( $<0.7T_m$ ) (Mohamed and Langdon, 1974a).

Based on the studies of Coble (1963a), Mohamed and Langdon (1974a), Ashby (1983), Langdon (2002) and Abe et al. (2008), a schematic diagram of GB diffusion creep can be plotted to illustrate GB diffusion behaviour.

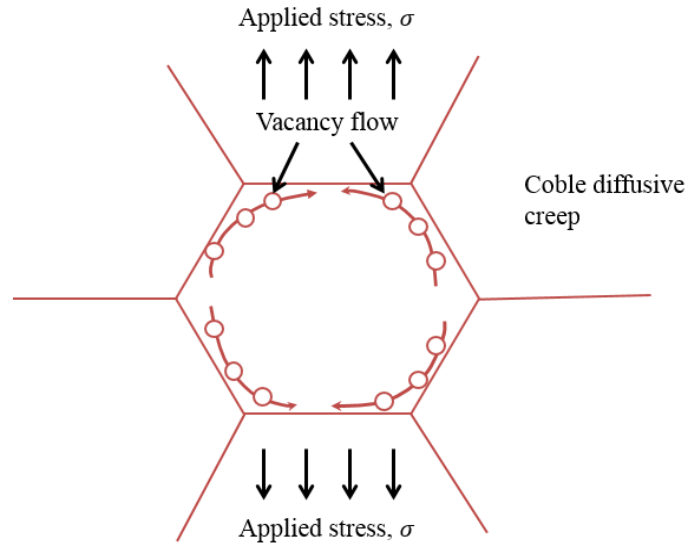


Figure 5.5: Schematic diagram of GB diffusion

Figure 5.5 shows a schematic diagram of how GB diffusion creep occurs in a crystal lattice. In the GB diffusion creep mechanism, the vacancy is driven by the applied stress and flows through the GB. This mechanism is usually caused by low applied stress and at a lower temperature than that of volume diffusion creep (Riedel, 1987). The GB acts as a planar channel about two atoms wide, with a high diffusion rate that is related to the applied stress (Milne et al., 2003). The vacancy flows through the GB from the high vacancy density area to the low density area (Mott, 1951). Then the atoms along the GB will diffuse in the opposite direction, which causes the creep rate to change (Li and Dasgupta, 1993).

At relatively low temperatures and small grain size, the GB diffusion mechanism prevails in lattice diffusion, and diffusional creep occurs through mass transport along grain boundaries. Coble (1963a) derived the following creep equation by assuming spherical grains:

$$\dot{\epsilon} = \frac{B_1(\delta_B D_B)\sigma\Omega}{\pi d^3 kT} \quad (5.4)$$

where  $D_B$  is the GB diffusion coefficient,  $\delta_B$  is the GB thickness and  $B_1$  is the constant. The coble creep rate is inversely proportional to  $d^3$ , and the activation energy for diffusional creep is equal to that for GB diffusion.

### **5.3 Creep damage mechanisms**

Creep damage is manifested by the nucleation and growth of creep cavities within the microstructure of the material (Myers, 1985). Studies monitoring cavity nucleation and growth with strain after creep deformation have provided limited information with regard to varying applied stresses. This information is especially limited for Low Cr alloy steels, which are extensively used for component operation at elevated temperatures and low stresses, and in particular for piping and pressure vessel applications of the power generating industry. The mechanisms contributing to the creep strength of low alloy steels have been shown to be complex, but they can generally be related to three main aspects: 1) cavity site; 2) cavity nucleation mechanism; and 3) cavity growth mechanism.

#### **5.3.1 Cavity site**

Cavities are often initiated at the intersection of a slip band with a GB or at ledges in the boundaries (Ashby, 1972). Commercial materials usually contain second phase particles in the vacancy path, causing obstruction on the GB in order to prevent or minimise GB sliding (Riedel, 1987). These particles are prone to nucleate cavitation and they can affect the mechanical properties of materials adversely (Benci et al., 1988). The experimental evidence from studies such as those by Cane and Middleton (1981), Chen and Argon (1981b), Myers (1985), Needham and Gladman (1986), Walker (1997), Kassner and Hayes (2003) and Binda et al. (2010) show that low Cr alloy cavities are often associated with the following sites:

- a) GB ledges: cavity nucleation at a ledge is the predominant nucleation mechanism in pure metals (Watanabe, 1983). The ledges can be grown-in features of the GB or they can result from slip in the adjacent grains which intersect the boundary (Riedel, 1987). In pure metals, the GB ledge sites experience a concentration of stress because they resist GB sliding (Stanley, 1978). The ledge experiences tensile or compressive stress and only the tensile ledges are expected to initiate cavities (Riedel, 1987). Due to their geometry, ledges are commonly compressive in

nature (Riedel, 1987). However, the application of an external compressive load leads to ledges which will in turn experience a tensile stress, and as a result it is possible for cavities to be initiated (Anderson and Rice, 1985).

- b) GB triple junctions: with GB diffusion, triple junction diffusion is capable of playing an important role in the creep deformation of low Cr alloy steels (Kassner and Hayes, 2003). Creep deformation in metals with a small grain size can provide diffusion along GB triple junctions, and creep strain rate associated with triple junction diffusional creep can contribute to cavity nucleation (Perry, 1974). The initial stress concentration at the GB triple junction is obviously larger than the applied stress, and even after relaxation by diffusion, the stress may still be elevated, leading to an increased local rate of cavity nucleation (Anderson and Shewmon, 2000).
- c) Secondary particles: second phase particles are a common location where cavities are nucleated. In low alloy steels, some previous works such as those by Lombard and Vehoff (1990), Svoboda and Sklenička (1990), Wu and Sandström (1995) and Horstemeyer et al. (2000) have proved that such cavitation can be observed in second phase particles. Furthermore, second phase particles can result in stress concentrations upon application of stress, and increase cavity nucleation at grain boundaries through vacancy condensation by increasing GB free energy (Loh, 1970). Moreover, particles can be effective barriers to dislocation pile-ups. However, the interface of the particle cannot accommodate the atom, and thus high stresses on particles may result in the possibility of promoting cavity nucleation (Riedel, 1987).

### **5.3.2 Cavity nucleation mechanism**

The influences of various macroscopic mechanisms, and their interaction, on the nature and severity of creep deformation have been outlined above. However, before creep damage constitutive equations can be developed

to depict the creep behaviour of structural components, account must be taken of the investigation of mechanisms of creep cavity nucleation.

The cavity nucleation mechanism can be described according to the category of creep deformation process as follows:

- I. The cavity nucleation mechanism based on dislocation creep.
- II. The cavity nucleation mechanism based on diffusion creep.

#### **5.3.2.1 Cavity nucleation mechanism based on dislocation creep**

Dislocation movement causes vacancy condensation on the GB and inside the grain, which causes the cavity to nucleate (Chokshi, 2005). Perry (1974) first presented experimental evidence for the dislocation mechanism of cavity nucleation, but there was a bewildering lack of certainty regarding the extent to which dislocation and local diffusion reduces the accumulation of stress concentrations. Later on, Rediel (1987) suggested that GB sliding is a prerequisite for the nucleation of cavities, and that cavities nucleate primarily along boundaries approximately perpendicular to the maximum principal stress axis (the direction along which sliding is minimal). Despite the difficulties of adequate metallographic examination, several studies on the number of cavities observed, such those of Loh (1970), Chen and Argon (1981b) and Riedel (1987), indicated that the stress and creep rate are independent of grain size. They also suggested that the dragging force is an outcome of solute atoms segregating to stacking faults, and the ordering of the region surrounding a dislocation reduces the total energy of the crystal by pinning the dislocation.

Based on the investigations of Bilby and Eshelby (1968), Greenwood (1970) and Riedel (1987), a schematic diagram of the formation and condensation of vacancy on GB under the dislocation process can be plotted to illustrate how dislocation influences the formation and condensation of a vacancy.

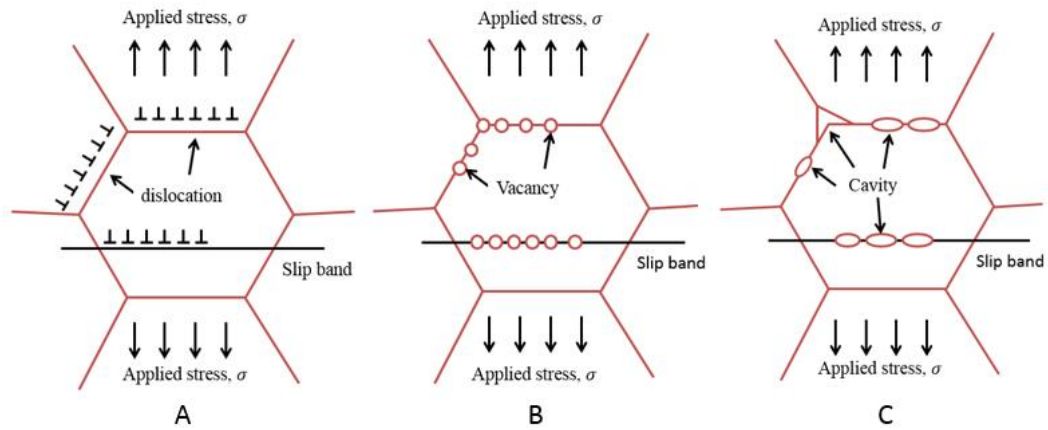


Figure 5.6 Schematic diagram of the formation and condensation of vacancy on GB under the dislocation process

Figure 5.6 (A to C) shows how vacancy condensation on the GB and inside the grain influence cavity nucleation. The formation and condensation of vacancies can be described by the power-law (Greenwood et al., 1954) as involving cell formation by climbing and being constrained by gliding. The condensation of dislocations on the G will cause an increase in the density of a vacancy; thus, the vacancies accumulate on the triple point of the GB, which is perpendicular to the applied stress direction (Riedel, 1987). The vacancy condensation at the triple point leads to a change in the cavity shape, and the vacancy condensation on the perpendicular GB causes stress redistribution (Beere and Rutter, 1978).

One of the most likely nucleation sites is that of the second phase particles contained in the boundary plane (Cane, 1979; Miller and Pilkington, 1978; Lonsdale and Flewitt, 1979). Based on the dislocation theories of Watanabe and Davies (1978), Nieh and Nix (1980) and Riedel (1987), a schematic diagram of how dislocation creep influences the cavity nucleation associated with carbides or particles can be plotted.

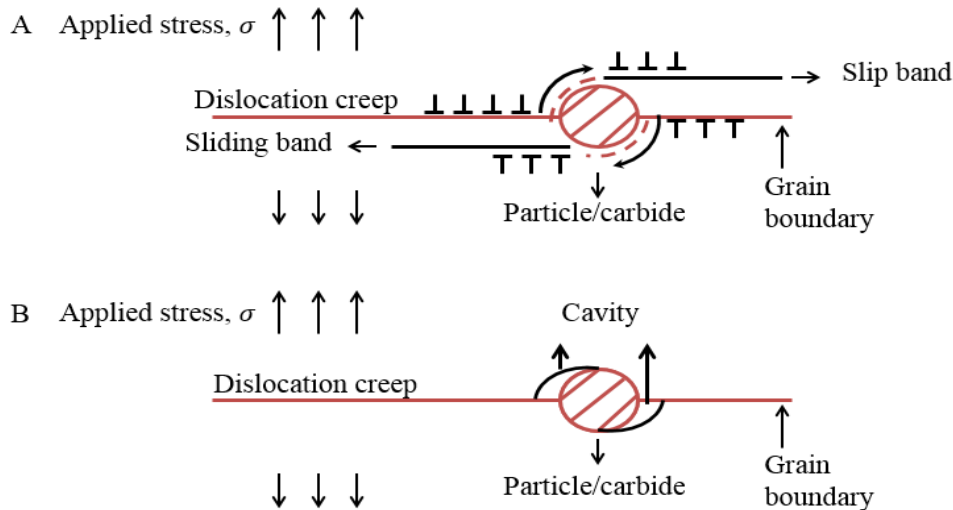


Figure 5.7: Schematic diagram of how dislocation creep influences the cavity nucleation associated with carbides or particles

Figure 5.7 shows how dislocation creep influences the cavity nucleation associated with carbides or particles. Figure 5.7 (A) illustrates the dislocation movement occurs which made the vacancies gather around the particle or carbide with the movement of the sliding band. Figure 5.7 (B) shows the cavity occurs due to the condensation of the vacancies caused by the dislocation movement. According to Figure 5.7, the dislocation motion can be arrested by obstacles such as second phase particles. Vacancies diffuse into the dislocation core, allowing dislocation to climb. The decohesion behaviour occurs at the particle or particle-matrix interface as a result of dislocation pile-ups.

### 5.3.2.2 Cavity nucleation mechanism based on diffusion creep

Cavity nucleation is still considered within classical diffusion theory (Goods and Nieh, 1983; Stanzl et al., 1983). The diffusion creep process is controlled by stress-directed atomic movement through structural components, and this movement of atoms leads to stress concentration at obstacles like second phase particles and triple grain junctions, resulting in the enhancement of cavity nucleation (Balluffi and Cahn, 1981) .

Experimental evidence from previous works such as those by Fleck et al. (1975), Cane and Greenwood (1975) and Chen and Argon (1981b) suggests that the nucleation process is controlled by diffusion. In the

diffusion process, vacancies generate and agglomerate on the GB, and a super saturation of vacancies can produce a cavity. A schematic diagram of the formation and condensation of vacancies on a GB under the diffusion process is shown in Figure 5.8.

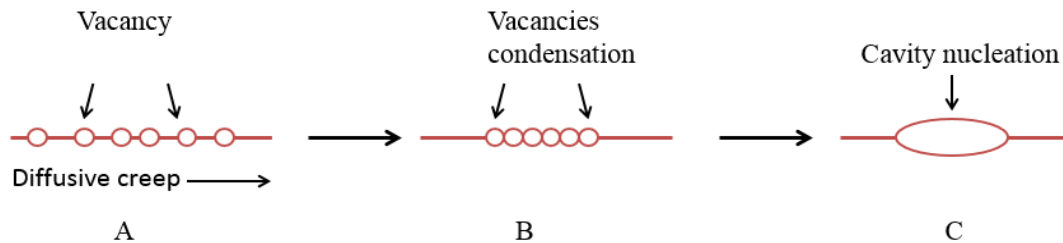


Figure 5.8: Schematic diagram of the formation and condensation of vacancy on GB under the diffusion process

Figure 5.8 shows a schematic diagram of how diffusion creep influences vacancy condensation (A and B) and forms a creep cavity (C). It should be noted that cavity nucleation is primarily stress controlled, but the stresses necessary for nucleation are found to be much greater than the applied stress (Seitz, 1952). Thus, the influence of stress concentrations must be considered in relation to the nucleation of a creep cavity. According to Riedel (1987), there is a critical stress for nucleation, above which voids nucleate almost at the instant of load application. If the stress is over this critical stress, the vacancy will aggregate on the G, which leads to the formation of a cavity.

Under the diffusion creep process, GB sliding can produce tensile stress concentrations at the particle-matrix interface which enhance the probability of a nucleation event (Burton, 1973). The following figure is presented to describe how GB creep influences the cavity nucleation associated with particles.

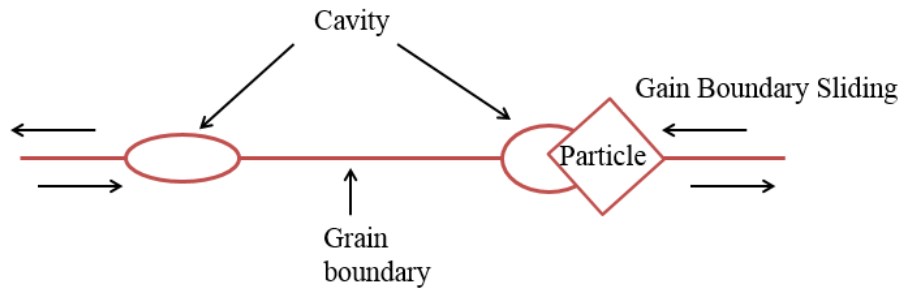


Figure 5.9: Schematic diagram of the generation of cavity nucleation associated with particles caused by GB sliding

According to Figure 5.9, high stress concentrations can be produced at particles by sliding grain boundaries. It should be emphasised that the stress concentration could be influenced by the thickness of particles, and that the nucleation stress is reduced with a decrease in the thickness of the particle (Riedel, 1987). As far as precipitate particles are concerned, an optimum size range will exist in the process of cavity nucleation. Furthermore, Chen and Argon (1981b) indicate that sudden rapid GB sliding can generate sufficiently large stresses for nucleation to be possible. Thus, cavity nucleation is dependent on the local stress and not simply on the overall applied stress.

### 5.3.3 CGM

There has been a great deal of discussion on the possible processes that contribute to cavity growth, such as those by Dyson (1976), Cocks and Ashby (1981) and Tvergaard (1990). Originally, in terms of modelling, a regular network of equilibrium cavities, with the number remaining constant throughout the life of a creep test, was considered by Dyson (1976). Later on, Tvergaard (1990) reported that the number remaining constant throughout the life of a creep test is not satisfactory, because creep cavities tend to nucleate continuously throughout a creep test and non-equilibrium cavity shapes may form at various creep stages during the test. Here, the CGM is described according to the category of creep deformation process as follows:

- I. The cavity growth process based on dislocation creep.
- II. The cavity growth process based on diffusion creep.

### 5.3.3.1 CGM-based on dislocation creep

The growth of cavities has received considerable attention over recent decades and it is apparent from the literature that most research work on the growth of cavities along grain interfaces is based on GB diffusion. However, a few publications, such as those of Hull and Rimmer (1959), Ishida and McLean (1967) and Raj and Ashby (1975), indicate that dislocation creep can contribute to creep cavity growth because extensive dislocation creep allows local accommodation of matter diffused into the GB. In dislocation creep, cavities grow with a spherical morphology by accepting vacancies from the surrounding material at low stress levels (Stanley, 1978).

Based on the investigations of Chen and Argon (1981a), Riedel (1987) and Kassner and Hayes (2003), a schematic diagram of the effect of dislocation creep on cavity growth associated with the triple point can be plotted to illustrate cavity growth behaviour.

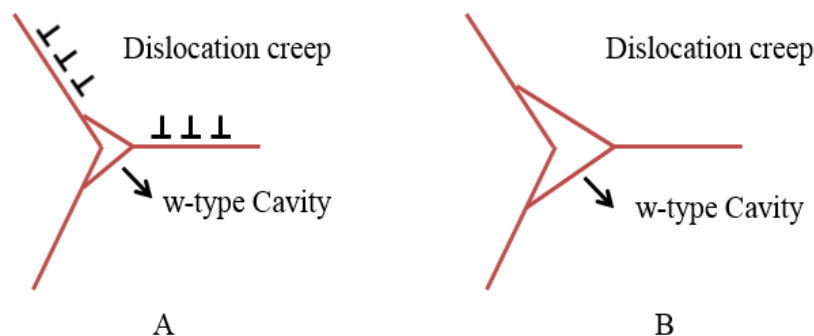


Figure 5.10: Schematic diagram of the effect of dislocation creep on cavity growth associated with the triple point

Figure 5.10 shows how dislocation creep influences the cavity growth associated with the triple point. Figure 5.10 (A) illustrates the condensation of vacancies at the small cavity. Figure 5.10 (B) shows the condensation of the vacancies at small cavity which has contributed to the growth of the cavity size. In this figure, the process of cavity growth associated with the wedge-type (w-type) cavity at the triple point of the GB is presented. The dislocation occurs along the GB and the interaction of the dislocation movement causes the vacancy to condensate; this then

causes stress concentration at the triple junction as a result of the growth of the cavity (Kassner and Hayes, 2003).

### **5.3.3.2 CGM-based on diffusion creep**

Most of the theories and models that have been proposed describe cavity growth as the coupling of diffusional cavity growth with the creep deformation of the material surrounding the cavity. Beere and Speight (1978) first addressed this problem by assuming that each cavity is surrounded by a non-deforming zone of material within the diffusional cavity growth. Later on, Edward and Ashby (1979) proposed a similar model which has different boundary conditions. These models are proposed through the use of a pure diffusion constitutive law for diffusion and creep deformation, and thus they are only an approximate solution for creep analysis. The use of a numerical finite element technique in analysing the growth of cavity has been demonstrated by Horstemeyer et al. (2000) and Isaac et al. (2008), and this can be used to obtain a more rigorous solution allowing for deformation to occur in the material immediately surrounding the cavity. The important finding achieved through the use of the finite element technique is that cavity growth is controlled by diffusional processes when they are close together, and by creep deformation when they are far apart (Ghosh and Raj, 1981). Pardoen and Hutchinson (2000) suggest that the radius of the diffusion zone extends a distance equal to the cavity spacing at low stress and temperature, and therefore growth is purely diffusional. At high stress and temperature, the size of the diffusion zone is less than the cavity spacing, so growth occurs by a coupled process (Cocks and Ashby, 1981). Based on the investigations of Jaeger and Gleiter (1978) and Rediel (1987), a schematic diagram of the effect of diffusion creep on creep cavity growth can be plotted to illustrate the processes of cavity growth under diffusion creep.

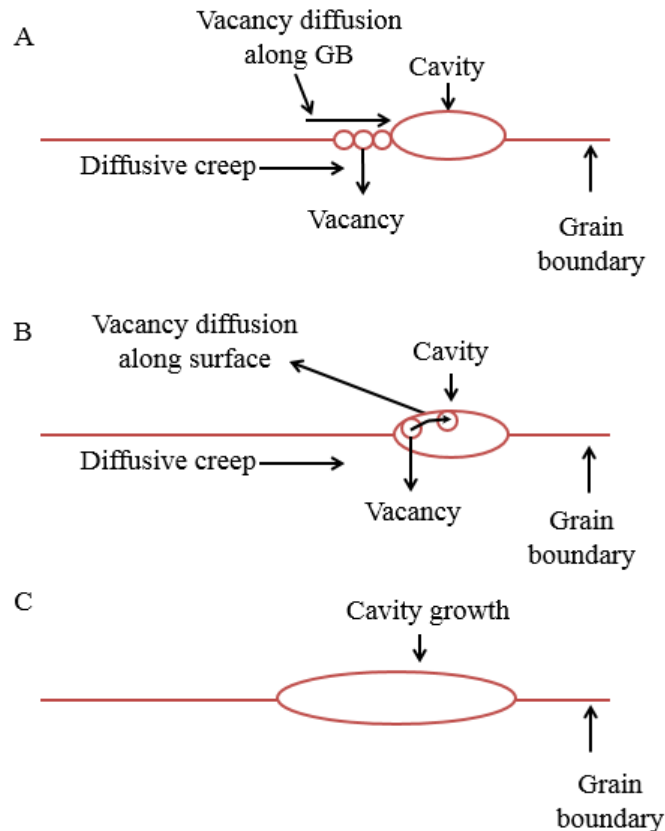


Figure 5.11: Schematic diagram of the effect of diffusion creep on cavity growth

Figure 5.11 shows a schematic diagram of the influence of diffusion creep on cavity growth. When the cavity is nucleated under stress, the vacancy will move from one side to another within the GB or through the lattice. The cavity aggregated on the GB, which is associated with a high density of vacancies, will lead to the formation of a crack with perpendicular stress applied on the GB. This behaviour will lead to the cavity size growing and coarsening, and will form into a crack contributing to damage in the tertiary stage.

Under the diffusion process, GB sliding represents a typical degree of freedom which becomes active at elevated temperatures. The process has at least three different aspects and each is related to a different size scale (Riedel, 1987). On an atomic scale, the resistance against sliding is determined by the mobility of grain-boundary dislocations. It is generally believed that in engineering high temperature materials, this intrinsic sliding resistance is negligible compared to the effect of hard second-phase particles in the boundary. The GB slide is forced by the applied

stress; therefore, GB sliding contributes to the elongation of the GB. As the grain elongates, the grain centres move to preserve GB continuity (Perry, 1974; Stanley, 1978; Riedel, 1987; Penny and Marriott, 1995). A schematic diagram of the effect of GB sliding on cavity growth at the GB is shown as follows:

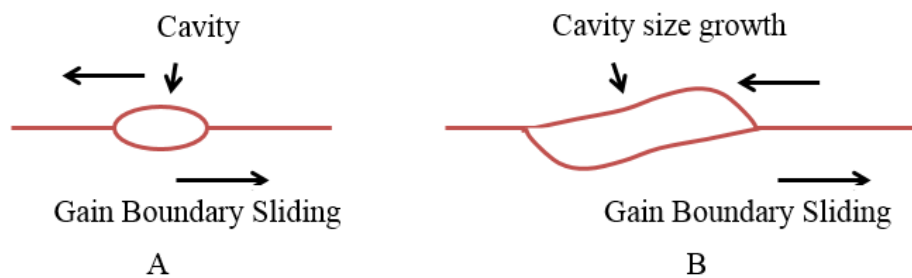


Figure 5.12: Schematic diagram of the effect of GB sliding on cavity growth at GB

Figure 5.12 shows the growth of cavity size in conjunction with the mechanisms of GB sliding. The sliding behaviour of the GB (Figure 5.12 A) causes the cavity to move from one side to another, and therefore, the size of the cavity is increased. At the triple junction, the stress concentration will increase the cavity growth (Figure 5.12 B).

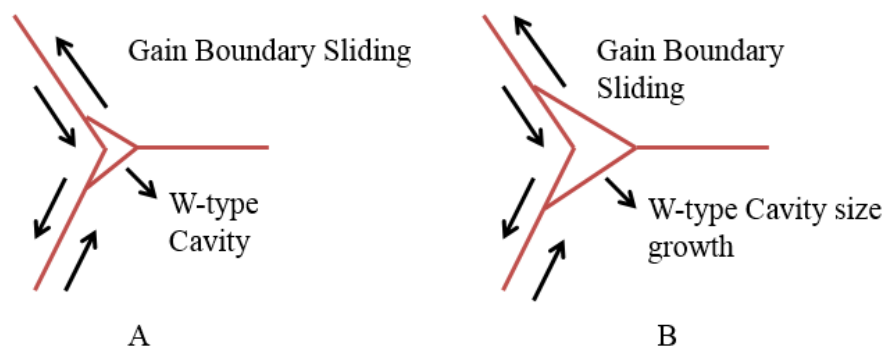


Figure 5.13: Schematic diagram of the effect of GB sliding on cavity growth at triple junction

Figure 5.13 shows the growth of cavity size at the triple junction in conjunction with GB sliding. This behaviour is caused by the GB sliding at the triple junction. At the triple point, the stress concentration will cause the GB sliding to become faster. The sliding behaviour of the GB (Figure

5.13 A) causes the cavity to move from one side to another, and as a result, the size of the cavity is increased (Figure 5.13 B).

According to Langdon (1970), Yoo and Trinkaus (1983) and Riedel (1987), GB sliding behaviour does not contribute significantly in a stable state. However, it is important in the initiation of inter-granular voids and this mechanism has a significant impact on the accumulation of damage. It is noted that this mechanism relies strongly on grain size. If the grain size is large, this process makes little contribution to the whole creep strain and has only a small influence on creep deformation; whereas if the grain size is small enough, this process makes a large contribution to creep strain and creep rate, which has a great influence on creep deformation.

#### **5.4 Creep rupture mechanisms**

Creep fracture is usually caused by the processes of nucleation and growth of cavities (Kassner and Hayes, 2003). With the continued growth of voids, creep cracks grow from the cusp and ultimately weaken the cross section to the point where failure occurs (Viswanathan, 1989). The cavitation process, which includes cavity nucleation, cavity growth and cavity linkage, is the most important factor that weakens the material and results in rupture. During the secondary stage and tertiary stage, the cavity density and cavity size increase. This behaviour causes the creep damage to accumulate, and this damage accumulation behaviour is significantly influenced by the stress level.

There are two typical types of rupture behaviour that predominantly lead to final rupture. One is controlled by continuous cavity nucleation and the other is controlled by cavity growth (Dyson, 2000). The creep fracture process usually initialises at the end of the secondary stage and continues in the tertiary stage (Kassner and Hayes, 2003). This means it is associated with the process of creep deformation that could form cavities.

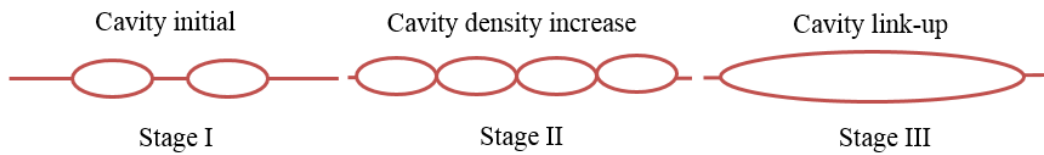


Figure 5.14: Schematic diagram of the effect of cavity nucleation on creep fracture

Figure 5.14 (Stage I to Stage III) shows the process of creep fracture under the cavity nucleation mechanism. With the nucleation of new cavities, the cavity density will be increased and the mutual connection of micro-cavities and micro-cracks will cause creep fracture. However, cavity nucleation is not the only factor that accelerates the creep rate. The second-phase particles and carbides can also accelerate the creep rate and cause the microstructure of material to degrade. These impurities behave as obstacles against dislocation, and against the GB sliding motion which causes the stress concentration on grain boundaries or triple points that contributes to creep rupture. In long-term service, some impurities which have grown into a larger size will lead to the loss of creep strength (Lonsdale and Flewitt, 1979).

It is noted that particle coarsening and concomitant softening of material have been observed in creep-resistant low Cr alloy steels by Williams and Wilshire (1977) and Williams and Cane (1979). Furthermore, Dyson and McLean (1983) have pointed out that damage accumulation cannot be explained by cavity nucleation alone. At least some aspects of accelerated creep rate are produced by particle coarsening. Therefore, the rupture mechanism for low Cr alloy should include cavity growth.

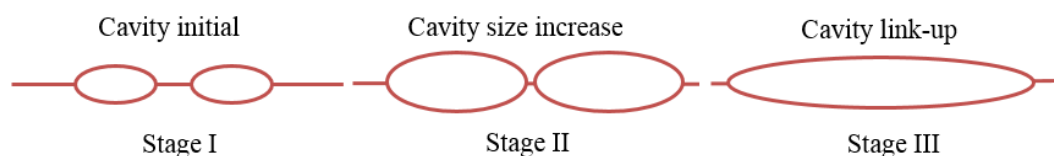


Figure 5.15: Schematic diagram of the effect of cavity growth on creep fracture

Figure 5.15 (Stage I to Stage III) shows the process of creep fracture under the cavity growth mechanism. With growth in the size of cavities, to

the stage of linkage, the mutual connection of micro-cavities and micro-cracks will cause creep fracture.

The fracture mechanism map, as an effective method of representing the fracture model at any combination of stress and temperature, was first proposed by Ashby (1977). This map indicates the different fracture mechanisms of creep operating in a material as a function of stress, temperature and grain size.

Fracture mechanism maps such as those produced by Ashby (1977), Miller and Langdon (1979) and Krishnamohanrao et al. (1986) have been summarized by Rediel (1987). A famous schematic diagram of the fracture-mechanism map was proposed by Rediel (1987) and is shown in Figure 5.16.

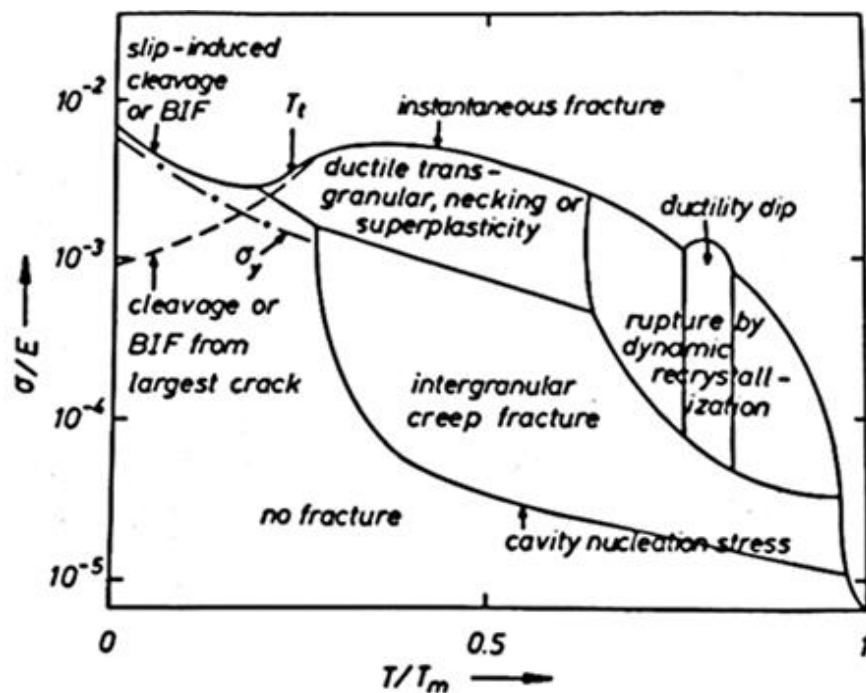


Figure 5.16: Schematic diagram of creep fracture mechanism map (Riedel, 1987)

Different regions are presented for a range of stresses and temperatures over which a specific mechanism is anticipated to be the principle process of creep (Riedel, 1987). The fracture mechanisms can be described according to the category of stress level. At high stress levels, creep fracture is usually associated with the trans-granular fracture mechanism,

whereas at low stress levels, creep fracture is mainly investigated based on the inter-granular fracture mechanism (Ashby et al., 1979).

The mechanisms appearing on the fracture mechanism map can be classified according to stress level category as follows:

- I. Creep fracture mechanisms under high stress levels.
- II. Creep fracture mechanisms under low stress levels.

#### **5.4.1 Creep rupture mechanisms under high stress levels**

In metals and alloys which creep at high stress levels, the key features of rupture mechanisms within this category can be classified as follows:

- a) Trans-granular creep rupture mechanism: trans-granular creep fracture requires either that voids pre-exist or that voids nucleate at inclusions which concentrate stress (Ashby et al., 1979). The size of voids grows by creep deformation around inclusions, elongating them in the direction where the stress is applied, and the flow stress is determined by the strain rate, which can be governed by power-law creep (Riedel, 1987).
- b) GB controlled rupture mechanism: at high stresses, trans-granular rupture behaviour may depend on GB controlled rupture, where w-type cracks or round types of voids are allowed to nucleate and grow at the GB, normally lying at the axis of tensile stress or lying at 45° to applied stress (Stanley, 1978). The local shear strain rate in the boundary is obviously greater than that in the grain because of the nucleation of boundary inclusions (Riedel, 1987). This mechanism can contribute to necking behaviour at the final rupture stage, and it can enhance the accumulation of creep deformation and the value of creep strain rate.
- c) Ductile rupture mechanism: ductile failure is usually found at low temperatures and high stresses. The process of this fracture mechanism is similar to that of trans-granular creep fracture (Benzerga and Leblond, 2010). Voids nucleate at inclusions and

the plasticity promotes their growth. When voids grow big enough, they may coalesce and trigger the fracture of components. As a new void is nucleated and connects with other voids, this could result in fracture. Ductile fracture usually accompanies trans-granular fracture. However, it may accompany inter-granular fracture if the void density becomes higher in the boundaries (Briant and Banerji, 1978).

- d) Plastic-hole growth controlled rupture mechanism: at high stresses, thermal- and strain-induced structural degeneration due to large plastic strains are produced by normal dislocation processes (Viswanathan, 1989). Rupture is associated with the plastic growth of internal holes that nucleate at the interface of coarse precipitate particles or inclusions. Internal necking of materials between the holes leads to coalescence (Stanley, 1978). Especially at high strain rates and stresses, void growth can be significantly improved by the plastic deformation of the surrounding material (Riedel, 1987).

#### **5.4.2 Creep rupture mechanisms under low stress levels**

In metals and alloys which creep at low stress levels, the key features of the rupture mechanisms can be classified as follows:

- a) Inter-granular rupture mechanism: the process of inter-granular fracture usually occurs at lower stresses and elevated temperatures. In this rupture process, void growth by creep becomes very slow as fracture by GB cavitation intervenes (Riedel, 1987). Rediel (1987) reports that the shear deformation observed at grain boundaries in inter-granular creep was much lower than that in trans-granular creep. Creep void growth is controlled by dislocation creep at the primary and secondary creep stages when voids are small, whereas diffusion creep contributes to void and crack growth synchronously.

- b) Pure diffusional rupture mechanism: at low stresses and high temperatures, particularly where the stress is extremely low, cavities on the GB are grown by the mechanism of diffusion alone (Ashby and Brown, 2014). Voids on grain boundaries subjected to tensile forces experience a gradient of chemical potential of vacancies. Vacancies migrate under the influence of the gradient which causes the void to grow. The exact rate of growth can be determined by the diffusion process and the shape of void (Raj and Ashby, 1975; Riedel, 1987). With the growth of cavities, this type of fracture will progress to either inter-granular fracture or trans-granular fracture. If the stress is over the critical value, vacancies will aggregate on the GB, leading to the formation of cavities.
- c) Brittle rupture mechanism: brittle failure is usually found at high temperatures and low stresses. The process of this fracture mechanism is similar to that of inter-granular creep fracture. Brittle rupture mechanism is the rupture of a metal at high temperature and low stress without appreciable prior plastic deformation. It is a break in a brittle piece of metal which has failed because stress has exceeded cohesion (Abe et al., 2008). It usually occurs at unpredictable levels of stress by rapid crack propagation, and the strain at failure is usually less than 5% (Viswanathan, 1989). In the fracture area, many pieces can be observed through the brittle fracture process (NIMS, M/CDS/No. 3B, 1986).
- d) Constrained cavity growth (continuous cavitation) controlled rupture: at low stresses, the local deformation due to the growth of inter-granular voids exceeds the deformation rate of the surrounding material. As a result, stresses are redistributed and the local strain rate increases dramatically (Hales, 1994).

## 5.5 Summary

This chapter has investigated creep deformation mechanisms based on the creep deformation processes of dislocation and diffusion. Subsequently, the identification of creep behaviour under different

temperature and stress ranges has been achieved through the investigation of mechanisms such as dislocation glide creep, dislocation climb creep, Nabarro-Herring diffusion creep and Coble creep.

The chapter has also illustrated creep damage mechanisms. The mechanisms involved with cavitation characteristics in creep damage behaviour have been understood through the investigation of cavity sites, the cavity nucleation mechanism and the cavity growth mechanism. Finally, rupture mechanisms under both high and low stress levels have been investigated.

# **Chapter 6 Analysis of the effects of stress level on creep damage behaviour for low Cr alloys**

## **6.1 Introduction**

All materials exhibit stress range dependent creep behaviour, and the respected power-law creep is widely used in practice to predict creep behaviour under a variable stress history. However, at transition stage, the superposition of two mechanisms may spontaneously produce an apparent rupture process at a relatively low creep rate. Furthermore, the existing creep damage constitutive equations, such as the Kachanov-Rabotnov equation which was developed based on power-law creep, does not include the related mechanisms for low Cr alloys, and the definition of stress level is still vague in this area. In order to develop a set of constitutive equations to accurately describe the process of creep, an analysis of the effects of physically-based stress on creep behaviour for low Cr alloys ought to be involved in this research.

The specific areas of focus for this chapter include:

- 1) To analyse the effects of stress level on creep curve. The typical creep curve and the effects of stress level on creep curve for low Cr alloys should be analysed in order to identify the dominative mechanism at different stress levels.
- 2) To analyse the effects of stress level on creep parameter. A physically-based analysis of the effects of stress level on the minimum creep rate, rupture time and strain at failure should be conducted; then, the stress level definitions involved in developing creep damage constitutive equations for low Cr alloys should be proposed.
- 3) To analyse the effects of stress level on creep cavity behaviour. The effects of stress level on creep cavity shape, cavity site, cavity

nucleation and growth should be analysed in order to contribute to the design of a rupture criterion associated with the damage equation.

## **6.2 Analysis of the effects of stress level on creep curve**

Practical lifetime design in newly-developed long-term structural components, and technical and financial restrictions in test durations, mean that extrapolation of short-term experimental test results to predict long-term rupture of high temperature service components is an area of concern when conducting a fitness for service or remaining life assessment. However, Sawada et al. (2009) report that in uniaxial creep rupture tests, some materials show lower rupture time during long-term creep tests, and the creep curves predicted by constitutive equations based on accelerated creep tests cannot fit the actual long-term creep behaviour. Thus, an analysis of the effects of stress from actual physically-based long-term creep tests on creep transformation at constant temperature should be addressed in this project.

### **6.2.1 Typical creep curve**

The creep curve usually changes with increases of stress and temperature (Nabarro and Villiers, 1995). It is noted that Viswanathan (1989) has summarised creep data and plotted a typical creep curve to show the trend of creep with stress and temperature changes.

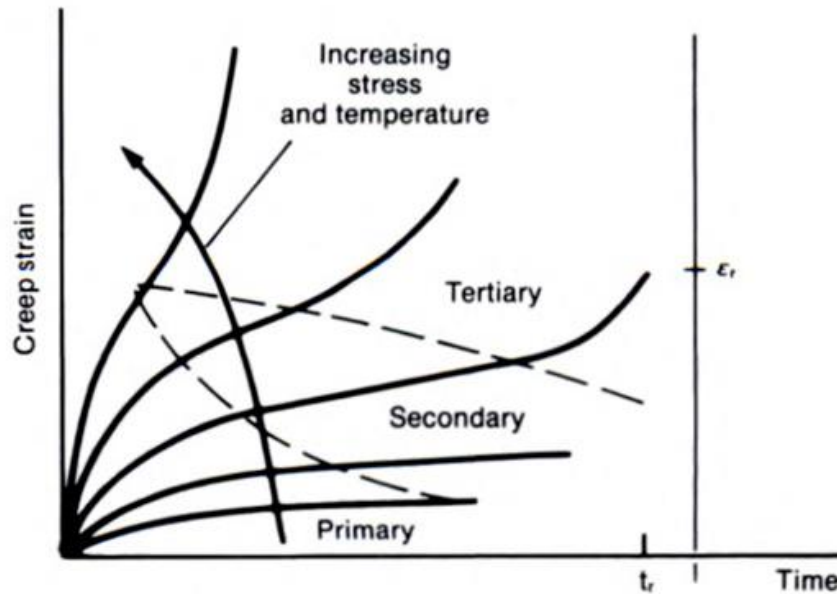


Figure 6.1: The typical creep curve (Viswanathan, 1989)

Figure 6.1 illustrates the general tendency of the effects of stress level on creep transformation. This curve can be applied in the analysis of creep transformation for various materials, and both low Cr alloys and high Cr alloys can be simply described through the use of this typical creep curve. According to Figure 6.1, the process of creep deformation under different stress levels can be summarised as follows:

- At low stresses, the primary and secondary creep stages account for approximately 80% of the total rupture time.
- At high stresses, the tertiary stage occupies about 80% of the total rupture lifetime and the creep strain at failure is obviously higher than that at low stresses.

### 6.2.2 Analysis of the effects of stress level on creep curve for low Cr alloys

Analysis of the effects of stress level on creep curve for low Cr alloys was undertaken through the investigation of experiment data for the evolution of creep strain under the stresses 40MPa ( $0.31\sigma_Y$ ), 54MPa ( $0.42\sigma_Y$ ) and 70MPa ( $0.54\sigma_Y$ ) at 640°C for 0.5Cr-0.5Mo-0.25V base material (Hyde et al., 1998). From these experiment data, the creep curve can be plotted as shown in Figure 6.2.

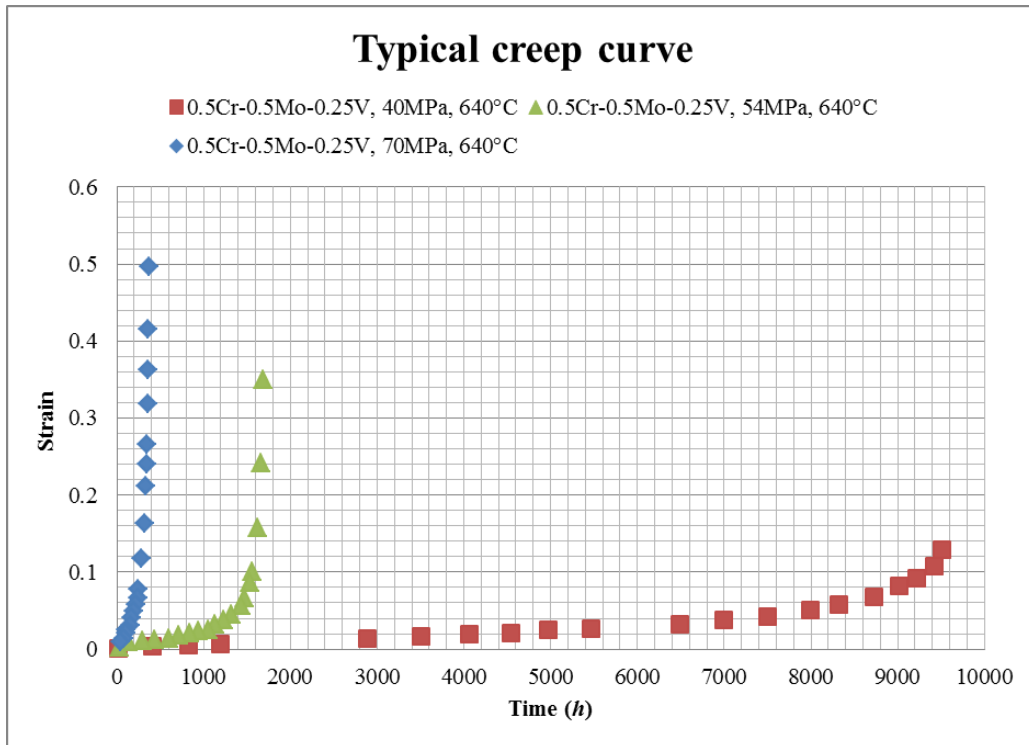


Figure 6.2: Creep curves under the stresses 40MPa ( $0.31\sigma_Y$ ), 54MPa ( $0.42\sigma_Y$ ) and 70MPa ( $0.54\sigma_Y$ ) at 640°C for 0.5Cr-0.5Mo-0.25V steel

Figure 6.2 shows the evolution of creep strain under the stresses 40MPa ( $0.31\sigma_Y$ ), 54MPa ( $0.42\sigma_Y$ ) and 70MPa ( $0.54\sigma_Y$ ) at 640°C for 0.5Cr-0.5Mo-0.25V base material. According to Figure 6.2, the percentage of tertiary creep stage in rupture time significantly increases from the low stress level to high stress level. Furthermore, the creep strain at failure time under the high stress level is obviously higher than that at the low stress level.

The above phenomenon is caused by the different dominant creep deformation mechanisms at the different stress levels. At high stresses, the accumulation of creep strain at the tertiary stage is controlled by ductility incensement (creep dislocation mechanisms), which is affected by the formation of nucleation and the reduction of surface load-carrying capacity. However, at low stresses, the rupture behaviour is found to be brittle (diffusion mechanisms) (Shibli and Holdsworth, 2009). Furthermore, at low stresses, cavity nucleation will cause reduction of the effective bearing area on the grain boundaries, which leads to brittle rupture. Thus, the creep strain at failure under low stresses is relatively low.

## **6.3 Analysis of the effects of stress level on creep parameter**

The creep strain trajectories over time at the different stress levels exhibit the different dominative mechanisms of damage accumulation at high and low stress levels. Recent developments in creep damage constitutive equations have led to a renewed interest in mechanistic creep failure analysis. However, it is still not certain which factor plays the key role in tertiary creep stage rupture. Recently, investigators have examined the effects of external section loss, internal section loss and the degradation of microstructure. In order to accurately develop constitutive equations to describe creep damage for low Cr alloys under long-term service, the analysis of the effects of stress level on creep parameters was focused on an investigation of minimum creep rate, rupture time and creep strain at failure on the basis of physically-based experiment data.

### **6.3.1 Analysis of the effects of stress level on minimum creep rate**

Creep often takes place in three stages. In the initial stage, strain occurs at a relatively rapid rate but the rate gradually decreases until it becomes approximately constant during the second stage. This constant creep rate is called the minimum creep rate, or steady-state creep rate, since it is the slowest creep rate during the test. The minimum creep rate is often chosen as a characteristic parameter representing the major part of the creep life for evaluated materials (Viswanathan, 1989). This parameter represents a vital role in creep damage constitutive equations. To address the deficiencies in current creep damage constitutive equations highlighted in Chapter 3, further enhancement should be focused on developing a new constitutive equation for describing minimum creep rate with particular regard to low stress levels for low Cr alloys.

In order to describe the stress dependence of creep, accurate identification of the effects of mechanisms on creep rupture is essential. The use of the stress exponent to identify the dominative mechanism in the process of rupture is widely adopted in developing a constitutive model based on power-law creep. Here, a classical schematic diagram to

illustrate the stress dependence of the steady-state creep rate, as proposed by Yavari and Langdon (1982), is shown in Figure 6.3.

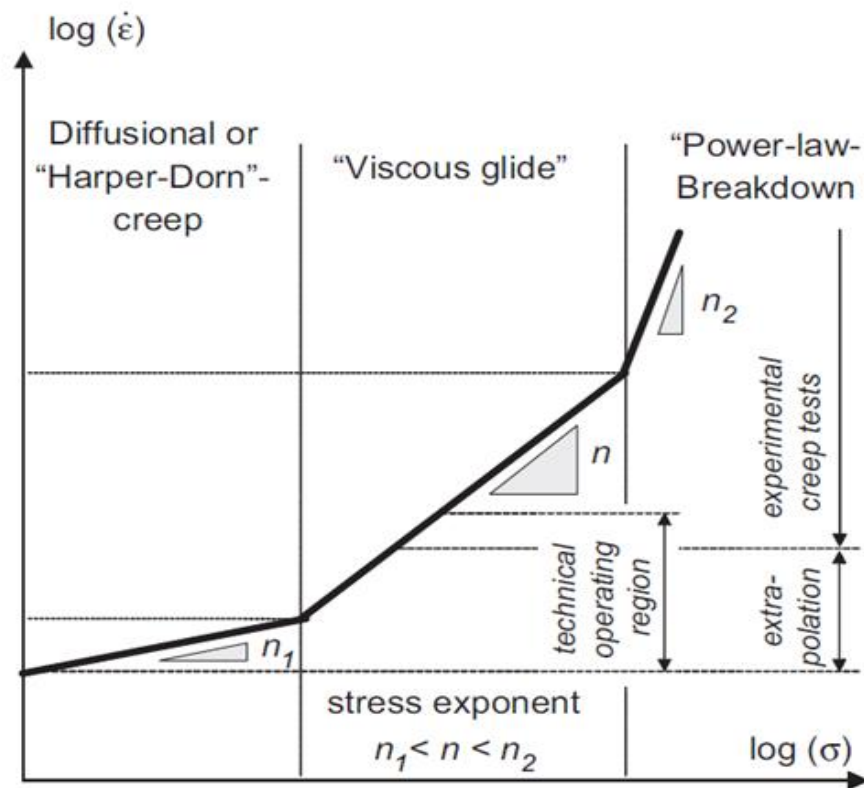


Figure 6.3: Schematic diagram of stress dependence of steady-state creep rate (Yavari and Langdon, 1982)

Figure 6.3 shows a schematic diagram to illustrate the stress dependence of the steady-state creep rate. According to Yavari and Langdon (1982), the slope in Figure 6.3 is presented as  $n = \frac{\log \dot{\epsilon}_{min}}{\log \sigma}$ . At low stresses, the  $n$  is shown as a constant value, whereas at high stresses, the  $n$  increases with the increase of stress level. The different mechanisms in the process of creep can be distinguished by a simple stress exponent. However, the main shortcoming of the use of this method is the lack of consideration of the stress breakdown phenomenon, where a significant change in dominative mechanism and the superposition of two mechanisms spontaneously produces an apparent rupture process at a relatively low creep rate. Thus, it was essential to soundly investigate the effects of stress level on minimum creep rate through examination of data from physically-based long-term creep tests.

Through investigation of experiment data for the evolution of minimum creep strain under the stress range from 60MPa to 200MPa ( $0.21\sigma_Y$ - $0.71\sigma_Y$ ) at 565°C for 2.25Cr-1Mo steel (Cane, 1979); the stress range from 60MPa to 180MPa ( $0.21\sigma_Y$ - $0.64\sigma_Y$ ) at 600°C for 2Cr-1Mo steel (Parker, 1995); and the stress range from 70MPa to 180MPa ( $0.33$ - $0.85\sigma_Y$ ) at 600°C for 1Cr-1Mo-1V steel (Parker, 1995), the relationship between minimum creep strain and stresses for low Cr alloys can be plotted as shown in Figure 6.4.

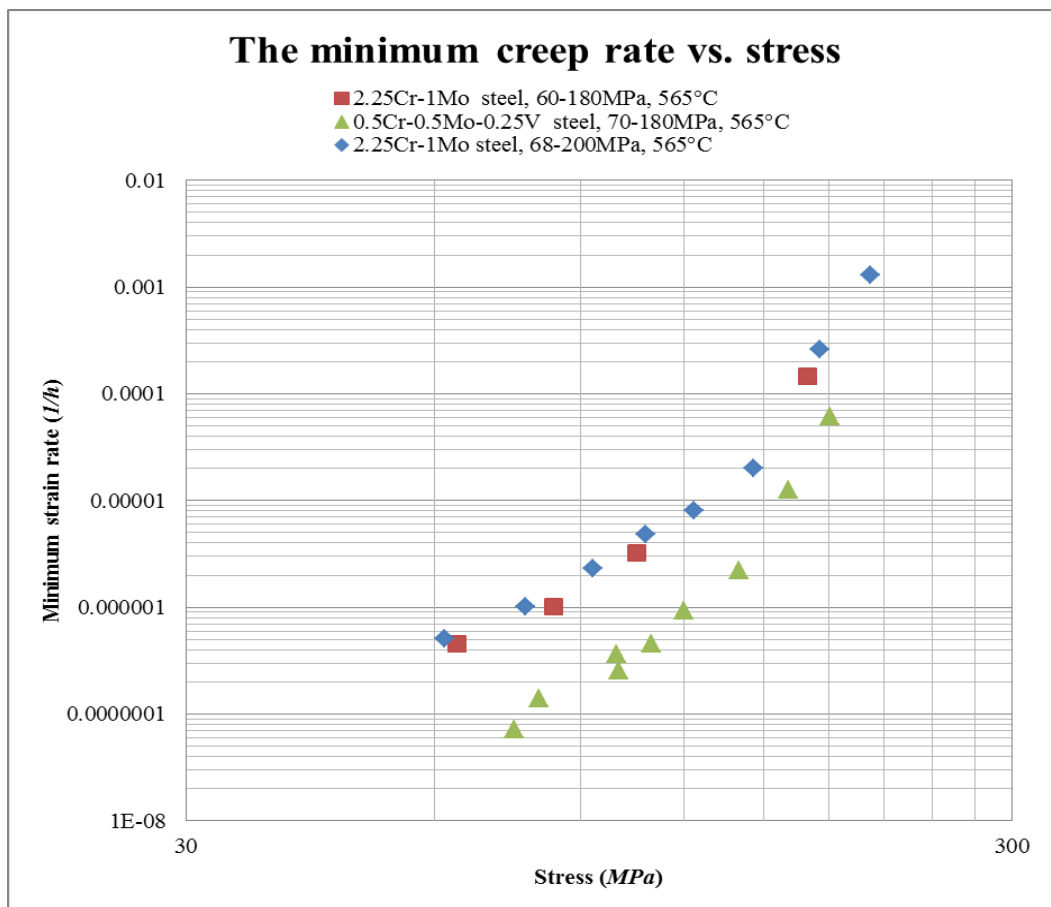


Figure 6.4: Log-log plot of stress versus minimum creep rate for low Cr alloys

Figure 6.4 shows a log-log plot of stress versus minimum creep rate for low Cr alloys. According to Figure 6.4, at the stress range from 68MPa to approximately 150MPa for 2.25Cr-1Mo steel, the minimum creep rate increases smoothly and in a linear manner with the increase of stress, while at the stress range from 150MPa to approximately 200MPa, the minimum creep rate increases dramatically with the increase of stress. A

similar phenomenon is also demonstrated by the data for 2Cr-1Mo steel and 1Cr-1Mo-1V steel creep tests.

The above observation indicates that stress level can influence the creep behaviour of the alloy, having a larger effect on the minimum creep rate. A careful analysis of the creep data was carried out to check the variation in minimum creep rate with stress, and to verify the possibility of expressing the data.

When comparing the conventional power-law creep equation with sinh law, which has been considered by Dyson and Osgerby (1993), the latter has obvious advantages in representing experimental data for minimum creep rate. Thus, the constitutive model which could express the physical meaning and fit with experimental observation could be developed based on sinh law.

### **6.3.2 Analysis of the effects of stress level on rupture time**

Creep rupture is usually caused by the growth of voids. With the continued growth of voids, creep cracks grow from the cusp and ultimately weaken the cross section to the point where failure occurs. At high stresses, creep rupture is usually associated with the trans-granular fracture mechanism, whereas at low stresses, the creep rupture is mainly investigated based on the inter-granular fracture mechanism. However, high local stress may occur when the stress is redistributed due to the growth and nucleation of cavitation, and the stress concentration in turn leads to premature failure. Thus, the effects of stress level on rupture time should be investigated in order to develop creep damage constitutive equations for describing creep rupture behaviour.

The analysis of the effects of stress level on rupture time was conducted through investigation of creep experiment data under a wide stress range from 10MPa to 1000MPa and the temperature range from 450°C to 650°C for 2.25Cr-1Mo steel (M/CDS/No.36B, 2003). The relationship between creep rupture time and stress levels for low Cr alloys can be plotted as shown in Figure 6.5.

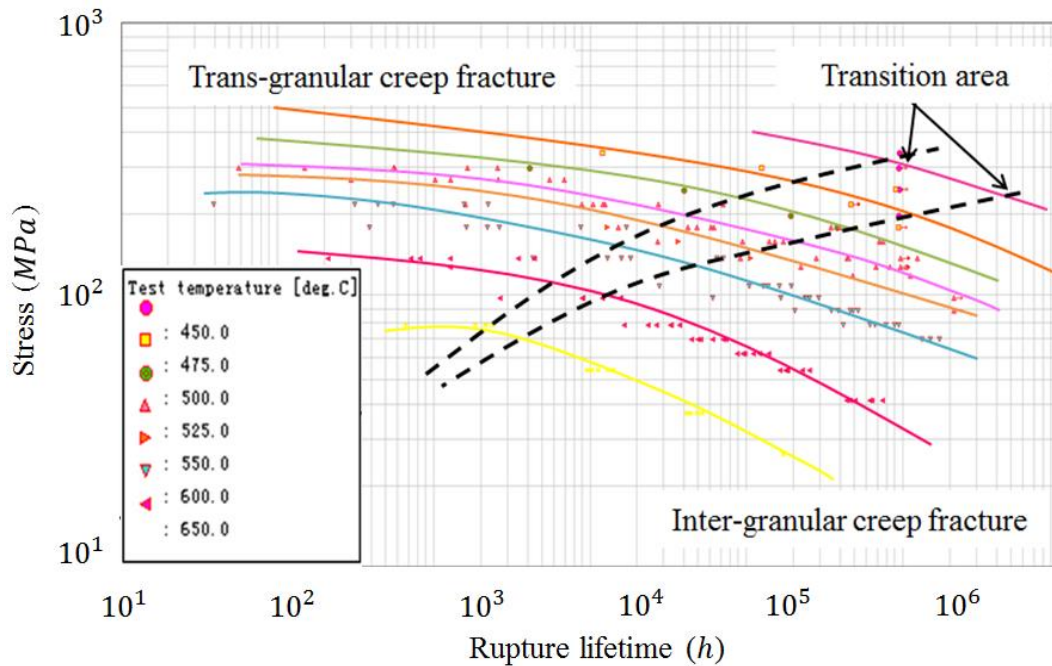


Figure 6.5: Log-log plot of stress versus creep rupture time for low Cr alloys

Figure 6.5 clearly demonstrates the effect of stress level on lifetime for the range of temperature tested (450°C to 650°C), and shows that at higher stress levels the damage mechanism differs from that at low stress levels. According to Figure 6.5, the creep rupture time decreases with the increase of stress levels and temperatures. At high stresses, trans-granular fracture is the dominative rupture mechanism; voids nucleate at inclusions and they may coalesce and trigger the fracture of components. Under low stresses, however, according to the experiment report (M/CDS/No.36B, 2003), many pieces were observed on the fracture surface. Therefore, at a low stress level, the dominative rupture mechanism is inter-granular fracture and the fracture process exhibits as brittle. This temperature-influenced phenomenon is also explained by the fact that higher temperatures could provide the high energy for atoms to move, and higher stresses also contribute to the same effect. The relationship demonstrated in Figure 6.5 between creep rupture time and stress levels for low Cr alloys shows good agreement with the results from the investigation of creep mechanisms in Chapter 5.

The above observation strongly indicates that extrapolation from short-term (high stress level) data to long-term (lower stress) conditions is highly

questionable, no matter how convenient and tempting it is. A specific creep damage constitutive equation needs to be developed according to the stress level in order to reflect the change of damage mechanisms. This is also in agreement with general observations of stress breakdown in creep modelling for other materials.

### 6.3.3 Analysis of the effects of stress level on creep strain at failure

Analysis of the effects of stress level on creep strain at failure was conducted through the investigation of creep experiment data under the stress range from 50MPa to 500MPa ( $0.13\sigma_Y$ - $0.92\sigma_Y$ ) at 550°C for 1.2Cr-0.7Mo-0.3V steel (Hall, 1990). These creep experiment data were obtained under conditions of constant uniaxial loading and constant temperature (Hall, 1990). Based on the typical experiment data, the relationship between creep rupture time and stress levels for low Cr alloys can be plotted as shown in Figure 6.6.

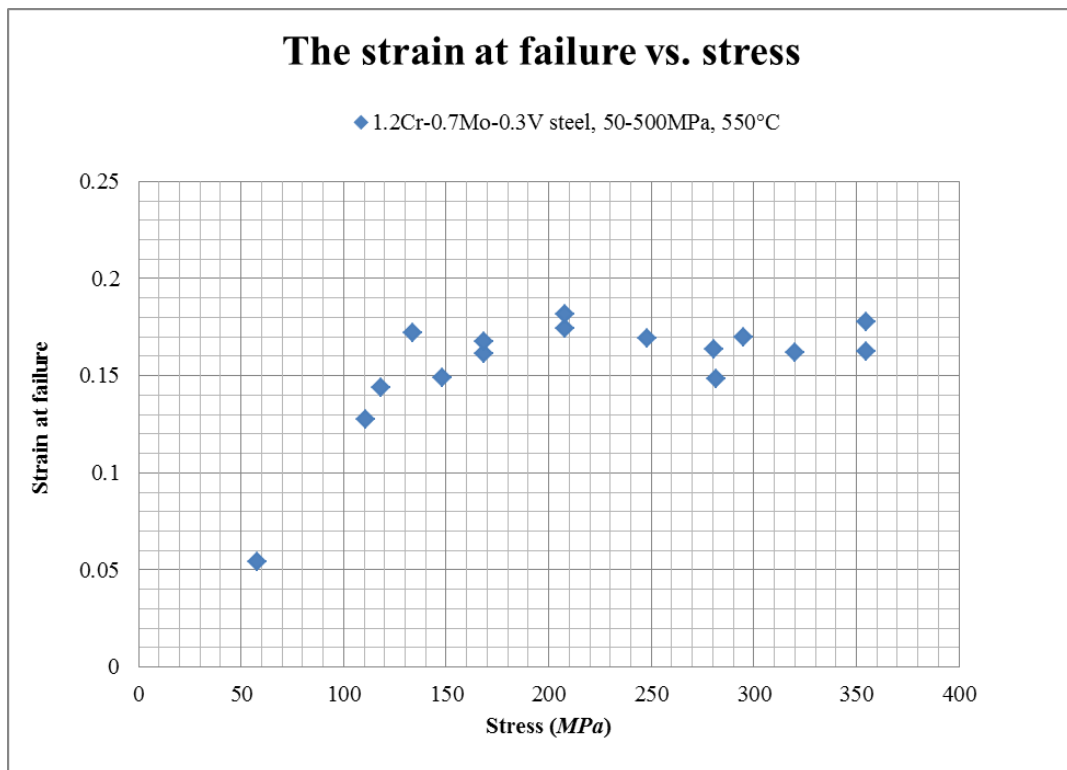


Figure 6.6: Relationship between creep strain at failure and stress levels for low Cr alloys

Figure 6.6 shows the relationship between creep strain at failure and stress levels for low Cr alloys. The test results are plotted as strain versus

stress at rupture time. In the third stage, the strain rate increases until failure occurs. According to Figure 6.6, the creep strain at failure time increases with the increase of stress levels. However, for 1.2Cr-0.7Mo-0.3V steel at 550°C, the maximum strain at failure is approximately 0.2, and the increase of stress levels will not affect the strain at failure when the value of strain at failure reaches 0.2.

Creep strain at failure is associated with the tertiary creep stage. In the tertiary creep stage, the strain rate exponentially increases with stress because of the necking phenomenon (Abe et al., 2008). Moreover, the increase in creep rate is also caused by metallurgical changes such as recrystallization, and the increase in stress as the area is reduced by a specimen's thinning under constant load, by internal fracture or by the nucleation of a creep cavity. In order to accurately design the rupture criterion, analysis of the effects of stress level on creep strain at failure should be involved in the development of a creep damage constitutive equation for low Cr alloys.

#### 6.3.4 Stress level definition in creep damage analysis of low Cr alloys

Based on the investigation of creep mechanisms and analysis of the effects of stress level on creep parameters, the stress level definitions associated with this project are shown in Table 6.1.

Table 6.1: Stress level definitions involved in developing constitutive equations for low Cr alloys

Stress level definition	Stress level	Characteristics
Low stress level	$0.2-0.4 \sigma_Y$	<p>The fracture process is related to the brittle manner of rupture.</p> <p>Under the low stress level, creep deformation is mainly based on the diffusional law (where low energy is required to motivate such deformation behaviour).</p> <p>Creep damage often occurs on the GB based on the inter-granular rupture mechanism.</p>

<p><b>Intermediate stress level</b></p>	<p>0.4-0.5 <math>\sigma_y</math></p>	<p>The fracture process is related to the brittle-ductile transitional manner.</p> <p>Under the intermediate stress level, creep deformation may be controlled by the diffusion or the dislocation mechanism. GB sliding can also be observed at this stress level.</p> <p>The superposition of two different mechanisms can spontaneously produce an apparent damage process of rupture. At this stress level, the strain at failure increases with stress.</p>
<p><b>High stress level</b></p>	<p>&gt;0.5 <math>\sigma_y</math></p>	<p>The fracture process is related to the ductile manner of rupture and the necking phenomenon can be observed at tertiary creep stage.</p> <p>Under the high stress level, creep deformation is mainly based on dislocation (where high energy is required to motivate such deformation behaviour).</p> <p>The creep damage process is based on the trans-granular rupture mechanism. At this stress level, the strain at failure remains the same regardless of increase in stress.</p>

### 6.4 Analysis of the effects of stress level on creep cavity

It is well known that the final rupture life of low Cr alloy material operated at elevated temperature is influenced by creep cavities, and a large amount of experiments indicate that the accumulated damage is predominantly caused by creep cavities. The mechanisms of creep cavity nucleation and growth have been investigated in Chapter 5. According to Kassner (2003), at low stress levels the process of creep fracture is exhibited to be brittle and the dominant damage evolution depends on cavity nucleation. However, the high local stresses which are caused by the stress breakdown phenomenon can lead to a brittle to ductile transition phenomenon under long-term conditions. Hence, qualitative observations of cavity nucleation and growth under different stress levels for low Cr alloys have been investigated. In order to obtain a precise understanding of the creep damage and rupture process, a critical analysis of creep

cavity shape, cavity site, cavity density and cavity nucleation and growth under different stress levels was carried out based on creep experiment tests.

#### **6.4.1 Effect of stress level on cavity shape**

Cavity shape plays an important role in the systematic study of cavitation. However, there are only a few published studies which describe this role because the investigation of cavity shape relies heavily on detection techniques and the detection process for cavity shape under low stresses is usually time-consuming. Nevertheless, the investigation of creep cavity shape should not be neglected since cavity nucleation sites are significantly affected by specific cavity shapes (Riedel, 1987).

The creep cavity shapes involved with failure mechanisms are significantly dependent on stress levels. According to Cane and Middleton (1981), Myers (1987), Chokshi (2005) and Singh and Kamaraj (2009), cavity shapes can be classified into the following two types: wedge shape 'w-type cracks' and spheroidal cavities appearing elsewhere on the boundary, which are termed round shape 'r-type voids' (Stanley, 1978). Wedge shape creep cavities have been observed through the creep experiment test in 0.5Cr-0.5Mo-0.25V steel under the constant stress 110MPa,  $0.55\sigma_Y$  at 600°C (Singh and Kamaraj, 2009). The wedge shape creep cavities are shown in Figure 6.7.

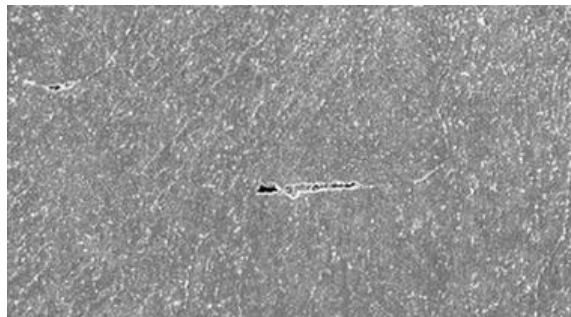


Figure 6.7: Wedge shape creep cavities in 0.5Cr-0.5Mo-0.25V steel under constant stress 110MPa ( $0.55\sigma_Y$ ) at 600°C (Singh and Kamaraj, 2009)

Figure 6.7 shows the wedge shape creep cavities in 0.5Cr-0.5Mo-0.25V steel under the constant stress 110MPa,  $0.55\sigma_Y$  at 600°C. According to

Figure 6.7, the wedge shape cavities can be clearly observed at the stress of 110MPa. At high stress levels, cavities nucleate at inclusions and time promotes their growth based on the ductile mechanism. Wedge shape creep cavities at high stress levels can be effectively explained by the ductile mechanism.

Spheroidal shape creep cavities have been observed though the creep experiment test in 1Cr-0.5Mo steel under the constant stress 35MPa,  $0.22\sigma_Y$  at 520°C (Dobrzański et al., 2006). The spheroidal shape creep cavities are shown in Figure 6.8.

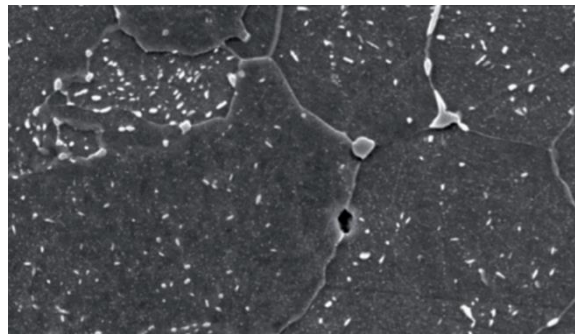


Figure 6.8: Round shape creep cavities in 1Cr-0.5Mo steel under constant stress 35MPa ( $0.22\sigma_Y$ ) at 520°C (Dobrzański et al., 2006)

Figure 6.8 shows the round shape creep cavities in 1Cr-0.5Mo steel under the constant stress 35MPa,  $0.22\sigma_Y$  at 520°C. According to Figure 6.8, the round shape cavities can be clearly observed at the stress of 35MPa. At low stresses, cavity growth by creep becomes very slow and many small voids are nucleated as a result of fracture by GB cavitation. The small round shape creep cavities can be effectively explained by the brittle mechanism. However, a few small wedge shape creep cavities can also be observed in Figure 6.8. This phenomenon might be explained as the result of high local stresses caused by the stress breakdown phenomenon, leading to a change of fracture mechanism.

#### **6.4.2 Effect of stress level on creep cavity site**

Analysis of the effects of stress level on creep cavity site was conducted through investigation of creep experiment data under the stress levels 35-120MPa and temperatures of 520-560°C for 1Cr-0.5Mo steel (Dobrzański

et al., 2006); the stress level 110MPa at 600°C for 0.5Cr-0.5Mo-0.25V steel (Singh and Kamaraj, 2009); and the stress level 60.6MPa and temperature range 565-650°C for 2.25Cr-1Mo steel (Lonsdale and Flewitt, 1979).

The creep experiment data were obtained under conditions of constant uniaxial loading and constant temperature. The creep cavity site data for low Cr alloys under the specified stress levels have been summarised in Table 6.2.

Table 6.2: Creep cavity site under different stress levels for low Cr alloys

Stress level	Yield stress	Temperature	Material type	Cavity sites	Experiment data source
35-120MPa	0.21-0.54 $\sigma_Y$	520-560°C	1Cr-0.5Mo steel	GB	(Dobrzański et al., 2006)
110 MPa	0.55 $\sigma_Y$	600°C	0.5Cr-0.5Mo0.25V steel	Triple junction	(Singh and Kamaraj, 2009)
60.6MPa	0.24-0.33 $\sigma_Y$	565-650°C	2.25Cr-1Mo steel	Second phase particles	(Lonsdale and Flewitt, 1979)

Table 6.2 shows the creep cavity sites for low Cr alloys under different stress levels. The stress levels have an influence on the cavities' preferential nuclei sites. Under low stresses, the distribution of cavities was observed perpendicular (90°) to the external applied stress; this has been confirmed by Lonsdale and Flewitt (1979). Dobrzański et al. (2006) indicate that under a low applied uniaxial stress, the failure of specimens results from the coalescence of discrete cavities on prior austenite grain boundaries which were oriented approximately to the tensile stress axis. Moreover, Dobrzański et al. (2006) state that cavitation has also been seen at 45° to the tension stress. At low stresses, the nucleation energy is not enough to promote GB sliding, as the cavity sites are usually observed on grain boundaries or second phase particles. At high stresses, however, the nucleation energy can significantly contribute to the dislocation of atoms and such behaviour will cause cavities to nucleate on a triple junction.

To sum up, the cavity site is significantly influenced by the stress levels. Creep cavities can nucleate at grain boundaries, second phase particles and triple junctions. It should also be noted that a cavity may nucleate at the stress concentration point on a triple junction under low stress levels.

#### **6.4.3 Creep cavity behaviour under low stress levels**

The process of nucleation and growth of cavities has been investigated through the literature of Cane (1979), Chen and Argon (1981b), Lonsdale and Flewitt (1979), Needham (1983), Myers et al. (1987), Dobrzański et al. (2006) and Maharaj et al. (2009). Numerous investigations, such as those of Lonsdale and Flewitt (1979), Walker (1997) and Owen et al. (1997), agree that cavity nucleation and growth generally start early and continue over an appreciable fraction of, or over the whole, creep life. Quantitative measurements of the cavity nucleation rate have been made by counting the number densities of observable cavities at various fractions of the lifetime.

At low stress ( $0.2\sim 0.4\sigma_Y$ ), nucleation-controlled constrained cavity growth is the predominant mechanism (Dyson, 1976). Fracture behaviour has been observed as inter-granular rupture along the grain boundaries (Dobrzański et al., 2006). Further analysis illustrates that the creep failure is associated with brittle rupture behaviour, as the reduction of area is less than approximately 10% (Kushima et al., 2005). Figure 6.9 summarizes the observations of cavitation reported by Dobrzański et al. (2006) for 1Cr-0.5Mo alloy steel at a temperature range of 520-560°C with a low stress range of 35-120MPa. These observations have been applied against the trend of typical creep stages by the authors, indicating the internal creep damage processes in low Cr-Mo alloy with time to fracture. Dobrzański et al. (2006) state that for the creep evolution of low Cr alloy steels, in the early stages (less than or equal to 0.4 of time to rupture  $T/T_f$ ) of creep damage development, individual voids are observed (at stage 1 in Figure 6.9). Their research reflects that under low stress level, 1Cr-0.5Mo, T/P23 and P92 steel start to nucleate at about  $0.4\sim 0.6 T_f$  (Gaffard, 2004; Dobrzański et al., 2006; Abe et al., 2008). Similar initial development of

the cavitation nucleation process has been seen at approximately  $0.25 T_f$  in EPRI's report of its creep specimens of 2.25Cr-1Mo steel (Viswanathan, 1989). As further damage accumulates, the density and size of voids will both increase (Needham, 1983). Eventually, the density of voids is sufficient for cracks to form (Dobrzański et al., 2006; Singh and Kamaraj, 2009).

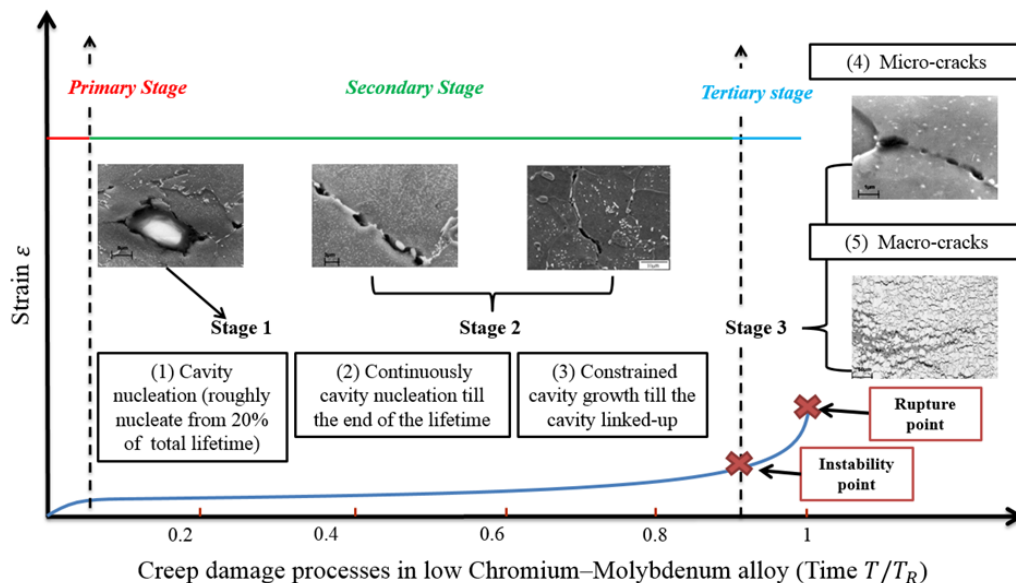


Figure 6.9: Typical damage microstructures associated with the typical curve reflecting dominant creep damage processes (cavitation) with typical creep curve for low Cr-Mo alloy steel at low stresses ( $0.2 \sim 0.4 \sigma_y$ )

Initiation behaviour in the development of cavity includes five different processes: cavity nucleation, growth, and coalescence, micro-cracks growth and macro-cracks growth; these five processes have been summarized in association with time to rupture in Table 6.3. As Table 6.3 shows, the majority of life span is involved, with cavity nucleation occurring from about  $0.2T_f$  to  $0.6T_f$  (stage 1), which represents more than 50% of the total lifetime (Kushima et al., 2005). In contrast, the final rupture process takes less than 30% of life to rupture (stage 3) (Shibli et al., 2005), indicating that the assumption that all voids nucleate at  $T_0 = 0$  is not appropriate for the development of a physically-based set of creep damage constitutive equations for low Cr-Mo alloy at low stresses.

Table 6.3: Initiation time for development of cavitation process

Initiation behaviour at time to rupture: $TT_f$	0-0.2	0.2-0.4	0.4-0.6	0.6-0.8	0.8-1
(1) cavity nucleation:		$\geq 0.25/0.26$	0.4~0.6		
(2) cavity growth:			0.38~0.56		
(3) cavity coalesce:			$\geq 0.4$		
(4) macro-crack growth:				$\geq 0.7$	0.96~1

Longsdale and Flewitt (1979) report that under low stresses (55.6, 60.6 and 70.6MPa) at 600°C for 2.25Cr-1Mo steel, the cavity nucleation rate of accumulation increased monotonically with time and at a given time was greatest for the largest applied stress (Myers et al., 1987; Riedel, 1987; Naumenko and Altenbach, 2007). In addition, the density of cavities observed on the grain surfaces increased continuously throughout the creep life (Walker, 1997) and cavity growth rate increased slightly with the accumulation of time (Wu and Sandström, 1995).

All in all, under a low stress level, failure is in a brittle manner controlled by inter-granular cavitation. The dominant process of creep damage accumulation that leads to eventual rupture is creep cavitation development, which is controlled by continuous cavity nucleation and the constrained CGM.

#### 6.4.3.1 Cavity nucleation rate induced stress dependence under low stress level

Needham (1983) found, by examining smooth specimens, that cavity nucleation rate depends strongly on stress rather than on creep strain. In comparing the relative contributions of the principal, maximum and equivalent stresses to the creep on the nucleation rate,  $\dot{N}$ , and cavity growth rate,  $\dot{R}$ , in two Cr-Mo steels, he found that it is the principal tensile stress,  $\sigma_1$ , which controls the nucleation rate. Needham (1983) suggests that under lower stresses, the functional relationship for cavity nucleation rate (Equation 6.4) cavity growth rate (Equation 6.5), and the rupture lifetime for 2.25Cr-1Mo steel and 1Cr-0.5Mo steel are related to maximum

principal stress,  $\sigma_1$ , by a power-law; the power-law index number has been presented in Table 6.4 for these two grades.

Under low stresses,  $\sigma_1$  controls the nucleation rate according to:

$$\dot{N} = a\sigma_1^n \quad (6.1)$$

Under low stresses,  $\sigma_1$  controls the nucleation growth rate according to:

$$\dot{R} = b\sigma_1^m \quad (6.2)$$

Under low stresses,  $\sigma_1$  controls the rupture lifetime according to:

$$T_f = 1/c\sigma_1^p \quad (6.3)$$

where  $a$ ,  $b$  and  $c$  are empirical factors, respectively;  $n$ ,  $m$  and  $p$  represent the power-law stress index.

Table 6.4: Summary of stress index for power-law behaviour under low stress

Under low stresses (0.2-0.4 $\sigma_Y$ ) MPa			
Depends on maximum principal stress	Cavity nucleation rate	Cavity growth rate	Rupture lifetime
Power law stress index ( $n$ , $m$ and $p$ )	5-7	3.5-4.5	4.8

Table 6.4 summarises the stress index for power-law behaviour under low stresses. It is apparent that the relative cavity density is dependent upon the stress level. The proportionality of the cavity density to stress sometimes holds until very close to final failure (Riedel, 1987; Wu and Sandström, 1995). This phenomenon shows that cavity nucleation occurs throughout most of the lifetime. Experimental observation also shows that the continuous formation of cavities throughout life fraction is stress dependent (Kassner and Hayes, 2003). The predominance of the principal tensile stress was found by Dyson and McLean (1997), who carried out tests on Nimonic 80A in tension and torsion. The von Mises stress,  $\sigma_e$ , is usually less important except at high stresses in 2.25Cr-1Mo steel, where Needham (1983) finds  $\dot{N} \propto \sigma_1^4 \sigma_e^4$ .

#### 6.4.3.2 Cavity density induced strain dependence under low stress level

As has been summarised in the previous section, it is agreed that cavity nucleation generally starts early and continues over an appreciable fraction of creep life. Quantitative measurements of cavity nucleation rate have been made by counting the number densities of observable cavities at various fractions of the lifetime. These counts are usually made at cavity sizes of 0.5 to 1  $\mu\text{m}$ , whereas cavity nuclei are much smaller, say, 20  $\text{nm}$ . Therefore the apparent nucleation kinetics may be distorted by cavity growth. Dyson (1976), however, points out that small cavities tend to grow rapidly and therefore the counting of cavities having a size of 0.5  $\mu\text{m}$  reflects the kinetics of cavity nucleation sufficiently accurately in many practical cases.

As Dyson (1983) further noticed, a common result of many experimental studies is that the number of cavities,  $N$ , per unit GB area increases approximately in proportion to creep strain with a factor of proportionality which, to a first approximation, is independent of stress. Likewise, Evans (1984) quotes a few other papers containing information on the increase in cavity number with strain. This observation can be expressed as:

$$N = \alpha' \varepsilon \quad (6.4)$$

where  $N$  is the cavities per unit GB area,  $\alpha'$  is an empirical factor of proportionality having the physical dimensions [ $\text{m}^{-2}$ ], and  $\varepsilon$  is creep strain for austenized 2.25Cr-1Mo steel at 1300°C,  $\alpha' = 4 \times 10^{12} \text{m}^{-2}$ . The empirical factors for other low Cr-Mo alloy steels, such as 1Cr-1Mo-0.25V steel austenized at 1300°C ( $\alpha' = 4 \times 10^{10} \text{m}^{-2}$ ) and 0.5Cr-0.5Mo-0.25V ( $\alpha' = 1.5 \times 10^{12} \text{m}^{-2}$ ), can be found in Evans (1984).

#### 6.4.4 Creep cavity behaviour under high stress level

At high stresses ( $> 0.5\sigma_Y$ ), the plasticity-controlled CGM is predominant, and there is increasing rupture strain with the increasing creep strain rate (Cane and Middleton, 1981; Sklenicka et al., 1987; Shibli et al., 2005). Under this stress level, creep rupture occurs based on w-type micro-cracks which form at a triple grain junction, and the growth of those cracks

will lead to local grain-boundary separation (Chen and Argon, 1981b; Riedel, 1987; Singh and Kamaraj, 2009). Furthermore, failure occurs relatively quickly and is accompanied by elongation deformation at this stress level (Shibli and Holdsworth, 2009). The speed of plastic strain increases rapidly after external loading is applied. In this condition, fracture is based on trans-granular cavities (Boyle and Spence, 2013). A further study shows that creep failure is associated with ductility because the reduction area of specimens represented around  $\frac{3}{4}$  of the cross section under high strength condition (Parker, 1995).

#### 6.4.4.1 Cavity growth rate induced stress dependence under high stress level

Creep deformation and rupture have been studied in 2.25Cr-1Mo steel over the range 100-210MPa at 565°C (Cane and Greenwood, 1975; Cane, 1979; Myers et al., 1987; Bissel et al., 1988). Kawashima et al.(1994) report that for this steel the creep rupture lifetime depends on the cavity nucleation rate and cavity growth size. Creep damage accumulates by the initiation and growth of extensive cavitation at prior austenite grain boundaries. Cavity formation predominates during the initial stage and individual cavities appear to nucleate on GB carbides. Quantitative analysis of cavitation kinetics in relation to creep deformation processes suggests that cavity growth is directly related to deformation occurring at grain boundaries. It is inferred that cavity growth is limited by the local creep process occurring at grain boundaries.

Table 6.5: Cavity growth rate versus stress in low Cr-Mo alloy under high stress (Rediel, 1987)

Cavity growth rate (m/s)	Stress (MPa)
3.16228E-14	117.5
5.62341E-14	127.5
7.49894E-14	145
1.77828E-13	160
3.16228E-13	170
1.77828E-12	190
3.16228E-12	225

As Table 6.5 shows, the growth rate increases with the increase of applied stress under higher stresses. These results indicate that cavity growth behaviour is associated with the creep diffusion growth mechanism.

#### 6.4.4.2 Cavity nucleation rate induced stress dependence under high stress level

Under high stress levels, Needham (1983) reports that under high stresses, the functional relationship for cavity nucleation rate, cavity growth rate and rupture lifetime for 2.25Cr-1Mo steel and 1Cr-0.5Mo steel are related to maximum principal stress,  $\sigma_1$ , and equivalent stress,  $\sigma_e$ , by a power-law; the power-law index number is presented in Table 6.6 for these two grades.

Under high stresses,  $\sigma_1$  and  $\sigma_e$  control the nucleation rate according to:

$$\dot{N} = d\sigma_1^a\sigma_e^b \quad (6.5)$$

Under high stresses,  $\sigma_1$  and  $\sigma_e$  control the nucleation growth rate according to:

$$\dot{R} = e\sigma_1^p\sigma_e^q \quad (6.6)$$

Under high stresses,  $\sigma_1$  and  $\sigma_e$  controls the rupture lifetime according to:

$$T_f = 1/f\sigma_1^x\sigma_e^y \quad (6.7)$$

where  $a, b, p, q, x$  and  $y$  represent the power-law stress index;  $d, e$  and  $f$  represent the power-law stress index as summarised in Table 6.6.

Table 6.6: Summary of stress index for power law behaviour under high stress

<b>Under intermediate and high stresses (&gt;0.4 <math>\sigma_Y</math>) MPa</b>			
Depends on maximum principal stress and equivalent stress	Cavity nucleation rate	Cavity growth rate	Rupture lifetime
Power law stress index ( $a, b, p, q, x$ and $y$ )	3.5~5	3.5~5	3.5~5

As the cavity nucleation rate is strongly dependent upon the maximum principal stress under low stress conditions, and dependent upon both the maximum principal stress and the equivalent stress under intermediate

and high stresses, the rupture lifetime could be predicted from knowledge of the nucleation rate determined under a uniaxial tensile (Abe et al., 2008). Therefore, further work is needed to focus on the critical value of the void nucleation rate and growth rate depending on creep life. Once this has been carried out, a hypothesis for a new creep rupture criterion can be developed to predict the physically-based creep rupture behaviour and mechanism.

## **6.5 Summary**

This chapter has firstly analysed the effects of stress level on creep curve. Subsequently, the typical creep curve and the effects of stress level on creep curve for low Cr alloys have been analysed and the dominative mechanisms at different stress levels have been identified.

The chapter has also illustrated the effects of stress level on creep parameter. The effects of stress level on the minimum creep rate, rupture time and strain at failure have been analysed, and the stress level definitions involved in developing creep damage constitutive equations for low Cr alloys have been proposed.

Finally, the effects of stress level on creep cavity behaviour have been investigated. The effects of stress level on creep cavity shape, cavity site, cavity nucleation and growth have been analysed, and the conclusions will be used in the design of a rupture criterion associated with the damage equation.

# **Chapter 7 Minimum creep rate and stress equation for low Cr alloys under long-term service**

## **7.1 Introduction**

The dominant creep deformation and rupture mechanisms are significantly influenced by applied stress, and the use of the typical minimum creep rate and stress constitutive model to extrapolate from high stresses to low stresses still runs the risk of over-estimating the creep lifetime of low Cr alloys. Thus, it is important to develop a new set of creep damage constitutive equations for creep damage analysis of low Cr alloys under long-term service. The minimum creep rate and stress constitutive equation is one of the most important aspects, among others such as rupture criteria and the coupling of damage and creep deformation. The deficiencies of the classical constitutive equations for describing the relationship between minimum creep rate and stress levels have been highlighted in Chapter 3. Based on the investigation of creep mechanisms and analysis of the effects of stress level on creep behaviour in Chapters 5 and 6 respectively, a novel constitutive equation to depict the relationship between minimum creep rate and stress levels is proposed in this chapter. This chapter presents the development of the minimum creep rate constitutive equation. The specific strategies required to determine the relationship between minimum creep rate and applied stresses can be described as follows:

- 1) To investigate the classical constitutive laws for depicting the relationship between minimum creep rate and stress levels.
- 2) To design and propose a novel constitutive equation based on investigation of the classical laws.

- 3) To validate the newly developed constitutive equation through the comparison of simulated results with physically-based creep experiment data.

## 7.2 Investigation of classical constitutive laws for minimum creep rate

An accurate depiction of the relationship between minimum creep rate and stress levels depends on a sound constitutive equation which is developed based on creep mechanisms and the effects of stress levels on minimum creep rate. The physically-based experiment data used for describing the relationship between minimum creep rate and stress levels for low Cr alloys are plotted in Figure 7.1.

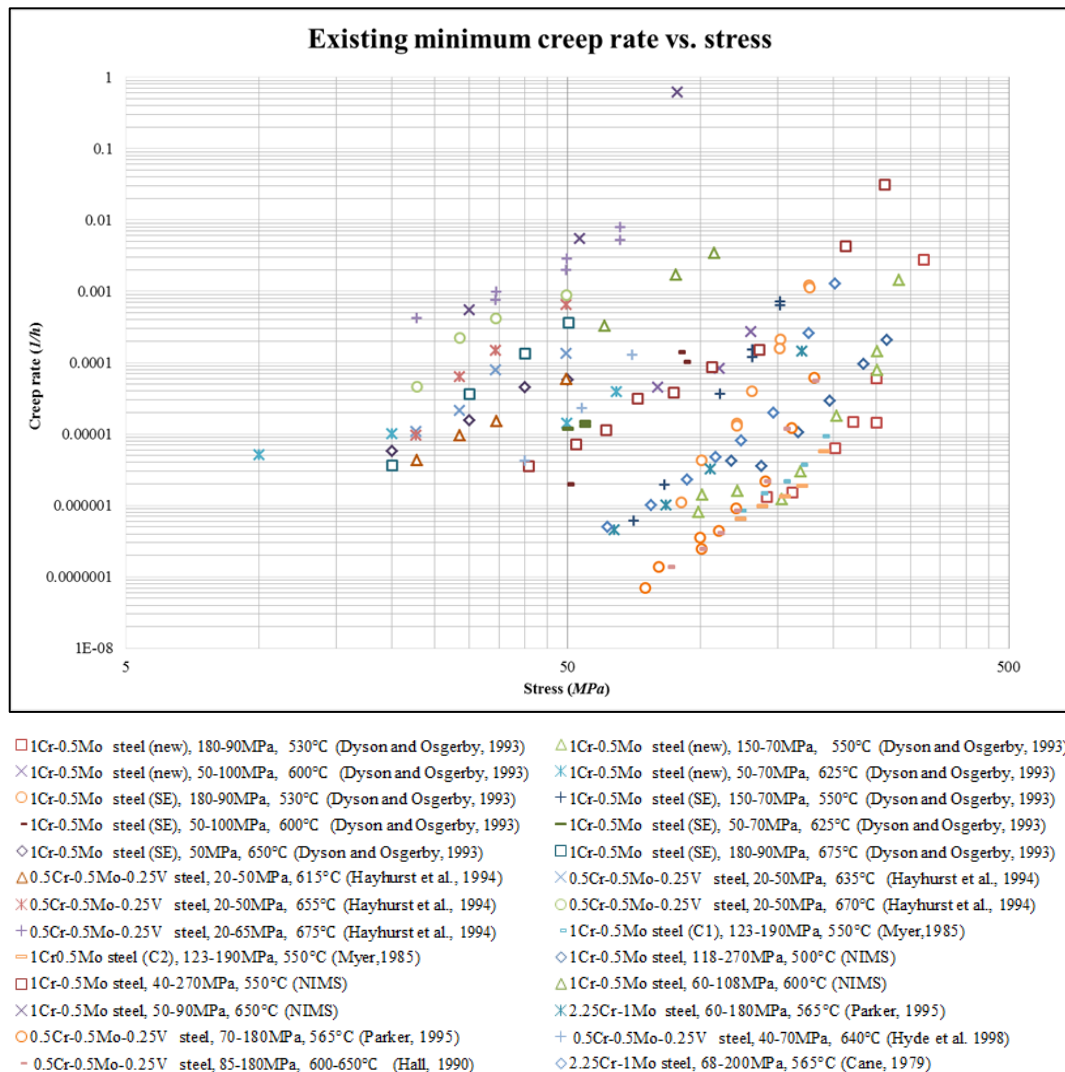


Figure 7.1: Log-log plot of stress versus minimum creep rate based on experiment data

Figure 7.1 shows a log-log plot of the relationship between minimum creep rate and stress as a parallel relationship among the different data sets (Cane, 1979; Cane, 1980; Dyson and Osgerby, 1993; Parker, 1995; Perrin and Hayhurst, 1996; Kern et al., 2004). For each data set, the curve indicates that there is a nonlinear relationship between minimum creep rate and stress. These experiment data sets were selected to test the different equations by combining data for materials under a wide range of stress regimes.

Typical well-known constitutive laws were investigated in order to identify the best mathematical model for developing a constitutive equation to describe the minimum creep rate for low Cr alloys under long-term service. The typical-well known constitutive laws are summarized in Table 7.1.

Table 7.1: Typical well-known constitutive laws for minimum creep rate

Constitutive law	Mathematical model
<b>Diffusion law (Coble, 1963b; Fessler and Hyde, 1994; Harper and Dorn, 1957)</b>	$\dot{\epsilon}_{min} \propto A\sigma$
<b>Power-law creep (Bailey, 1930; Norton, 1929)</b>	$\dot{\epsilon}_{min} \propto A\sigma^n$
<b>Linear + power-law (Naumenko and Altenbach, 2007; Naumenko et al., 2010)</b>	$\dot{\epsilon}_{\dot{\epsilon}_{min}} \propto A\sigma[1 + (B\sigma)^n]$
<b>Hyperbolic sine law (Dyson and McLean, 1997; Dyson and McLean, 2001)</b>	$\dot{\epsilon}_{min} \propto A \sinh(B\sigma) = A \frac{e^{B\sigma} - e^{-B\sigma}}{2}$

### 7.2.1 Investigation of the diffusion law

The diffusion law was first proposed based on the diffusion of atoms and vacancies under low stresses (Coble, 1963a). Applied stress generates an excess of vacancies at grain boundaries, which is normally along the loading direction, and depletion along other boundaries which experience

compressive stresses. To reach an equilibrium, a vacancy flux occurs from boundaries experiencing tensile stresses to boundaries experiencing compressive stresses. Diffusion may occur through the lattice or along the grain boundaries.

According to the diffusion law, the minimum creep rate is directly dependent on the stress applied. The mathematical equation for illustrating the relationship between minimum creep rate and stress under the diffusion law can be shown as:

$$\dot{\epsilon} = A\sigma \tag{7.1}$$

where  $A$  is the material parameter and  $\sigma$  is the applied stress.

In order to understand the effects of material properties on minimum creep rate, six material parameters, representing different material properties, were utilized in this investigation. The values of these material parameters are shown in Table 7.2.

Table 7.2: Material parameters under the diffusion law

Material parameter	A <sub>1</sub>	A <sub>2</sub>	A <sub>3</sub>	A <sub>4</sub>	A <sub>5</sub>	A <sub>6</sub>
Value	2E-10	2E-9	2E-8	2E-7	2E-6	2E-5

With stress ranges from 10MPa to 300MPa, the effects of material properties on minimum creep rate under the diffusion law can be plotted as shown in Figure 7.2.

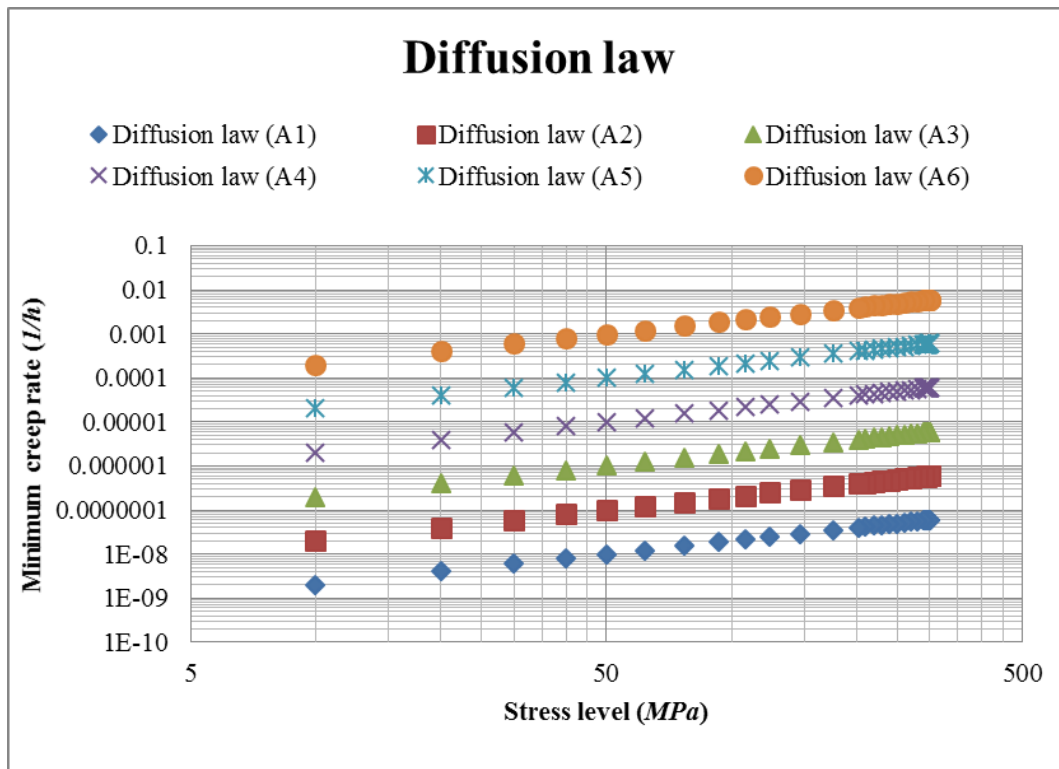


Figure 7.2: Log-log plot of material parameter versus minimum creep rate under the diffusion law

Figure 7.2 shows the effects of material properties on minimum creep rate under the diffusion law. According to Figure 7.2, the minimum creep rate increases in a linear manner with the increase in value of the material parameter. The effects of changing mechanisms on creep material properties are not involved in this model, as such a simple mathematical model cannot give an accurate description of the creep deformation process. Furthermore, the effects of stress level on minimum creep rate, which were highlighted in Chapter 6, are not considered. Thus, the diffusion law does not satisfy the requirements for the development of creep damage constitutive equations for low Cr alloys.

### 7.2.2 Investigation of the power-law

The power-law usually assumes the movement of crystal dislocations into systematic patterns, usually polygonal, within a stress field (Yavari and Langdon, 1982). High stress creep levels are often described as power-law creep, as a steady-state strain rate can be represented by a simple Norton power-law. The power-law is widely utilized in analysis of the

performance of many metals and heat resistant steels. The power-law is consistent with the developments introduced by Weertman (1955), Nabarro (1967), Edward and Ashby (1979), Pharr (1981) and Raj (2002). All these researchers have extensively studied the steady-state creep regime controlled by dislocation creep. The secondary stage maintains a constant creep rate, signifying that a steady state is achieved through a balance of recovery. Moreover, this rate is often adequately described by a power-law expression, such as the well-known Norton relationship:

$$\dot{\epsilon} = A\sigma^n \quad (7.2)$$

where  $A$  is constant and  $n$  are stress-independent constants.

In order to understand the effects of material properties on minimum creep rate, six material parameters, representing different material properties, were utilized in this investigation. The values of these material parameters are shown in Table 7.3.

Table 7.3: Material parameters under the power-law

Material parameter	A <sub>1</sub>	A <sub>2</sub>	A <sub>3</sub>	A <sub>4</sub>	A <sub>5</sub>	A <sub>6</sub>	n
Value	1.4E-11	1.4E-10	1.4E-9	1.4E-8	1.4E-7	1.4E-6	3

With a wide stress range from 10MPa to 300MPa, the effects of material properties on minimum creep rate under the power-law can be plotted as shown in Figure 7.3.

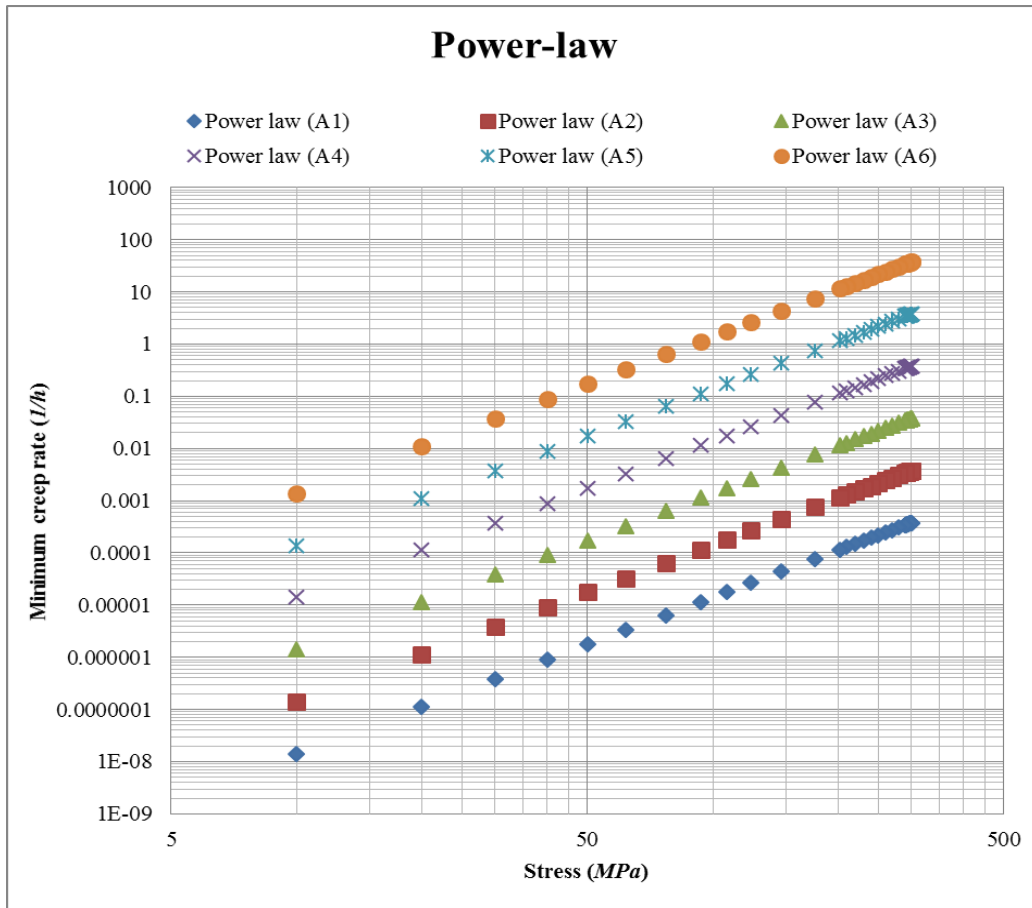


Figure 7.3: Log-log plot of material parameter versus minimum creep rate under the power-law

Figure 7.3 shows the effects of material properties on minimum creep rate under the power-law. According to Figure 7.3, the minimum creep rate increases in a linear manner with the increase in value of the material parameter, and the change in value of the parameter only allows a parallel translation movement of the minimum creep rate curve with stress.

In order to understand the effects of the stress exponent on minimum creep rate, six stress exponents, representing different stress levels, were utilized in this investigation. The values of these exponents are shown in Table 7.4.

Table 7.4: Stress exponents under the power-law

Material parameter	$n_1$	$n_2$	$n_3$	$n_4$	$n_5$	$n_6$	A
Value	1	2	4	6	8	10	1.4E-11

With a wide stress range from 10MPa to 300MPa, the effects of the stress exponent on minimum creep rate under the power-law can be plotted as shown in Figure 7.4.

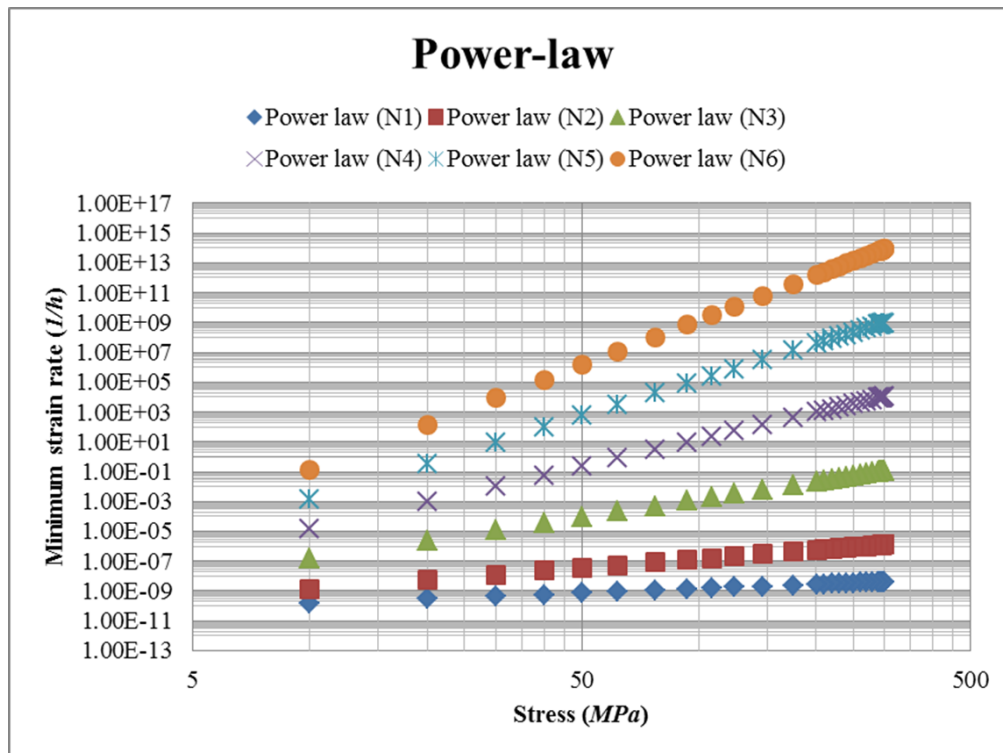


Figure 7.4: Log-log plot of stress exponent versus minimum creep rate under the power-law

Figure 7.4 shows the effects of the stress exponent on minimum creep rate under the power-law. According to Figure 7.4, the stress exponent can obviously change the slope of the curve. However, at the same stress exponent the minimum creep rate is log-linear, increasing with the increase of stress, and this behaviour is not consistent with the physically-based experiment observation conducted by Dimmler et al. (2008). According to Dimmler et al. (2008), at the temperature range of 600-750°C, the minimum creep rate changes in a non-linear manner at different stress regimes.

To sum up, the power-law has considered the effects of stress level on minimum creep rate in developing a constitutive model. However, the effects of changing micro-structure mechanisms and material properties on minimum creep rate are not involved in this model, and the typical

minimum creep rate constitutive model's use of extrapolation from high stresses to low stresses based on power-law creep still runs the risk of over-estimating the creep lifetime of low Cr alloys. Thus, the design of a new constitutive equation to depict minimum creep rate, derived from physically-based experiment data, is still necessary, and the idea of implementing the stress exponent through the use of power-law creep can be utilized in developing the new constitutive minimum creep rate equation.

### 7.2.3 Investigation of the linear + power-law

Under the intermediate stress level, creep deformation may be controlled by either the diffusion or the dislocation mechanism, and GB sliding can be observed at this stress level. It is very difficult to determine which creep mechanism prevails at this stress level because the superposition of two different mechanisms may spontaneously produce an apparent creep damage process of rupture.

In order to extend the power-law creep constitutive model from a high stress level to a low stress level, a transition stage becomes unavoidable. From experiment observation of 9Cr-1Mo-V-Nb (ASTM P91) steel at 600°C, 625°C and 650°C, Gorash (2008) reports that at intermediate stress there is a sharp transition rather than a smooth transition, which is different from the experiment observation of low Cr alloys. Following the observation of transition stage creep behaviour, Gorash (2008) proposes a constitutive equation which couples the power-law with the diffusion law for high Cr alloys:

$$\dot{\epsilon} = A\sigma[1 + (B\sigma)^{n-1}] \quad (7.3)$$

where  $A$  is the material parameter and  $n$  is the stress exponent;

$$B = \frac{1}{\sigma_0} \quad (7.4)$$

where  $\sigma_0$  is the transition stress, and according to Gorash (2008),  $\sigma_0 = 100\text{MPa}$ .

$$B = \frac{1}{100}$$

when,

$$\sigma \leq 100$$

thus,

$$\dot{\epsilon} = A\sigma \quad (7.5)$$

This equation shows a linear relationship between the minimum creep rate and the applied stress, and when

$$\sigma \geq 100$$

thus,

$$\dot{\epsilon} = A\sigma(B\sigma)^{n-1} \quad (7.6)$$

This equation shows a log-linear relationship between minimum creep rate and applied stress.

In order to understand the effects of material properties on minimum creep rate, six material parameters, representing different material properties, were utilized in this investigation. The values of these material parameters are shown in Table 7.5.

Table 7.5: Material parameters under the diffusion + power-law

Material parameter	A <sub>1</sub>	A <sub>2</sub>	A <sub>3</sub>	A <sub>4</sub>	A <sub>5</sub>	A <sub>6</sub>	n
Value	4E-12	4E-11	4E-10	4E-9	4E-8	4E-7	12

With a wide stress range from 10MPa to 300MPa, the effects of material properties on minimum creep rate under the linear + power-law can be plotted as shown in Figure 7.5.

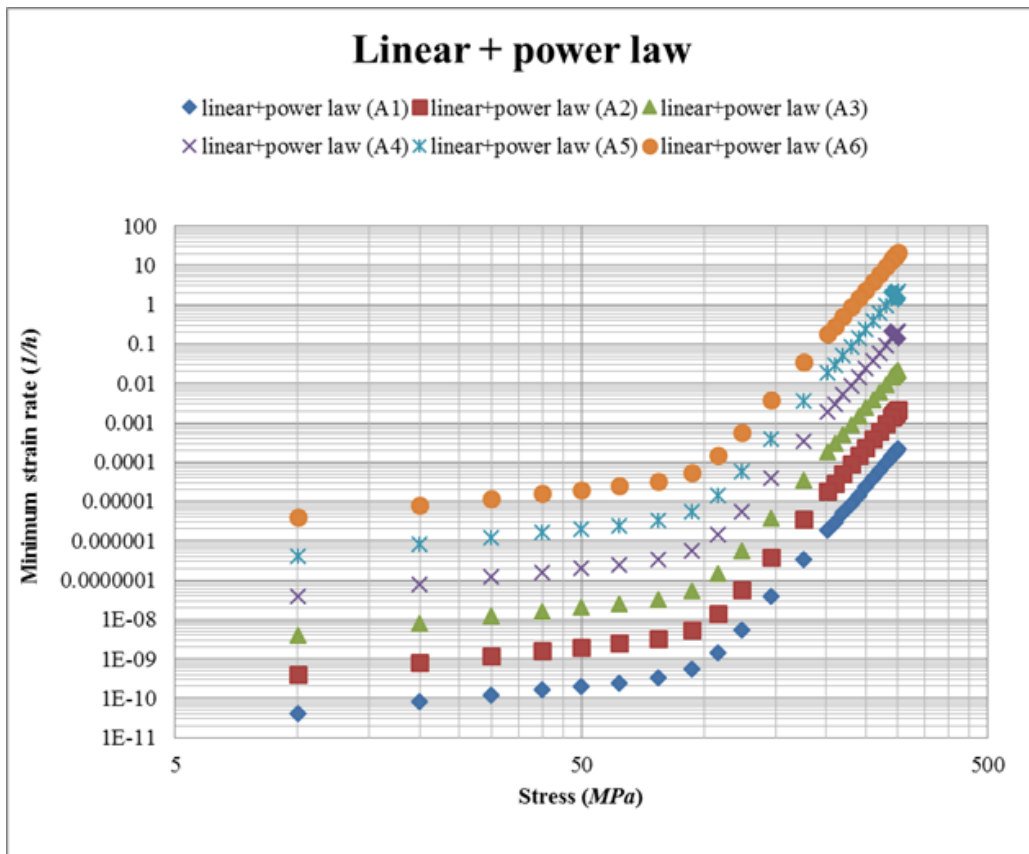


Figure 7.5: Log-log plot of material parameter versus minimum creep rate under the linear + power-law

Figure 7.5 shows the effects of material properties on minimum creep rate under the linear + power-law. According to Figure 7.5, the minimum creep rate increases in a log-linear and smooth manner with the increase in value of the material parameter under the stress range from 10MPa to approximately 100MPa. Between 100MPa and 300MPa, the minimum creep rate increases in a linear manner but more dramatically. The use of piecewise function considers the effect of different mechanisms on micro-structural changes and material properties. However, the evolution process of creep deformation shows high nonlinearity and the piecewise method cannot accurately depict such nonlinear behaviour.

In order to understand the effects of the stress exponent on minimum creep rate under the linear + power-law, six stress exponents, representing different stress levels, were utilized in this investigation. The values of these exponents are shown in Table 7.6.

Table 7.6: Stress exponents under the linear + power-law

Stress exponent	n <sub>1</sub>	n <sub>2</sub>	n <sub>3</sub>	n <sub>4</sub>	n <sub>5</sub>	n <sub>6</sub>	A
Value	11	9	7	5	3	1	4E-9

With a wide stress range from 10MPa to 300MPa, the effects of the stress exponent on minimum creep rate under the linear + power-law can be plotted as shown in Figure 7.6.

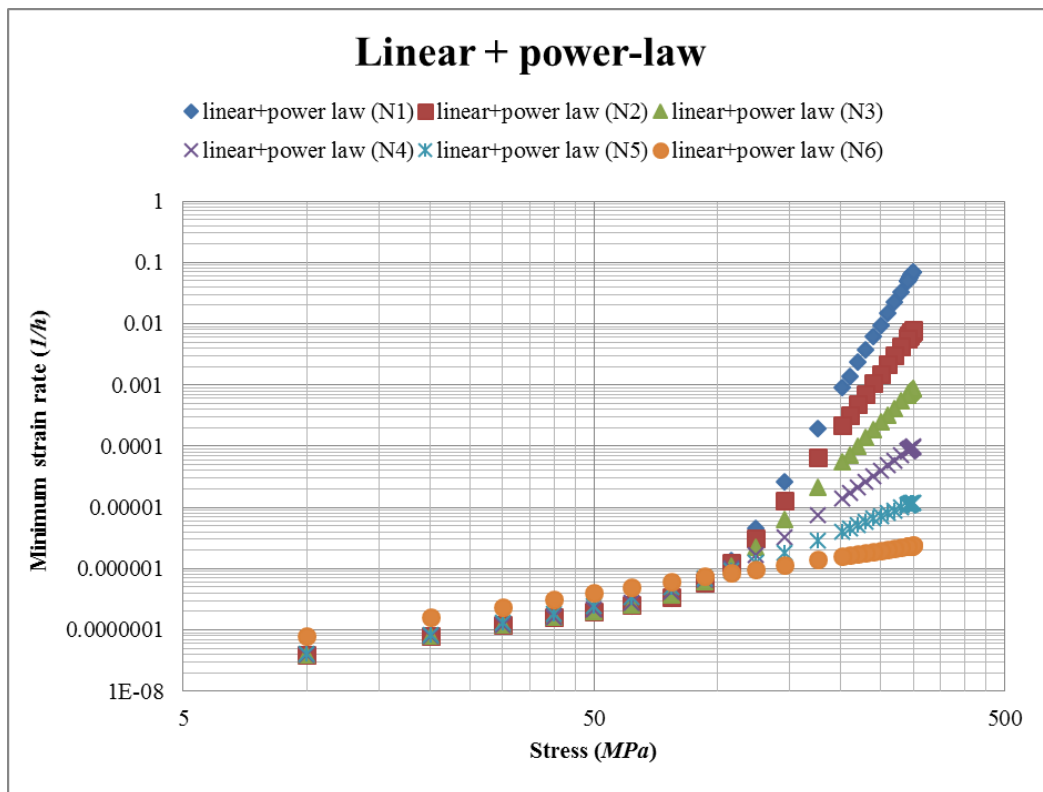


Figure 7.6: Log-log plot of stress exponent versus minimum creep rate under the linear + power-law

Figure 7.6 shows the effects of the stress exponent on minimum creep rate under the linear + power-law. According to Figure 7.6, the stress exponent can obviously change the slope of the curve under the stress range from 100MPa to 300MPa, and the characteristic demonstrated through the use of the linear + power-law is similar to that of power-law creep. Between 10MPa and 100MPa, the slope of the curve is not changed with the increase in value of the stress exponent. Furthermore, the behaviour of minimum creep rate among the different stress levels is

almost the same. This behaviour is due to the lack of effect of low stresses on creep mechanisms.

In order to understand the effects of parameter B on minimum creep rate, six parameters were utilized in this investigation. The values of these parameters are shown in Table 7.7.

Table 7.7: Parameter B under the diffusion + power-law

Material parameter	B <sub>1</sub>	B <sub>2</sub>	B <sub>3</sub>	B <sub>4</sub>	B <sub>5</sub>	B <sub>6</sub>	A <sub>1</sub>	n
Value	7.14E-3	8.33E-3	1E-2	1.25E-2	1.67E-2	2.5E-2	4E-12	12

With a wide stress range from 10MPa to 300MPa, the effects of parameter B on minimum creep rate under the linear + power-law can be plotted as shown in Figure 7.7.

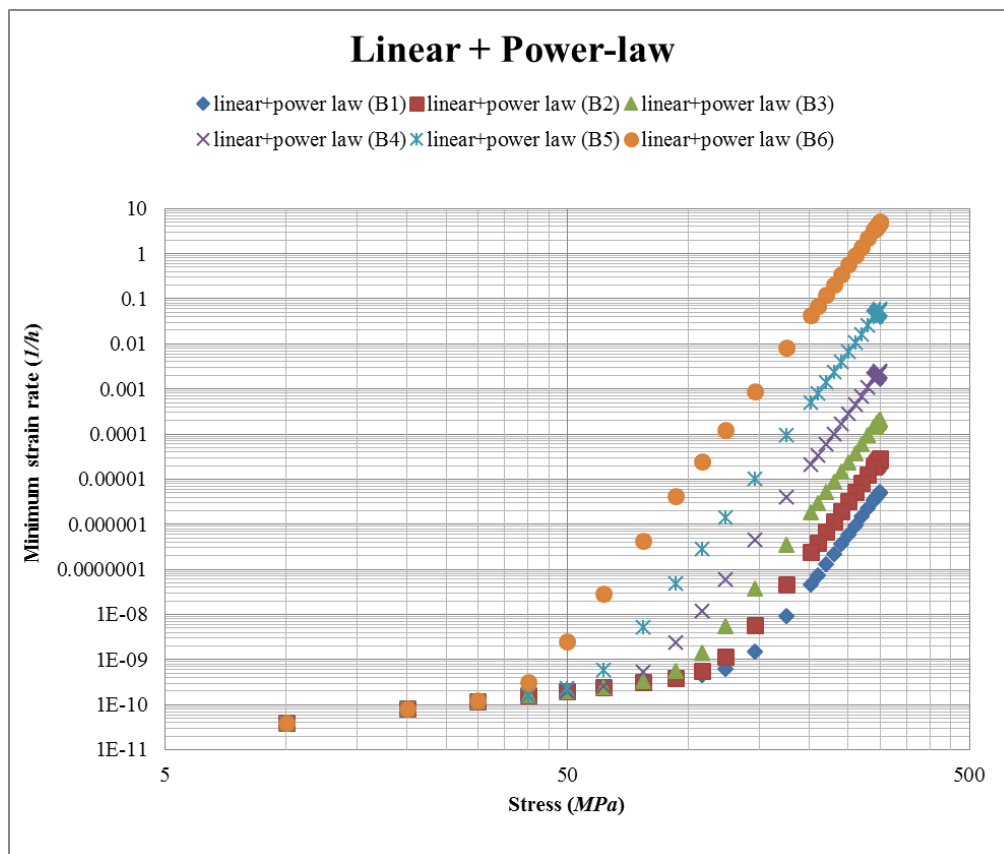


Figure 7.7: Log-log plot of parameter B versus minimum creep rate under the linear + power-law

Figure 7.7 shows the effects of parameter B on minimum creep rate under the linear + power-law. According to Figure 7.7, at low stress levels (under 40MPa), the minimum creep rate is not influenced by the change of parameter B. From 40MPa to 300MPa, the key point of the curve increases with the decrease in value of parameter B, and the characteristic demonstrated through the use of linear + power-law is similar to that of power-law creep.

To sum up, the use of the linear + power-law has combined the characteristics of both linear law and power-law. The effects of intermediate and high stress levels on minimum creep rate have been considered in this method. However, the effects of changing micro-structure mechanisms and material properties on minimum creep rate cannot be described through the use of a piecewise method, and the typical minimum creep rate constitutive model's use of extrapolation from high stresses to low stresses based on power-law creep still runs the risk of over-estimating the creep lifetime of low Cr alloys. Thus, the design of a new constitutive equation to describe minimum creep rate, derived from physically-based experiment data, is still necessary, and the idea of implementing the stress exponent through the use of power-law creep can be utilized in developing the new constitutive minimum creep rate equation.

#### **7.2.4 Investigation of the hyperbolic sine law**

The evolution of creep strain can be explained by recalling that the rate of GB sliding is an approximately constant fraction of the overall creep rate. This fractional relationship requires that GB sliding must be accommodated by creep within the grains. Thus, the creep of the grain interior, due to the climb and glide of dislocations, controls the rate of GB sliding. Conventionally, such dislocation creep is described by a power-law relationship; however, Dyson and Osgerby (1993) propose that climb and glide occur as parallel rather than sequential processes. These parallel processes lead to the creep strain having a hyperbolic sine dependence on the applied stress, rather than the conventional power-law dependence. Osgerby and Dyson (1993) have applied hyperbolic sine law

to the investigation of creep behaviour of Ni 80A and 1Cr-0.5Mo steels, and this hyperbolic sine law can be represented as:

$$\dot{\varepsilon} = ASinh(B\sigma) \quad (7.7)$$

where A and B are the material parameters.

$$Sinh(x) = x + \frac{x^3}{3!} + \frac{x^5}{5!} + \frac{x^7}{7!} + \dots = \sum_{n=0}^{\infty} \frac{x^{2n+1}}{(2n+1)!} \quad (7.8)$$

In order to understand the effects of parameter A on minimum creep rate, six parameters were utilized in this investigation. The values of these parameters are shown in Table 7.8.

Table 7.8: Parameter A under the hyperbolic sine law

Material parameter	A <sub>1</sub>	A <sub>2</sub>	A <sub>3</sub>	A <sub>4</sub>	A <sub>5</sub>	A <sub>6</sub>	B
Value	4.078E-10	4.078E-9	4.078E-8	4.078E-7	4.078E-6	4.078E-5	9.053E-3

With a wide stress range from 10MPa to 300MPa, the effects of parameter A on minimum creep rate under the hyperbolic sine law can be plotted as shown in Figure 7.8.

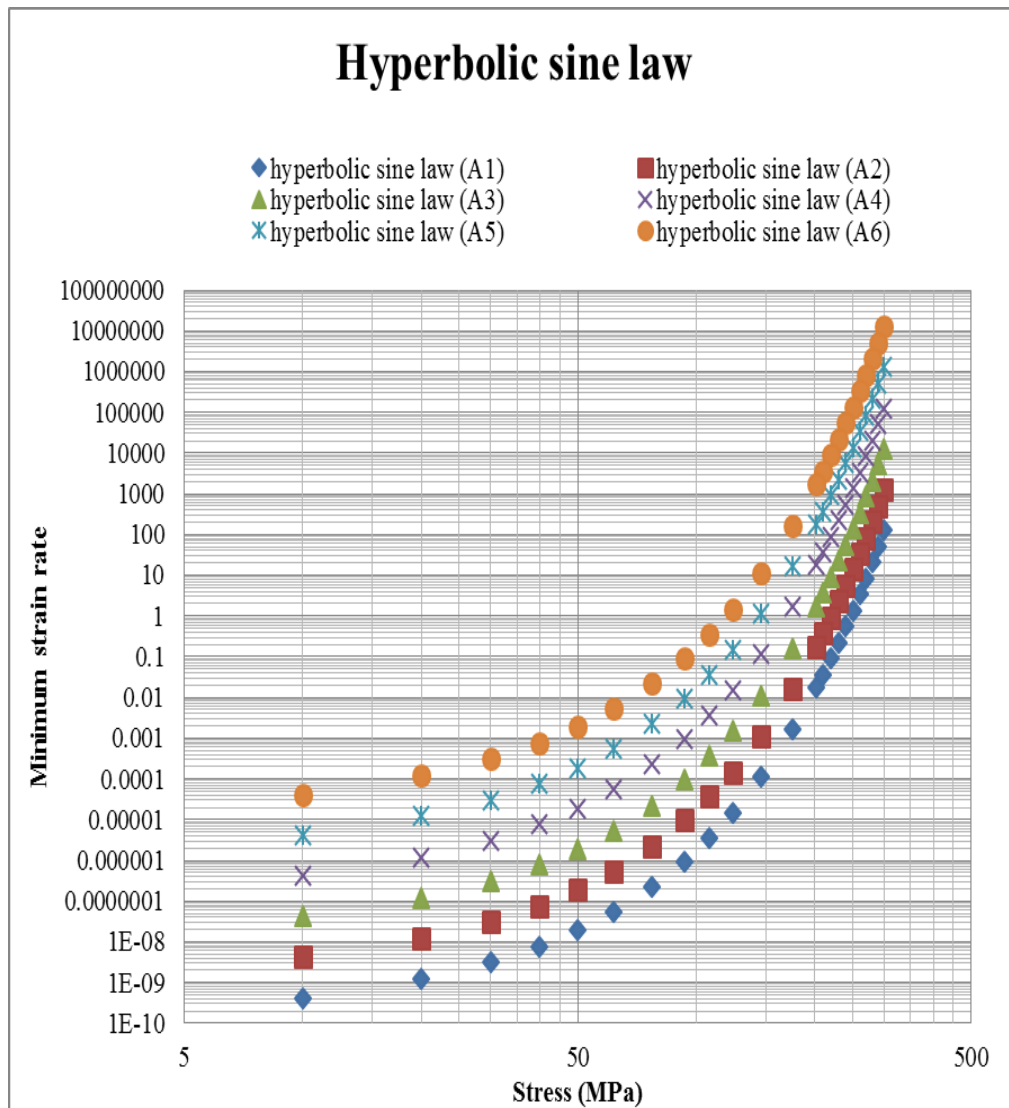


Figure 7.8: Log-log plot of parameter A versus minimum creep rate under the hyperbolic sine law

Figure 7.8 shows the effects of parameter A on minimum creep rate under the hyperbolic sine law. According to Figure 7.8, the change in value of parameter A only allows a parallel translation movement of the minimum creep rate curve with stress. Furthermore, the minimum creep rate increases in a non-linear manner with the increase of stress level.

In order to understand the effects of parameter B on minimum creep rate under the hyperbolic sine law, six parameters were utilized in this investigation. The values of these parameters are shown in Table 7.9.

Table 7.9: Parameter B under the hyperbolic sine law

Material parameter	B <sub>1</sub>	B <sub>2</sub>	B <sub>3</sub>	B <sub>4</sub>	B <sub>5</sub>	B <sub>6</sub>	A
Value	4.54E-7	4.54E-6	4.54E-5	4.54E-4	4.54E-3	4.54E-3	6.78E-08

With a wide stress range from 10MPa to 300MPa, the effects of parameter B on minimum creep rate under the hyperbolic sine law can be plotted as shown in Figure 7.9.

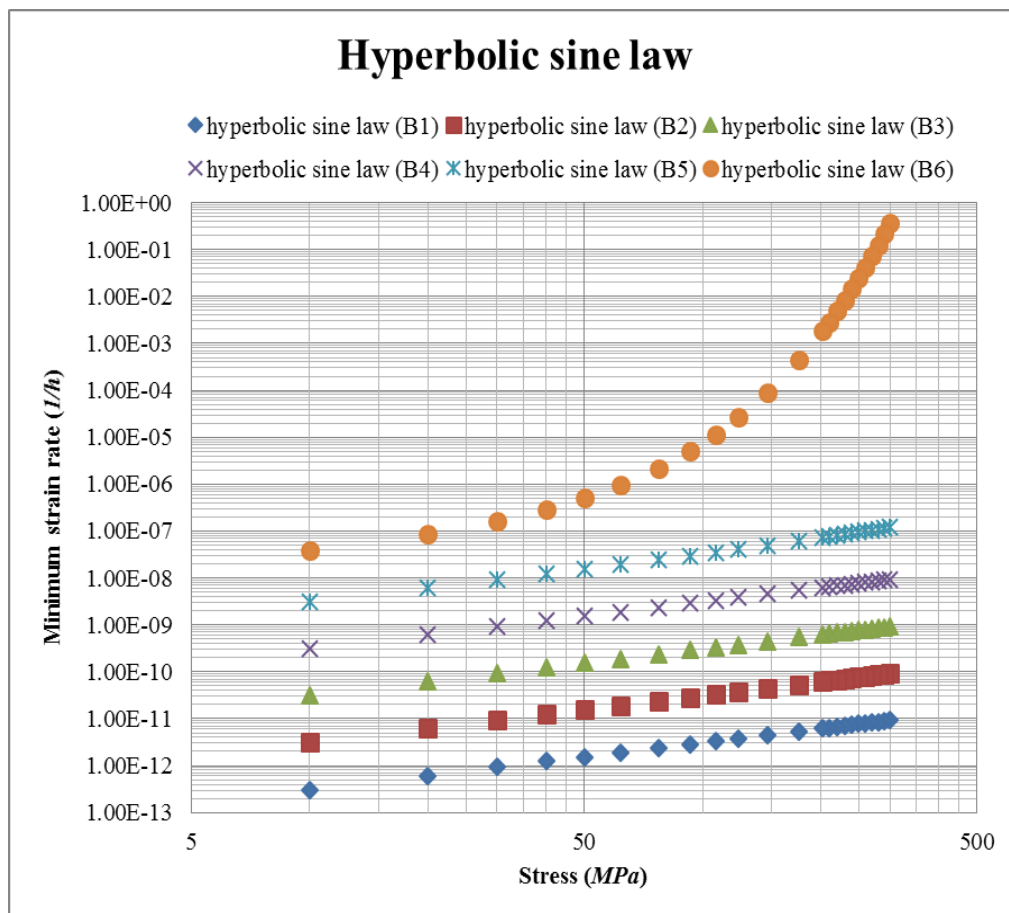


Figure 7.9: Log-log plot of parameter B versus minimum creep rate under the hyperbolic sine law

Figure 7.9 shows the effects of parameter B on minimum creep rate under the hyperbolic sine law. According to Figure 7.9, the plot of traditional sinh law illustrates that the change in value of B can affect the curvature of the curve, and the minimum creep rate increases in a nonlinear manner with the increase of stress level. Due to the nonlinear relationship between minimum creep rate and stress, as shown in the experiment observation

illustrated in Figure 7.1, the hyperbolic sine law should be investigated through comparison with creep experiment data. Experimental data for 2.25Cr-1Mo steel (Cane, 1979), under the stress range 60-200MPa, were utilized in this investigation. The comparison between the hyperbolic sine law and experiment data is shown in Figure 7.10.

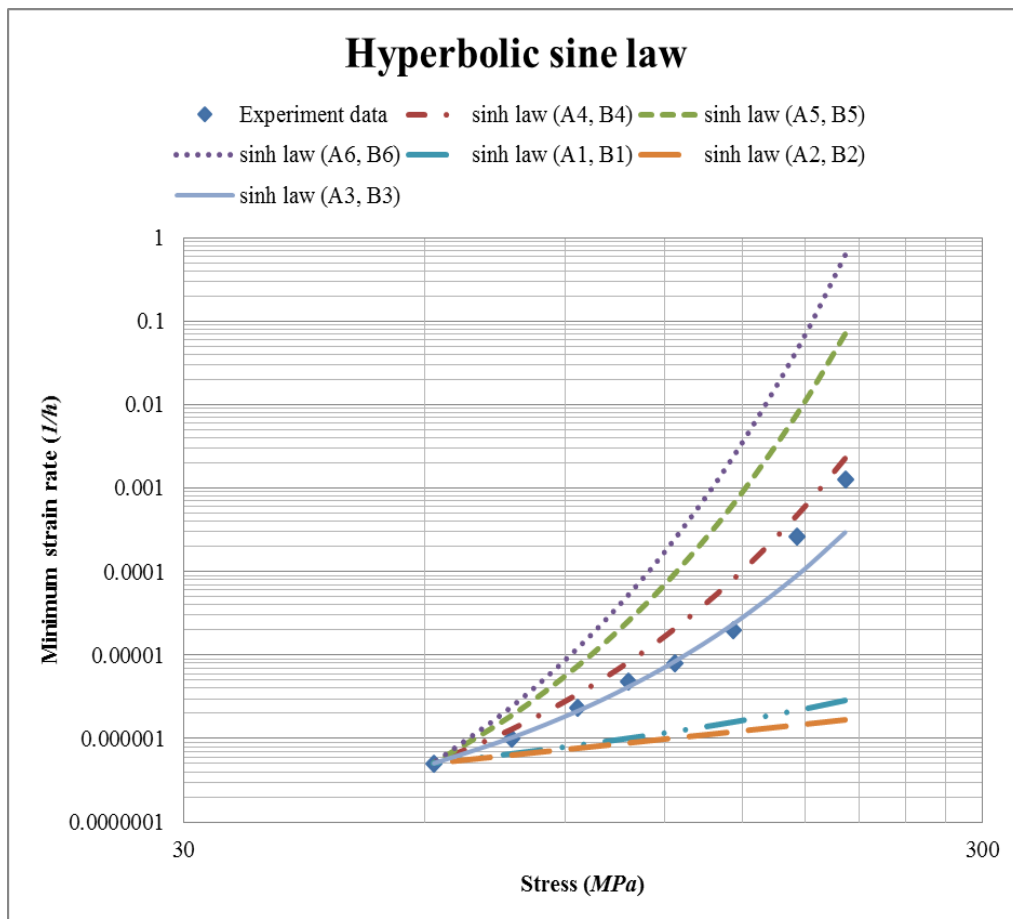


Figure 7.10: Comparison of hyperbolic sine law and experiment data

Figure 7.10 shows a log-log plot of stress versus minimum creep rate under the hyperbolic sine law and from experiment data. Different material parameters were used to fit the experiment data, and the use of sinh law (A3, B3) exhibits good agreement with the experiment data for the stress range from 60MPa to 140MPa. However, at the stress range from 140MPa to 200MPa, the hyperbolic sine law curve is obviously higher than the experiment curve. Thus, the hyperbolic sine law is shown to be in good agreement with the experimental data at low stress regimes. However, with an increase of stress level, the traditional sinh law cannot

predict the minimum creep rate accurately. At low stresses, the stress breakdown phenomenon can significantly improve the stress level, and the minimum creep rate cannot be accurately described through the use of the traditional sinh law function when high local stresses are occurring. The fact is that sinh law cannot predict creep rate accurately for both low and high stress. Thus, the traditional sinh law is not accurate in estimating the secondary creep stage for low Cr alloys, and it is necessary to design a new equation to cope with the deficiencies in the traditional sinh law.

### **7.3 Development of a novel minimum creep rate equation**

Based on investigation of the classical constitutive laws for minimum creep rate, the hyperbolic sine law has shown good agreement with experimental data at low stress regimes. However, at high stress regimes the simulated result is shown to be lower than that of the experiment data. This phenomenon may be due to the lack of consideration of the changing fracture mechanisms which influence microstructural changes at different stress levels. Thus, the newly designed constitutive equation to characterize the stress dependence of minimum creep rate should involve the effects of stress level on minimum creep rate.

With the implementation of the stress exponent, the newly designed constitutive equation to depict the relationship between minimum creep rate and stress levels is expressed as follows:

$$\dot{\epsilon}_{min} = A \sinh(B\sigma^q) \quad (7.9)$$

where  $A$  and  $B$  are material parameters and  $q$  is the stress exponent.

#### **7.3.1 Data fitting method for the determination of the constants in the constitutive equations**

Creep damage constitutive equations based on CDM are characterized by their complexity due to the coupled form of the multi-damage state variables that represent the current state of the material and allow creep rate and temperature history effects as well as the coupling of rate- and temperature-dependence with material hardening over a wide range of stresses.

However, the inclusion of internal state variables increases significantly the number of unknown material constants that need to be found through fitting of the model to experimental stress–strain data at different strain rates and temperatures. This makes the fitting process extremely challenging and increases the uncertainty in the material constants. Thus, the determination of the material constants involved in these equations requires the application of an optimization technique.

Gong et al. (2010) proposed a numerical method to determine the material constants in the nonlinear constitutive model. A new objective function was designed where the errors between the predicted and experimental normalized deformation and lifetime were used in conjunction of the minimal least square method.

In this project, curve fitting procedures were examined for determination of the three unknown creep parameters A, B and q. Its use is simpler, more compact, and less uncertain and is able to obtain an accurate solution for a sample material (0.5Cr-0.5Mo-0.25V ferritic steel) at the temperature range of 560-590<sup>0</sup> C. Later on, Igual and Xu (2015) proposed another data fitting method to determine the parameters of the creep damage constitutive equations for low Cr alloy steels. The data fitting method (Igual and Xu, 2015) can simulate the creep damage behaviours of 0.5Cr-0.5Mo-0.25V ferritic steel at high temperatures, and this project has considered the data fitting method proposed by Gong et al. (2010) and Igual and Xu (2015).

In order to determine the parameters a least square method can be used. The global minimum creep strain can be achieved through the use of the square sum of the predicted creep strain to minus the he square sum of the experimental creep strain. The mathematic equation (Igual and Xu, 2015) is shown in following.

$$f(b) = \sum_{i=1}^m [\sum_{j=1}^n (\varepsilon(b)_j^{pred} - \varepsilon_j^{exp})^2] \quad (7.10)$$

$b \in R^n$ ; where b is an array to include the creep parameters for the constitutive equations,  $b = [A, B, q]^T$ ,  $\varepsilon(b)_j^{pre}$  and  $\varepsilon_j^{exp}$  are the sum of

simulated creep strain and the sum of experimental creep strain, respectively,  $j$  is the loop of time,  $i$  is the given creep curve and  $m$  is the number of the given curves.

The ordinary differential equation is integrated for obtaining the creep parameters array at different temperature and stress levels. From the proposed creep damage constitutive equations the primary creep damage fields such as creep strain, hardening, particle and damage could be identified through the integration of the ordinary differential equation.

According to Gong et al. (2010), the Levenberg-Marquadt approach is integrated in the '**lsqnonlin**' function in a Matlab program. This approach needs for a primary value for Equation 7.10:

$$f(b) = [f_1(b) \ f_2(b) \ \dots \ f_n(b)] \quad (7.11)$$

where  $b$  is an array includes the predicted primary values, and  $f_n(b)$  are the arrays of the specific formulation. The mathematic calculation process is used the least square method and this process can be represented as following formulation (Gong et al., 2010):

$$\min_b \|f(b)\|_2^2 = \min_b [f_1(b)^2 + f_2(b)^2 + \dots + f_n(b)^2] \quad (7.12)$$

where  $b$  is an array to include the creep parameters for the constitutive equations,  $b=[A,B,q]T$ ,  $\varepsilon_{bjpre}$  and  $\varepsilon_{jexp}$  are the sum of simulated creep strain and the sum of experimental creep strain, respectively,  $j$  is the loop of time,  $i$  is the given creep curve and  $m$  is the number of the given curves.

The new formulation to fit the parameters for creep damage constitutive equations have been proposed in this research group (Igal and Xu, 2015) and it can be written as:

$$F_\varepsilon(b) = \sum_{i=1}^m \left[ \sum_{j=1}^n \left\{ \left( \frac{\varepsilon(b)_j^{pred} - \varepsilon_j^{exp}}{\varepsilon_{fi}^{exp}} \right)^2 \right\} + w_i \left( \frac{t(b)_{fi}^{pred} - \varepsilon_{fi}^{exp}}{t_{fi}^{exp}} \right)^2 \right] \quad (7.13)$$

where the new variables are:  $F_\varepsilon(b)$ , the new formulation,  $w_i$ , a reduction coefficient for the specific creep curve  $i$ ,  $t(b)_{fi}^{pred}$  and  $t_{fi}^{exp}$  represent the simulated creep curve and experimental creep curve at a specific lifetime, and  $\varepsilon_{fi}^{exp}$  is the stress curve at the rupture time.

The general flow chart of the optimization process to determine creep parameters is shown in Figure 7.11 (Igal and Xu, 2015). This flow chart of the optimization process to determine creep parameters has been considered in developing and validating the creep damage constitutive equations for low Cr alloys.

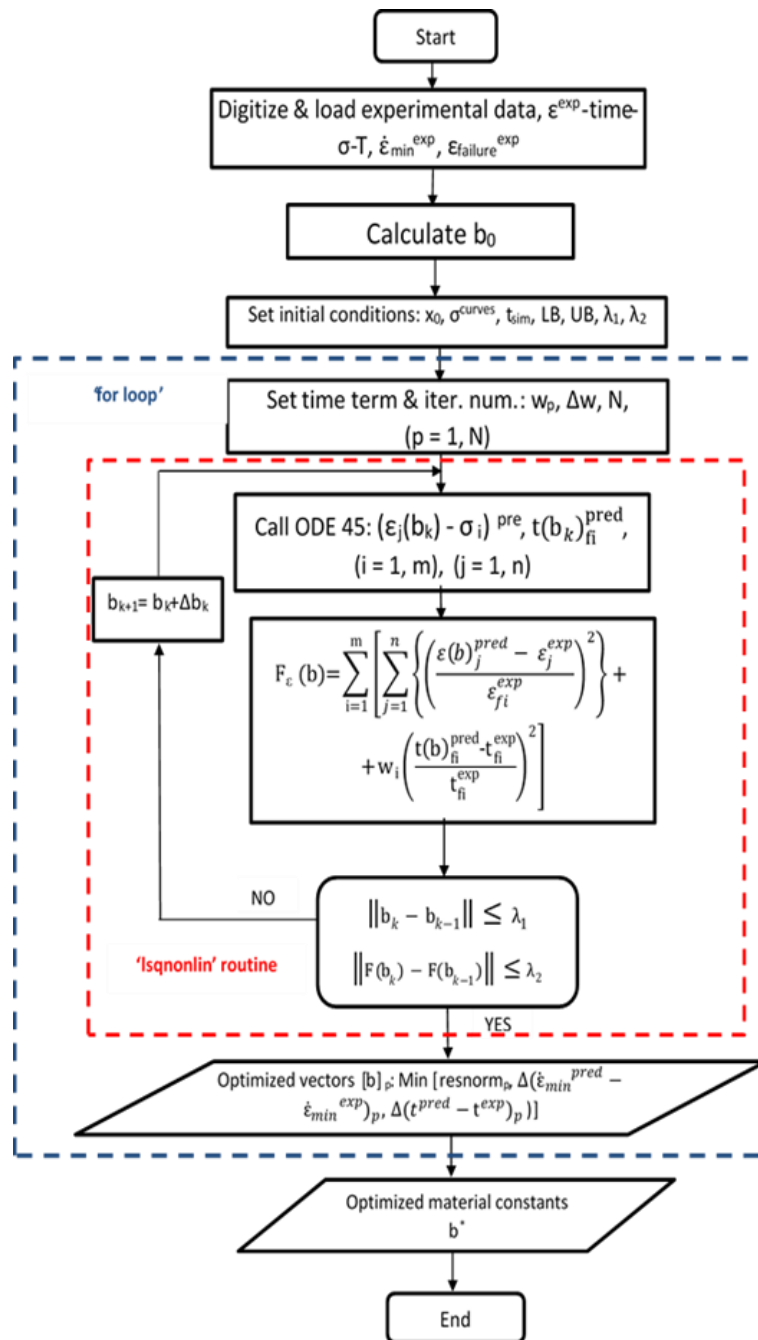


Figure 7.11 General flow chart of the optimization process for determination of material constants (Igal and Xu, 2015)

The determination of the material constants which give the best curve fitting can be divided in four stages (Igal and Xu, 2015).

- a. to plot the experimental creep data and calculate the initial creep parameters for the constitutive equations’.
- b. to build the initial conditions, initial values of the creep damage fields such as creep strain, hardening, particle and damage, the tolerances

for the calculation process, and the boundary constraints for the optimization creep constants. Then, reduction coefficient for the specific creep curve can be achieved through the start of the time loop.

- c. to execute the specific iteration loop for the integration of the proposed ordinary differential creep damage constitutive equation, and simulate the creep strain for each the specific loop can be achieved.
- d. to achieve the new array which includes different creep parameters of the lifetime coefficient. If the experimental creep data are available, the best data to fit the experimental curve can be achieved through the finding of minimum creeps rate.

### 7.3.2 Investigation of the effects of parameter A on minimum creep rate

In order to investigate the effects of parameter *A* on minimum creep rate through the use of the newly designed constitutive equation, six parameters were utilized. The values of these parameters are shown in Table 7.10.

Table 7.10: Parameter A in newly designed constitutive equation

Material parameter	A <sub>1</sub>	A <sub>2</sub>	A <sub>3</sub>	A <sub>4</sub>	A <sub>5</sub>	A <sub>6</sub>	B	q
Value	6.1E-10	6.1E-9	6.1E-8	6.1E-7	6.1E-6	6.1E-5	2.14E-4	2

With a wide stress range from 10MPa to 300MPa, the effects of parameter *A* on minimum creep rate using the newly designed constitutive equation can be plotted as shown in Figure 7.12.

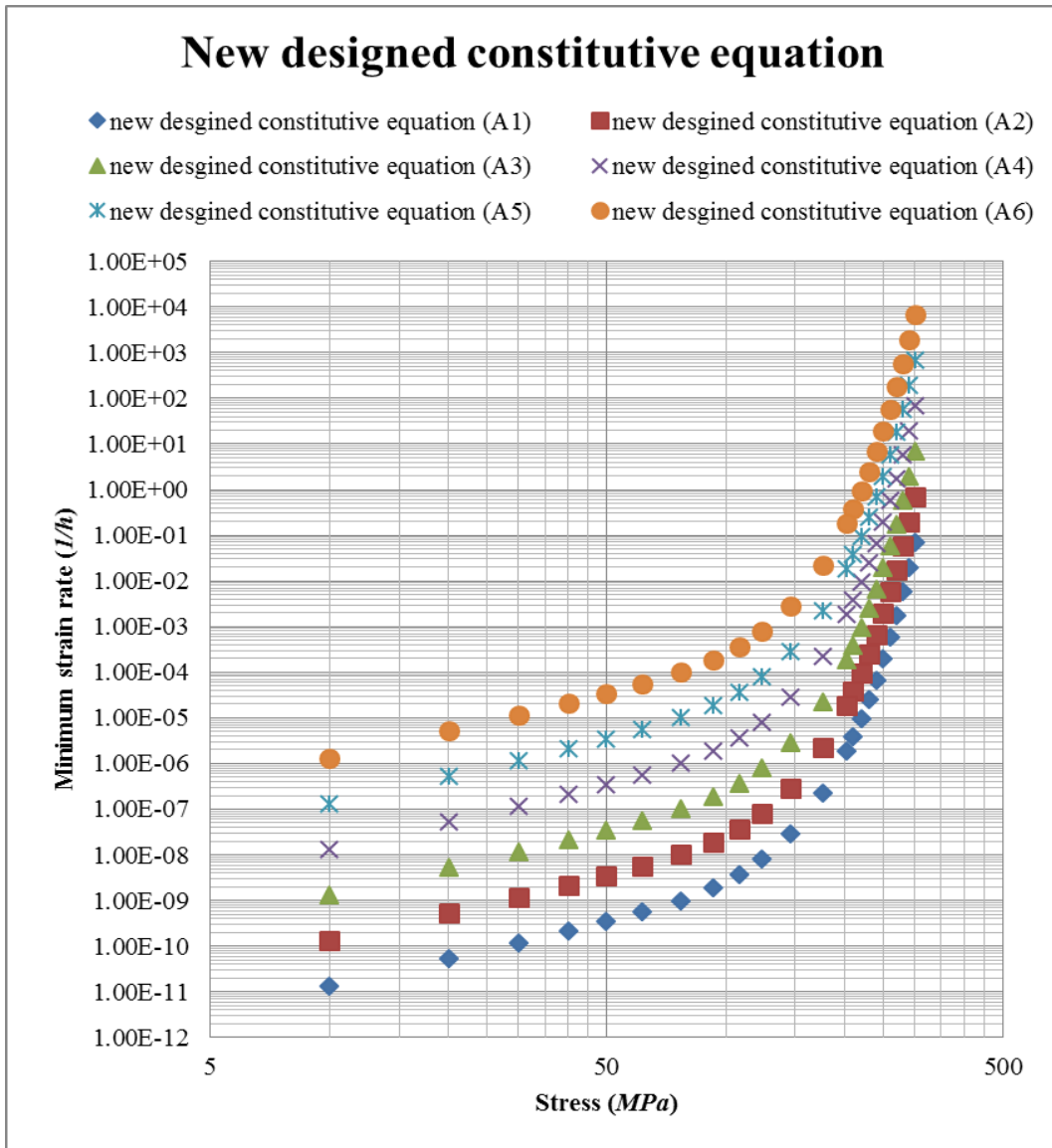


Figure 7.12: Log-log plot of parameter A versus minimum creep rate using newly designed constitutive equation

Figure 7.12 shows the effects of parameter A on minimum creep rate through the newly designed constitutive equation. According to Figure 7.12, changing the value of A allows simulation curves which move in parallel sequence. Furthermore, the minimum creep rate increases in a nonlinear manner with the increase of stress level.

### 7.3.3 Investigation of the effects of parameter B on minimum creep rate

In order to investigate the effects of parameter B on minimum creep rate through the use of the newly designed constitutive equation, six

parameters were utilized. The values of these parameters are shown in Table 7.11.

Table 7.11: Parameter B in newly designed constitutive equation

Material parameter	B <sub>1</sub>	B <sub>2</sub>	B <sub>3</sub>	B <sub>4</sub>	B <sub>5</sub>	B <sub>6</sub>	A	q
Value	2.14E-9	2.14E-8	2.14E-7	2.14E-6	2.14E-5	2.14E-4	6.1E-7	2

With a wide stress range from 10MPa to 300MPa, the effects of parameter B on minimum creep rate using the newly designed constitutive equation can be plotted as shown in Figure 7.12.

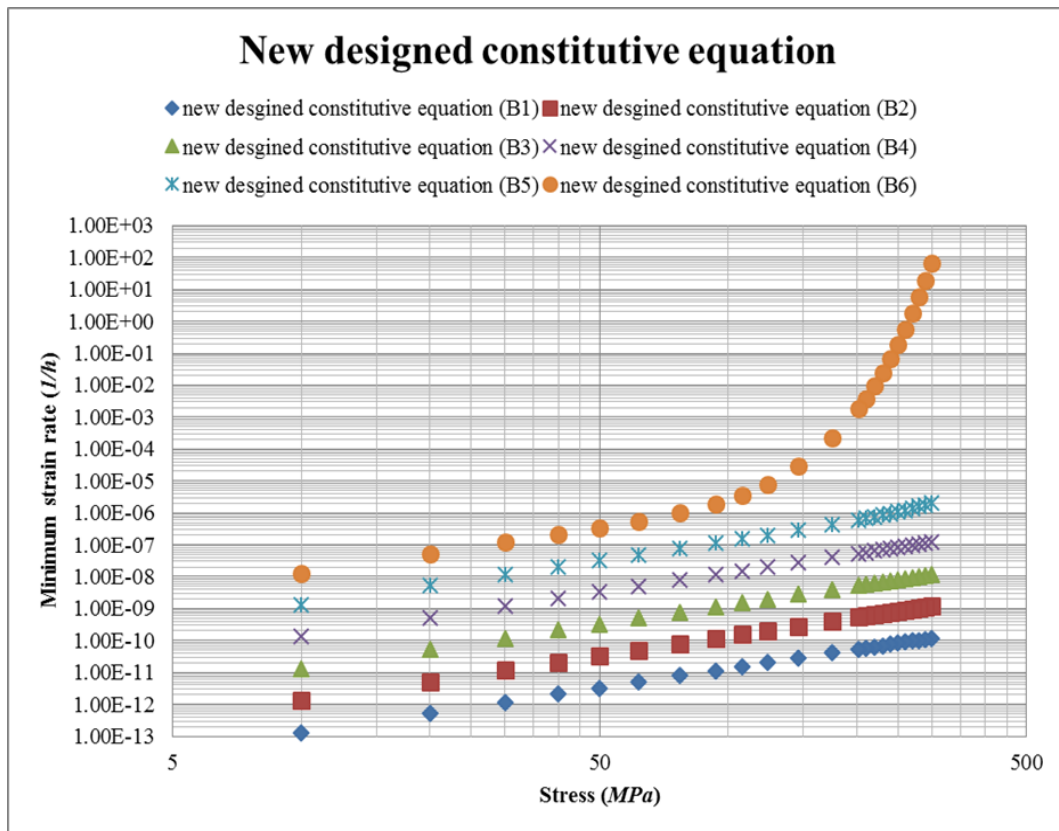


Figure 7.13: Log-log plot of parameter B versus minimum creep rate using newly designed constitutive equation

Figure 7.13 shows the effects of parameter B on minimum creep rate through the newly designed constitutive equation. According to Figure 7.13, changing the value of B can affect the curvature of the curve, and the minimum creep rate increases in a nonlinear manner with the increase

of stress level. The characteristic of change for a large parameter B is similar to that of the hyperbolic sine law.

### 7.3.4 Investigation of the effects of stress exponent on minimum creep rate

In order to investigate the effects of the stress exponent on minimum creep rate through the use of the newly designed constitutive equation, six parameters were utilized. The values of these parameters are shown in Table 7.12.

Table 7.12: Stress exponent parameters in newly designed constitutive equation

Material parameter	q <sub>1</sub>	q <sub>2</sub>	q <sub>3</sub>	q <sub>4</sub>	q <sub>5</sub>	q <sub>6</sub>	A	B
Value	1.5	1.6	1.7	1.8	1.9	2	6.1E-7	2.14E-4

With a wide stress range from 10MPa to 300MPa, the effects of the stress exponent parameter on minimum creep rate using the newly designed constitutive equation can be plotted as shown in Figure 7.14.

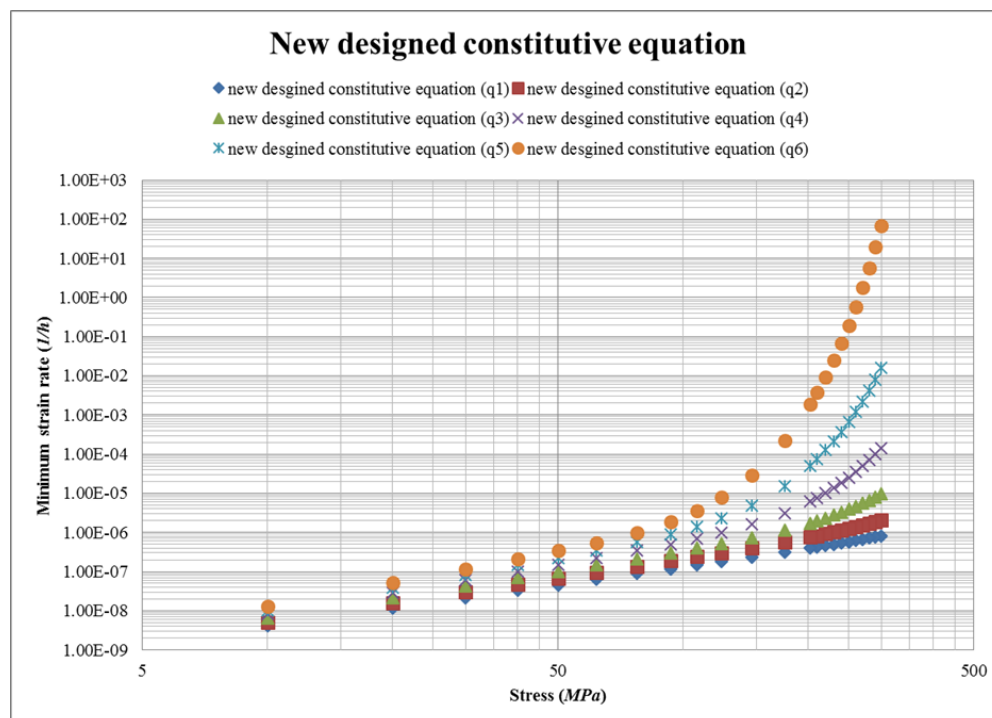


Figure 7.14: Log-log plot of stress exponent versus minimum creep rate in newly designed constitutive equation

Figure 7.14 shows the effects of the stress exponent on minimum creep rate using the newly designed constitutive equation. According to Figure 7.14, the stress exponent can obviously change the slope of the curve. Furthermore, at the same stress exponent, the minimum creep rate increases in a nonlinear manner with the increase of stress, and this behaviour supports the physically-based experiment observation. Increase of parameter  $q$  has the similar effects as the increase of parameter  $B$ .

## **7.4 Validation of the newly developed minimum creep rate equation**

Experiment data for the evolution of minimum creep strain under the stress range 60MPa to 180MPa ( $0.21\sigma_Y$ - $0.64\sigma_Y$ ) at 600°C for 2.25Cr-1Mo steel (Parker, 1995), and the stress range 70MPa to 180MPa ( $0.33$ - $0.85\sigma_Y$ ) at 600°C for 0.5Cr-0.5Mo-0.25V steel (Parker, 1995), were utilized to demonstrate the validity of the newly designed minimum creep rate equation.

The current approach to analysing creep damage behaviour for low Cr alloys under long-term service (low stress levels) is to use the typical stress constitutive model to extrapolate the minimum creep rate from high stresses to low stresses. Here, a demonstration of why simply extrapolating from high stresses to low stresses runs the risk of over-estimating the creep lifetime is conducted through validation of the newly developed minimum creep rate equation.

### **7.4.1 Validation of the newly developed minimum creep rate equation based on 2.25Cr-1Mo steel experiment test**

The experimental data set for the evolution of minimum creep strain rate under a stress range from 60MPa to 180MPa ( $0.21\sigma_Y$ - $0.64\sigma_Y$ ) at 600°C for 2.25Cr-1Mo steel (Parker, 1995) was utilized in validating the newly designed minimum creep rate equation. Furthermore, Dyson's conventional sinh law equation was investigated and the simulated results were compared with the experiment data and the results from the newly developed minimum creep rate equation.

Table 7.13: Material parameters in newly developed constitutive equation for 2.25Cr-1Mo steel

Material parameter	A	B	q
Value	5.57E-7	2.4E-4	2

With a wide stress range from 10MPa to 300MPa, comparison of the newly developed constitutive equation with the experiment data for 2.25Cr-1Mo steel (Cane, 1979) can be plotted as shown in Figure 7.15.

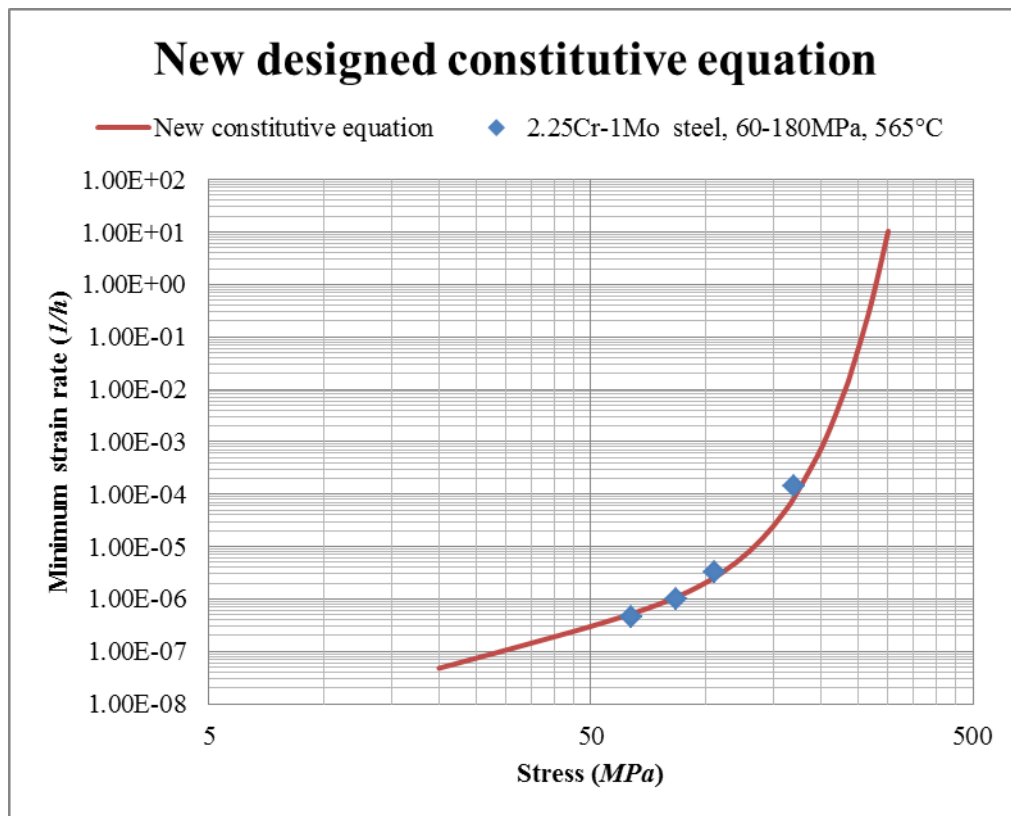


Figure 7.15: Comparison of newly developed constitutive equation with experiment data for 2.25Cr-1Mo steel

Figure 7.15 shows the comparison of the newly developed constitutive equation with the experiment data for 2.25Cr-1Mo steel (Parker, 1995). As Figure 7.15 shows, the minimum creep rate predicted by the newly designed constitutive equation is in good agreement with the experiment data.

Table 7.14: Material parameters in conventional sine law for 2.25Cr-1Mo steel

Material parameter	A	B
Value	7.44E-9	6.2E-2

With a wide stress range from 10MPa to 300MPa, comparison of the conventional sinh law with the experiment data for 2.25Cr-1Mo steel (Parker, 1995) can be plotted as shown in Figure 7.16.

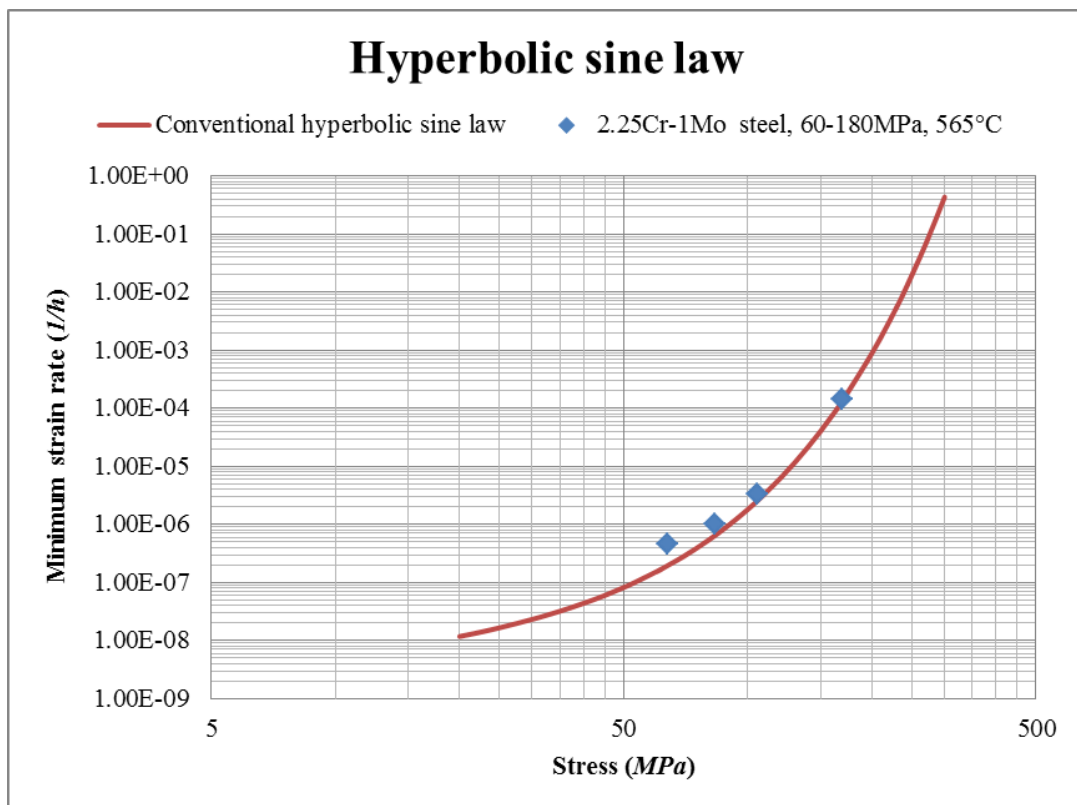


Figure 7.16: Comparison of conventional sinh law with experiment data for 2.25Cr-1Mo steel

Figure 7.16 shows the comparison of the conventional sinh law with the experiment data for 2.25Cr-1Mo steel (Parker, 1995). As Figure 7.16 shows, the minimum creep rate predicted by the conventional sinh law is in good agreement with the experiment data at high stresses. However, at low stresses, the minimum creep rate is lower than that of the experiment test. In order to clearly compare the minimum creep rate predicted by the newly developed constitutive equation and that predicted by the

conventional sinh law, simulated results from the two different models are plotted in Figure 7.17.

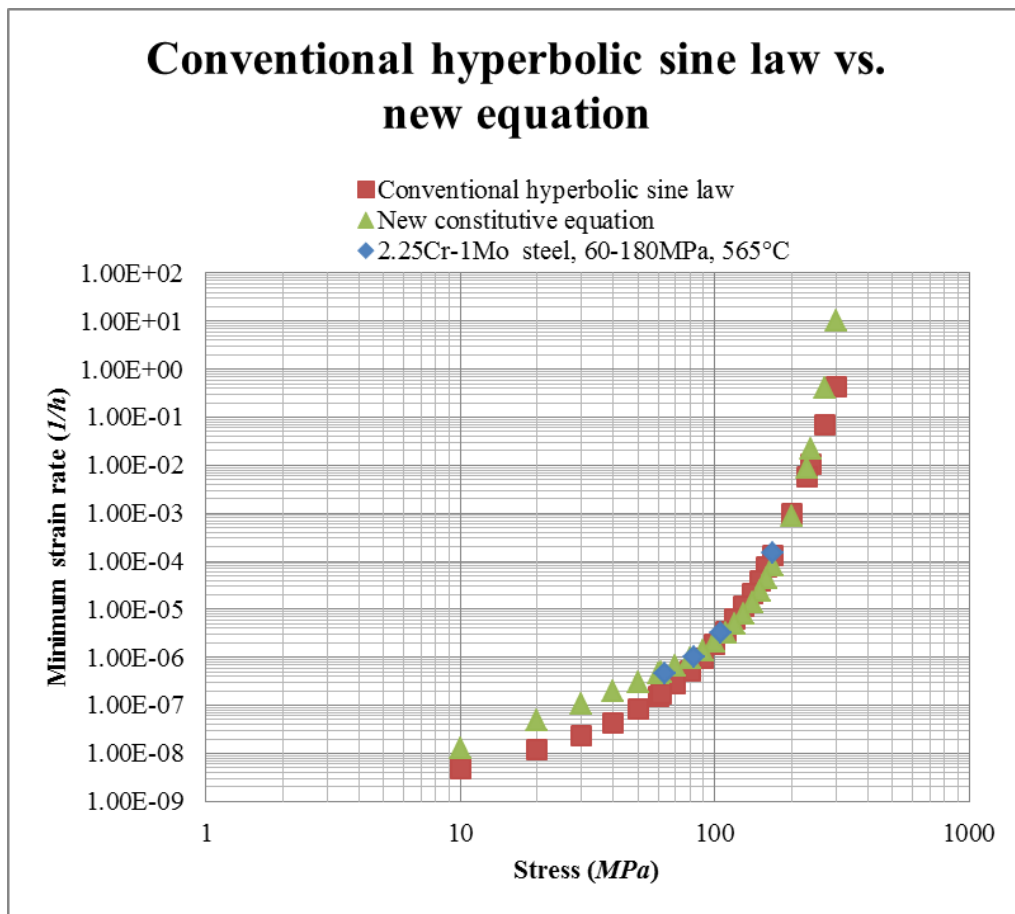


Figure 7.17: Comparison of the conventional sinh law with newly designed constitutive equation for 2.25Cr-1Mo steel

Figure 7.17 shows the comparison of the conventional sinh law with the newly designed constitutive equation for 2.25Cr-1Mo steel. According to Figure 7.17, the minimum creep rate predicted by the newly designed constitutive equation fits much better with the experiment data than that predicted by the conventional sinh law. Furthermore, at low stresses, the minimum creep rate predicted by the conventional sinh law is lower than that of the experiment test. Thus, the use of the conventional sinh law to simply extrapolate from high stresses to low stresses runs the risk of over-estimating the creep lifetime.

#### 7.4.2 Validation of the newly developed minimum creep rate equation based on 1Cr-1Mo-1V steel experiment test

The experimental data set for the evolution of minimum creep strain under a stress range from 70MPa to 180MPa ( $0.33-0.85\sigma_Y$ ) at 600°C for 0.5Cr-0.5Mo-0.25V steel (Parker, 1995) was utilized in validating the newly designed minimum creep rate equation. Furthermore, Dyson's conventional sinh law equation was investigated and the simulated results were compared with the experiment data and the result from the newly developed minimum creep rate equation.

Table 7.15: Material parameters in newly developed constitutive equation for 0.5Cr-0.5Mo-0.25V steel

Material parameter	A	B	q
Value	4.12E-8	2.51E-4	2

With a wide stress range from 10MPa to 300MPa, comparison of the newly developed constitutive equation with the experiment data for 0.5Cr-0.5Mo-0.25V steel (Parker, 1996) can be plotted as shown in Figure 7.18.

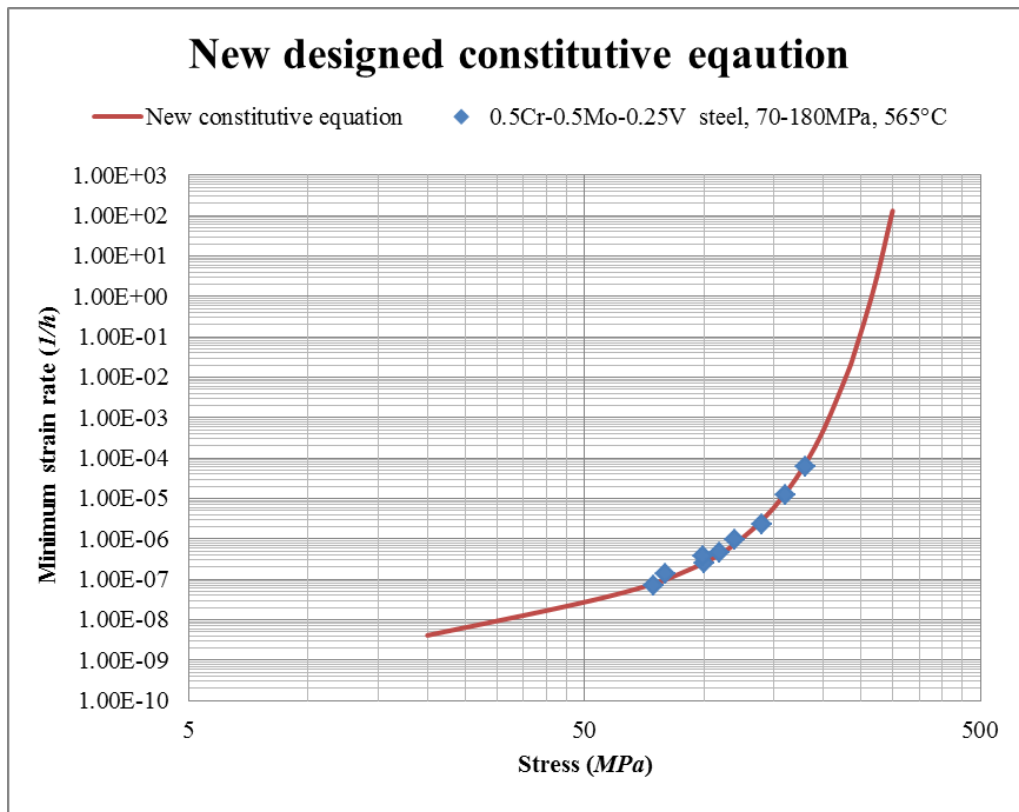


Figure 7.18: Comparison of newly developed constitutive equation with experiment data for 0.5Cr-0.5Mo-0.25V steel

Figure 7.18 shows the comparison of the newly developed constitutive equation with the experiment data for 0.5Cr-0.5Mo-0.25V steel (Parker, 1996). As Figure 7.18 shows, the minimum creep rate predicted by the newly designed constitutive equation is in good agreement with the experiment data.

Table 7.16: Material parameters in conventional sinh law for 0.5Cr-0.5Mo-0.25V steel

Material parameter	A	B
Value	3.6E-12	9.87E-2

With a wide stress range from 10MPa to 300MPa, comparison of the conventional sinh law with the experiment data for 0.5Cr-0.5Mo-0.25V steel (Parker, 1996) can be plotted as shown in Figure 7.19.

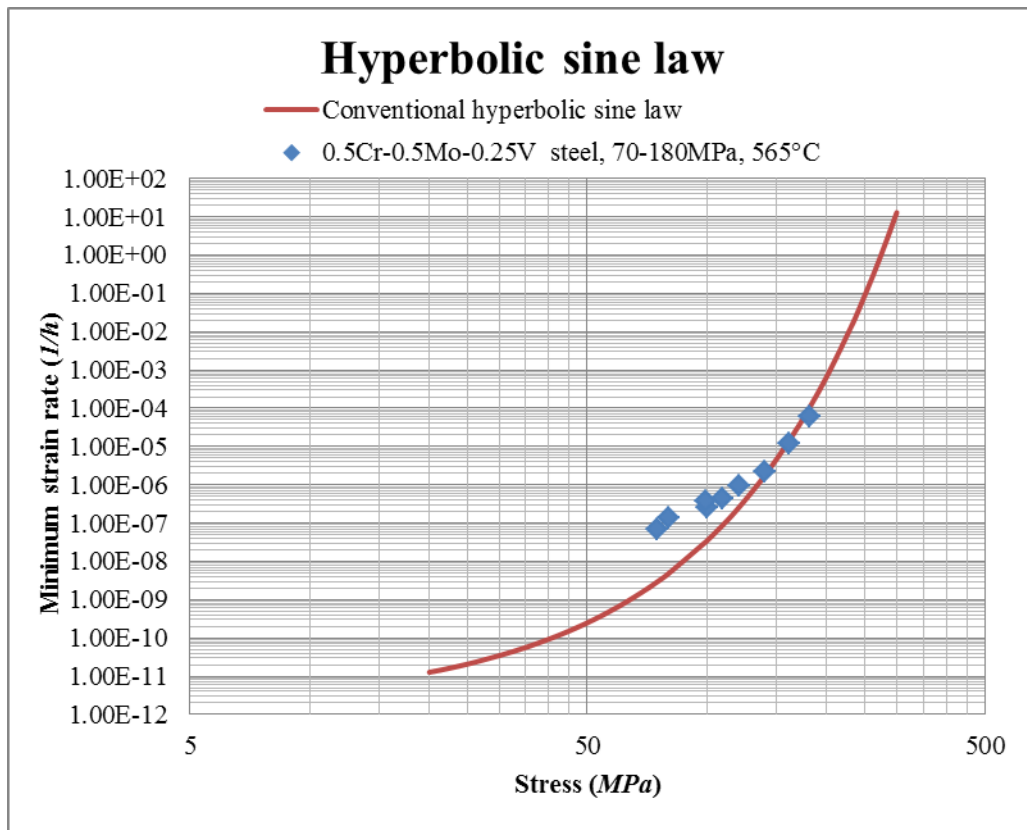


Figure 7.19: Comparison of conventional sinh law with experiment data for 0.5Cr-0.5Mo-0.25V steel

Figure 7.19 shows the comparison of the conventional sinh law with the experiment data for 0.5Cr-0.5Mo-0.25V steel (Parker, 1995). As Figure 7.19 shows, the minimum creep rate predicted by the conventional sinh law is in good agreement with the experiment data at high stresses. However, at low stresses, the minimum creep rate is obviously lower than that of the experiment test. In order to clearly compare the minimum creep rate predicted by the newly developed constitutive equation and the conventional sinh law, simulated results from the two different models are plotted in Figure 7.20.

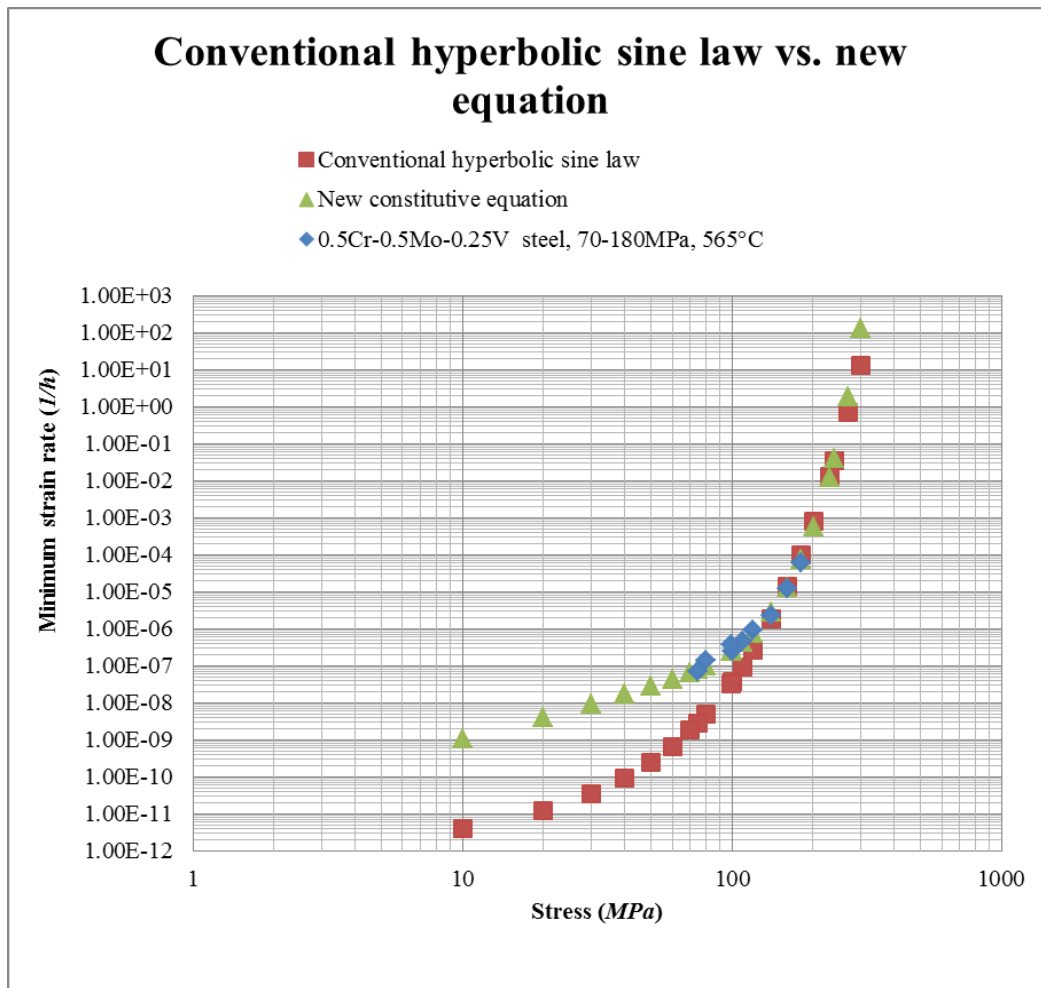


Figure 7.20: Comparison of conventional sinh law with newly designed constitutive equation for 0.5Cr-0.5Mo-0.25V steel

Figure 7.20 shows the comparison of the conventional sinh law with the newly designed constitutive equation for 0.5Cr-0.5Mo-0.25V steel. According to Figure 7.20, the minimum creep rate predicted by the newly designed constitutive equation fits much better with the experiment data than that predicted by the conventional sinh law. Furthermore, at low stresses, the minimum creep rate predicted by the conventional sinh law is lower than that of the experiment test. Thus, the use of the conventional sinh law to simply extrapolate from high stresses to low stresses runs the risk of over-estimating the creep lifetime for low Cr alloys.

## 7.5 Summary

This chapter has investigated the classical constitutive laws for depicting the relationship between minimum creep rate and stress levels. The

advantages and disadvantages of each constitutive law for creep analysis of low Cr alloys under long-term service have been commented on, and the mathematical model for developing a new constitutive equation for minimum creep rate has been explained.

Secondly, a novel minimum creep rate equation has been proposed. This chapter has also illustrated the effects of different parameters in analysing the relationship between minimum creep rate and stress levels through the use of the newly designed constitutive equation.

Finally, validation of the newly designed minimum creep rate constitutive equation has been presented, and the results have been shown to be in good agreement with the results of experimental tests. Furthermore, the chapter has demonstrated why simply using constitutive models to extrapolate from high stresses to low stresses runs the risk of over-estimating the creep lifetime.

# **Chapter 8 Damage evolution equation and rupture criterion for low Cr alloys under long-term service**

## **8.1 Introduction**

Creep fracture is caused by the processes of nucleation and growth of cavities. With the continued growth of voids, creep cracks grow from the cusp and ultimately weaken the cross section to the point where failure occurs. In order to characterize creep damage behaviour and the evolution of the fracture process, an accurate damage evolution equation and rupture criterion should be developed and implemented into the constitutive equations. This chapter presents the development of a damage evolution equation and rupture criterion for low Cr alloys under long-term service. The description of long-term damage behaviour for advanced low Cr alloy steels is based on the assumption that transition from a brittle to ductile character of damage occurs with an increase of stress. The rupture mechanisms and the effects of stress level on creep cavity have been investigated in Chapter 5 and Chapter 6, respectively. Here, a novel creep damage equation with the rupture criterion for evaluating the failure time of low Cr alloys has been developed through the evaluation of physically-based experiment data and analysis of the effects of stress level on creep mechanisms. The procedure required in order to fulfil the above aims can be described as follows:

- 1) To investigate the evolution of creep cavity during the rupture process. The characteristics of initial creep cavity and cavity at rupture time should be analysed, and then the dominative mechanisms during the creep rupture process should be determined.
- 2) To design a rupture criterion for the new constitutive equations. The typical rupture criteria should first be investigated, and then a new

rupture criterion should be developed according to physically-based experiment observation.

- 3) To develop and validate the new damage evolution equation. The new damage evolution equation should first be proposed, and the validation should be conducted through comparison of simulated results with physically-based creep experiment data.

## 8.2 Investigation of the evolution of creep cavity during rupture process

### 8.2.1 Creep cavity at initial damage time

The characteristics of initial creep cavities were analysed based on experiment data from observation of the micro-structural changes of 1Cr-0.5Mo steel under the stress 35MPa at a temperature of 520 °C (Dobrzański et al., 2006). The micro-structure of creep cavities at initial damage time is shown in Figure 8.1.

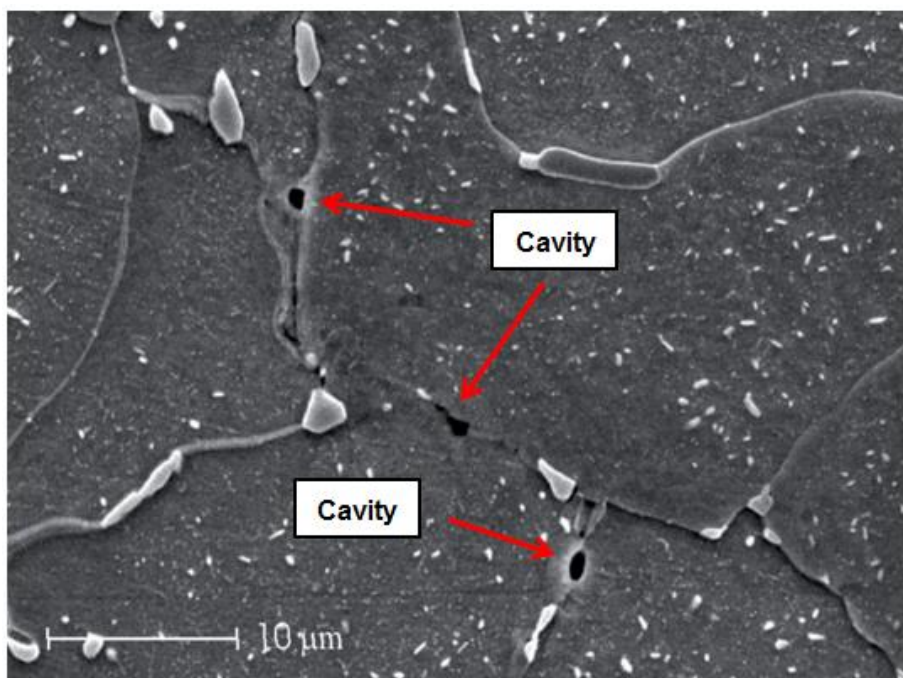


Figure 8.1: Cavity at initial damage stage of 1Cr-0.5Mo steel under stress range from 35MPa at temperature of 520°C (Dobrzański et al., 2006)

As shown in Figure 8.1, three cavities were captured through the use of transmission electron microscopy (TEM) by Dobrzański et al. (2006). The

size and shape of cavities can be represented by a cavity semi-axis schematic diagram.

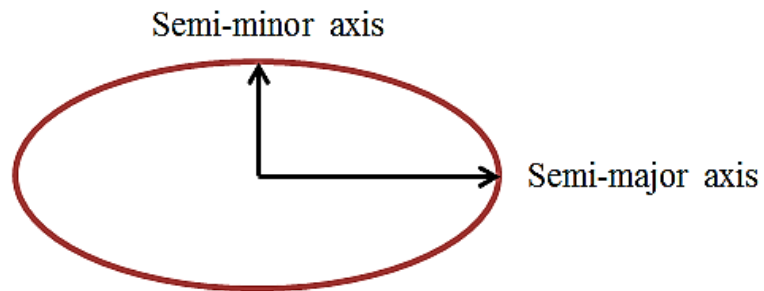


Figure 8.2: Cavity semi-axis schematic diagram

From the experiment data for cavities at initial damage stage of 1Cr-0.5Mo steel (Dobrzański et al., 2006), the radii of initial cavities in the semi-minor axis can be summarised and plotted as shown in Figure 8.3.

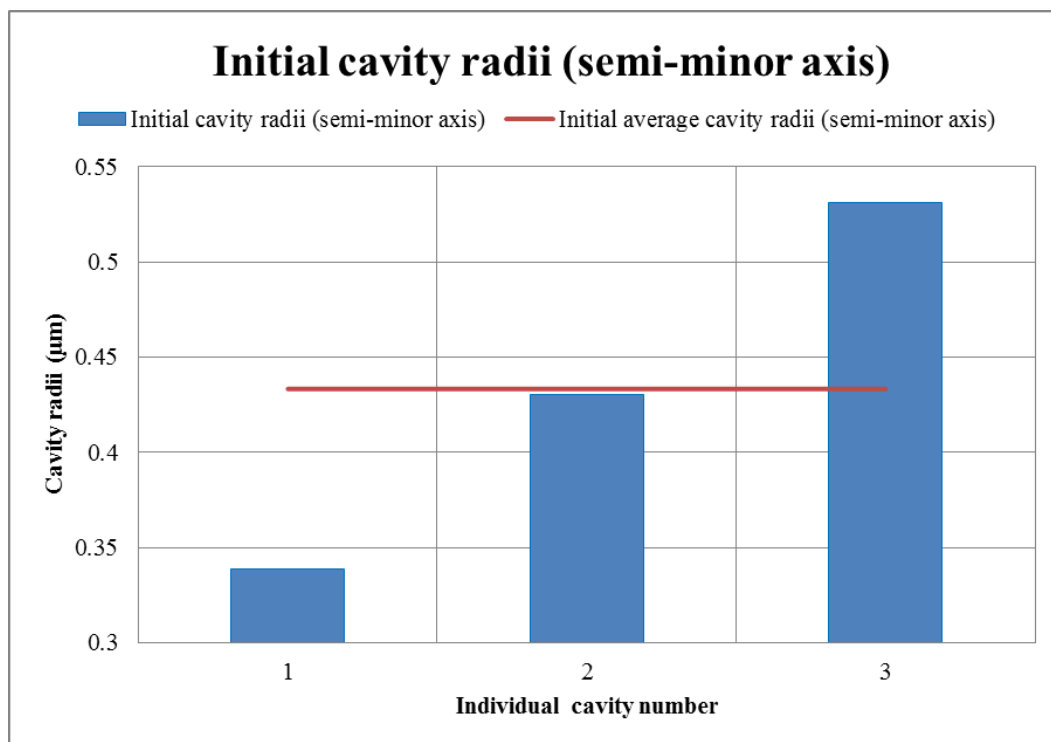


Figure 8.3: Radii of initial cavities of 1Cr-0.5Mo steel in semi-minor axis

Figure 8.3 shows the radii of initial cavities of 1Cr-0.5Mo steel in the semi-minor axis. As Figure 8.3 demonstrates, the average initial cavity radius  $R_i$  ( $\mu\text{m}$ ) can be plotted and the value of the average initial cavity radius is

0.433. The radii of initial cavities in the semi-major axis can be summarised and plotted as shown in Figure 8.4.

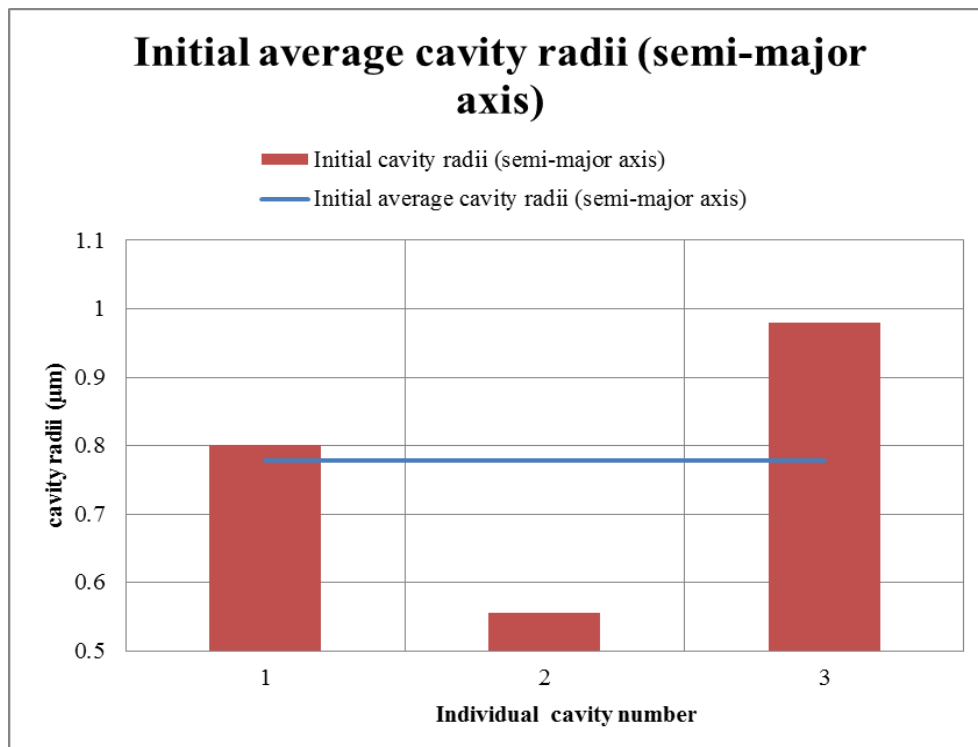


Figure 8.4: Radii of initial cavities of 1Cr-0.5Mo steel in semi-major axis

Figure 8.4 shows the radii of initial cavities of 1Cr-0.5Mo steel in the semi-major axis. As Figure 8.4 demonstrates, the average initial cavity radius  $R_i$  ( $\mu\text{m}$ ) can be plotted and the value of the average initial cavity radius is 0.778.

### 8.2.2 Creep cavity at rupture time

The characteristics of creep cavity at rupture time were analysed based on experiment data from the observation of micro-structural changes of 1Cr-0.5Mo steel under the stress 35MPa at a temperature of 520 °C (Dobrzański et al., 2006). The micro-structure of creep cavities at rupture time is shown in Figure 8.5.

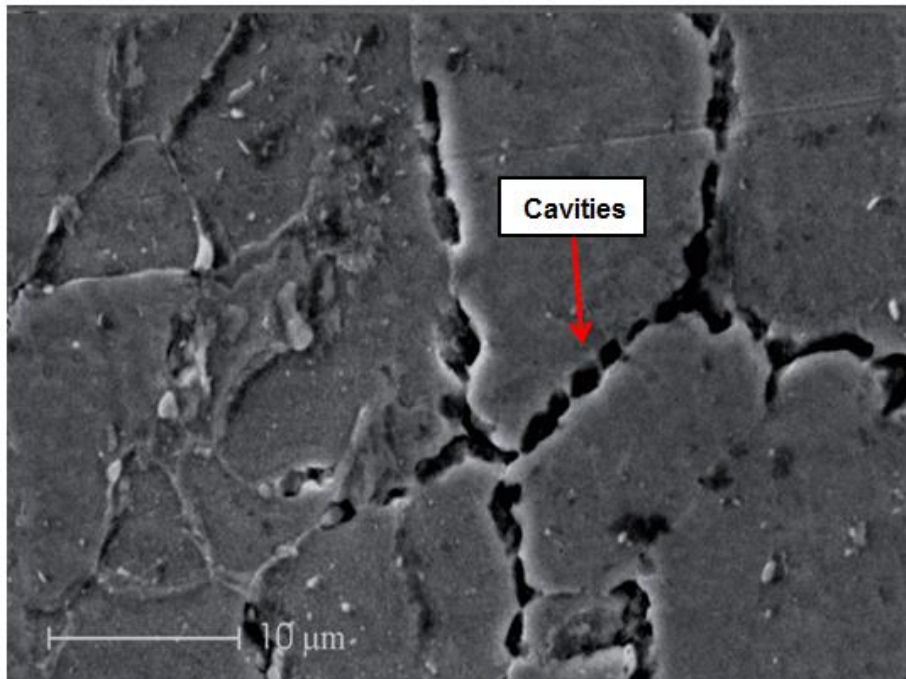


Figure 8.5: Cavities at coalescence stage of 1Cr-0.5Mo steel under stress range from 35MPa at temperature of 520°C (Dobrzański et al., 2006)

According to Figure 8.5, the number of cavities has significantly increased and the characteristics of creep cavities on the fracture surface were observed through the use of SEM by Dobrzański et al., (2006). The coalescence of cavities can be illustrated as shown in Figure 8.6.

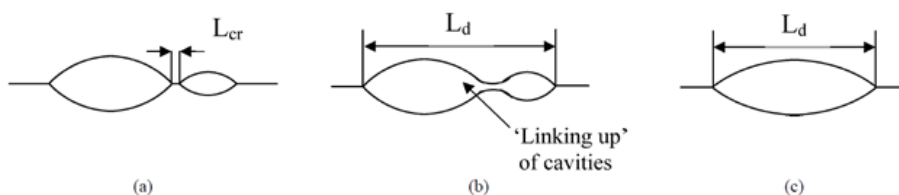


Figure 8.6: Schematic diagram of cavity linkup behaviour at rupture stage (Westwood et al., 2004)

Cavities coalesce by mid-way through the tertiary stage, though many retain their individuality even at rupture. Once the size of voids grows sufficiently large, they will coalesce either with nearby cracks or with neighbouring voids. From the experiment data for cavities in 1Cr-0.5Mo steel at rupture time (Dobrzański et al., 2006), the radii of cavities in the semi-minor axis at rupture time can be summarised and plotted as shown in Figure 8.7.

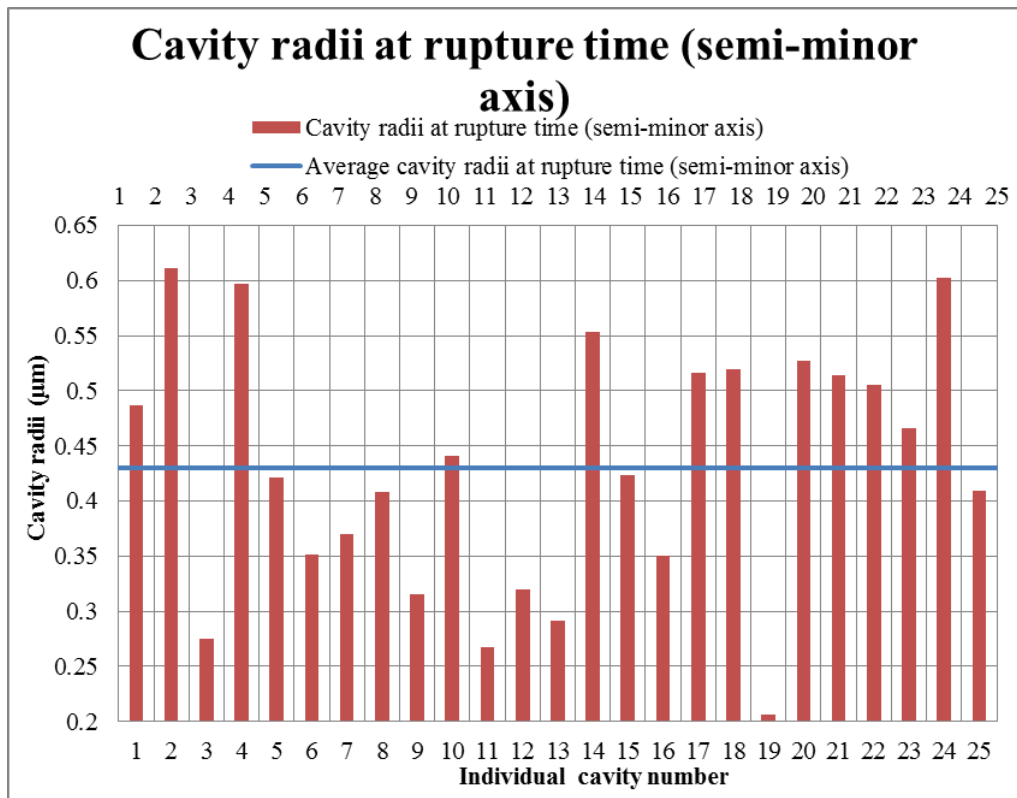


Figure 8.7: Radii of cavities of 1Cr-0.5Mo steel in semi-minor axis at rupture time

Figure 8.7 shows the radii of cavities of 1Cr-0.5Mo steel in the semi-minor axis at rupture time. As Figure 8.7 demonstrates, the average cavity radius  $R_c$  ( $\mu\text{m}$ ) at rupture time can be plotted and the value of the average initial cavity radius is 0.430. The number of cavities has increased from three (initial damage stage) to twenty-five (rupture time). The radii of cavities in the semi-major axis at rupture time can be summarised and represented as shown in Figure 8.8.

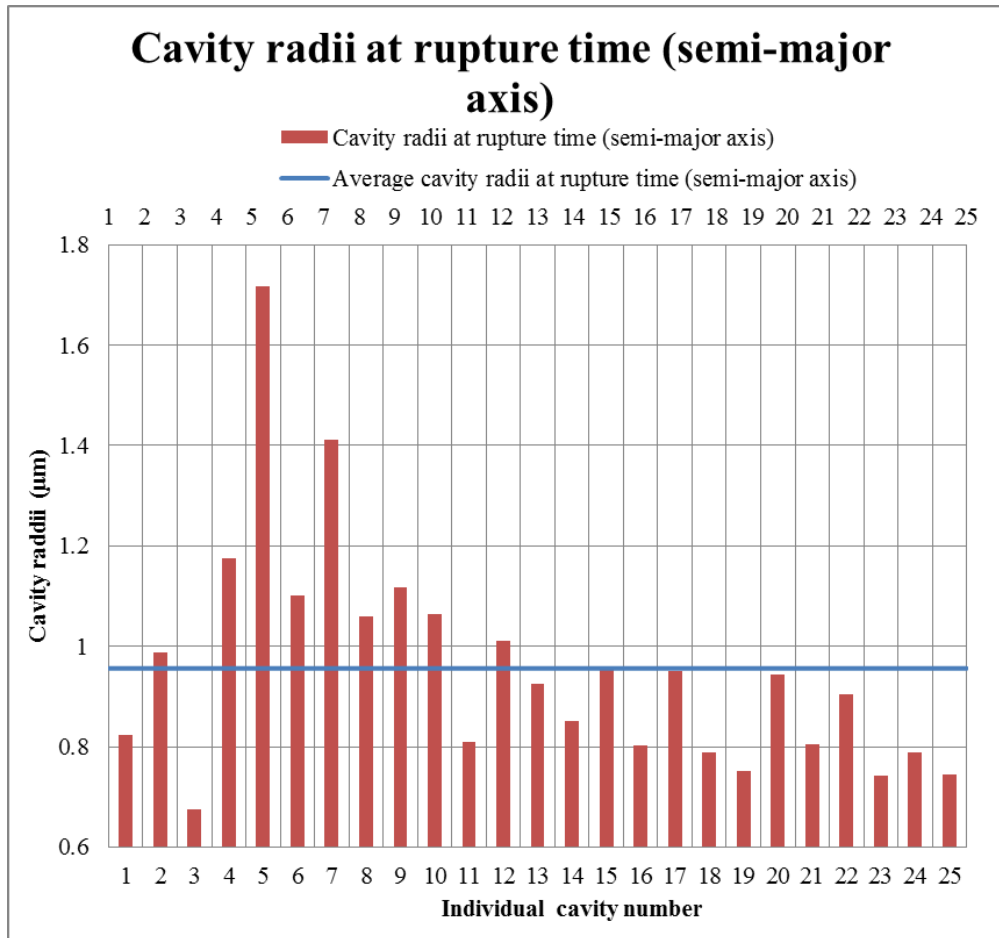


Figure 8.8: Radii of cavities of 1Cr-0.5Mo steel in semi-major axis at rupture time

Figure 8.8 shows the radii of cavities of 1Cr-0.5Mo steel in the semi-major axis at rupture time. As Figure 8.8 demonstrates, the average initial cavity radius  $R_c$  ( $\mu\text{m}$ ) can be plotted and the value of the average initial cavity radius is 0.956.

### 8.2.3 Discussion

Creep rupture is caused by the accumulation of cavity nucleation and growth. At a low stress level it is usually associated with brittle rupture behaviour and the dominative rupture mechanism is based on cavity nucleation. At high stresses, however, it is normally associated with ductile rupture behaviour and the dominative rupture mechanism is based on cavity growth. Furthermore, the model of cavity growth is controlled by the diffusion process, because the cavity growth process involves vacancy condensation. Dobrzański et al. (2006) report that the majority of cavities appear along the GB which is transverse to the stress axis, and that cavity

growth is affected by the absorption of excess stress-induced vacancies. Due to the fact that the short radii of cavities are controlled by the GB, the cavity profile can evolve over time into an elongated crack.

Based on observations presented in Figures 8.1 to 8.8, the evolution of creep cavities in 1Cr-0.5Mo steel can be summarised as shown in Table 8.1.

Table 8.1: Evolution of creep cavities in 1Cr-0.5Mo steel

Creep cavity	Average initial cavity radius, $R_i$ ( $\mu m$ )	Average cavity radius ( $\mu m$ ), $R_c$ at rupture time	Percentage change in cavity radius $\left  \frac{R_i - R_r}{R_r} \right $
Semi-minor axis	0.433	0.430	0.7%
Semi-major axis	0.778	0.956	18.6%
Observation	<ol style="list-style-type: none"> <li>1. The coalescence of cavities to form micro-cracks appeared at the rupture stage</li> <li>2. A slight decrease of cavity radius in the semi-minor axis direction was observed</li> <li>3. An increase of cavity radius in the semi-major axis direction was observed</li> <li>4. Within areas of the same size, initial cavity density was approximately 10 times less than the cavity density at rupture time</li> <li>5. Cavities associated with particles were observed at rupture stage</li> </ol>		

Table 8.1 summarises the evolution of creep cavity in 1Cr-0.5Mo steel. According to Table 8.1, the percentage change in cavity radius was not obvious in the semi-minor axis direction, but the percentage change in cavity radius in the semi-major axis direction increased by approximately 20% from the initial damage stage to rupture time. The cavities on the GB were constrained by the GB and surrounding material, as the growth of the cavities' radii in the semi-minor axis direction were restricted by the width of the GB. Furthermore, the size of newly nucleated cavities was not large as a result of a slight decrease in the average cavity radius in the semi-minor axis direction. The number of cavities increased significantly from initial damage stage to rupture stage because this experiment was conducted under low stress level, and thus the dominative rupture mechanism was based on cavity nucleation. However, an increase in

cavity radius in the semi-major axis direction was observed. Such behaviour may have been caused by the occurrence of high local stresses during the damage process and the fact that the rupture mechanism based on cavity growth promotes the growth of cavity radii in the semi-major axis, which is along the transverse GB direction.

Thus, the creep rupture process in 1Cr-0.5Mo steel is not only dependent on cavity nucleation but also affected by cavity growth. Although the observation was conducted at a low stress level, high local stresses caused by the stress breakdown phenomenon can also change the dominative rupture mechanism in specific areas where such high local stress occurs.

### 8.3 Design of the rupture criterion for constitutive equation

#### 8.3.1 Investigation of the typical creep rupture criterion

In order to determine the failure time of high temperature structural components, an accurate rupture criterion should be developed to meet the physics. Many efforts have been made to develop a rupture criterion for low Cr alloy creep damage constitutive equations, and the typical rupture criteria have been summarized in Table 8.2.

Table 8.2: Summary of typical rupture criteria for low Cr alloy creep damage constitutive equations

Creep models used for low Cr-Mo alloy	Originated from year	Failure criterion
Kachanov-Rabotnov (1969)	1969	Critical damage $D = 1$
Lemaitre (1985)	1985	Critical damage $D = 0.5$
Lai (1989)	1989	Critical reduction in load-bearing area = $A$ (addressed as 63%)
Dyson and Osgerby (1993)	1993	Critical damage $\omega_c = 1/3$
Pétry and Lindet (2009)	2009	Critical strain at failure $\epsilon_f = 5\%$

Table 8.2 summarizes the different creep rupture criteria which have been applied in creep damage constitutive equations for low Cr alloys, where  $D$  represents the damage rate and  $\omega_c$  is the area fraction of cavitation. However, these creep rupture criteria do not have realistic physical meanings in terms of reflecting real creep rupture and the rupture

mechanism. The results summarized in Chapters 6 and 7, regarding the effects of strain at failure, cavity nucleation and growth, illustrate that the relationship between strain at failure and stress levels is nonlinear and that cavitation behaviour at rupture time varies with different stress levels. Thus, the use of a fixed value as a rupture criterion has obvious limitations. Dyson and Osgerby (1993) suggest that the percentage of boundary area fraction may be a suitable creep rupture criterion. They report that in a uniaxial creep test, the failure condition was met when all of the grain boundaries normal to the applied load were completely cavitated. The area fraction of such cavities at failure is approximately 1/3, and since the damage variable represents a cavitated area fraction, then the damage at failure is equal to 1/3. The main advantage of using the percentage of boundary area fraction method is that cavity size and shape can be detected at the fracture surface in a physically-based experimental creep test.

### **8.3.2 New physically-based creep rupture criterion**

Cavities are often initiated at the intersection of a slip band with a GB or at ledges in the boundaries (Riedel, 1987). The cavitated area fraction changes when the stress level changes. Furthermore, strain at failure increases in a nonlinear manner with the increase of stress level, as the damage varies with the stress level. With experiment data for the evolution of creep cavity for 2.25Cr-1Mo steel under stresses of 55.6MPa, 60.6MPa and 70.6MPa at a temperature of 565°C (Lonsdale and Flewitt, 1979), a new creep rupture criterion can be developed through use of the percentage of boundary area fraction (Dyson and Osgerby, 1993). Based on this experiment data (Lonsdale and Flewitt, 1979), the relationship between area fraction of cavitation and rupture time can be plotted as shown in Figure 8.9.

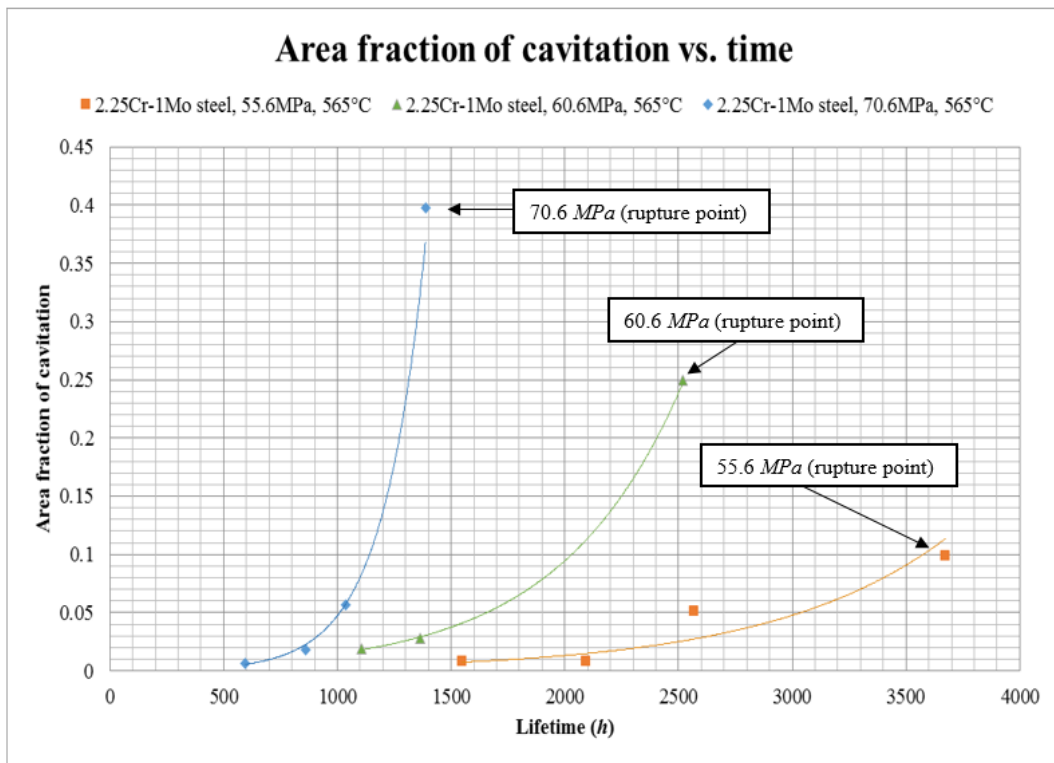


Figure 8.9: Area fraction of cavitation versus time for 2.25Cr-1Mo under the stresses 55.6MPa, 60.6MPa and 70.6MPa at temperature of 565°C

Figure 8.9 shows that the area fraction of cavitation increases in a nonlinear manner with time. Based on the limited experiment data available (only a small volume) describing the evaluation of creep cavity under different stresses for low Cr alloys, the relationship between area fraction of cavitation and stresses can be simply plotted as shown in Figure 8.10.

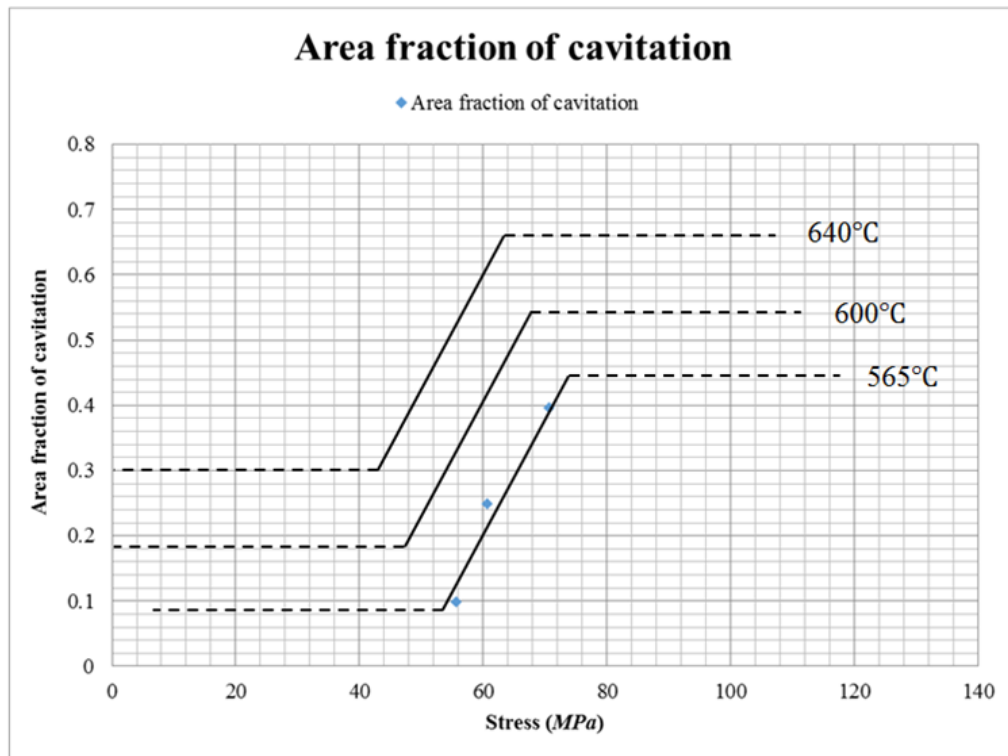


Figure 8.10: Area fraction of cavitation at rupture time versus stress for 2.25Cr-1Mo under the stresses 55.6MPa, 60.6MPa and 70.6MPa at temperature of 565°C, and assumption of the area fraction of cavitation at 600°C and 640°C

Figure 8.10 shows the area fraction of cavitation at rupture time versus stress for 2.25Cr-1Mo under the stresses 55.6MPa, 60.6MPa and 70.6MPa at a temperature of 565°C, and an assumption of the area fraction of cavitation at 600°C and 640°C (Cane, 1979; Lonsdale and Flewitt, 1979). According to Figure 8.10, the area fraction of cavitation at rupture time obviously differs under the different stress levels and is not a fixed value. Thus, the use of a fixed value as rupture criterion has obvious limitations.

The area fraction at rupture time in Figure 8.10 increases with the increase of stress level, and an approximately linear increase occurs at an intermediate stress level ( $0.4\sigma_Y$ - $0.5\sigma_Y$ ). Thus, the new damage creep rupture criterion can be described as follows:

$$\omega_c = \begin{cases} a & 0.2\sigma_Y \leq \sigma \leq 0.4\sigma_Y \\ \alpha\sigma - \delta & 0.4\sigma_Y \leq \sigma \leq 0.5\sigma_Y \\ b & \sigma > 0.5\sigma_Y \end{cases} \quad (8.1)$$

where  $\alpha$  and  $\delta$  are the material parameters and  $\sigma$  is the applied stress. It should be noted that at relatively low stress level ( $0.2\sigma_Y$ - $0.4\sigma_Y$ ) and high stress level ( $>0.5\sigma_Y$ ), the rupture criterion is shown as an approximately constant value in Figure 8.10. Moreover, as has been stated in the previous section, the cavity density is affected by temperature. The degree of cavity nucleation and growth increases with the increase of temperature; therefore, in the absence of any other relationship between relative creep cavitation rupture area and stress, further assumptions can be made as plotted in Figure 8.10.

## **8.4 Development and validation of new damage evolution equation**

### **8.4.1 Development of new damage evolution equation**

In order to develop the new damage evolution equation, two classical damage concepts have been explored in relation to ductile and brittle damage accumulation characteristics. These concepts are based on the same long-term strength equation describing creep rupture versus time, but caused by different types of fracture. Ductile fracture, with progressive deformation and necking, occurs at high stress levels and is accompanied by conventional *sinh* law creep deformations, whereas brittle fracture, caused by thermal exposure and material micro-structure degradation, occurs at low stress levels. They are predominantly accompanied by nonlinear creep deformations, and therefore two corresponding ductile and brittle damage evolution equations based on the *sinh* law concept have been formulated to be used in combination with the creep constitutive equation.

The proposed damage evolution equation has been extended to include stress dependence using Dyson's damage model. According to Dyson (2000), the creep damage variables  $D_N$  and  $D_G$  are proposed to describe the cavity nucleation damage mechanism and cavity growth damage mechanism respectively. The dimensionless damage parameter  $D_N$  demonstrates the area fraction of GB facets cavitated. When cavity evolution is growth controlled, the rate of cavity nucleation is  $\dot{D}_N = 0$ .

When cavities are nucleated continuously, the evolution of  $D_N$  can be written as:

$$\dot{D}_N = N \left( \frac{K_N}{\varepsilon_{fu}} \right) \dot{\varepsilon} \quad (8.2)$$

The parameter of  $K_N$  has a maximum value of 1/3, where  $\varepsilon_{fu}$  is the uniaxial strain at failure.

The dimensionless damage parameter  $D_G$  demonstrates the volume fraction of GB facets cavitated. When creep damage is cavity growth controlled, the rate of cavity growth can be written as:

$$\dot{D}_G = \frac{d}{2lD_G} \dot{\varepsilon} \quad (8.3)$$

where  $l$  is the inter-cavity spacing and  $d$  is the grain size (Dyson, 1988, 2000).

By coupling with the cavity nucleation damage mechanism and cavity growth damage mechanism, Dyson's damage evolution equation can be written as:

$$\dot{\omega} = C \dot{\varepsilon} \quad (8.4)$$

where  $C$  is the material parameter;  $\dot{\varepsilon}$  is the creep strain rate and  $\dot{\omega}$  is the damage rate. The use of creep damage variables  $D_N$  and  $D_G$  can be decided by the parameter  $C$ .

However, the creep rupture process in low Cr alloy steel is not only dependent on cavity nucleation but also affected by cavity growth at the same time. At low stress levels, due to the creep rupture mechanism, it is suggested that the evolution of cavity is the result of continuous cavitation nucleation and a constrained cavity growth mechanism, which has a dominant influence on the accumulation of damage leading to final rupture behaviour.

According to Table 8.1, the occurrence of high local stresses during the damage process and the fact that the rupture mechanism based on cavity

growth promotes the growth of cavity radii in the semi-major axis, which is along the transverse GB direction. Although the observation was conducted at a low stress level, high local stresses caused by the stress breakdown phenomenon can also change the dominative rupture mechanism in specific areas where such high local stress occurs. Thus, a strain exponent should be implemented into Dyson's respected damage model and the improved damage evolution equation can be written as:

$$\dot{\omega} = C\dot{\epsilon}^x \quad (8.5)$$

where  $C$  and  $x$  are the material parameter and strain exponent, respectively;  $\dot{\epsilon}$  is the creep strain rate and  $\dot{\omega}$  is the damage rate.

#### 8.4.2 Validation of new damage evolution equation

Experiment data for the evolution of creep damage under the stress 40MPa ( $0.31\sigma_Y$ ) at 640°C for 0.5Cr-0.5Mo-0.25V base material (Hyde et al., 1998) was utilized to demonstrate the validity of the newly developed damage evolution equation. Furthermore, Dyson's conventional damage evolution equation was investigated, and the simulated results compared with experiment data and the result from the newly developed damage evolution equation.

Table 8.3: Material parameters in validating newly developed damage evolution equation for 0.5Cr-0.5Mo-0.25V base material (Dyson and Osgerby, 1993)

Material parameter	A (MPa/h)	B (MPa <sup>-1</sup> )	C	H (MPa)	H*	Kc (MPa <sup>-3</sup> /h)
Value	4.316E-8	0.15	0.8	1.0E6	0.35	4.998E-4

With the stress 40MPa and the time increment of 50 hours, comparison of Dyson's damage evolution equation with the experiment data for 0.5Cr-0.5Mo-0.25V base material (Hyde et al., 1998) can be plotted as shown in Figure 8.11.

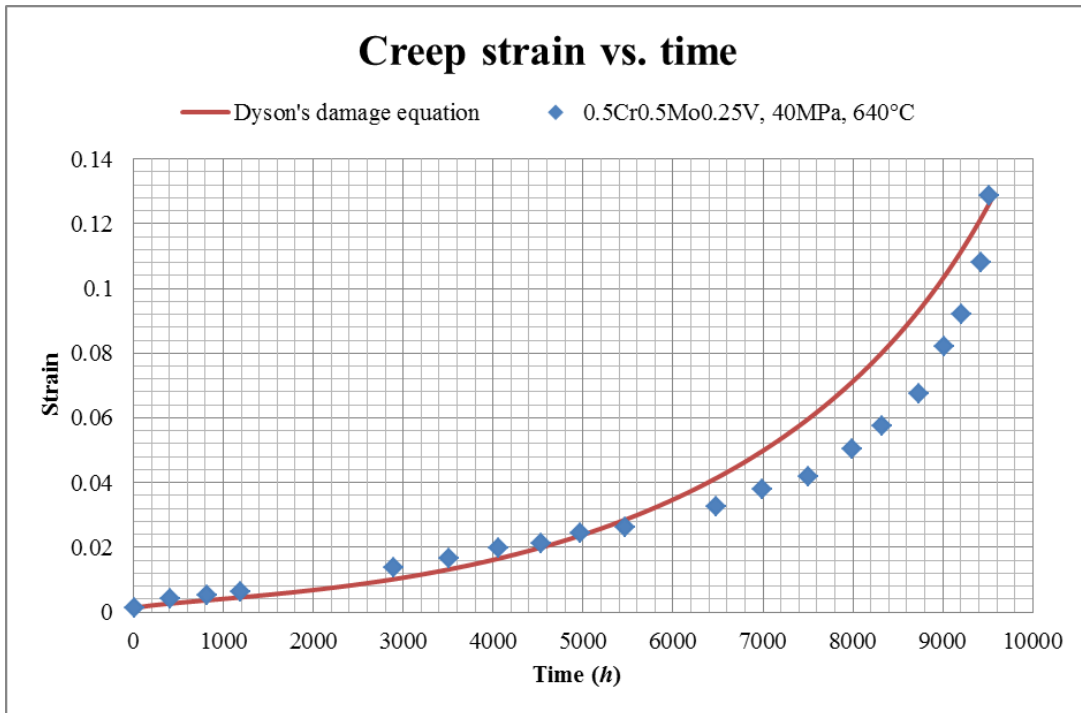


Figure 8.11: Comparison of Dyson’s damage evolution equation with experiment data for 0.5Cr-0.5Mo-0.25V base material

Figure 8.11 shows the comparison of Dyson’s damage evolution equation with the experiment data for 0.5Cr-0.5Mo-0.25V base material. As Figure 8.11 demonstrates, the creep strain predicted by Dyson’s damage evolution equation is in good agreement with the experiment data from the initial time to almost the 6000<sup>th</sup> hour; however, from the 6000<sup>th</sup> hour to rupture time the predicted creep strain is obviously larger than that of the experiment data.

With the stress 40MPa and the time increment of 50 hours, comparison of the newly developed damage evolution equation with the experiment data for 0.5Cr-0.5Mo-0.25V base material (Hyde et al., 1998) can be plotted as shown in Figure 8.12.

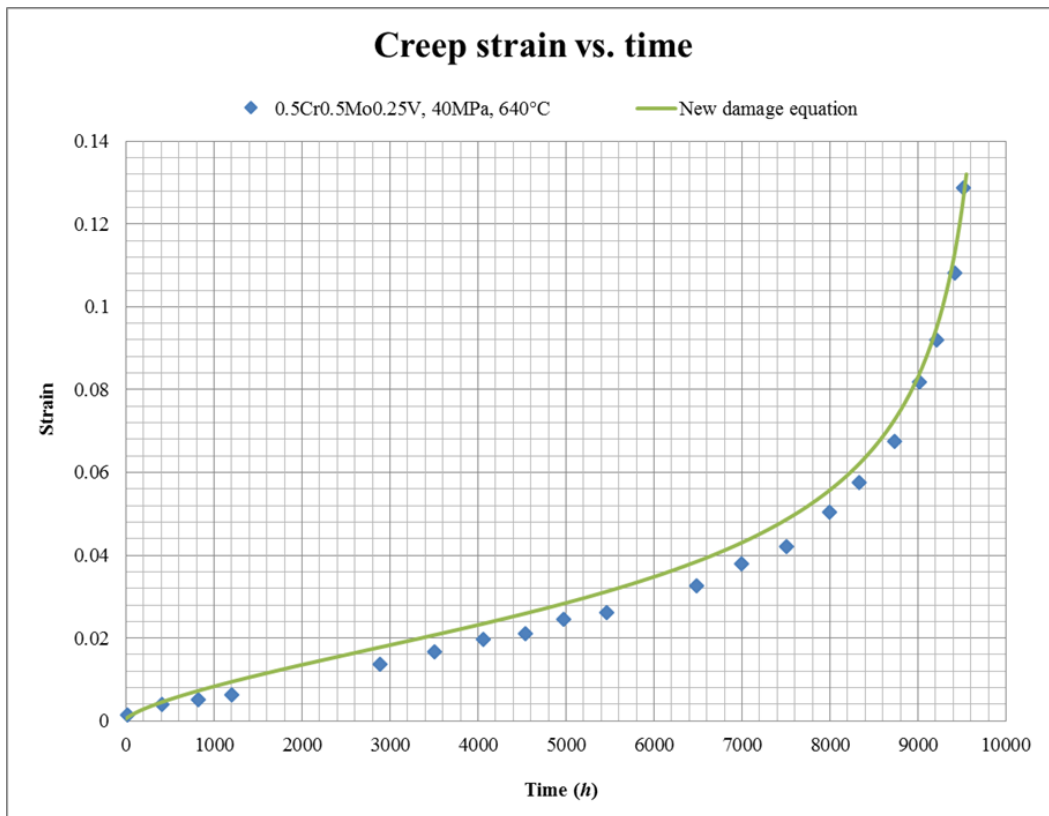


Figure 8.12: Comparison of newly developed damage evolution equation with the experiment data for 0.5Cr-0.5Mo-0.25V base material

Figure 8.12 shows the comparison of the newly developed damage evolution equation with the experiment data for 0.5Cr-0.5Mo-0.25V base material. As shown in Figure 8.12, the creep strain predicted by the newly developed damage evolution equation is in good agreement with the experiment data from the initial time to rupture time. In order to clearly compare the creep strain predicted by the newly developed damage evolution equation and Dyson's damage evolution equation, simulated results from the two different models are plotted in Figure 8.13.

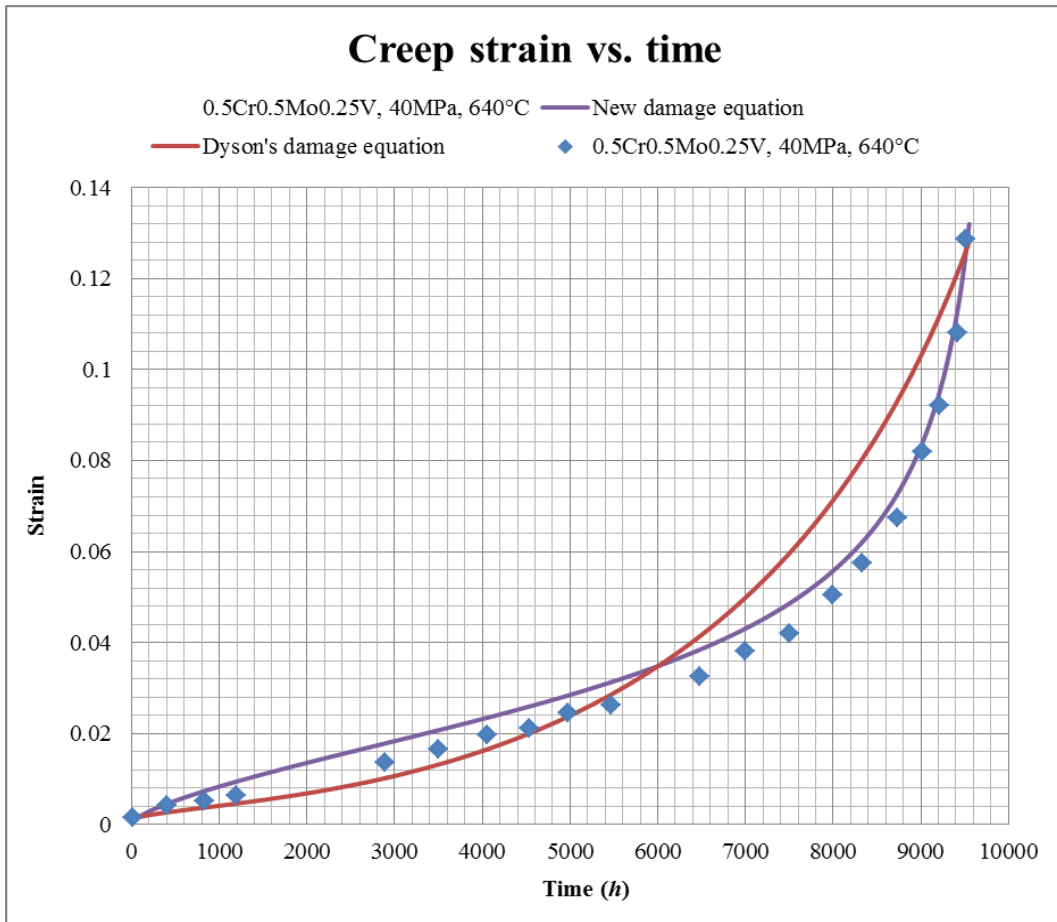


Figure 8.13: Comparison of newly developed damage evolution equation with Dyson's damage evolution equation for 0.5Cr-0.5Mo-0.25V base material

Figure 8.13 shows the comparison of the newly developed damage evolution equation with Dyson's damage evolution equation for 0.5Cr-0.5Mo-0.25V base material. According to Figure 8.13, the creep strain predicted by the newly developed damage evolution equation fits much better with the experiment data than that predicted by Dyson's damage evolution equation. Thus, the newly developed damage evolution equation should be utilized in developing constitutive equations for creep damage analysis of low Cr alloys under long-term service.

## 8.5 Summary

This chapter has investigated the evolution of creep cavity during the rupture process, and the creep mechanisms involved in the rupture process of low Cr alloys under long-term service have been determined.

Secondly, a new rupture criterion for constitutive equations has been proposed. This chapter also illustrates why the typical rupture criteria do not satisfy the requirements for developing creep damage constitutive equations.

Finally, a new damage evolution equation has been proposed, and validation of the damage evolution equation has been presented which shows the results to be in good agreement with those of the experiment test.

# **Chapter 9 Implementation and verification of creep damage constitutive equations for creep damage analysis**

## **9.1 Introduction**

This chapter presents the implementation and verification of creep damage constitutive equations for creep damage analysis of low Cr alloys under long-term service.

The specific areas of focus for this chapter include the following:

- 1) To implement the newly developed minimum creep rate equation and damage evolution equation into constitutive equations for creep damage analysis of low Cr alloys.
- 2) To verify the new set of creep damage equations by comparing them with results from the well-known Kachanov-Rabotnov constitutive equations and experiment data.
- 3) To verify the new set of creep damage equations via extension of the low stress level to intermediate stress level.

## **9.2 Implementation of the newly developed minimum creep rate equation and damage evolution equation into constitutive equations**

The development of the hardening constitutive equation and particle coarsening constitutive equation has reached maturity, and further enhancements to advance knowledge of creep constitutive equations need to be focused on the accurate depiction of minimum creep strain rate and the evolution of damage over time for low Cr alloys. The newly developed minimum creep rate equation and damage evolution equation have been proposed in Chapter 7 and Chapter 8, respectively.

The new minimum strain rate versus stress constitutive equation can be expressed as follows:

$$\dot{\epsilon}_{min} = A \sinh(B\sigma^q) \quad (9.1)$$

where  $A$  and  $B$  are material parameters and  $q$  is the stress exponent.

The new creep damage equation and rupture criterion can be written as:

$$\dot{\omega} = C\dot{\epsilon}^x \quad (9.2)$$

where  $C$  and  $x$  are the material parameter and strain exponent, respectively;  $\dot{\epsilon}$  is the creep strain rate and  $\dot{\omega}$  is the damage rate.

$$\omega_c = \begin{cases} a & 0.2\sigma_Y \leq \sigma \leq 0.4\sigma_Y \\ \alpha\sigma - \delta & 0.4\sigma_Y \leq \sigma \leq 0.5\sigma_Y \\ b & \sigma > 0.5\sigma_Y \end{cases} \quad (9.3)$$

where  $\alpha$  and  $\delta$  are the material parameters,  $\sigma$  is the applied stress and  $\omega_c$  is the rupture criterion.

In order to predict the three creep deformation stages, the minimum creep rate equation should be coupled with the hardening equation and the particle coarsening equation. Through combining these constitutive equations, a new set of creep damage constitutive equations for creep damage analysis of low Cr alloys under long-term service can be written as:

$$\dot{\epsilon} = A \sinh \left[ \frac{B\sigma^q(1-H)}{(1-\phi)(1-\omega)} \right] \quad (9.4)$$

$$\dot{H} = \left( \frac{h\dot{\epsilon}}{3} \right) \left[ 1 - \left( \frac{H}{H^*} \right) \right] \quad (9.5)$$

$$\dot{\phi} = \left( \frac{K_c}{3} \right) (1 - \phi)^4 \quad (9.6)$$

$$\dot{\omega} = C\dot{\epsilon}^x \quad (9.7)$$

$$\omega_c = \begin{cases} a & 0.2\sigma_Y \leq \sigma \leq 0.4\sigma_Y \\ \alpha\sigma - \delta & 0.4\sigma_Y \leq \sigma \leq 0.5\sigma_Y \\ b & \sigma > 0.5\sigma_Y \end{cases} \quad (9.8)$$

where  $A$ ,  $B$ ,  $C$ ,  $h$ ,  $H^*$ ,  $K_c$ ,  $\alpha$  and  $\delta$  are material parameters. The material parameters which appear in this model may be divided into three groups: (1) the constants  $h$  and  $H$  which describe primary creep; (2) the

parameters  $A$  and  $B$  which characterize secondary creep; and (3) the parameters  $K_c$  and  $\omega$  which are responsible for damage evolution.

The equation set contains two damage state variables used to model tertiary softening mechanisms. The first damage state variable,  $\phi$ , is defined by the physics for ageing as lying lie within a range of 0 to 1 for mathematical convenience. The second damage variable,  $\omega$ , describes GB creep constrained cavitation, the magnitude of which is strongly sensitive to alloy composition and to process route.

### 9.3 Verification of the new constitutive equations by comparing with results from the respected Kachanov-Rabotnov constitutive equations and experiment data

Experiment data for the evolution of creep strain under the stress 40MPa ( $0.31\sigma_Y$ ) at 640°C for 0.5Cr-0.5Mo-0.25V base material (Hyde et al., 1998) have been used here in order to demonstrate the validity of the newly developed creep damage constitutive equations. Furthermore, the respected Kachanov-Rabotnov constitutive equations have been investigated and the simulated results compared with experiment data and the results from the newly developed constitutive equations.

Table 9.1: Material parameters in Kachanov-Rabotnov constitutive equations for 0.5Cr-0.5Mo-0.25V base material

Material parameter	A (MPa/h)	B MPa <sup>-1</sup>	n	v
Value	3.1E-5	1.85E-13	4.6	4

With the stress 40MPa and the time increment of 50 hours, comparison of creep strain predicted by the Kachanov-Rabotnov constitutive equations and the experiment data for 0.5Cr-0.5Mo-0.25V base material (Hyde et al., 1998) can be plotted as shown in Figure 9.1.

Kachanov (1958) and Rabotnov (1969) used a power-law creep rate formulation, coupled with a power-law dependence of damage evolution equation, as illustrated in Equation 9.7 and Equation 9.8.

$$\frac{d\varepsilon}{dt} = A \left( \frac{\sigma}{1-\omega} \right)^n \quad (9.7)$$

$$\frac{d\omega}{dt} = B \left( \frac{\sigma}{1-\omega} \right)^v \quad (9.8)$$

where  $\varepsilon$  is creep strain,  $\omega$  is the creep damage and the  $\sigma$  is the applied stress;  $A$  and  $B$  are material constants;  $n$  and  $v$  are stress exponents.

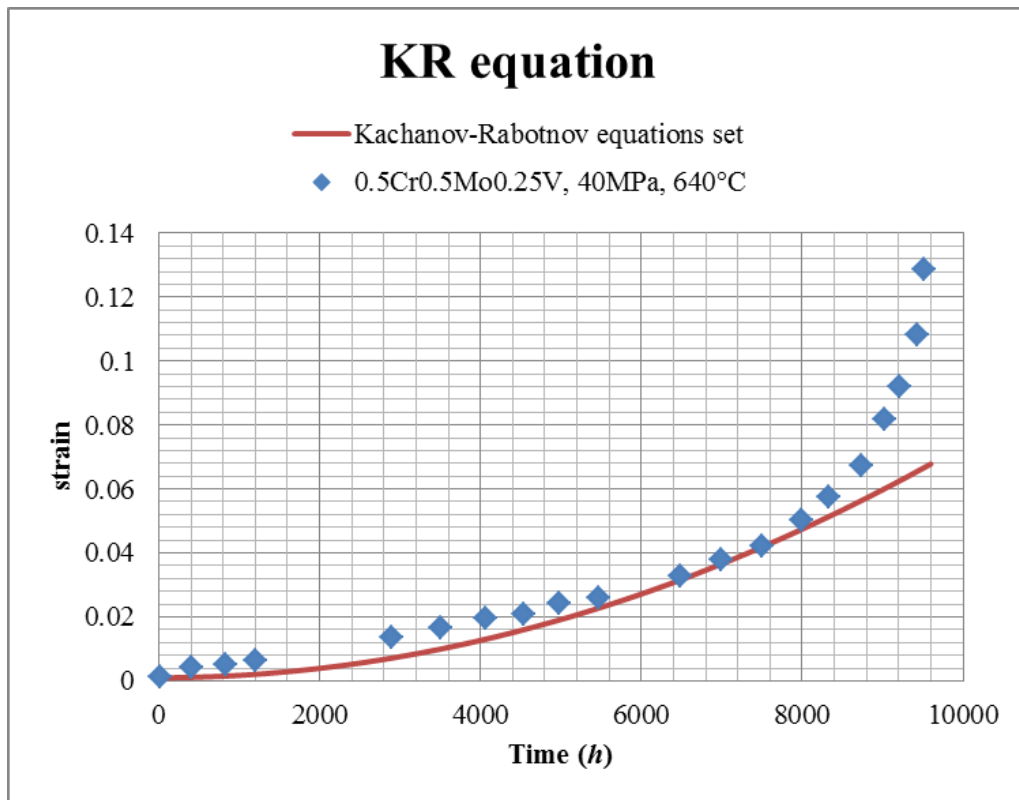


Figure 9.1: Comparison of creep strain predicted by Kachanov-Rabotnov constitutive equations and experiment data for 0.5Cr-0.5Mo-0.25V base material

In order to clearly compare the initial creep strain predicted by Kachanov-Rabotnov constitutive equations with the experiment data, the initial creep strain is plotted in Figure 9.2.

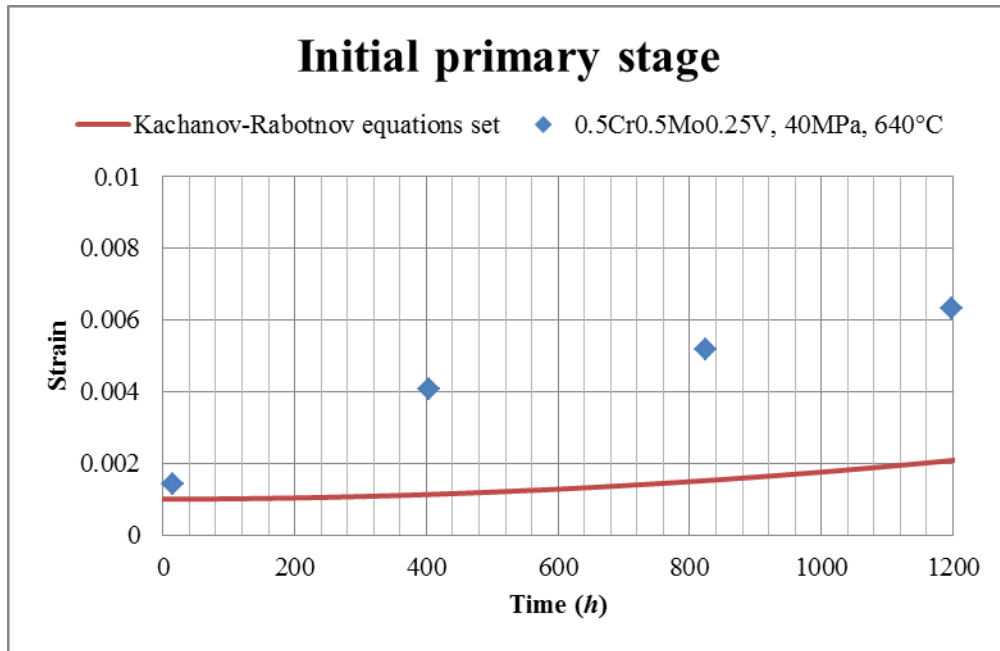


Figure 9.2: Comparison of initial creep strain predicted by Kachanov-Rabotnov constitutive equations and experiment data for 0.5Cr-0.5Mo-0.25V base material

Figure 9.1 shows that the creep strain predicted by the Kachanov-Rabotnov constitutive equations exhibits good agreement with the experiment data for 0.5Cr-0.5Mo-0.25V base material overall; however, at the primary and tertiary creep stages, the strain predicted by the Kachanov-Rabotnov equations is higher than that of the experiment data. In addition, the strain at failure predicted by the Kachanov-Rabotnov equations is about 0.068 and the experimental strain at failure is 0.126. The percentage of error in strain at failure between the Kachanov-Rabotnov equations and the experiment data is about 0.4. Since the nature of creep is very complex, the respected Kachanov-Rabotnov equations are still valuable in creep damage analysis of high temperature structures. However, efforts should be made to improve the accuracy of creep strain prediction at the primary and tertiary creep stages.

Table 9.2: Material parameters in newly developed constitutive equations for 0.5Cr-0.5Mo-0.25V base material

Material parameter	A (MPa/h)	B (MPa <sup>-1</sup> )	C	H (MPa)	H*	Kc (MPa <sup>-3</sup> /h)	q	x
Value	2.21618E-9	5.898E-3	9.85E-2	2.43E6	0.5929	9.227E-4	2	0.3

With the stress 40MPa and the time increment of 50 hours, the  $\omega_c$  at a temperature of 640 °C is approximately 0.3 (for low stress level). Comparison of the creep strain predicted by the newly developed constitutive equations with the experiment data for 0.5Cr-0.5Mo-0.25V base material (Hyde et al., 1998) can be plotted as shown in Figure 9.3.

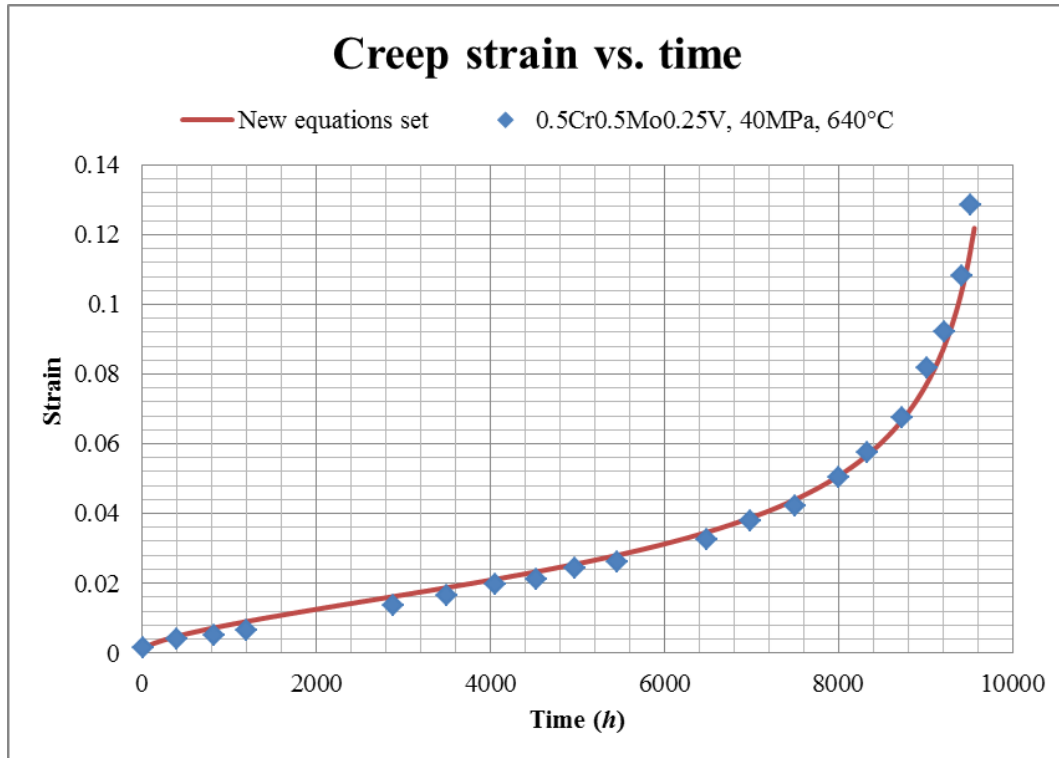


Figure 9.3: Comparison of creep strain predicted by new constitutive equations and experiment data for 0.5Cr-0.5Mo-0.25V base material

In order to clearly compare the initial creep strain predicted by the new constitutive equations with the experiment data, the initial creep strain is plotted in Figure 9.4.

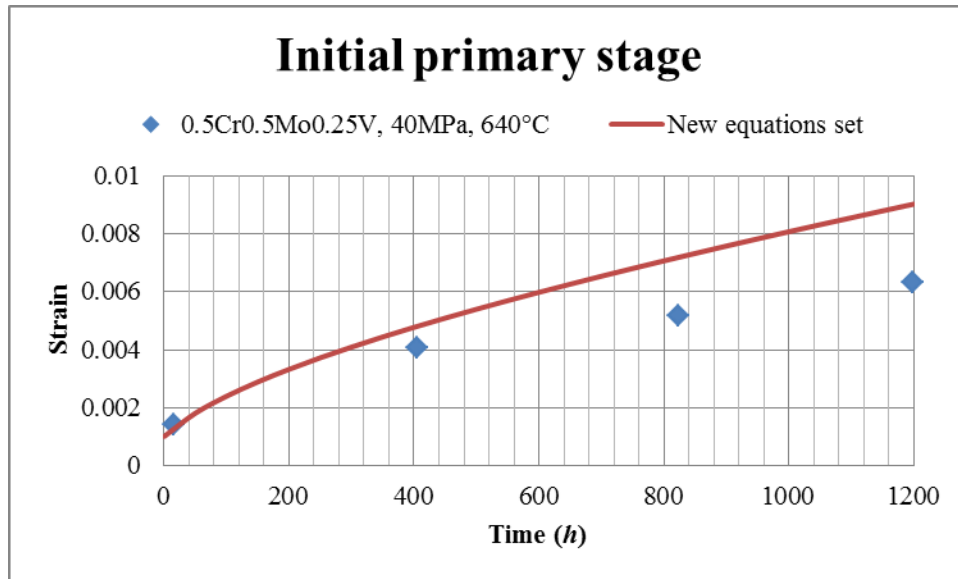


Figure 9.4: Comparison of initial creep strain predicted by new constitutive equations and experiment data for 0.5Cr-0.5Mo-0.25V base material

Figure 9.3 shows that the creep strain predicted by the new constitutive equations exhibits good agreement with the experiment data for 0.5Cr-0.5Mo-0.25V base material. The primary period is small but well represented by the new set of constitutive equations. Furthermore, the strain at failure predicted by the new constitutive equations is about 0.122 and the experimental strain at failure is 0.126. The percentage of error in strain at failure between the new constitutive equations and the experiment data is about 0.03. In comparison with the respected Kachanov-Rabotnov equations, at the primary and tertiary creep stages the accuracy of creep strain prediction is significantly improved by the new constitutive equations.

#### 9.4 Verification of the new constitutive equations via extension of the low stress level to intermediate stress level

Experiment data for the evolution of creep strain under the stress 54MPa ( $0.42\sigma_Y$ ) at 640°C for 0.5Cr-0.5Mo-0.25V base material (Hyde et al., 1998) have been used here in order to demonstrate the validity of the new constitutive equations via extension of the low stress level to intermediate stress level.

Table 9.3: Material parameters in newly developed constitutive equations for 0.5Cr-0.5Mo-0.25V base material at the stress 54MPa

Material parameter	A (MPa/h)	B (MPa <sup>-1</sup> )	C	H (MPa)	H*	Kc (MPa <sup>-3</sup> /h)	q	x
Value	2.21618E-9	3.473E-3	9.85E-2	2.43E6	0.5929	9.227E-4	2	0.54

With the stress 54MPa and the time increment of 50 hours, the  $\omega_c$  at a temperature of 640°C is approximately 0.4. The comparison of creep strain predicted by the newly developed constitutive equations with the experiment data for 0.5Cr-0.5Mo-0.25V base material (Hyde et al., 1998) can be plotted together with the creep deformation curves under low stresses (30, 35 and 40MPa) as shown in Figure 9.5. It should be noted that the material parameters used for 30MPa and 35MPa are the same as those for 40MPa.

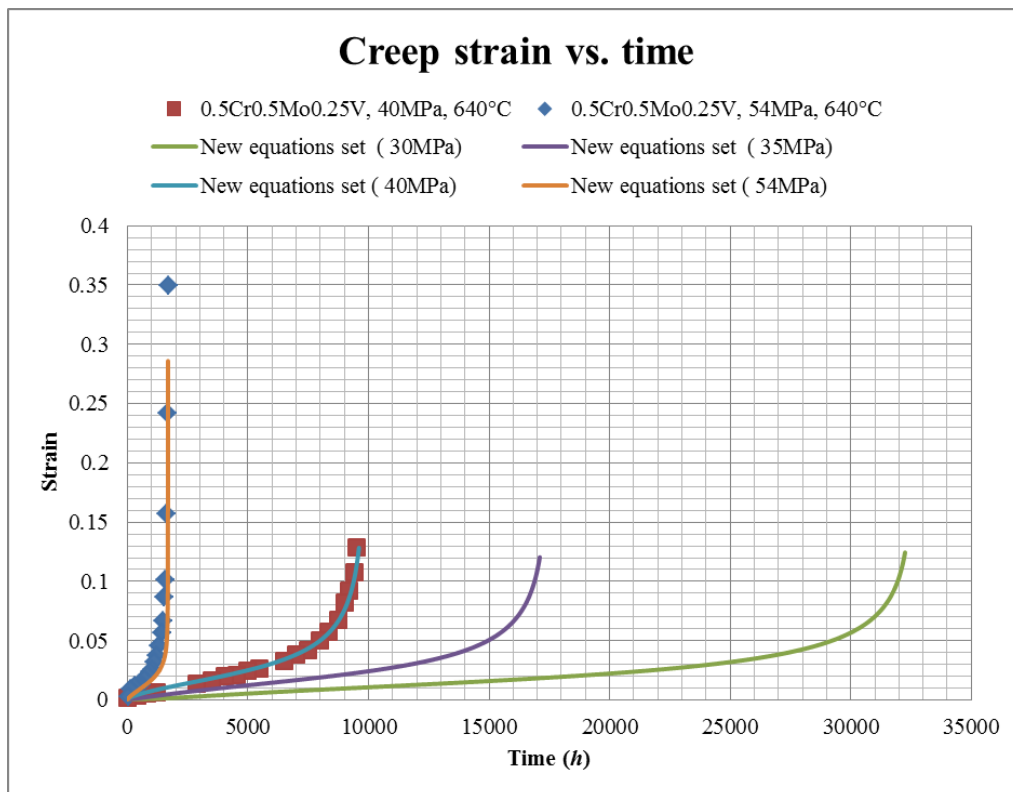


Figure 9.5: Comparison of creep strain predicted by new constitutive equations and experiment data for 0.5Cr-0.5Mo-0.25V base material under intermediate stress level and low stress level

Figure 9.5 shows the comparison of creep strain predicted by the new constitutive equations with the experiment data for 0.5Cr-0.5Mo-0.25V base material under intermediate stress level and low stress level. As shown in Figure 9.5, the creep behaviour predicted by the new constitutive equations is in good agreement with the experiment data (40MPa and 54MPa) for 0.5Cr-0.5Mo-0.25V base material.

## **9.5 Summary**

This chapter has proposed a new set of creep damage constitutive equations based on implementation of the newly developed minimum creep rate equation and damage evolution equation.

It has also demonstrated verification of the new set of creep damage equations by comparing them with results from the respected Kachanov-Rabotnov constitutive equations and experiment data at low stress level. Furthermore, verification of the new constitutive equations via extension of the low stress level to intermediate stress level has been conducted.

## **Chapter 10 Conclusion and Future Work**

This chapter summarizes the outcomes of this research and highlights its contributions to the research topics described in previous chapters. Future works relative to the development of creep damage constitutive equations for creep damage analysis of low Cr alloys under long-term service are also discussed.

### **10.1 Contributions and conclusions**

This dissertation has documented the design and development of creep damage constitutive equations for creep damage analysis of low Cr alloys under long-term service. A novel set of creep damage constitutive equations, which allow the scientist to simulate the behaviour of creep damage and, in particular, to analyse the evolution of creep damage at low stress levels, has been proposed. This thesis contributes to computational creep damage mechanics in general and particularly to the design and development of a constitutive model for creep damage analysis of low Cr alloys under long-term service. It is perceived that the dissertation has made several contributions to knowledge in this domain.

#### **10.1.1 Background of low Cr alloys in high temperature industries**

The first contribution of this project is a critical analysis of current issues regarding the application of low Cr alloys in high temperature industries. A brief overview and discussion of the problem domains relating to this project have been presented. In addition, methods of stress level definition and the nature of the stress breakdown phenomenon in creep damage analysis have been analysed.

- Creep behaviour and characteristics in low Cr alloys have been reviewed in order to develop a clear understanding of the nature of the creep damage problem. The importance of investigating creep damage behaviour in low Cr alloys has been identified.

- The characteristics of current stress level definition methods have been reported and the advantages of adopting the modified stress dependence method have been illustrated.
- The nature of the stress breakdown phenomenon in creep damage analysis has been examined. The significance of premature failure has been reported, and the causes of stress breakdown behaviour have been demonstrated.

### **10.1.2 Literature survey of classical creep damage constitutive equations**

The second contribution of this project is a critical analysis of the performance of existing creep damage constitutive equations in modelling the creep behaviour of low Cr alloys. Current approaches and creep damage constitutive equations utilized in predicting creep failure time have been presented. The specific areas which need to be enhanced in developing constitutive equations for low Cr alloys have been reported.

- Through the CDM approach, the way in which material becomes damaged does not necessarily have to be understood in detail, and the physical mechanisms of material deformation and deterioration can be represented by explicitly stated variables.
- Based on the investigation of current constitutive equations, the need for further enhancements in the accurate depiction of minimum creep strain rate and the evolution of damage over time for low Cr alloys has been commented on.

### **10.1.3 Development strategy in developing creep damage constitutive equations**

The third contribution of this project is the proposal of an integrated development strategy. An integrated strategy involving seven development stages has been proposed for the design of creep damage constitutive equations for low Cr alloys. The development approach for the constitutive equation to depict minimum creep strain rate under different

stress regions, and that for the constitutive equation to depict creep damage and rupture criterion at different time stages, have been detailed.

- Based on this development strategy, the developer can understand the requirements for developing creep damage constitutive equations and the method adopted to make the development procedures more logical and integrated.
- Based on the development approach for the minimum creep rate equation, the details of how the physically-based constitutive equation to depict the relationship between minimum creep rate and stress levels has been developed are clear.
- Based on the development approach for the damage evolution equation, the details of how the physically-based damage evolution equation and rupture criterion have been developed are clear.

#### **10.1.4 Investigation of creep mechanisms for low Cr alloys**

The fourth contribution of this project is a sound investigation of creep mechanisms in creep damage analysis of low Cr alloys. A critical understanding of which mechanisms are dominative in the process of creep has been presented, covering the mechanisms of creep deformation, damage, rupture behaviour and creep failure in low Cr alloys.

- The investigation of creep deformation mechanisms has contributed to an identification of the dominative mechanisms affecting the creep deformation process. In addition, the identification of creep behaviour under different temperature and stress ranges has been achieved through the investigation of mechanisms such as dislocation glide creep, dislocation climb creep, Nabarro-Herring diffusion creep and Coble creep.
- The investigation of creep damage mechanisms has contributed to an identification of the dominative mechanisms affecting the creep damage process. The mechanisms involving cavitation characteristics in creep damage behaviour have also been

understood through investigation of cavity sites, the cavity nucleation mechanism and the cavity growth mechanism.

- The investigation of creep rupture mechanisms has contributed to an identification of the dominative rupture mechanisms affecting the creep fracture process. Furthermore, the mechanisms involving stress levels in creep damage behaviour have been understood through the investigation of the trans-granular creep rupture mechanism, GB controlled rupture mechanism, ductile rupture mechanism, inter-granular rupture mechanism, pure diffusional rupture mechanism, brittle rupture mechanism and cavity growth mechanism.

#### **10.1.5 Analysis of the effects of stress level on creep behaviour for low Cr alloys**

The fifth contribution of this project is a critical analysis of the effects of stress level on creep behaviour for low Cr alloys. A detailed evaluation of the effects of stress level on creep damage constitutive equations has been presented, covering the effects of stress level on creep curve, creep parameter and creep cavitation.

- Analysis of the effects of stress level on creep curve for low Cr alloys has contributed to the identification of the dominative mechanism at different stress levels.
- Analysis of the effects of stress level on creep parameter has contributed to accurate stress level definition, and the effects of stress level on minimum creep rate, rupture time and strain at failure have been commented on.
- Analysis of the effects of stress level on creep cavity behaviour has contributed to the design of a rupture criterion, and the effects of stress level on creep cavity shape, cavity site, cavity nucleation and growth have been commented on.

### **10.1.6 New constitutive equation to depict relationship between minimum creep rate and stress**

The sixth contribution of this project is that a novel constitutive equation to depict the relationship between minimum creep rate and stress has been proposed. The classical constitutive laws for depicting the relationship between minimum creep rate and stress have been investigated, and then the development and validation of a new minimum creep rate constitutive equation have been presented.

- The investigation of classical constitutive laws for depicting the relationship between minimum creep rate and stress has contributed to the identification of the best mathematical model for developing a new minimum creep rate constitutive equation.
- The development of the minimum creep rate equation has contributed an understanding of the effects of different parameters on the relationship between minimum creep rate and stress levels. A detailed analysis of these effects has been conducted through the use of the newly designed constitutive equation.
- The validation of the newly designed minimum creep rate constitutive equation has contributed a clear demonstration of the reasons why simply using existing constitutive models to extrapolate from high stresses to low stresses runs the risk of over-estimating creep lifetime.

### **10.1.7 New constitutive equation to depict relationship between damage evolution and rupture criterion**

The seventh contribution of this project is that a novel creep damage evolution equation, with rupture criterion, for the creep analysis of low Cr alloys has been proposed. The evolution of creep cavity during the rupture process has been investigated, and then the development and validation of a new damage evolution equation and rupture criterion have been presented.

- Investigation of the evolution of creep cavity during rupture process has contributed to identification of the dominative mechanism in the creep rupture process at low stress level.
- Designing the rupture criterion for the constitutive equation has contributed to the ability to determine the failure time of high temperature structural components. Typical rupture criteria and the effects of stress level on the evolution of cavity have also been commented on.
- The development and validation of the new damage evolution equation has contributed to explaining why existing damage evolution equations do not satisfy the requirements for describing creep damage behaviour of low Cr alloys under long-term service.

#### **10.1.8 Implementation and verification of creep constitutive equations for low Cr alloys**

The eighth contribution of this project is that a novel set of creep constitutive equations for creep analysis of low Cr alloys has been proposed, allowing scientists to simulate the behaviour of creep damage.

- Implementation of the newly developed minimum creep rate equation and damage evolution equation into constitutive equations has contributed a demonstration of the use of the newly developed constitutive equations.
- Verification of the new set of creep damage equations has contributed to ensuring the newly developed creep constitutive equations can accurately describe the creep damage process in relation to the primary, secondary and tertiary creep stages.

### **10.2 Future Work**

Following the research work undertaken for this thesis, the author believes that there are several ideas which should be taken forward:

- 1) The newly developed constitutive equations could be broadened and assessed under non-proportional loading conditions and in specific cases such as notched bars.
- 2) The new constitutive equations could be extended from low and intermediate stress levels to high stress level through investigation of relevant creep data at high stresses (experiment data for low Cr alloys under high stress levels would need to be collected and analysed).
- 3) Multi-material zones should be considered in further development work, to cope with more complex structural features and conditions.
- 4) Butt-welded pipework may be subjected to more complicated loading and operating conditions depending upon the location of weldment in pipework circuits; thus, it is important to implement investigation of multi-axial stress states.
- 5) The development of the creep rupture criterion was conducted based on limited experiment data for the evolution of creep cavity in low Cr alloys. With more integrated experiment data, the accuracy of the creep rupture criterion can be improved.

## References

1. Abe, F., Kern, T.-U., and Viswanathan, R. (2008). *Creep-resistant steels*: Elsevier.
2. Adamantiades, A., and Kessides, I. (2009). Nuclear power for sustainable development: current status and future prospects. *Energy Policy*, 37(12), 5149-5166.
3. Ainsworth, R. A., Dowling, A. R., Sharples, J. K., and Technology, A. (1999). Advances in structural integrity assessment procedures within the UK nuclear industry.
4. Anderson, P., and Rice, J. (1985). Constrained creep cavitation of grain boundary facets. *Acta metallurgica*, 33(3), 409-422.
5. Anderson, P. M., and Shewmon, P. G. (2000). Stress redistribution and cavity nucleation near a diffusively growing grain boundary cavity. *Mechanics of materials*, 32(3), 175-191.
6. Armaki, H. G., Maruyama, K., Yoshizawa, M., and Igarashi, M. (2008). Prevention of the overestimation of long-term creep rupture life by multiregion analysis in strength enhanced high Cr ferritic steels. *Materials Science and Engineering: A*, 490(1), 66-71.
7. Arzt, E., Ashby, M. F., and Verrall, R. (1983). Interface controlled diffusional creep. *Acta metallurgica*, 31(12), 1977-1989.
8. Ashby, F. (1977). *Fracture-mechanism Maps*: University of Cambridge, Engineering Department.
9. Ashby, M. (1969). On interface-reaction control of Nabarro-Herring creep and sintering. *Scripta Metallurgica*, 3(11), 837-842.
10. Ashby, M. (1972). Boundary defects, and atomistic aspects of boundary sliding and diffusional creep. *Surface Science*, 31, 498-542.

11. Ashby, M., Gandhi, C., and Taplin, D. (1979). Overview No. 3 Fracture-mechanism maps and their construction for fcc metals and alloys. *Acta metallurgica*, 27(5), 699-729.
12. Ashby, M. F., and Brown, L. (2014). *Perspectives in creep fracture*: Elsevier.
13. Bailey, R. (1930). Creep of steel under simple and compound stress. *Engineering*, 121, 129-265.
14. Balluffi, R. (1969). Mechanisms of dislocation climb. *Physica status solidi (b)*, 31(2), 443-463.
15. Balluffi, R., and Cahn, J. (1981). Mechanism for diffusion induced grain boundary migration. *Acta metallurgica*, 29(3), 493-500.
16. Balluffi, R., and Mehl, R. (1982). Grain boundary diffusion mechanisms in metals. *Metallurgical Transactions A*, 13(12), 2069-2095.
17. Bauer, C. L. (1965). The free energy of a pinned dislocation. *Philosophical Magazine*, 11(112), 827-840.
18. Beere, W., and Rutter, E. (1978). Stresses and Deformation at Grain Boundaries [and Discussion]. *Philosophical Transactions of the Royal Society of London A: Mathematical, Physical and Engineering Sciences*, 288(1350), 177-196.
19. Beere, W., and Speight, M. (1978). Creep cavitation by vacancy diffusion in plastically deforming solid. *Metal Science*, 12(4), 172-176.
20. Benac, D. (2002). Failure analysis and life assessment of structural components and equipment. *Materials Park, OH: ASM International, 2002*, 227-242.
21. Benci, J., Pope, D., and George, E. (1988). Creep damage nucleation sites in ferrous alloys. *Materials Science and Engineering: A*, 103(1), 97-102.
22. Benzerga, A., and Leblond, J.-B. (2010). Ductile fracture by void growth to coalescence. *Advances in Applied Mechanics*, 44, 169-305.

23. Berry, G. (1976). The stress - strain behavior of materials exhibiting andrade creep. *Polymer Engineering & Science*, 16(11), 777-781.
24. Bilby, B., and Eshelby, J. (1968). *Fracture*, edited by H. Liebowitz: Academic Press.
25. Binda, L., Holdsworth, S., and Mazza, E. (2010). The exhaustion of creep ductility in 1CrMoV steel. *International journal of pressure vessels and piping*, 87(6), 319-325.
26. Bissel, A., Cane, B., and De-Long, J. (1988). *Remanent Life Assessment of Seam Welded Pipework*. Paper presented at the ASME Pressure Vessel and Piping Conference, American Society of Mechanical Engineers.
27. Bollerup, J., Hertzman, S., Ludvigsen, P., Sandstrom, R., and von Walden, E. (1986). Cavitation in New and Service-Exposed 1Cr--0.5Mo Steel. *High Temp. Technol.*, 4(1), 3-11.
28. Boyle, J. T., and Spence, J. (2013). *Stress analysis for creep*: Elsevier.
29. Briant, C., and Banerji, S. (1978). Intergranular failure in steel: the role of grain-boundary composition. *International metals reviews*, 23(1), 164-199.
30. Brown, A., and Ashby, M. (1980). On the power-law creep equation. *Scripta Metallurgica*, 14(12), 1297-1302.
31. Bueno, L., and Sobrinho, J. (2012). Correlation between creep and hot tensile behaviour for 2.25 Cr-1Mo steel from 500°C to 700°C Part 1: an assessment according to usual relations involving stress, temperature, strain rate and rupture time. *Matéria (Rio de Janeiro)*, 17(3), 1098-1108.
32. Burton, B. (1972). Interface reaction controlled diffusional creep: a consideration of grain boundary dislocation climb sources. *Materials Science and Engineering*, 10, 9-14.
33. Burton, B. (1973). On the mechanism of the inhibition of diffusional creep by second phase particles. *Materials Science and Engineering*, 11(6), 337-343.
34. Cane, B. (1979). Interrelationship Between Creep Deformation and Creep Rupture in 2.25 Cr--1Mo Steel. *Met. Sci.*, 13(5), 287-294.

35. Cane, B. (1980). Creep cavitation and rupture in 2 1/4 Cr-1Mo steel under uniaxial and multiaxial stresses. *Mechanical behaviour of materials*.
36. Cane, B. (1981). Creep fracture of dispersion strengthened low alloy ferritic steels. *Acta metallurgica*, 29(9), 1581-1591.
37. Cane, B., and Greenwood, G. (1975). The nucleation and growth of cavities in iron during deformation at elevated temperatures. *Metal Science*, 9(1), 55-60.
38. Cane, B., and Middleton, C. (1981). Intergranular creep-cavity formation in low-alloy bainitic steels. *Metal Science*, 15(7), 295-301.
39. Chen, I.-W., and Argon, A. (1981a). Creep cavitation in 304 stainless steel. *Acta metallurgica*, 29(7), 1321-1333.
40. Chen, I.-W., and Argon, A. (1981b). Diffusive growth of grain-boundary cavities. *Acta metallurgica*, 29(10), 1759-1768.
41. Chen, Y., Yan, W., Wang, W., Shan, Y., and Yang, K. (2012). Constitutive equations of the minimum creep rate for 9% Cr heat resistant steels. *Materials Science and Engineering: A*, 534, 649-653.
42. Chokshi, A. H. (2005). Cavity nucleation and growth in superplasticity. *Materials Science and Engineering: A*, 410, 95-99.
43. Chowdhury, S. G., Mukhopadhyay, N., Das, G., Das, S. K., and Bhattacharya, D. (1998). Failure analysis of a weld repaired steam turbine casing. *Engineering Failure Analysis*, 5(3), 205-218.
44. Coble, R. (1963a). A model for boundary diffusion controlled creep in polycrystalline materials. *Journal of Applied Physics (US)*, 34.
45. Coble, R. (1963b). A model for boundary diffusion controlled creep in polycrystalline materials. *Journal of Applied Physics*, 34(6), 1679-1682.
46. Cocks, A., and Ashby, M. (1981). *Creep fracture by void growth*: Springer.
47. Coleman, M., and Kimmins, S. (1990). *The behaviour of 1/2Cr1/2Mo1/4V pipe weldments in high temperature plant*. Paper presented at the Proc. Inst. Mech. Engrs. Conf. on Life of Welds at High Temperature.

48. Coleman, M., Parker, J., and Walters, D. (1985). The behaviour of ferritic weldments in thick section 12Cr12Mo14V pipe at elevated temperature. *International journal of pressure vessels and piping*, 18(4), 277-310.
49. Cottrell, A. (1997). Logarithmic and Andrade creep. *Philosophical magazine letters*, 75(5), 301-308.
50. Dimmler, G., Weinert, P., and Cerjak, H. (2008). Extrapolation of short-term creep rupture data—The potential risk of over-estimation. *International journal of pressure vessels and piping*, 85(1), 55-62.
51. Dobrzański, J., Sroka, M., and Zieliński, A. (2006). Methodology of classification of internal damage the steels during creep service. *Journal of achievements in materials and manufacturing engineering*, 18(1-2).
52. Dyson, B. (1976). Constraints on diffusional cavity growth rates. *Metal Science*, 10(10), 349-353.
53. Dyson, B. (1983). Continuous cavity nucleation and creep fracture. *Scripta Metallurgica*, 17(1), 31-37.
54. Dyson, B. (2000). Use of CDM in materials modeling and component creep life prediction. *Journal of pressure vessel technology*, 122(3), 281-296.
55. Dyson, B. (2009). Microstructure based creep constitutive model for precipitation strengthened alloys: theory and application. *Materials science and technology*, 25(2), 213-220.
56. Dyson, B., and McLean, M. (1983). Particle-coarsening,  $\sigma_0$  and tertiary creep. *Acta metallurgica*, 31(1), 17-27.
57. Dyson, B., and McLean, M. (1997). Microstructural evolution and its effects on the creep performance of high temperature alloys. *Microstructural stability of creep resistant alloys for high temperature plant applications*, 371-393.
58. Dyson, B., and McLean, M. (2001). *Micromechanism-quantification for creep constitutive equations*. Paper presented at the IUTAM Symposium on Creep in Structures.

59. Dyson, B., and Osgerby, D. (1993). Modelling and analysis of creep deformation and fracture in a 1 Cr-1/2 Mo ferritic steel. *NASA STI/Recon Technical Report N, 94*, 29121.
60. Edward, G., and Ashby, M. (1979). Intergranular fracture during power-law creep. *Acta metallurgica*, 27(9), 1505-1518.
61. Es-Souni, M. (2000). Primary, secondary and anelastic creep of a high temperature near  $\alpha$ -Ti alloy Ti6242Si. *Materials characterization*, 45(2), 153-164.
62. Evans, H. (1984). Mechanisms of creep fracture. *Elsevier Applied Science Publishers Ltd., 1984*, 319.
63. Evans, W., and Wilshire, B. (1970). The high temperature creep and fracture behavior of 70-30 alpha-brass. *Metallurgical Transactions*, 1(8), 2133-2139.
64. Fedeli, G., and Mori, S. (1993). Grain Boundary Creep Cavitation of 0.5 Cr--0.5 Mo--0.25 V Steel During Service and Post Exposure Testing. *Creep and Fracture of Engineering Materials and Structures*, 733-742.
65. Fessler, H., and Hyde, T. (1994). The use of model materials to simulate creep behaviour. *The Journal of Strain Analysis for Engineering Design*, 29(3), 193-200.
66. Finnie, I., and Heller, W. R. (1959). *Creep of Engineering Materials*.
67. Fleck, R., Taplin, D., and Beevers, C. (1975). An investigation of the nucleation of creep cavities by 1 MV electron microscopy. *Acta metallurgica*, 23(4), 415-424.
68. Frost, H. J., and Ashby, M. F. (1982). Deformation mechanism maps: the plasticity and creep of metals and ceramics.
69. FUJIYAMA, K., ISEKI, T., KOMATSU, A., and OKABE, N. (1997). Creep life assessment of 2.25 Cr-1Mo piping steel and of its simulated HAZ material. *Material*, 46 (12Appendix), 237-243.

70. Gaffard, V. (2004). Experimental study and modelling of high temperature creep flow and damage behaviour of 9Cr1Mo-NbV. *École Nationale Supérieure des Mines de Paris*.
71. Galiyev, A., Kaibyshev, R., and Gottstein, G. (2001). Correlation of plastic deformation and dynamic recrystallization in magnesium alloy ZK60. *Acta Materialia*, 49(7), 1199-1207.
72. Garofalo, F. (1963). An empirical relation defining the stress dependence of minimum creep rate in metals. *Trans Metall Soc AIME*, 227(2), 351-355.
73. Ghosh, A., and Raj, R. (1981). Grain size distribution effects in superplasticity. *Acta metallurgica*, 29(4), 607-616.
74. Goldhoff, R., and Woodford, D. (1972). The evaluation of creep damage in a Cr-Mo-V steel. *ASTM STP*, 515, 89-106.
75. Gooch, D. (2003). Remnant creep life prediction in ferritic materials. *Comprehensive structural integrity*, 5, 309-359.
76. Goods, S., and Nieh, T. (1983). Mechanisms of intergranular cavity nucleation and growth during creep. *Scripta Metallurgica*, 17(1), 23-30.
77. Gong, Y. P., Hyde, C. J., Sun, W., and Hyde, T. H. (2010). Determination of material properties in the Chaboche unified viscoplasticity model. *Proceedings of the Institution of Mechanical Engineers, Part L: Journal of Materials Design and Applications*, 224(1), 19-29.
78. Gorash, E., Lvov, G., Harder, J., Kostenko, Y., and Wieghardt, K. (2005). Comparative analysis of the creep behaviour in a power plant component using different material models. *Creep and Fracture in High Temperature Components—Design and Life Assessment Issues*.
79. Gorash, Y. (2008). Development of a creep-damage model for non-isothermal long-term strength analysis of high-temperature components operating in a wide stress range. *Martin Luther University of Halle-Wittenberg, Halle Germany*.
80. Greenwood, G. (1956). The growth of dispersed precipitates in solutions. *Acta metallurgica*, 4(3), 243-248.

81. Greenwood, G. (1970). The possible effects on diffusion creep of some limitation of grain boundaries as vacancy sources or sinks. *Scripta Metallurgica*, 4(3), 171-173.
82. Greenwood, J. N., Miller, D., and Suiter, J. (1954). Intergranular cavitation in stressed metals. *Acta metallurgica*, 2(2), 250-258.
83. Hales, R. (1994). The role of cavity growth mechanisms in determining in creep rupture under multi-axial stresses. *Fatigue & Fracture of Engineering Materials & Structures*, 17(5), 579-591.
84. Hall, F., and Hayhurst, D. (1991). *Continuum damage mechanics modelling of high temperature deformation and failure in a pipe weldment*. Paper presented at the Proceedings of the Royal Society of London A: Mathematical, Physical and Engineering Sciences.
85. Hall, F. R. (1990). Development of continuum damage mechanics models to predict the creep deformation and failure of high temperature structures. University of Sheffield.
86. Harper, J., and Dorn, J. E. (1957). Viscous creep of aluminum near its melting temperature. *Acta Metallurgica*, 5(11), 654-665.
87. Hayhurst, D. (1972). Creep rupture under multi-axial states of stress. *Journal of the Mechanics and Physics of Solids*, 20(6), 381-382.
88. Hayhurst, D., Hayhurst, R., and Vakili-Tahami, F. (2005). Continuum damage mechanics predictions of creep damage initiation and growth in ferritic steel weldments in a medium bore branched pipe under constant pressure at 590° C using a five-material weld model. Paper presented at the Proceedings of the Royal Society of London A: Mathematical, Physical and Engineering Sciences.
89. Hayhurst, D., Lin, J., and Hayhurst, R. (2008). Failure in notched tension bars due to high-temperature creep: Interaction between nucleation controlled cavity growth and continuum cavity growth. *International Journal of Solids and Structures*, 45(7), 2233-2250.

90. Herring, C. (1950). Diffusional viscosity of a polycrystalline solid. *Journal of Applied Physics*, 21(5), 437-445.
91. Hill, R. (1998). *The mathematical theory of plasticity* (Vol. 11): Oxford university press.
92. Hondros, E., and Henderson, P. (1983). Role of grain boundary segregation in diffusional creep. *Metallurgical Transactions A*, 14(3), 521-530.
93. Horstemeyer, M., Matalanis, M., Sieber, A., and Botos, M. (2000). Micromechanical finite element calculations of temperature and void configuration effects on void growth and coalescence. *international Journal of Plasticity*, 16(7), 979-1015.
94. Hull, D., and Bacon, D. J. (2001). *Introduction to dislocations*: Butterworth-Heinemann.
95. Hull, D., and Rimmer, D. (1959). The growth of grain-boundary voids under stress. *Philosophical Magazine*, 4(42), 673-687.
96. Hult, J. A. (1966). *Creep in engineering structures*: Blaisdell Pub. Co.
97. Hyde, T., Becker, A., Sun, W., and Williams, J. (2006). Finite-element creep damage analyses of P91 pipes. *International journal of pressure vessels and piping*, 83(11), 853-863.
98. Hyde, T., Hyde, C., and Sun, W. (2013). *Applied creep mechanics*: McGraw-Hill Professional.
99. Hyde, T., Sun, W., and Tang, A. (1998). Determination of material constants in creep continuum damage constitutive equations. *Strain*, 34(3), 83-90.
100. Igual, J. Z., and Xu, Q. (2015, September). Determination of the material constants of creep damage constitutive equations using Matlab optimization procedure. In *Automation and Computing (ICAC), 2015 21st International Conference on* (pp. 1-6). IEEE.
101. Ion, J., Barbosa, A., Ashby, M., Dyson, B. H., McLean, M., and National Physical Lab., T. D. o. M. A. (1986). *The Modelling of Creep for Engineering Design-1*: National Physical Laboratory Division of Materials Applications.

102. Isaac, A., Sket, F., Reimers, W., Camin, B., Sauthoff, G., and Pyzalla, A. (2008). In situ 3D quantification of the evolution of creep cavity size, shape, and spatial orientation using synchrotron X-ray tomography. *Materials Science and Engineering: A*, 478(1), 108-118.
103. Ishida, Y., and McLean, D. (1967). The formation and growth of cavities in creep. *Metal Science*, 1(1), 171-172.
104. Jaeger, W., and Gleiter, H. (1978). Grain boundaries as vacancy sources in diffusional creep. *Scripta Metallurgica*, 12(7), 675-678.
105. Jaffee, R. (2013). *Fundamental Aspects of Structural Alloy Design*: Springer Science & Business Media.
106. Jovanovic, A. (2003). Risk-based inspection and maintenance in power and process plants in Europe. *Nuclear Engineering and Design*, 226(2), 165-182.
107. Kachanov, L. (1958). On rupture time under condition of creep. *Izvestia Akademi Nauk USSR, Otd. Techn. Nauk, Moskwa*, 8, 26-31.
108. Kachanov, L. (2013). *Introduction to continuum damage mechanics* (Vol. 10): Springer Science & Business Media.
109. Kassner, M., and Hayes, T. (2003). Creep cavitation in metals. *international Journal of Plasticity*, 19(10), 1715-1748.
110. Kassner, M. E. (2015). *Fundamentals of creep in metals and alloys*: Butterworth-Heinemann.
111. Kern, T.-U., Merckling, G., and Yagi, K. (2004). Introduction *Creep Properties of Heat Resistant Steels and Superalloys* (pp. 1-7): Springer.
112. Kowalewski, Z., Hayhurst, D., and Dyson, B. (1994). Mechanisms-based creep constitutive equations for an aluminium alloy. *The Journal of Strain Analysis for Engineering Design*, 29(4), 309-316.
113. Krishnamohanrao, Y., Kutumbarao, V., and Rao, P. R. (1986). Fracture mechanism maps for titanium and its alloys. *Acta metallurgica*, 34(9), 1783-1806.

114. Kushima, H., Watanabe, T., Murata, M., Kamihira, K., Tanaka, H., and Kimura, K. (2005). *Metallographic atlas for 2.25 Cr-1Mo steels and degradation due to long-term service at the elevated temperatures*. Paper presented at the Proc. ECCC Creep Conference.
115. Lai, J. (1989). A simple model for assessing the degradation of creep rupture strength after exposure to high temperatures at low stresses. *Materials Science and Engineering: A*, 111, 81-84.
116. Langdon, T. G. (1985). Dislocations and creep. *Dislocations and properties of real materials*, 221-238.
117. Langdon, T. G. (1970). Grain boundary sliding as a deformation mechanism during creep. *Philosophical Magazine*, 22(178), 689-700.
118. Langdon, T. G. (2002). Creep at low stresses: an evaluation of diffusion creep and Harper-Dorn creep as viable creep mechanisms. *Metallurgical and Materials Transactions A*, 33(2), 249-259.
119. Langdon, T. G., and Mohamed, F. A. (1978). A new type of deformation mechanism map for high-temperature creep. *Materials Science and Engineering*, 32(2), 103-112.
120. Lee, J. S., Armaki, H. G., Maruyama, K., Muraki, T., and Asahi, H. (2006). Causes of breakdown of creep strength in 9Cr–1.8 W–0.5 Mo–VNb steel. *Materials Science and Engineering: A*, 428(1), 270-275.
121. Lemaitre, J. (1985). Coupled elasto-plasticity and damage constitutive equations. *Computer Methods in Applied Mechanics and Engineering*, 51(1), 31-49.
122. Li, J., and Dasgupta, A. (1993). Failure-mechanism models for creep and creep rupture. *Reliability, IEEE Transactions on*, 42(3), 339-353.
123. Lifshitz, I. M., and Slyozov, V. V. (1961). The kinetics of precipitation from supersaturated solid solutions. *Journal of Physics and Chemistry of Solids*, 19(1), 35-50.

124. Liu, D. Z., Xu, Q., Lu, Z. Y., Xu, D. L., and Xu, Q. H. (2013). *The techniques in developing finite element software for creep damage analysis*. Paper presented at the Advanced Materials Research.
125. Loh, B. (1970). Stress concentration and cavity growth. *Scripta Metallurgica*, 4(4), 299-303.
126. Lombard, R., and Vehoff, H. (1990). Nucleation and growth of cavities at defined grain boundaries in bicrystals. *Scripta Metallurgica et Materialia*, 24(3), 581-586.
127. Lonsdale, D., and Flewitt, P. (1979). Damage accumulation and microstructural changes occurring during the creep of a 2 1/4% Cr1% Mo steel. *Materials Science and Engineering*, 39(2), 217-229.
128. Maharaj, C., Dear, J., and Morris, A. (2009). A Review of Methods to Estimate Creep Damage in Low - Alloy Steel Power Station Steam Pipes. *Strain*, 45(4), 316-331.
129. Mainprice, D., Bouchez, J.-L., Blumenfeld, P., and Tubià, J. M. (1986). Dominant c slip in naturally deformed quartz: implications for dramatic plastic softening at high temperature. *Geology*, 14(10), 819-822.
130. Martin, J., and Leckie, F. (1972). On the creep rupture of structures. *Journal of the Mechanics and Physics of Solids*, 20(4), 223-238.
131. Maruyama, K., Nakamura, J., and Yoshimi, K. (2015). Prediction of Long-Term Creep Rupture Life of Grade 122 Steel by Multiregion Analysis. *Journal of pressure vessel technology*, 137(2), 021403.
132. Maruyama, K., Sawada, K., and Koike, J.-i. (2001). Strengthening mechanisms of creep resistant tempered martensitic steel. *ISIJ international*, 41(6), 641-653.
133. Massé, T., and Lejeail, Y. (2013). Creep mechanical behaviour of modified 9Cr1Mo steel weldments: Experimental analysis and modelling. *Nuclear Engineering and Design*, 254, 97-110.

134. Miller, D., and Pilkington, R. (1978). The effect of temperature and microstructure on the creep damage found in low alloy ferritic steels. *Metallurgical Transactions A*, 9(9), 1221-1227.
135. Miller, D. A., and Langdon, T. G. (1979). Creep fracture maps for 316 stainless steel. *Metallurgical Transactions A*, 10(11), 1635-1641.
136. Milne, I., Ritchie, R. O., and Karihaloo, B. (2003). Comprehensive structural integrity:[fracture of materials from nano to macro]. Vol. 4, Cyclic loading and fatigue: Elsevier Pergamon.
137. Mohamed, F. A., and Langdon, T. G. (1974a). Deformation mechanism maps based on grain size. *Metallurgical Transactions*, 5(11), 2339-2345.
138. Mohamed, F. A., and Langdon, T. G. (1974b). The transition from dislocation climb to viscous glide in creep of solid solution alloys. *Acta metallurgica*, 22(6), 779-788.
139. Mott, N. (1951). The mechanical properties of metals. *Proceedings of the Physical Society. Section B*, 64(9), 729.
140. Murakami, S. (1983). Notion of continuum damage mechanics and its application to anisotropic creep damage theory. *Journal of Engineering Materials and Technology*, 105(2), 99-105.
141. Murti, K., and Sundaresan, S. (1985). Thermal-behavior of austenitic-friction welding. *Welding Journal*, 64(12), S327-S334.
142. Myers, M. (1985). Damage accumulation in a low alloy ferritic steel. University of Manchester.
143. Myers, M., Pilkington, R., and Needham, N. (1987). Cavity nucleation and growth in a 1% Cr- 0.5% Mo steel. *Materials Science and Engineering*, 95, 81-91.
144. Nabarro, F. R. (1967). Steady-state diffusional creep. *Philosophical Magazine*, 16(140), 231-237.
145. Nabarro, F. R. (2002). Creep at very low rates. *Metallurgical and Materials Transactions A*, 33(2), 213-218.

146. Nabarro, F. R. (1948). Report of a Conference on the Strength of Solids. *The Physical Society, London*, 75.
147. Nabarro, F. R. N., and De Villiers, F. (1995). *Physics of creep and creep-resistant alloys*: CRC press.
148. Naumenko, K., and Altenbach, H. (2007). *Modeling of creep for structural analysis*: Springer.
149. Naumenko, K., Altenbach, H., and Kutschke, A. (2010). A combined model for hardening, softening, and damage processes in advanced heat resistant steels at elevated temperature. *International Journal of Damage Mechanics*, 1056789510386851.
150. Needham, N. (1983). Cavitation and fracture in creep resisting steels. *Commision of the European Communities, Brussels*, 7.
151. Needham, N., and Gladman, T. (1986). Intergranular cavity damage and creep fracture of 1Cr–0.5Mo steels. *Materials science and technology*, 2(4), 368-373.
152. Nicolas, A., and Poirier, J.-P. (1976). *Crystalline plasticity and solid state flow in metamorphic rocks*: Wiley London.
153. Nieh, T., and Nix, W. (1980). A comparison of the dimple spacing on intergranular creep fracture surfaces with the slip band spacing for copper. *Scripta Metallurgica*, 14(3), 365-368.
154. Norton, F. H. (1929). *The creep of steel at high temperatures*: McGraw-Hill Book Company, Incorporated.
155. Orowan, E. (1940). Problems of plastic gliding. *Proceedings of the Physical Society*, 52(1), 8.
156. Osgerby, S., and Dyson, B. (1993). A methodology for modelling tertiary creep behaviour of engineering alloys under oxidising conditions. *International journal of pressure vessels and piping*, 55(2), 333-341.
157. Owen, D. M., Chokshi, A. H., and Nutt, S. R. (1997). Nucleation and growth characteristics of cavities during the early stages of tensile creep deformation

- in a superplastic zirconia–20 wt% alumina composite. *Journal of the American Ceramic Society*, 80(9), 2433-2436.
158. Pardoën, T., and Hutchinson, J. (2000). An extended model for void growth and coalescence. *Journal of the Mechanics and Physics of Solids*, 48(12), 2467-2512.
  159. Parker, J. (1995). Creep behaviour of low alloy steel weldments. *International journal of pressure vessels and piping*, 63(1), 55-62.
  160. Penny, R., and Marriott, D. (1995). Design for creep: Chapman and Hall, London.
  161. Perrin, I., and Hayhurst, D. (1996). Creep constitutive equations for a 0.5 Cr–0.5 Mo–0.25 V ferritic steel in the temperature range 600–675°C. *The Journal of Strain Analysis for Engineering Design*, 31(4), 299-314.
  162. Perrin, I., and Hayhurst, D. (1999). Continuum damage mechanics analyses of type IV creep failure in ferritic steel crossweld specimens. *International journal of pressure vessels and piping*, 76(9), 599-617.
  163. Perry, A. (1974). Cavitation in creep. *Journal of Materials Science*, 9(6), 1016-1039.
  164. Petry, C., and Lindet, G. (2009). Modelling creep behaviour and failure of 9Cr–0.5 Mo–1.8 W–VNb steel. *International journal of pressure vessels and piping*, 86(8), 486-494.
  165. Pharr, G. M. (1981). Some observations on the relation between dislocation substructure and power law breakdown in creep. *Scripta Metallurgica*, 15(7), 713-717.
  166. Poirier, J.-P. (1985). Creep of crystals: high-temperature deformation processes in metals, ceramics and minerals: Cambridge University Press.
  167. Rabotnov, Y. N. (1969a). *Creep problems in structural members* (Vol. 7): North-Holland Pub. Co.
  168. Rabotnov, Y. N. (1969b). Creep rupture *Applied mechanics* (pp. 342-349): Springer.

169. Raj, R. (1975). Transient behavior of diffusion-induced creep and creep rupture. *Metallurgical Transactions A*, 6(8), 1499-1509.
170. Raj, R., and Ashby, M. (1975). Intergranular fracture at elevated temperature. *Acta metallurgica*, 23(6), 653-666.
171. Raj, S. (2002). Power-law and exponential creep in class M materials: discrepancies in experimental observations and implications for creep modeling. *Materials Science and Engineering: A*, 322(1), 132-147.
172. Ratcliffe, R., and Greenwood, G. (1965). The mechanism of cavitation in magnesium during creep. *Philosophical Magazine*, 12(115), 59-69.
173. Riedel, H. (1987). *Fracture at high temperatures*: Springer.
174. Robin, P.-Y. F. (1978). Pressure solution at grain-to-grain contacts. *Geochimica et Cosmochimica Acta*, 42(9), 1383-1389.
175. Rodgers, J., and Tilley, R. (1999). Summary of field experience for acoustic emission monitoring of seam-welded high energy piping.
176. Rollason, E. C. (1973). *Metallurgy for engineers*.
177. Roy, N., Bagui, S., Sahu, J., and Ray, A. (2013). Creep characterization and damage assessment of long term service exposed P-22 grade of steel. *Materials Science and Engineering: A*, 560, 802-810.
178. Sawada, K., Tabuchi, M., and Kimura, K. (2009). Analysis of long-term creep curves by constitutive equations. *Materials Science and Engineering: A*, 510, 190-194.
179. Segle, P. (2002). Numerical simulation of weldment creep response.
180. Seitz, F. (1952). On the generation of vacancies by moving dislocations. *Advances in Physics*, 1(1), 43-90.
181. Sherby, O. D., and Burke, P. M. (1968). Mechanical behavior of crystalline solids at elevated temperature. *Progress in Materials Science*, 13, 323-390.
182. Shibli, I., and Holdsworth, S. (2009). Proceedings: Creep & Fracture in High Temperature Components: Design & Life Assessments Issues: 2nd ECCC

Creep Conference, April 21-23, 2009, Zurich, Switzerland: DEStech Publications, Inc.

183. Shibli, I., Holdsworth, S., and Merckling, G. (2005). Creep and Fracture in High Temperature Components: Design and Life Assessment Issues: DEStech Publications, Inc.
184. Singh, K., and Kamaraj, M. (2009). Creep ductility of 1Cr1Mo1/4V low alloy forging and casting steels. *Materials Science and Engineering: A*, 510, 51-57.
185. Sklenicka, V., Kucharova, K., Foldyna, V., and Cadek, J. (1987). Interrelationship between creep deformation and creep rupture in a low alloy CrMoV steel after service. *The Institute of Metals*, 361-374.
186. Smith, D., Walker, N., and Kimmins, S. (2003). Type IV creep cavity accumulation and failure in steel welds. *International journal of pressure vessels and piping*, 80(9), 617-627.
187. Speight, M., and Beere, W. (1975). Vacancy potential and void growth on grain boundaries. *Metal Sci.*, 9(4), 190-191.
188. Spindler, M. (2004). The multiaxial creep ductility of austenitic stainless steels. *Fatigue & Fracture of Engineering Materials & Structures*, 27(4), 273-281.
189. Spindler, M., Hales, R., and Ainsworth, R. (1997). Multiaxial creep-fatigue rules.
190. Stanley, R. G. (1978). *Creep fracture and some low-alloy steels*. University of Sheffield.
191. Stanzl, S., Argon, A., and Tschegg, E. (1983). Diffusive intergranular cavity growth in creep in tension and torsion. *Acta metallurgica*, 31(6), 833-843.
192. Svensson, L.-E., and Dunlop, G. (1981). Growth of intergranular creep cavities. *International metals reviews*, 26(1), 109-131.
193. Svoboda, J., and Sklenička, V. (1990). Thermal cavity nucleation at intergranular inclusions in high temperature creep. *Acta Metallurgica et Materialia*, 38(6), 1141-1149.

194. Tabuchi, M., and Takahashi, Y. (2006). *Evaluation of creep strength reduction factors for welded joints of modified 9Cr-1Mo steel (P91)*. Paper presented at the ASME 2006 Pressure Vessels and Piping/ICPVT-11 Conference.
195. Tipler, H., and Hopkins, B. (1976). The creep cavitation of commercial and high-purity Cr-Mo-V steels. *Metal Science*, 10(2), 47-56.
196. Tu, S.-T., Segle, P., and Gong, J.-M. (2004). Creep damage and fracture of weldments at high temperature. *International journal of pressure vessels and piping*, 81(2), 199-209.
197. Tvergaard, V. (1990). Material failure by void growth to coalescence. *Advances in Applied Mechanics*, 27(1), 83-151.
198. Vakili-Tahami, F., Hayhurst, D., and Wong, M. (2005). High-temperature creep rupture of low alloy ferritic steel butt-welded pipes subjected to combined internal pressure and end loadings. *Philosophical Transactions of the Royal Society of London A: Mathematical, Physical and Engineering Sciences*, 363(1836), 2629-2661.
199. Viswanathan, R. (1989). Damage mechanisms and life assessment of high temperature components: ASM international.
200. Wagner, C. (1961). Theory of precipitate change by redissolution. *Z. Elektrochem*, 65, 581-591.
201. Walker, N., Kimmins, S., and Smith, D. (1996). *Type IV creep cavitation in ferritic steel welds*. Paper presented at the IMECHE CONFERENCE TRANSACTIONS.
202. Walker, N. S. (1997). Type IV creep cavitation in low alloy ferritic steel weldments. University of Bristol.
203. Watanabe, T. (1983). Grain boundary sliding and stress concentration during creep. *Metallurgical Transactions A*, 14(3), 531-545.
204. Watanabe, T., and Davies, P. W. (1978). Grain boundary sliding and intergranular fracture behaviour of copper bicrystals. *Philosophical Magazine A*, 37(5), 649-681.

205. Webster, G., and Ainsworth, R. A. (1994). *High temperature component life assessment*. Springer Science & Business Media.
206. Weertman, J. (1955). Theory of Steady - State Creep Based on Dislocation Climb. *Journal of Applied Physics*, 26(10), 1213-1217.
207. Weertman, J. (1957). Steady-state creep through dislocation climb. *Journal of Applied Physics*, 28, 362-364.
208. Westwood, C., Pan, J., and Crocombe, A. (2004). Nucleation, growth and coalescence of multiple cavities at a grain-boundary. *European Journal of Mechanics-A/Solids*, 23(4), 579-597.
209. Whittaker, M., and Wilshire, B. (2011). Long term creep life prediction for Grade 22(2. 25 Cr-1 Mo) steels. *Materials science and technology*, 27(3), 642-647.
210. Whittaker, M. T., and Wilshire, B. (2013). Advanced procedures for long-term creep data prediction for 2.25 chromium steels. *Metallurgical and Materials Transactions A*, 44(1), 136-153.
211. Williams, K., and Cane, B. (1979). Creep behaviour of 12Cr12Mo14V steel at engineering stresses. *Materials Science and Engineering*, 38(3), 199-210.
212. Williams, K., and Wilshire, B. (1977). Effects of microstructural instability on the creep and fracture behaviour of ferritic steels. *Materials Science and Engineering*, 28(2), 289-296.
213. Wilshire, B., and Bache, M. (2009). *Cost effective prediction of creep design data for power plant steels*. Paper presented at the ECCC Creep Conference.
214. Wu, R., and Sandström, R. (1995). Creep cavity nucleation and growth in 12Cr–Mo–V steel. *Materials science and technology*, 11(6), 579-588.
215. Xu, Q. (2001). Creep damage constitutive equations for multi-axial states of stress for 0.5 Cr0. 5Mo0. 25V ferritic steel at 590 C. *Theoretical and applied fracture mechanics*, 36(2), 99-107.
216. Xu, Q., Wright, M., and Xu, Q. (2011). *The development and validation of multi-axial creep damage constitutive equations for P91*. Paper presented at

the Automation and Computing (ICAC), 2011 17th International Conference on.

217. Yaghi, A., Hyde, T., Becker, A., and Sun, W. (2008). Finite element simulation of welding and residual stresses in a P91 steel pipe incorporating solid-state phase transformation and post-weld heat treatment. *The Journal of Strain Analysis for Engineering Design*, 43(5), 275-293.
218. Yamaguchi, M., and Umakoshi, Y. (1990). The deformation behaviour of intermetallic superlattice compounds. *Progress in Materials Science*, 34(1), 1-148.
219. Yao, H.-T., Xuan, F.-Z., Wang, Z., and Tu, S.-T. (2007). A review of creep analysis and design under multi-axial stress states. *Nuclear Engineering and Design*, 237(18), 1969-1986.
220. Yavari, P., and Langdon, T. G. (1982). An examination of the breakdown in creep by viscous glide in solid solution alloys at high stress levels. *Acta metallurgica*, 30(12), 2181-2196.
221. Yin, Y., and Faulkner, R. (2006). Continuum damage mechanics modelling based on simulations of microstructural evolution kinetics. *Materials science and technology*, 22(8), 929-936.
222. Yin, Y., Faulkner, R. G., Morris, P., and Clarke, P. (2008). Modelling and experimental studies of alternative heat treatments in Steel 92 to optimise long term stress rupture properties. *Energy Materials*, 3(4), 232-242.
223. Yoo, M., and Trinkaus, H. (1983). Crack and cavity nucleation at interfaces during creep. *Metallurgical Transactions A*, 14(3), 547-561.
224. Yoo, M., and Trinkaus, H. (1986). Interaction of slip with grain boundary and its role in cavity nucleation. *Acta metallurgica*, 34(12), 2381-2390.
225. Zhang, J., Wang, G., Xuan, F., and Tu, S. (2015). The influence of stress-regime dependent creep model and ductility in the prediction of creep crack growth rate in Cr–Mo–V steel. *Materials & Design*, 65, 644-651.

226. Zinkle, S. J., and Was, G. (2013). Materials challenges in nuclear energy. *Acta Materialia*, 61(3), 735-758.